EMILIE M. HERZOG

PRE ECL AMP SIA

AND THE DEVELOPMENT AND PROGRAMMING OF MATERNAL AND NEWBORN TISSUES

CLINICAL AND EPIGENETIC STUDIES

PREECLAMPSIA AND THE DEVELOPMENT AND PROGRAMMING OF MATERNAL AND NEWBORN TISSUES

CLINICAL AND EPIGENETIC STUDIES

Emilie M. Herzog

ISBN: 978-94-028-0849-0
Cover photography: M. Vidovic - www.magdalenavidovic.de
Cover and graphic design: A. Spindler - www.annaspindler.com
Printing: Ipskamp printing, Amsterdam, the Netherlands

Financial support by the Dutch Heart Foundation for the publication of this thesis is gratefully acknowledged. The printing of this thesis was additionally supported by the HELLP Foundation, Herzog Medical, the department of Obstetrics and Gynaecology of the Erasmus MC, University Medical Centre Rotterdam and the Erasmus University Rotterdam, the Netherlands.

PREECLAMPSIA AND THE DEVELOPMENT AND PROGRAMMING OF MATERNAL AND NEWBORN TISSUES

CLINICAL AND EPIGENETIC STUDIES

Preeclampsie en de ontwikkeling en programmering
van maternale en neonatale weefsels
Klinische en epigenetische studies

Proefschrift

ter verkrijging van de graad van doctor aan de
Erasmus Universiteit Rotterdam
op gezag van de Rector Magnificus

Prof. dr. H.A.P. Pols

en volgens besluit van het College voor Promoties.

De openbare verdediging zal plaatsvinden op
vrijdag 8 december 2017 om 09.30 uur

door

Emilie Marjolein Herzog
geboren te Amersfoort

Erasmus University Rotterdam

PROMOTIECOMMISSIE

Promotor	Prof. dr. R.P.M. Steegers-Theunissen
Copromotor	Dr. A.J. Eggink
Overige leden	Prof. dr. A.H.J. Danser
	Prof. dr. A. Franx
	Prof. dr. C.M. van Duijn
Paranimfen	Dr. M.H. van Coevorden - Hameete
	M.E. Herzog

TABLE OF CONTENTS

009 CHAPTER 1 General introduction

017 **PART I** **CLINICAL STUDIES**

019 CHAPTER 2 The impact of early- and late-onset preeclampsia on umbilical cord blood cell populations
Journal of Reproductive Immunology, 2016 Aug. 116: p. 81-85

033 CHAPTER 3 Impact of early- and late-onset preeclampsia on features of placental and newborn vascular health
Placenta, 2017 Jan. 49: p. 72-79

049 CHAPTER 4 Microcirculation in women with severe preeclampsia and HELLP syndrome: a case-control study
British Journal of Obstetrics and Gynaecology, 2014. 121: p. 363–370

063 **PART II** **EPIGENETIC STUDIES**

065 CHAPTER 5 Tissue-specific DNA methylation profiles in newborns
Clinical Epigenetics, 2013. 5: p. 8-12

073 CHAPTER 6 The tissue-specific aspect of genome-wide DNA-methylation in newborn and placental tissues: implications for epigenetic epidemiologic studies
Submitted

107 CHAPTER 7 Early- and late-onset preeclampsia and the tissue-specific epigenome of the placenta and newborn
Placenta, 2017. 58: p. 122-132

137 CHAPTER 8 DNA hypomethylation of placental growth factor and decreased SAM:SAH ratio in placental tissue of preeclampsia-complicated pregnancies
Submitted

149 PART III

151 CHAPTER 9 General discussion

167 CHAPTER 10 Summary / Samenvatting
De dans van DNA: een aanvulling op de Nederlandse samenvatting

179 ADDENDUM

180 References
192 Authors and affiliations
194 List of abbreviations
196 List of publications
198 About the author
199 PhD Portfolio
203 Acknowledgements

CHAPTER 1

General introduction

In line with the Developmental Origins of Health and Disease (DOHaD) paradigm, epidemiological and experimental animal studies have associated adverse intrauterine conditions with increased susceptibility to cardiovascular disease throughout the offspring's lifespan [1, 2]. For instance, offspring exposed to pregnancies complicated by preeclampsia (PE) have enhanced risks of increased blood pressure and body mass index in childhood and early adolescence and nearly a double risk of stroke in adulthood [3-7]. Moreover, the American Heart Association has recently added PE to the list of risk factors for developing cardiovascular disease, as women who experienced PE have a fourfold increased risk of developing hypertension and a more than twofold increased risk of dying from cardiovascular diseases [3, 8, 9].

PREECLAMPSIA

PE affects 2-8% of all pregnancies and is considered a major obstetric problem due to the high prevalence of maternal and perinatal morbidity and mortality [3]. This complex disorder is characterised by gestational hypertension of at least 140/90 mmHg accompanied by an urine protein/creatinine ratio of ≥ 30 mg/mmol arising *de novo* at or after 20 weeks of pregnancy, although the new clinical definition also includes gestational hypertension with one or more of the following new-onset conditions: proteinuria, thrombocytopenia, impaired liver function, renal insufficiency, pulmonary oedema or cerebral or visual disturbances [3, 10]. Two main disease entities have been identified with early-onset PE (EOPE) as the more severe phenotype, diagnosed before 34 weeks of gestation, and late-onset PE (LOPE) diagnosed at or after 34 weeks of gestation [3, 11].

Although the pathophysiology of both phenotypes is not yet fully understood, there is extensive evidence that EOPE originates from poor first trimester placentation, characterised by early unplugging of spiral arteries, superficial trophoblast invasion and insufficient remodelling of spiral arteries in the myometrium, causing episodes of placental hypoxia and reperfusion [12]. The poor and restricted placental development in EOPE is associated with small placental volume and often fetal growth restriction (**Figure 1A**). Whereas LOPE is considered a more maternal disorder originating from underlying maternal cardiovascular- and metabolic risk factors, with potential trophoblast dysfunction at the end of gestation due to villous overcrowding in large, term placentas without prior pathology and typically well-grown fetuses [13]. Both phenotypes are characterised by an excessive production of placental induced reactive oxygen species (ROS) which induce a hyperoxidative state to which the developing

embryo and fetus are exposed. In LOPE this occurs more towards the end of gestation than in EOPE (**Figure 1B**) [11]. As a result, pro-inflammatory cytokines and (anti)angiogenic factors are released into the maternal circulation inducing maternal endothelial dysfunction, leading to the clinical symptoms of PE [14].

EPIGENETICS

The adverse prenatal PE environment can disturb the development and programming of placental and newborn tissues [15-17]. This development and programming is subject to complex interactions between genes and environmental conditions. The process of developmental programming is strongly mediated by various epigenetic mechanisms [18, 19], that can be defined as '*chromosome-based mechanisms that change the phenotypic plasticity in a cell or organism*' [20]. This allows for the generation of diverse cell phenotypes and functions of an organism from a single genome, and for the regulation of gene-expression in response to a range of environmental exposures [21]. Epigenetic processes generally involve the regulation of gene-expression without changing the underlying DNA sequence [18].

DNA methylation is the best-characterised epigenetic modification, involving the attachment of a methyl group on predominantly cytosine nucleotides that precede a guanosine nucleotide in the DNA sequence (so-called CpG dinucleotides) [22]. DNA methylation is established in a tissue-specific manner and takes place at various positions on the genome, relative to genes and CpG-density. The function of DNA methylation seems to vary within this context affecting the relationship between DNA methylation and transcription [23-26]. Disturbed epigenetic programming of specific tissues such as the placenta, is suggested to be involved as cause or consequence, in the development of PE [18].

HYPOTHESIS

From this background we hypothesize that prenatal PE exposure is associated with a disturbed development (1) and epigenetic programming (2) of placental and newborn cardiovascular tissues, resulting in a cardiovascular phenotype of the newborn that is more susceptible to develop cardiovascular diseases later in life [22] (**Figure 1**).

FIGURE 1. A

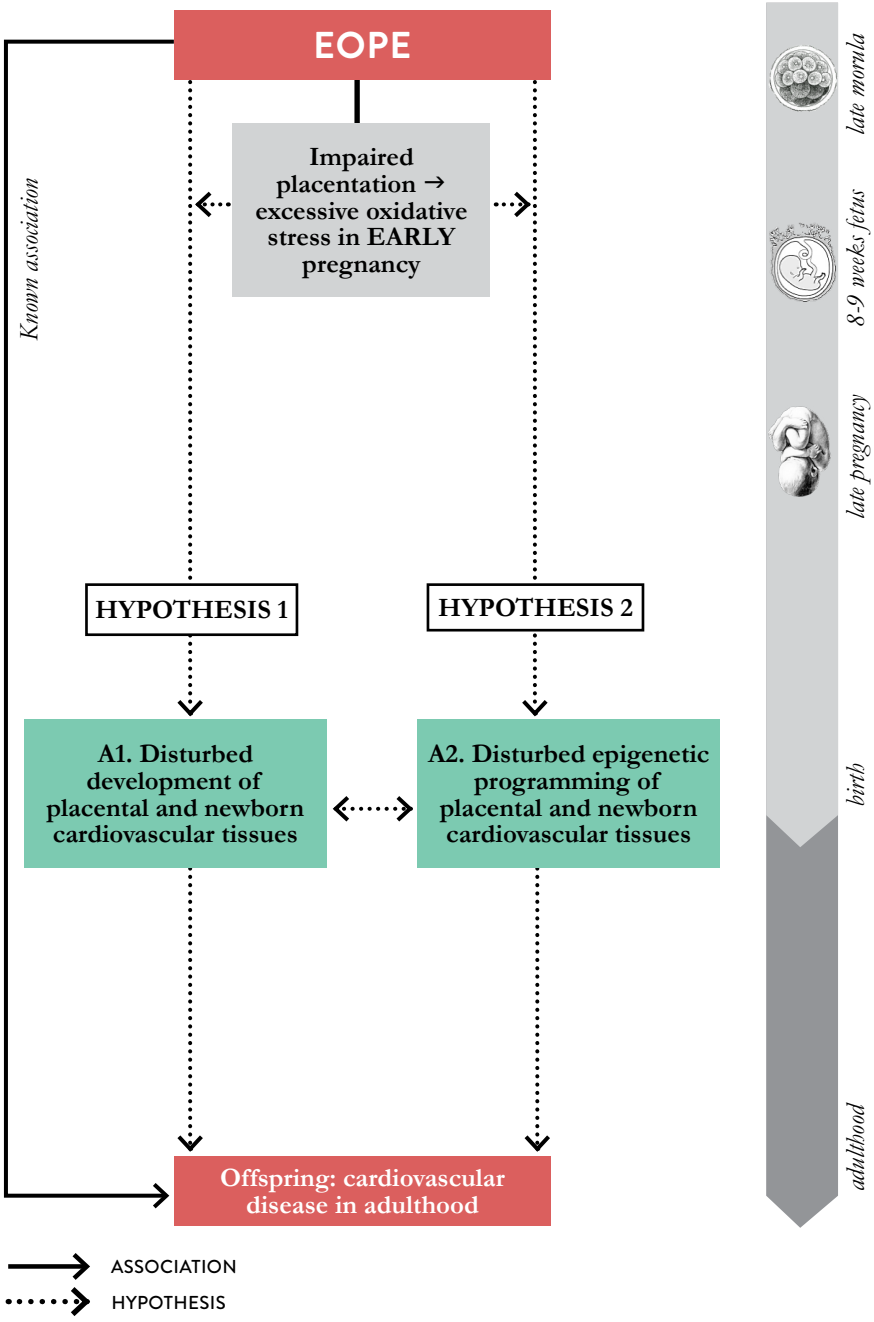
EOPE
Impaired placentation → excessive oxidative stress in EARLY pregnancy
Known association
HYPOTHESIS 1
HYPOTHESIS 2
A1. Disturbed development of placental and newborn cardiovascular tissues
A2. Disturbed epigenetic programming of placental and newborn cardiovascular tissues
Offspring: cardiovascular disease in adulthood
late morula
8-9 weeks fetus
late pregnancy
birth
adulthood
ASSOCIATION
HYPOTHESIS

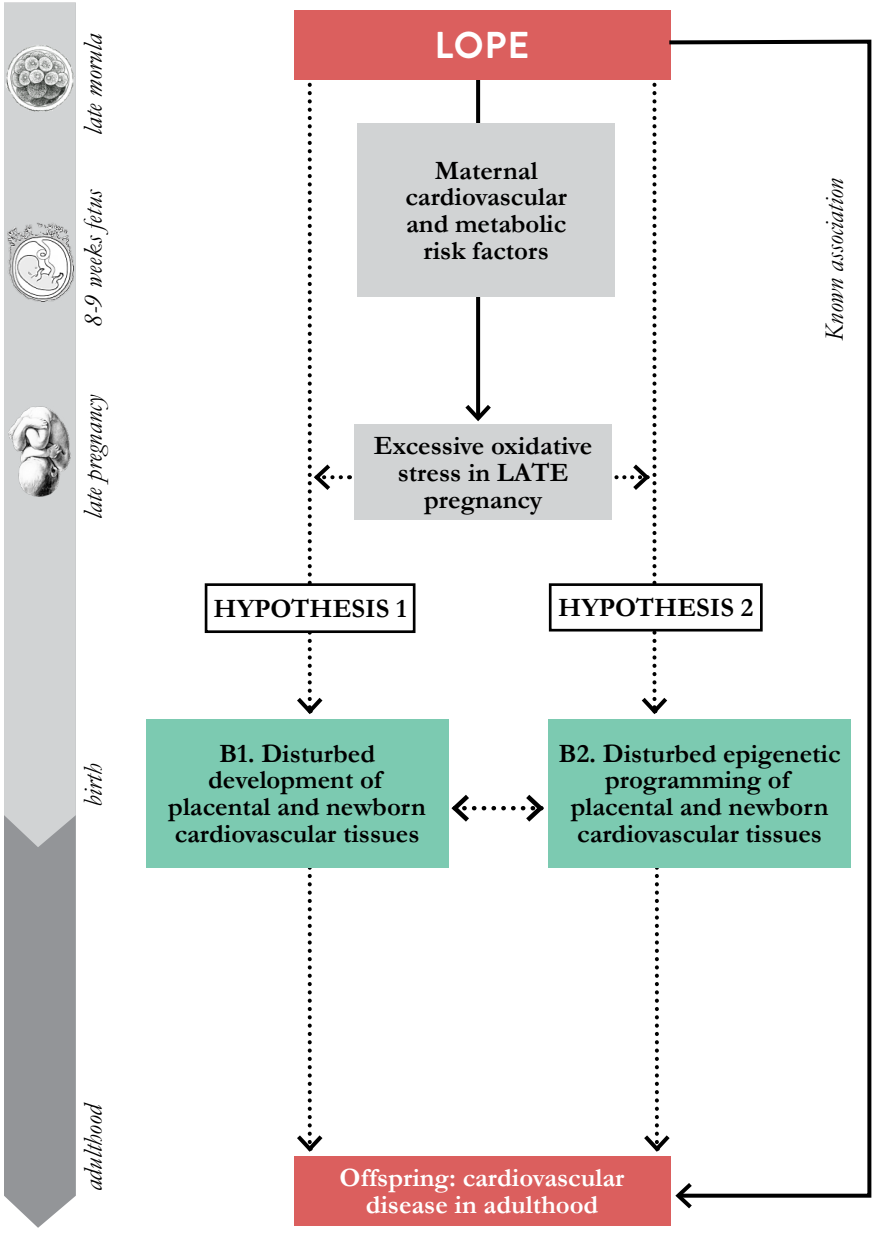
late morula
8-9 weeks fetus
late pregnancy
birth
adulthood
LOPE
Maternal cardiovascular and metabolic risk factors
Excessive oxidative stress in LATE pregnancy
HYPOTHESIS 1
HYPOTHESIS 2
B1. Disturbed development of placental and newborn cardiovascular tissues
B2. Disturbed epigenetic programming of placental and newborn cardiovascular tissues
Offspring: cardiovascular disease in adulthood
Known association

PLACENTAL AND NEWBORN TISSUES

Since it is not feasible to study our hypotheses in the cardiovascular tissues of the human embryo and fetus directly, we aimed to examine human umbilical cord vein endothelial cells (HUVEC), umbilical cord blood, and placental tissue in clinical and epigenetic studies. It is known that these tissues are essential for normal embryonic and fetal development and involved in the pathophysiology of PE. They may therefore provide novel insights into the potential development and programming of long-term cardiovascular disease susceptibility, and unravel underlying mechanisms.

The umbilical cord vasculature, originating from the intra- and extra-embryonic mesodermal layers, is the best accessible representative tissue of the newborn vasculature, and its development is highly influenced by local haemodynamic conditions of pregnancy, such as blood flow, oxygen tension and oxidative stress [20, 21, 27]. The umbilical cord vessels are responsible for transport of oxygen- and nutrient-rich blood and deoxygenated blood and metabolic waste between mother and child [28, 29]. Umbilical cord blood (UCB) originates from the same embryonic mesodermal layers as HUVEC and provides information on the prenatal inflammatory- and haematopoietic systemic conditions and as such represents a widely-studied, easily-accessible newborn tissue [27]. The main regulatory organ of the intrauterine environment is the placenta, serving as a metabolic, immunologic and endocrine organ of extra-embryonic origin. By monitoring fetal demands and intrauterine adaptations, the placenta regulates fetal growth and development. Due to its involvement in the pathophysiology of PE, the investigation of placental tissue is crucial in this context [30, 31].

OBJECTIVES OF THE THESIS

The main objectives of this thesis are to investigate:

1. The development of placental and newborn cardiovascular tissues in association with EOPE and LOPE (a), and of the maternal microcirculation in association with PE (b) (**Part I**)
2. The tissue-specific DNA methylation in placental and newborn cardiovascular tissues in association with EOPE and LOPE (**Part II**)

METHODOLOGY

Data for the studies in this thesis was obtained from a nested case-control study embedded in the Rotterdam Periconceptional Cohort (Predict Study), a prospective tertiary hospital-based cohort study conducted at the Department of Obstetrics and Gynaecology of the Erasmus MC, University Medical Centre

Rotterdam, the Netherlands [32]. Pregnant women and their newborns were recruited between June 2011 and June 2013. Enrolment was aimed early in the first trimester of pregnancy, but was also possible if patients were admitted to our hospital after the first trimester, meeting the inclusion criteria. Maternal and newborn characteristics were obtained from hospital medical records. Umbilical cord tissue (including HUVEC), umbilical cord blood and placental tissue were collected and subjected to flow-cytometric, histological and (genome-wide) epigenetic analysis.

Cases comprised of women with pregnancies that were complicated by EOPE or LOPE. PE is known to be complicated by fetal growth restriction (FGR) in 12% and iatrogenic preterm birth (PTB) in 20% [33]. These conditions can independently influence the intrauterine development and epigenetic programming of placental and newborn tissues [34-36]. In order to examine associations with EOPE and LOPE independent of FGR and PTB, control pregnancies comprised of both uncomplicated and complicated normotensive FGR and PTB pregnancies.

To investigate associations with the maternal microcirculation, women with severe PE with or without HELLP syndrome (haemolysis, elevated liver enzymes and low platelets), and healthy controls were included between November 2009 and September 2012 for the study described in chapter 4. Both study populations were recruited and conducted at the same hospital department.

THESIS OUTLINE

The first objective is addressed in Part I of this thesis by performing three clinical studies. Chapter 2 describes the associations between EOPE, LOPE and umbilical cord blood cell populations. In chapter 3 we address whether EOPE and LOPE are associated with placental and umbilical cord (vascular) (histo-) morphological alterations. The associations between the maternal microcirculatory perfusion and severe PE are studied in chapter 4.

Part II describes both gene-specific and epigenome-wide DNA methylation studies. The first two chapters (chapter 5 and 6) address the tissue-specific characteristics of DNA methylation in newborn tissues, on a genome-wide level and of the imprinted Insulin-like growth factor 2 *(IGF2)/H19* genes. This is followed by chapter 7 and 8 that evaluate the associations between EOPE, LOPE and variations in tissue-specific DNA methylation, both genome-wide and in placental-specific angiogenic genes.

Chapter 9 covers the general discussion of the main findings, methodological considerations, clinical implications and recommendations for future research.

CHAPTER 2

The impact of early- and late-onset preeclampsia on umbilical cord blood cell populations (Journal of Reproductive Immunology, 2016 Aug. 116: p. 81-85)

CHAPTER 3

Impact of early- and late-onset preeclampsia on features of placental and newborn vascular health (Placenta, 2017 Jan. 49: p. 72-79)

CHAPTER 4

Microcirculation in women with severe preeclampsia and HELLP syndrome: a case-control study (British Journal of Obstetrics and Gynaecology, 2014. 121: p. 363–370)

PART 01

CLINICAL STUDIES

CHAPTER 2

The impact of early- and late-onset preeclampsia on umbilical cord blood cell populations

E.M. Herzog, A.J. Eggink, M. van der Zee, J. Lagendijk, S.P. Willemsen, R. de Jonge, E.A.P. Steegers, R.P.M. Steegers-Theunissen

Journal of Reproductive Immunology, 2016 Aug. 116: p. 81-85

ABSTRACT

Pregnancies complicated by preeclampsia (PE) are characterised by an enhanced maternal and fetal inflammatory response with increased numbers of leukocytes in maternal peripheral blood. The impact of PE on newborn umbilical cord blood cell (UCBC) populations however, has been scarcely studied. We hypothesise that PE deranges fetal haematopoiesis and subsequently UCBC populations. Therefore, the objective of this study was to investigate newborn umbilical cord blood cell populations in early- (EOPE) and late-onset PE (LOPE).

A secondary cohort analysis in the Rotterdam Periconceptional cohort was conducted comprising 23 PE cases, including 11 EOPE and 12 LOPE, and 195 controls, including 153 uncomplicated and 23 fetal growth restriction and 19 preterm birth complicated controls. UCBC counts and differentials were quantified by flow cytometry and analysed as main outcome measures.

Multivariable regression analysis revealed associations of EOPE with decreased leucocytes (monocytes, neutrophils , eosinophils , immature granulocytes) and thrombocyte counts and increased NRBC counts (all $p < 0.05$). EOPE remained associated with neutrophils (β-0.92, 95%CI -1.27,-0.57, $p < 0.001$) and NRBC counts (β1.11, 95%CI 0.27,1.95, $p = 0.010$) after adjustment for gestational age and birth weight. LOPE did not reveal any significant association.

We conclude that derangements of fetal haematopoiesis, in particular of neutrophils and NRBC counts, are associated with EOPE only, with a potential impact for future health of the offspring. This heterogeneity in UCBC should be considered as confounder in epigenetic association studies examining EOPE.

INTRODUCTION

Preeclampsia (PE) is a heterogeneous disease with early-onset (EOPE) and late-onset (LOPE) PE as the main phenotypes. Due to inadequate spiral artery remodelling with suboptimal placental perfusion, excessive amounts of oxidative stress can lead to an enhanced release of syncytiotrophoblast microparticles and cytokines, which particularly contributes to the pathogenesis of the more severe EOPE phenotype [11]. In contrast, LOPE shows a relatively normal initial placentation and is associated with conditions that enhance excessive oxidative stress and placental inflammation later in pregnancy, such as obesity and pre-existing hypertension [3, 14]. Circulating syncytiotrophoblast microparticles can induce an increased maternal systemic inflammatory response with increased numbers of neutrophils and total leukocytes in maternal peripheral blood [37, 38]. The impact of PE on newborn umbilical cord blood cell (UCBC) populations, however, has been scarcely studied.

During pregnancy, haematopoiesis takes place in the yolk sac, liver, bone marrow as well as in the placenta, generating all blood cell types from a small population of pluripotent hematopoietic stem cells as pregnancy advances [39-42]. We hypothesise that PE, in particular EOPE, deranges fetal haematopoiesis resulting in heterogeneity of UCBC populations [43], and investigated the associations between UCBC counts and differentials in early- and late-onset PE.

MATERIALS AND METHODS

Study design. Between June 2011 and June 2013 we included pregnant women in a prospective hospital based periconception birth cohort: The Rotterdam Predict Study, at the Erasmus MC, University Medical Centre Rotterdam, the Netherlands [32]. For the current secondary cohort analysis, we selected EOPE and LOPE as cases and uncomplicated pregnancies as controls. To adjust for the often accompanied fetal growth restriction (FGR) and iatrogenic preterm birth (PTB) in PE, we oversampled the uncomplicated control group with FGR and PTB as complicated controls. Pregnancies were included in the cohort during the first trimester (early cohort inclusions) or after the first trimester when they were referred to our hospital (late cohort inclusions).

PE was defined according to the International Society for the Study of Hypertension in Pregnancy as gestational hypertension of at least 140/90 mmHg accompanied by an urine protein/creatinine ratio of $\geq$ 30 mg/mmol, arising *de novo* after the 20th week of gestation [44]. EOPE was defined when PE was diagnosed

before 34 weeks of gestation, LOPE when diagnosed after 34 weeks of gestation [45]. Uncomplicated control pregnancies were defined as pregnancies without the presence of PE, gestational hypertension, FGR or PTB. FGR inclusion was based on an estimated fetal weight below the 10th percentile for gestational age based on ultrasound measurements performed between 20 and 38 weeks gestational age [46]. Birth weight percentiles were calculated using the reference curves of the Dutch Perinatal Registry to validate birth weight ≤ 10th percentile and exclude those newborns with birth weight > 10th percentile [47]. Spontaneous preterm deliveries between 22 and 37 weeks of gestation were defined as PTB [48]. Women with HIV infection, age < 18 years and insufficient knowledge of the Dutch language could not participate and pregnancies complicated with a fetal congenital malformation and twins were excluded for the current study. Maternal comorbidity was defined by any concurrent cardiovascular-, hematologic-, endocrine-, metabolic-, auto-immune- or renal disease. Maternal and fetal characteristics were obtained from hospital medical records. All women gave written informed consent before participation and written parental informed consent was obtained for the child. Ethical approval was given by the Erasmus MC, University Medical Centre Research Ethics Board (MEC-2004-227).

Collection and handling of blood samples. UCB samples from the umbilical vein were obtained in vacutainer tubes (Ethylenediaminetetraacetic acid as anticoagulant), immediately after delivery and clamping of the umbilical cord. Samples were transported at room temperature and subjected to flow cytometric analysis within 48 hours after delivery (Sysmex XE-5000, Sysmex XN-3000 and XS-800i, Etten-Leur, the Netherlands) to quantify erythrocyte, thrombocyte and leucocyte differentials. Between arrival at the Clinical Chemistry Laboratory and time of analysis, samples were stored at four to eight °C. Quality of the blood cell counts was guaranteed by a manual check whereby flow cytometric data of suspect plots or reported system errors were excluded for further analysis.

Statistical analysis. We used cell numbers/L for the analysis of leucocyte differentials and NRBC, which is preferable to the widely used percentages of total leucocyte count, since the largely variable total leucocyte count could result in misleading percentages [49]. The normal distributed maternal and newborn characteristics were tested using Analysis of Variance (ANOVA) to detect overall differences between the groups, followed by the posthoc Dunnett t-test for pairwise comparisons of EOPE and LOPE with uncomplicated controls and FGR and PTB complicated controls. The Dunnett t-test limits the multiple testing problem by comparing each group to one reference group

only. The Kruskall-Wallis-test was applied to all non-parametric maternal and newborn characteristics, followed by pairwise Mann-Whitney tests for posthoc comparisons.

Log-transformation was applied to the non-parametric UCBC to achieve normal distributions of neutrophils, monocytes, eosinophils, basophils, nucleated red blood cells (NRBC) and immature granulocytes. We converted zero values of neutrophils and NRBC into half of the lowest detectable value of the Sysmex haematology system, prior to log-transformation. Linear regression analysis was performed to investigate the association between UCBC counts and differentials and EOPE/LOPE versus the pooled group of (un) complicated controls. In the crude linear regression analyses, UCBC counts were estimated with group (case-control) as the only predictive variable. In the adjusted multivariable analyses, gestational age and birth weight were additionally entered to the model as covariates, in formula: $[UCBC] = \beta_0 + \beta_1 group + \beta_2 GA + \beta_3 BW + \varepsilon$. Here group is an indicator variable that is 1 for EOPE or LOPE and 0 for the pooled group of (un)complicated controls. [UCBC] represents the concentration of a certain UCBC population. All measurements were performed with IBM SPSS Statistics version 21.0 (SPSS Inc, Chicago, IL, USA).

RESULTS

From the Predict Study we included all eligible women for this secondary cohort analysis that met the inclusion criteria as described earlier (n=412). After exclusion of 194 pregnancies due to missing blood samples (n=117) or poor quality of blood cell counts (n=77), 218 pregnancies were included for analysis. Patients with missing data were characterised by a shorter gestational age (38.2 versus 39.1 weeks, $p < 0.001$) and lower birth weight (3065 versus 3363 grams, $p < 0.001$) as compared to the final study population, and contained twice as much EOPE- (10.3% versus 5.0%) and LOPE pregnancies (9.3% versus 5.5%, $p = 0.076$), as depicted in **Supplementary table 1**. The final study population comprised 23 cases of PE including 11 EOPE and 12 LOPE, and 195 controls, including 153 uncomplicated controls and 23 FGR and 19 PTB complicated controls (**Supplementary figure 1**).

Maternal and newborn characteristics are shown in **Table 1.** In addition to the case specific parameters blood pressure, proteinuria, gestational age and birth weight, a significant lower mean maternal age in EOPE versus LOPE and uncomplicated controls was shown (27.1 year, versus 34.1 and 32.2 year respectively, overall $p = 0.002$). EOPE pregnancies ended more often in a

TABLE 1. Maternal and newborn characteristics

Maternal characteristics	EOPE (n=11)	LOPE (n=12)	Uncomplicated controls (n=153)	Complicated controls FGR (n=23)	Complicated controls PTB (n=19)	Overall p-value
Age (years)	27.1 (5.2)	34.1* (3.8)	32.2* (5.1)	29.3# (5.8)	30.6 (5.2)	0.002
Nulliparous, n (%)	8 (72.7)	7 (58.3)	66 (43.1)	11 (47.8)	6 (31.3)	0.204
Ethnicity, n (%)						
Western	9 (81.8)	7 (58.3)	122 (80.3)	14 (60.9)	15 (83.3)	0.152
Non-Western	1 (18.2)	5 (41.7)	30 (19.7)	9 (39.1)	3 (16.7)	
Preconception BMI[a] (kg/m^2)	26.8 (9.3)	26.4 (2.8)	24.1 (7.1)	23.6 (5.6)	24.1 (7.1)	0.785
Smoking during pregnancy (yes), n (%)	1 (12.5)	0 (0.0)	8 (5.4)	2 (9.1)	1 (6.3)	0.813
Co-morbidity (yes), n (%)	1 (9.1)	3 (25.0)	61 (39.9)	4 (17.4)	3 (15.8)	0.022
Newborn characteristics						
Male gender, n (%)	9 (81.8)	7 (58.3)	77 (50.3)	14 (60.9)	9 (47.4)	0.210
Gestational age at birth[a] (weeks)	31.0 (3.7)	37.4* (1.9)	39.6*# (1.7)	39.0*# (2.6)	35.9*# (4.9)	<0.001
Birth weight[a] (grams)	1155 (353)	3238* (1689)	3515* (563)	2625*# (600)	2650*# (1455)	<0.001
Birth weight <10th percentile, n (%)	2 (18.2)	2 (16.7)	0*# (0.0)	23*# (100.0)	0 (0.0)	<0.001

Data are presented as mean (standard deviation) with corresponding ANOVA testing to examine overall differences between the groups, followed by the post hoc Dunnett t-test for pairwise comparisons of EOPE and LOPE with (un) complicated controls.
Data are presented as number (%) with corresponding Chi^2/Fischer's exact testing.
[a] Non-parametric data are presented as median (interquartile range) with corresponding Kruskall-Wallis testing and post-hoc Mann-Whitney testing. * p <0.05 versus EOPE pregnancies. # p <0.05 versus LOPE pregnancies.
ANOVA analysis of variance; *BMI* body mass index; *EOPE* early onset preeclampsia; *LOPE* late onset preeclampsia; *FGR* fetal growth restriction; *PTB* preterm birth.

caesarean section compared to LOPE and (un)complicated controls (90%, versus 25% and up to 35% respectively, overall p = 0.003). Comorbidity was significantly different between the groups and highest in uncomplicated controls, but no significant differences were observed in the posthoc analysis. Neonatal temperature at birth was similar for each group.

We observed significantly lower cell counts for all UCBC populations and a significantly higher NRBC count in EOPE versus (un)complicated controls. In LOPE only significantly higher neutrophil and erythrocyte counts and lower reticulocyte counts compared to PTB complicated controls were observed (**Supplementary table 2**).

In **Table 2** we show the results of the linear regression analyses of the UCBC counts and differentials of both EOPE and LOPE versus the pooled (un)

complicated controls. The crude estimates revealed that EOPE was associated with the decreased counts of total leucocytes (β -7.6, 95% CI -10.53, -4.76, p <0.001); monocytes (β -0.88, 95% CI -1.26, -0.51, p <0.001); neutrophils (β -1.92, 95% CI -2.25, -1.60, p <0.001); eosinophils (β -0.67, 95% CI -1.16, -0.18, p = 0.007); immature granulocytes (β -1.82, 95% CI -2.60, -1.03, p <0.001) and thrombocytes (β -80.19, 95% CI -126.7, -33.7, p = 0.001). EOPE was associated with increased NRBC count (β 1.20, 95% CI 0.57, 1.84, p <0.001). After adjustment for gestational age and birth weight, EOPE remained associated with decreased neutrophil count (β -0.92, 95% CI -1.27, -0.57, p <0.001) and increased NRBC count (β 1.11, 95% CI 0.27, 1.95, p = 0.010). The linear regression analyses did not reveal any significant association with LOPE versus the (un)complicated control group.

DISCUSSION

In this study we observed that pregnancies complicated by EOPE are associated with decreased leucocyte (monocytes, neutrophils, eosinophils, immature granulocytes) and thrombocyte counts and with increased NRBC counts in umbilical cord blood. After adjustment for gestational age and birth weight, EOPE remained associated with decreased neutrophil and increased NRBC counts.

Our findings demonstrate that the associations of most UCBC counts (total leucocyte, monocyte, eosinophil, immature granulocyte and thrombocyte counts) with EOPE are confounded by gestational age and birth weight, which is in agreement with previous studies [39, 42]. It revealed that LOPE compared to EOPE has a marginally impact on UCBC populations, which may be explained by its milder phenotype as well as the absence of FGR and PTB in this group. The four to sevenfold decrease of neutrophil count and fivefold increase of NRBC count in association with EOPE however, were independent of gestational age and birth weight. Because the innate immune-system matures during pregnancy, this system of the newborn is prepared to be fully functional at birth by a sudden neutrophil rise during the late third trimester [39]. The excessive oxidative stress from early pregnancy onwards might have affected UCB neutrophil counts in EOPE by generating enhanced inflammation in the fetal circulation, as demonstrated earlier by higher activated neutrophils and monocytes as well as increased CRP, α-1-antitrypsin and plasma chemokine levels [50, 51]. As a consequence, fetal endothelial cell dysfunction might occur, by which the maturation and development of fetal haematopoiesis can be

TABLE 2. Linear regression analysis of UCBC count and differentials in EOPE and LOPE versus the (un)complicated control group (n=195)

	EOPE (n=11)		LOPE (n=12)	
	Crude β	Adjusted β (GA+BW)	Crude β	Adjusted β (GA+BW)
Haemoglobin (mmol/L)	-0.51 (-1.22, 0.21)	0.37 (-0.54, 1.29)	0.36 (-0.28, 1.01)	0.48 (-0.15, 1.12)
Haematocrit (L/L)	0.00 (-0.03, 0.04)	0.05* (0.00, 0.09)	0.02 (-0.01, 0.05)	0.03 (-0.01, 0.06)
Leucocytes				
Total leucocytes (x10^9/L)	-7.6* (-10.53, -4.76)	0.32 (-3.14, 3.78)	-0.75 (-3.66, 2.16)	-0.07 (-2.68, 2.55)
Lymphocytes (10^9/L)	-0.62 (-1.68, 0.44)	0.98 (-0.32, 2.28)	-0.40 (-1.29, 0.50)	-0.19 (-1.05, 0.66)
Monocytes[a] (10^9/L)	-0.88* (-1.26, -0.51)	-0.05 (-0.49, 0.39)	-0.10 (-0.41, 0.22)	-0.05 (-0.33, 0.23)
Granulocytes				
Neutrophils[a] (10^9/L)	-1.92* (-2.25, -1.60)	-0.92* (-1.27, -0.57)	0.05 (-0.22, 0.32)	0.14 (-0.08, 0.36)
Eosinophils[a] (10^9/L)	-0.67* (-1.16, -0.18)	-0.37 (-1.01, 0.26)	-0.08 (-0.49, 0.34)	-0.10 (-0.51, 0.31)
Basophils[a] (10^9/L)	-0.51 (-1.12, 0.09)	0.59 (-0.15, 1.32)	-0.05 (-0.56, 0.45)	0.04 (-0.44, 0.52)
Immature gran.[a] (10^9/L)	-1.82* (-2.60, -1.03)	-0.15 (-0.78, 1.07)	-0.26 (-0.90, 0.37)	-0.16 (-0.73, 0.41)
Erythroid cells				
NRBC[a] (10^9/L)	1.20* (0.57, 1.84)	1.11* (0.27, 1.95)	0.07 (-0.54, 0.68)	0.08 (-0.53, 0.70)
Reticulocytes (x10^9/L)	18.93 (-9.72, 47.58)	-24.25 (-60.40, 11.91)	1.12 (-25.36, 27.60)	-5.34 (-30.48, 19.80)
Erythrocytes (x10^{12}/L)	-0.63* (-0.96, -0.30)	0.04 (-0.37, 0.44)	0.12 (-0.17, 0.42)	0.21 (-0.07, 0.49)
Thrombocytes				
Thrombocytes (x10^9/L)	-80.19* (-126.7, -33.7)	-40.4 (-11.6, 19.8)	-32.05 (-72.25, 8.16)	-28.93 (-69.12, 11.27)

Data are presented as β (95% Confidence Interval) with corresponding multivariable linear regression analysis of EOPE and LOPE versus the (un)complicated controls, crude and with adjustment for gestational age and birth weight. The regression coefficient (β) indicates the increase or decrease (-) change per unit.
[a] Log-transformed data. * p <0.05. *GA* gestational age; *BW* birth weight; *NRBC* nucleated red blood cells; *UCB* umbilical cord blood; *EOPE* early onset preeclampsia; *LOPE* late onset preeclampsia; *Immature gran.* Immature granulocytes.

affected. Fetal haematopoiesis originates from endothelial cells in the ventral aorta of the developing embryo and is thus extremely sensitive to endothelial damage [52]. It has been suggested that the maternal endothelial cell damage is of more importance in EOPE than LOPE and that the excessive oxidative stress develops only towards the end of gestation in LOPE [11]. This is in line with the observed difference in leucocyte counts between EOPE and LOPE. The association between PE and decreased UCB leucocyte count has been described before and is in agreement with our findings [39, 53]. Low neutrophil counts might result in a temporarily reduced immune capacity of the newborn,

especially if the child is also born preterm. This might increase the vulnerability for infections.

The observed increase of UCB NRBC in EOPE pregnancies is in line with earlier studies [53-57]. However, Akercan- and Catarino et al. did not observe this increase independent of gestational age, which can be explained by the lack of separate analysis for EOPE and LOPE. High numbers of circulating NRBC can reflect an activation of erythropoiesis as a response to the placental ischemia-reperfusion phenomenon resulting from diminished and intermittent perfusion of the intervillous space or a compensation of the erythrocyte-damage, both more profoundly present in EOPE than in LOPE [11, 53, 55, 58]. The suboptimal placental perfusion results in a relatively hypoxic placental environment, which is beneficial for early invasion of the cytotrophoblast into the maternal decidua. However a prolonged hypoxic placental state may lead to an over-expression of hypoxia-inducible factor 1α (HIF-1α), regulating several processes such as erythropoiesis [59]. Placental over-expression of HIF-1α has been described in PE pregnancies, which may explain our finding of enhanced NRBC counts in umbilical cord blood, being a result of HIF-1α-induced erythropoietin-release [59, 60].

Strengths and limitations. A strength of the study is that we investigated associations between PE and UCBC counts and differentials in EOPE and LOPE separately which revealed a much stronger association between UCBC counts and EOPE, and is relevant concerning the different aetiologies of both. Moreover, associations were investigated independent of gestational age and birth weight.

Pregnancies complicated by EOPE in our study population ended more often in a Caesarean section. This unfortunately resulted in more missing blood samples (n=25, 59.5%) compared to LOPE (n=7, 26.9%, p = 0.009) due to the emergency of the Caesarean sections. Due to the sample size we were not able to adjust for many confounders and therefore inherent to an observational study residual confounding cannot be excluded. The wide confidence intervals demonstrate that the sample size also resulted in a limited power of the study. This implies that certain UCBC values with seemingly clinical relevant UCBC differences between groups might have failed to achieve statistical significance because of lack of power. Additionally, a selection bias due to the relatively high percentage of EOPE and LOPE pregnancies with missing data might be present, but this is an often occurring problem in high-risk patients where medical care is a priority. Another limitation of our study is the tertiary university hospital-setting, in which uncomplicated pregnancies presented

with a relatively high percentage of concurrent comorbidity (40%), for which they were referred. These patients were mostly included in the cohort study in the first trimester of pregnancy. Complicated PE, FGR and PTB pregnancies were more often included as late cohort inclusions after the first trimester. They presented with less additional comorbidity, as visualised in **Supplementary figure 1**. Two neonates only in EOPE and LOPE were complicated by FGR. Therefore, future studies may address differences in UCBC populations in a subgroup of early- and late-onset PE complicated by FGR.

CONCLUSION

Derangements of fetal haematopoiesis, in particular of neutrophils and NRBC counts, are associated with EOPE only. These findings imply potential impact on the future health of offspring and that heterogeneity in UCBC should be considered as confounder in epigenetic association studies examining EOPE. Further investigation is needed to establish the potential impact for future health of offspring.

SUPPLEMENTARY DATA

SUPPLEMENTARY FIGURE 1. Flowchart of the study population. *UCB* umbilical cord blood; *EOPE* early onset preeclampsia; *LOPE* late onset preeclampsia; *Unc. controls*; *FGR* fetal growth restriction; *PTB* preterm birth.

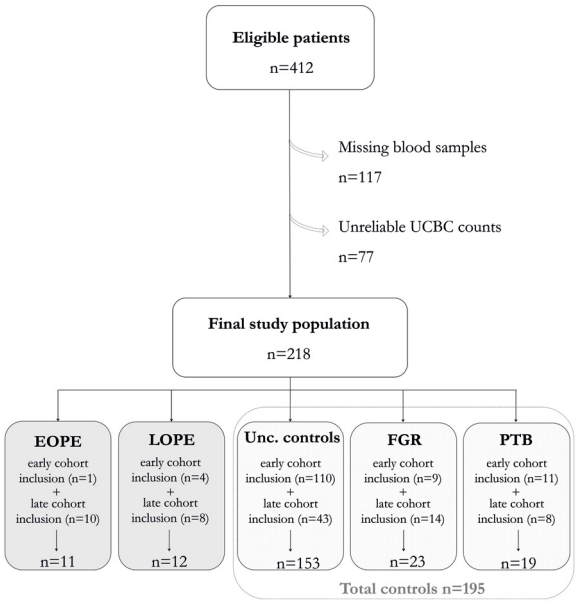

SUPPLEMENTARY TABLE 1. Sensitivity analysis of maternal and newborn characteristics between patients with missing data and the final study population.

		Patients with missing data	Final study population	p-value
Maternal characteristics		**(n=194)**	**(n=218)**	
Age (years)		31.5 (4.9)	31.6 (5.3)	0.818
Nulliparous, n (%)		95 (49.0)	98 (45.0)	0.415
Caesarean section, n (%)		78 (402)	80 (36.7)	0.465
Ethnicity, n (%)	Western	23 (20.7)	49 (22.7)	0.685
	Non-Western	88 (79.3)	167 (77.3)	
Preconception BMI[a] (kg/m^2)		23.3 (4.8)	24.2 (7.0)	0.113
Smoking during pregnancy (yes), n (%)		6 (5.9)	12 (5.8)	0.968
Co-morbidity (yes), n (%)		43 (35.8)	72 (33.0)	0.602
Case-control status, n (%)	EOPE	11 (10.3)	11 (5.0)	0.076
	LOPE	10 (9.3)	12 (5.5)	
	FGR	13 (12.1)	23 (10.6)	
	PTB	14 (13.1)	19 (8.7)	
	Uncomplicated controls	59 (55.1)	153 (70.2)	
Newborn characteristics				
Male gender, n (%)		96 (49.7)	107 (49.1)	0.894
Gestational age at birth[a] (weeks)		38.2 (4.7)	39.1 (2.4)	<0.001
Birth weight[a] (grams)		3065 (1488)	3363 (814)	<0.001
Birth weight <10th percentile, n (%)		37 (19.5)	27 (12.4)	0.050

Data are presented as mean (standard deviation) with corresponding independent t-testing to examine differences between the groups.
Data are presented as number (%) with corresponding Chi^2/Fischer's exact testing.
[a] Non-parametric data are presented as median (interquartile range) with corresponding Mann-Whitney testing. *BMI* body mass index; *EOPE* early onset preeclampsia; *LOPE* late onset preeclampsia; *FGR* fetal growth restriction; *PTB* preterm birth.

SUPPLEMENTARY TABLE 2. UCB cell counts and differentials

				Complicated controls		
	EOPE	LOPE	Uncom-plicated controls	FGR	PTB	Overall
	(n=11)	(n=12)	(n=153)	(n=23)	(n=19)	p-value
Haemoglobin (mmol/L) Missings	9.24 (1.41) 1	10.11 (1.08) 0	9.78 (0.96) 2	9.82 (1.32) 0	9.39 (1.71) 1	0.254
Haematocrit (L/L) Missings	0.47 (0.07) 1	0.49 (0.05) 0	0.47 (0.05) 2	0.47 (0.07) 0	0.45 (0.09) 1	0.387
Leucocytes						
Total leucocytes (x10^9/L) Missings	6.22 (1.97) 0	13.11*(3.29) 1	14.61* (4.62) 8	12.42* (3.74) 2	9.53 (5.01) 1	<0.001
Lymphocytes (10^9/L) Missings	3.99 (1.10) 4	4.21 (1.02) 2	4.70 (1.39) 29	4.76 (1.44) 4	3.60 (1.18) 5	0.034
Monocytes[a] (10^9/L) Missings	0.55 (0.25) 4	1.16* (0.42) 2	1.41* (0.57) 29	1.05* (0.48) 4	0.90 (0.44) 5	<0.001
Granulocytes						
Neutrophils[a] (10^9/L) Missings	1.04 (0.61) 4	6.90* (2.21) 2	7.21* (2.49) 30	5.71* (2.03) 4	4.16*# (2.89) 6	<0.001
Eosinophils[a] (10^9/L) Missings	0.19 (0.10) 4	0.36 (0.17) 2	0.42* (0.24) 29	0.30 (0.17) 4	0.37 (0.26) 6	0.008
Basophils[a] (10^9/L) Missings	0.07 (0.06) 4	0.10 (0.08) 2	0.14 (0.14) 30	0.07 (0.04) 4	0.08 (0.07) 5	0.027
Immature gran.[a] (10^9/L) Missings	0.06 (0.07) 5	0.41* (0.51) 2	0.45* (0.44) 30	0.19* (0.15) 4	0.31* (0.56) 7	<0.001
Erythroid cells						
NRBC[a] (10^9/L) Missings	5.44 (6.64) 0	0.99* (0.63) 1	1.18* (1.24) 12	1.01* (0.53) 2	1.68* (2.82) 1	<0.001
Reticulocytes (x10^9/L) Missings	201.83 (61.83) 1	184.02 (34.39) 1	178.36 (35.04) 12	175.17 (42.86) 2	227.43# (73.92) 1	<0.001
Erythrocytes (x10^{12}/L) Missings	3.79 (0.60) 1	4.54* (0.40) 0	4.47* (0.42) 2	4.37* (0.56) 0	4.08# (0.89) 1	<0.001
Thrombocytes						
Thrombocytes (x10^9/L) Missings	182.11 (83.19) 2	230.25 (68.23) 0	266.57* (66.83) 2	254.61* (72.83) 0	236.28 (74.48) 1	0.002

Data are presented as mean (standard deviation) with corresponding ANOVA testing to examine overall differences between the groups, followed by the post hoc Dunnett t-test for pairwise comparisons of EOPE and LOPE with (un)complicated controls.

[a] Log-transformed data are presented as back-transformed mean (standard deviation).

* p <0.05 versus EOPE pregnancies. # p <0.05 versus LOPE pregnancies. *ANOVA* analysis of variance; *UCB* umbilical cord blood; *NRBC* nucleated red blood cells; *Immature gran.* Immature granulocytes; *EOPE* early onset preeclampsia; *LOPE* late onset preeclampsia; *FGR* fetal growth restriction; *PTB* preterm birth.

CHAPTER 3

The impact of early- and late-onset preeclampsia on features of placental and newborn vascular health

E.M. Herzog, A.J. Eggink, A. Reijnierse, M.A.M. Kerkhof, R.R. de Krijger, A.J.M. Roks, I.K.M. Reiss, A.L. Nigg, P.H.C. Eilers, E.A.P. Steegers, R.P.M. Steegers-Theunissen

Placenta, 2017 Jan. 49: p. 72-79

ABSTRACT

Introduction. Offspring exposed to preeclampsia (PE) show an increased risk of cardiovascular disease in adulthood. We hypothesize that this is mediated by a disturbed vascular development of the placenta, umbilical cord and fetus. Therefore, we investigated associations between early-onset PE (EOPE), late-onset PE (LOPE) and features of placental and newborn vascular health.

Methods. We performed a nested case-control study in The Rotterdam Periconceptional Cohort, including 30 PE pregnancies (15 EOPE, 15 LOPE) and 218 control pregnancies (164 uncomplicated controls, 54 complicated controls including 28 fetal growth restriction, 26 preterm birth) and assessed macroscopic and histomorphometric outcomes of the placenta and umbilical cord.

Results. A significant association was observed between PE and a smaller umbilical vein area and wall thickness, independent of gestational age and birth weight. In EOPE we observed significant associations with a lower weight, length and width of the placenta, length of the umbilical cord, and thickness and wall area of the umbilical vein and artery. These associations attenuated after gestational age and birth weight adjustment. In LOPE a significant association with a larger placental width and smaller umbilical vein wall thickness was shown, independent of gestational age and birth weight.

Discussion. Our study suggests that PE is associated with a smaller umbilical cord vein area and wall thickness, independent of gestational age and birth weight, which may serve as a proxy of disturbed cardiovascular development in the newborn. Follow-up studies are needed to ultimately predict and lower the risk of cardiovascular disease in offspring exposed to PE.

INTRODUCTION

In line with the developmental origins of health and disease paradigm, epidemiological studies substantiated by animal studies strongly suggest that adverse prenatal exposures increase the risk of cardiovascular diseases in child- and adulthood [1, 2]. Preeclampsia (PE) occurs in approximately 2-8% of all pregnancies and accounts for one of the major placental-related pregnancy complications. PE is a complex disease characterised by increased maternal blood pressure and proteinuria during pregnancy and increased risks of fetal growth restriction (FGR) in 12% and preterm birth (PTB) in 20% [33]. Evidence is accumulating that offspring exposed to PE have enhanced risks of increased blood pressure and body mass index in childhood and nearly a double risk of stroke in adulthood [3-6]. Early-onset PE (EOPE) is often more severe than late-onset PE (LOPE) and largely originates from poor first trimester placentation. LOPE seems to be exaggerated by predisposing cardiovascular and metabolic risks for endothelial dysfunction in the second half of pregnancy [3]. It was recently suggested that also LOPE may be associated with trophoblast dysfunction due to villous overcrowding in term placentas, leading to diminished intervillous perfusion and increased hypoxia [13]. Both PE phenotypes show enhanced systemic inflammatory responses resulting in exposure of vessels and tissues to excessive oxidative stress [11].

Impaired placentation is a result of inadequate invasion of the maternal spiral arteries by the trophoblast, and has been suggested to affect placental and fetal growth. A lower placental weight at birth has been shown to predict the risk of hypertension in later life, suggesting an association between placental morphological features and offspring vascular health [61]. The umbilical- cord and fetal vasculature share the same embryonic origin and are derived from intra- and extra-embryonic mesodermal layers [28, 29]. Therefore umbilical cord vessels are often used as a model for the investigation of non-accessible fetal vessels to reflect newborn vascular health [62-66]. These vessels are essential for prenatal transport of oxygen, nutrient-rich and deoxygenated blood and metabolic waste [28, 29]. The development of the umbilical cord is highly influenced by systemic and local haemodynamic conditions of pregnancy, such as blood flow, oxygen tension and oxidative stress [20, 21, 27].

Here we hypothesize that a poor placental development particularly in severe EOPE induces excessive inflammatory responses and changes in the intrauterine haemodynamics, contributing to the remodelling of the umbilical cord and fetal vasculature and resulting in a vascular phenotype of the newborn at

risk for cardiovascular disease in later life. Therefore, the *objective* of our study was to investigate associations between PE and the phenotypes EOPE and LOPE, and placental and umbilical cord vessel morphology as features of placental and newborn vascular health, in which gestational age and birth weight are taken into account.

METHODS

Study design. Between June 2011 and June 2013 mother-child pairs were recruited before delivery and included in a nested case-control study embedded in the Rotterdam periconception cohort (Predict study), an ongoing prospective hospital-based cohort conducted at the Erasmus MC, University Medical Centre Rotterdam, the Netherlands [32]. We selected EOPE and LOPE as cases and uncomplicated pregnancies as controls. In order to reduce confounding by FGR and iatrogenic PTB, we also included FGR and PTB as complicated control groups.

Maternal characteristics. PE was defined according to the International Society for the Study of Hypertension in Pregnancy as gestational hypertension of at least 140/90 mmHg accompanied by an urine protein/creatinine ratio of ≥ 30 mg/mmol arising de novo after the 20th week of gestation [44]. EOPE and LOPE were defined as being diagnosed before and after 34 weeks of gestation, respectively [45]. Uncomplicated control pregnancies were defined as pregnancies without PE, gestational hypertension, FGR or PTB. FGR was defined as an estimated fetal weight below the 10th percentile for gestational age based on ultrasound measurements performed between 20 and 38 weeks gestational age [46]. Birth weight percentiles were calculated using the reference curves of the Dutch Perinatal Registry to validate birth weight < 10th percentile [47]. PTB was defined as a spontaneous delivery between 22 and 37 weeks of gestation [48]. Maternal comorbidity was defined by any concurrent presence of cardiovascular-, endocrine-, metabolic-, auto-immune- and/or renal disease. Women with HIV infection, aged < 18 years, not able to read and understand the Dutch language, multiple birth pregnancies or women with pregnancies complicated by fetal congenital malformations were excluded.

Maternal and neonatal characteristics were obtained from hospital medical records. All women gave written informed consent before participation and parental informed consent was obtained for the child. The research has been carried out in accordance with the Declaration of Helsinki (2013) of the World Medical Association.

Data collection. Macroscopic morphological outcomes including weight, length and width of the placenta and length, diameter, number of vessels and number of coils of the umbilical cord, were performed immediately after delivery. The umbilical coiling index was calculated as the total number of coils divided by the total length of the cord in centimetres. After clamping of the umbilical cord, samples of two centimetres for microscopic morphological examination were obtained next to the clamping site within one hour after delivery and immediately fixed in a 4% formaldehyde solution for paraffin sections. All samples and measurements were obtained by trained researchers according to protocol. Between 00:00h and 07.00h and during weekends, placental measurements were not performed due to logistic constraints.

Umbilical cord sample processing. Formalin-fixed umbilical cord samples were cut in transversal slices of four millimetres, perpendicular to the umbilical cord vessels. The slices were dehydrated in graded ethanol series, cleaned in xylene and embedded in paraffin. Paraffin samples were sectioned at 4 micrometre. Sections were deparaffinised and hydrated, before Haematoxylin/eosin (HE) staining and Elastica Von Gieson (EVG) staining was performed. Sections were digitally scanned using a digital slide scanner (NanoZoomer 2.0-HT, C9600-13, Hamamatsu Photonics, Japan) and analysed using the software NDP.view2, U12388-01 (Hamamatsu Photonics, Japan), IMAGE J version 2.0 (National Institutes of Health, US) and KS400 version 3.0 (Carl Zeiss Vision GmbH, Aalen, Germany).

The following parameters of the umbilical cord were measured in digitised HE stained sections; umbilical cord area, Wharton jelly area, vessel area, vessel lumen area and vessel wall thickness. Every individual area was measured manually with Image J [67]. Vessel wall thickness was measured manually in NDP viewer, as the mean of the smallest and largest wall diameter. Artery wall measurements were performed for both the internal and external muscular layer. EVG stained sections were used for the measurement of the percentage of elastin content in the wall of the umbilical artery and umbilical vein and internal elastic lamina (IEL) of the umbilical vein with KS400. The area of elastic fibres in the vessels was digitally marked and divided by the total vessel area to calculate the percentage of elastin content in the vein and in one artery separately.

All measurements were performed blinded by one researcher. Only sections without artefacts were used for analysis. Accuracy of the digital slices and measurements were checked by an experienced pathologist at the Erasmus MC, University Medical Centre in Rotterdam.

Statistical analysis. For normal distributed maternal and neonatal characteristics

FIGURE 1. Flowchart of the study groups

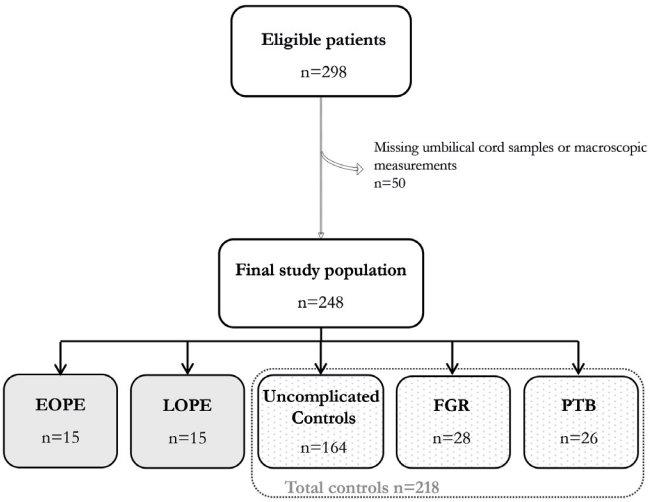

and outcomes of the umbilical cord and placenta Analysis of Variance (ANOVA) was applied to assess overall differences between the groups, followed by the post hoc Dunnett t-test for pairwise comparisons between EOPE, LOPE and uncomplicated and complicated control groups. Kruskall-Wallis was applied to skewed variables, followed by pairwise Mann-Whitney tests for posthoc comparisons.

In the comparisons between PE and the total control group, multivariable linear regression analysis with adjustment for gestational age and birth weight was applied. We additionally applied the multivariable linear regression model to compare EOPE and LOPE with the total control group.

Differences were considered statistically significant at $p < 0.05$. All analyses were performed with Statistical Package for Social Sciences (SPSS, version 21.0, SPSS Inc, Chicago, IL, USA) and logistic regression with SAS version 9.3 (SAS Campus Drive, Cary, NC, USA 27513).

RESULTS

298 women met the inclusion criteria and after exclusion of 50 pregnancies because of missing umbilical cord samples or macroscopic outcomes, 248 pregnancies

remained for further analysis (**Figure 1**). PE cases comprised 15 EOPE and 15 LOPE, and controls included 164 uncomplicated and 54 complicated pregnancies (28 FGR, 26 PTB). Microscopic outcomes were assessed in all EOPE, 14 LOPE, a random selection of 24 uncomplicated- and in 52 complicated control pregnancies.

Maternal and neonatal characteristics are depicted in **Table 1**. Except for the case specific parameters, such as blood pressure, proteinuria, gestational age and birth weight, we observed a higher frequency of nulliparous women in EOPE (80.0%) and LOPE (86.7%) versus uncomplicated controls (40.9%) and PTB (46.2%, overall $p < 0.001$). The frequency of caesarean section was higher in EOPE (80%) compared to LOPE and (un)complicated controls (23.1-37.5%, overall $p = 0.004$). In EOPE, one pregnancy was complicated by FGR (6.7%) versus two in LOPE (13.3%, $p = 1.000$) and all pregnancies were complicated by PTB (100%) versus two in LOPE (13.3%, $p < 0.001$).

Table 2 depicts the results of the multivariable linear regression analyses with gestational age and birth weight adjustments for the associations between the macroscopic morphological placental and umbilical cord outcomes and total PE, EOPE and LOPE versus the total control group. A negative association with placental weight, length and width and umbilical cord length was observed in total PE and EOPE, which attenuated after adjustment for birth weight and gestational age. LOPE was only positively associated with placental width, which remained statistically significant after adjustment for birth weight and gestational age ($p = 0.009$).

Macroscopic morphological outcomes of the placenta and umbilical cord are also depicted in **Supplementary table 1**. In EOPE we observed negative associations with placental weight, length and width and umbilical cord length versus (un)complicated controls (overall $p < 0.001$). In LOPE Dunnett t-testing revealed a significantly higher placental weight compared to FGR, and a higher placental width compared to FGR and PTB complicated controls.

The multivariable linear regression analyses for the microscopic umbilical cord outcomes are depicted in **Table 3**. Since there were no significant differences between the two individual artery measurements, the mean of both measurements was used for further analysis. In PE we revealed a negative association with umbilical cord length, total vessel area, vein area and wall thickness, total artery area, outer artery wall area and artery wall thickness (all $p < 0.05$). After adjustment for gestational age and birth weight, PE remained inversely associated with the vein area (β -1.05, 95% CI -2.05,

TABLE 1. Maternal and newborn characteristics

	Cases		Uncomplicated	Complicated controls		
	EOPE	LOPE	controls	Normotensive FGR	Normotensive PTB	Overall
Maternal characteristics	**(n=15)**	**(n=15)**	**(n=164)**	**(n=28)**	**(n=26)**	**p-value**
Age (years)	30.4 (5.2)	33.3 (4.7)	32.3 (4.9)	29.7 (5.9)	30.9 (5.1)	0.051
Nulliparous, n (%)	12 (80.0)	13 (86.7)	67*† (40.9)	17 (60.7)	12*† (46.2)	<0.001
Geographical origin, n (%)						
Western	13 (86.7)	8 (53.3)	130 (79.8)	18 (64.3)	22 (84.6)	0.172
Non-Western	2 (13.3)	7 (46.7)	33 (20.2)	10 (35.7)	4 (15.4)	
Preconception BMI‡ (kg/m^2)	24.1 (9.1)	24.2 (4.3)	24.1 (7.1)	22.5 (6.2)	23.9 (6.4)	0.620
Smoking in pregnancy (yes), n (%)	2 (15.4)	0 (0.0)	9 (5.7)	2 (7.7)	2 (8.7)	0.549
Co-morbidity (yes), n (%)	1 (6.7)	7 (46.7)	49 (30.1)	7 (25.0)	5 (19.2)	0.115
Neonatal characteristics						
Gender (male), n (%)	5 (33.3)	6 (40.0)	85 (51.8)	15 (53.6)	13 (50.0)	0.622
Gestational age at birth‡ (weeks)	30.7 (3.4)	37.4* (1.9)	39.6*† (1.7)	38.9* (2.6)	35.1*† (6.6)	<0.001
Birth weight‡ (grams)	1185 (435)	3200* (1250)	3560*† (565)	2628*† (593)	2568*† (1674)	<0.001
Birth weight <10th percentile, n (%)	1 (6.7)	2 (13.3)	0† (0.0)	28*† (100.0)	0 (0.0)	<0.001

Data are presented as mean (standard deviation) with corresponding ANOVA testing to examine overall differences between the groups, followed by the post hoc Dunnett t-test for pairwise comparisons between EOPE, LOPE and the uncomplicated and complicated control groups.

Data are presented as number (%) with corresponding Chi^2/Fischer's exact testing. ‡ Skewed data are presented as median (interquartile range) with corresponding Kruskall-Wallis testing and posthoc Mann-Whitney testing. * p <0.05 versus EOPE pregnancies. † p <0.05 versus LOPE pregnancies. *ANOVA* analysis of variance; *BP* blood pressure; *BMI* body mass index; *EOPE* early onset preeclampsia; *LOPE* late onset preeclampsia; *FGR* fetal growth restriction; *PTB* preterm birth.

TABLE 2. Multivariable linear regression analysis of the macroscopic morphology of the placenta and umbilical cord in EOPE and LOPE versus the total control group

	PE (n=30)		EOPE (n=15)		LOPE (n=15)	
	Crude β	Adjusted β (GA+BW)	Crude β	Adjusted β (GA+BW)	Crude β	Adjusted β (GA+BW)
Macroscopy of the placenta						
Weight (gr)	-148.0 (-236, -60)*	34.0 (-31, 98)	-300.1(-408.7,-191.5)*	6.7 (-86.6, 100.1)	41.9 (-81.7, 165.5)	55.5 (-28.8, 139.8)
Length (cm)	-2.38 (-3.84, -0.92)*	-0.52 (-1.99, 0.95)	-3.9 (-5.8, -2.0)*	-0.2 (-2.4, 2.1)	-0.7 (-2.7, 1.3)	-0.8 (-2.6, 1.0)
Width (cm)	-1.51 (-2.85, -0.18)*	0.99 (-0.22, 2.21)	-4.8 (-6.4, -3.2)*	-0.8 (-2.6, 1.0)	2.1 (0.3, 3.8)*	2.0 (0.5, 3.6)*
Macroscopy of the umbilical cord						
Length (cm)	-6.92 (-11.75, -2.08)*	-0.33 (-5.50, 4.84)	-15.6 (-22.1, -9.2)*	-5.2 (-13.4, 3.0)	1.8 (-4.7, 8.4)	-2.4 (-4.0, 8.7)
Diameter (mm)	0.69 (-0.71, 2.09)	1.02 (-0.54, 2.58)	0.2 (-1.8, 2.1)	1.1 (-1.4, 3.6)	1.2 (-0.7, 3.1)	1.1 (-0.7, 3.0)
Coiling index (coils/cm)	-0.01 (-0.04, 0.03)	-0.02 (-0.06, 0.02)	0.0 (-0.0, 0.1)	0.0 (-0.0, 0.1)	-0.0 (-0.1, 0.0)	-0.0 (-0.1, 0.0)

Data are presented as β (95% Confidence Interval) with corresponding multivariate linear regression analysis of both EOPE (on the left) and LOPE (on the right) versus the total control group (*n*=218), crude and with adjustment for gestational age and birth weight. The regression coefficient (β) indicates the increase or decrease (-) change per unit.

* p <0.05. *GA* gestational age; *BW* birth weight; *PE* preeclampsia; *EOPE* early-onset preeclampsia; *LOPE* late-onset preeclampsia. Missings are depicted in Supplementary table 1.

TABLE 3. Multivariable linear regression analysis of the microscopic morphology of the umbilical cord in EOPE and LOPE versus the total control group

	PE (n=29)		EOPE (n=15)		LOPE (n=14)	
	Crude β	Adjusted β (GA+BW)	Crude β	Adjusted β (GA+BW)	Crude β	Adjusted β (GA+BW)
Total cord area (mm^2)	-8.92 (-21.39, 3.55)	-5.17 (-17.77, 7.43)	-12.1 (-28.7, 4.5)	6.9 (-12.5, 26.3)	-5.8 (-22.8, 11.3)	-11.1 (-27.5, 5.3)
Wharton jelly area (mm^2)	-2.53 (-16.00, 10.93)	-1.41 (-15.09, 12.27)	-3.7 (-22.1, 14.7)	12.4 (-9.4, 34.2)	-1.5 (-19.2, 16.1)	-7.3 (-24.1, 9.5)
Total vessel area (mm^2)	-2.01 (-3.49, -0.52)*	-1.25 (-2.64, 0.14)	-3.3 (-5.3, -1.2)*	-0.3 (-2.7, 2.0)	-0.9 (-2.8, 1.1)	-1.6 (-3.4, 0.2)
Total lumen area (mm^2)	-0.10 (-0.50, 0.31)	-0.32(-0.46, 0.39)	-0.4 (-1.0, 0.1)	-0.3 (-1.0, 0.4)	0.2 (-0.3, 0.7)	0.1 (-0.4, 0.7)
Umbilical vein						
Total area (mm^2)	-1.67 (-2.71, -0.63)*	-1.05 (-2.05, 00.04)*	-2.6 (-4.0, -1.2)*	-0.8 (-2.4, 0.9)	-0.7 (-2.1, 0.7)	-1.1 (-2.5, 0.2)
Wall thickness (mm)	-0.19 (-0.29.-0.09)*	-0.15 (-0.26, -0.04)*	-0.3 (-0.4, -0.1)*	-0.1 (-0.3, 0.0)	-0.1 (-0.3, 0.0)	-0.1 (-0.3, -0.0)*
Lumen area (mm^2)	-0.11 (-0.44, 0.23)	0.04 (-0.30, 0.37)	-0.4 (-0.8, 0.0)	-0.1 (-0.6, 0.5)	0.2 (-0.3, 0.7)	0.1 (-0.3, 0.6)
Elastin content %	-0.73 (-1.75, 0.29)	-0.26 (-1.31, 0.78)	-1.2 (-2.6, 0.1)	0.4 (-1.2, 2.0)	-0.2 (-1.6, 1.2)	-0.5 (-1.9, 0.9)
Umbilical artery						
Total area (mm^2)	-0.46 (-0.88, -0.05)*	-0.23(-0.64, 0.18)	-0.7 (-1.3, -0.2)*	-0.0 (-0.7, 0.6)	-0.2 (-0.8, 0.4)	-0.4 (-0.9, 0.2)
External wall layer area (mm^2)	-0.41 (-0.71, -0.11)*	-0.24 (-0.54, 0.06)	-0.6 (-1.0, -0.2)*	-0.2 (-0.6, 0.3)	-0.2 (-0.6, 0.2)	-0.3 (-0.7, 0.1)
Internal wall layer area (mm^2)	-0.14 (-0.29, 0.02)	-0.05 (-0.20, 0.10)	-0.2 (-0.4, -0.0)*	0.1 (-0.2 0.3)	-0.1 (-0.3, 0.2)	-0.1 (-0.3, 0.10)
Wall thickness (mm)	-0.07 (-0.13, -0.00)*	-0.03 (-0.09, 0.03)	-0.1 (-0.2, -0.0)*	0.0 (-0.1, 0.1)	-0.0 (-0.1, 0.0)	-0.1 (-0.1, 0.0)
Lumen area (mm^2)	0.05 (-0.03, 0.13)	0.03 (-0.57, 0.12)	0.1 (-0.0, 0.2)	0.1(-0.1, 0.2)	-0.0 (-0.1, 0.1)	0.0 (-0.1, 0.1)
Elastin content %	-0.06 (-0.90, 0.77)	0.13 (-0.74, 1.00)	-0.1 (-1.3, 1.0)	0.4 (-1.0, 1.8)	0.0 (-1.0, 1.1)	-0.0 (-1.1, 1.1)

Data are presented as β (95% Confidence Interval) with corresponding multivariate linear regression analysis of both EOPE (on the left) and LOPE (on the right) versus the total control group (*n*=76), crude and with adjustment for gestational age and birth weight. The regression coefficient (β) indicates the increase or decrease (-) change per unit.
* p <0.05. *GA* gestational age; *BW* birth weight; *PE* preeclampsia; *EOPE* early-onset preeclampsia; *LOPE* late-onset preeclampsia. Missings are depicted in Supplementary table 2.

FIGURE 2. Microscopic morphological outcomes of the umbilical cord

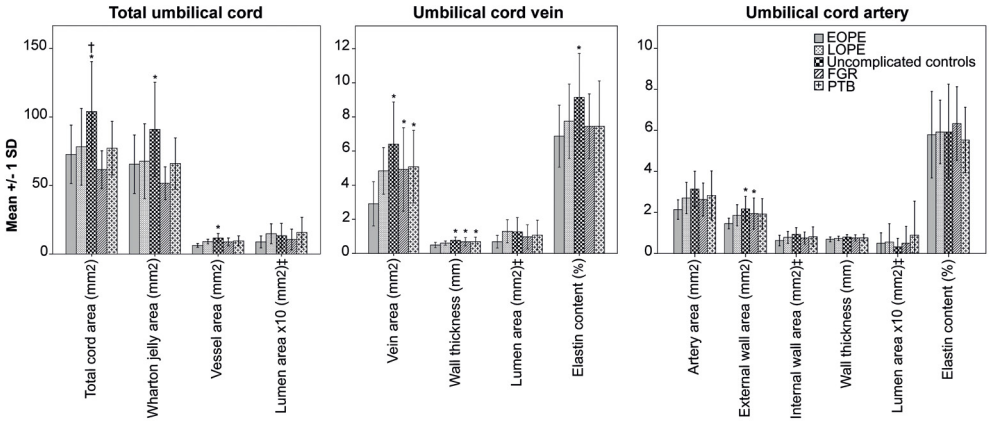

Microscopic morphological outcomes of the umbilical cord are presented as mean (+/- standard deviation) with corresponding ANOVA testing to examine overall differences between the groups, followed by the post hoc Dunnett t-test for pairwise comparisons of EOPE and LOPE with the (un)complicated control groups. ‡ Skewed data are analysed by Kruskall-Wallis testing.
* p <0.05 versus EOPE pregnancies. † p <0.05 versus LOPE pregnancies. *ANOVA* analysis of variance; *EOPE* early onset preeclampsia; *LOPE* late onset preeclampsia; *FGR* fetal growth restriction; *PTB* preterm birth.

0.04, p = 0.041) and vein wall thickness (β -0.15, 95% CI -0.26, -0.04, p = 0.006). EOPE was negatively associated with total umbilical cord vessel area, vein area, wall thickness and artery areas and wall thickness, which attenuated after adjustment for gestational age and birth weight.
A negative association was observed between LOPE and vein wall thickness, only after adjustment for gestational age and birth weight.

In **Figure 2, 3** and **Supplementary table 2**, the microscopic morphological outcomes of the umbilical cord are depicted per group. In EOPE we observed smaller total umbilical cord areas, vein area, wall thickness, external artery wall area and vein elastin content compared to uncomplicated controls. In EOPE vein total area and vein wall thickness were also significantly smaller compared to FGR and PTB (overall p = 0.001 and p = 0.004 respectively). In LOPE we only observed a smaller Wharton jelly area versus uncomplicated controls (p = 0.030).

DISCUSSION

Main findings. This study shows a negative association between the umbilical

FIGURE 3. Microscopic Transversal sections of the umbilical cord in an uncomplicated control (A) and EOPE (B).

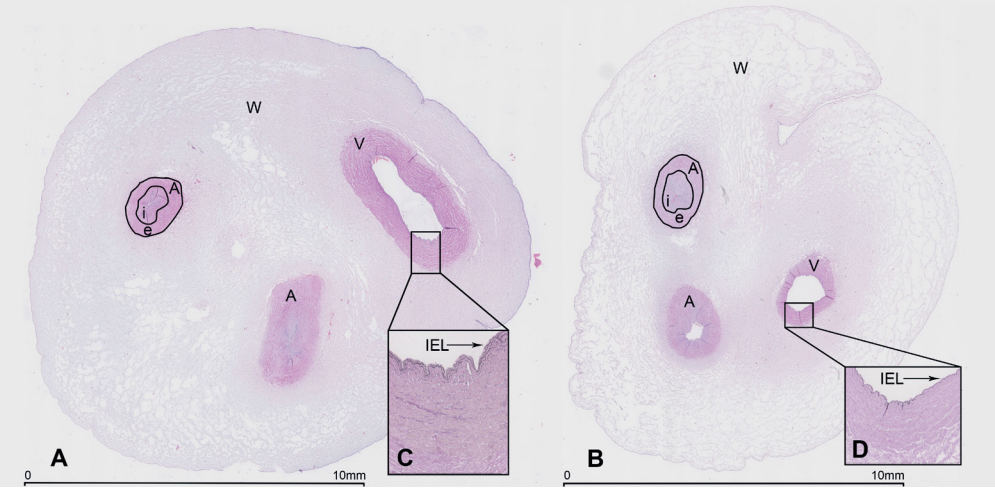

Umbilical cord paraffin section with Haematoxylin Eosin staining. Veins consist of a single layer circular smooth muscle cells and an internal elastic lamina (IEL). The umbilical arteries have a double-layered muscular wall divided in an internal layer of longitudinal smooth muscle cells and an external layer of crossing spiralled smooth muscle cells. Umbilical arteries do not contain an IEL.
A and **B**. Umbilical cord transversal section of an uncomplicated control (A) and EOPE (B) with a smaller vein area versus (un)complicated pregnancies.
C and **D**. Umbilical cord transversal paraffin sections with Elastic Van Gieson staining in an uncomplicated control (C) and EOPE (D) with a lower total vein elastin content versus uncomplicated pregnancies (x5).
W Wharton jelly; *V* vein; *A* artery; *i* internal muscular layer; *e* external muscular layer; *IEL* internal elastic lamina.

vein area and vein wall thickness in the total group of PE pregnancies, independent of gestational age and birth weight. In EOPE, the negative associations with placental weight, length and width and umbilical cord length, vein and artery wall area and wall thickness are largely explained by a shorter gestational age and lower birth weight. This is in contrast to LOPE showing a positive association with placental width and a negative association with umbilical vein wall thickness independent of gestational age and birth weight.

Strengths and limitations. Strengths of our study are that we established different associations between EOPE and LOPE and microscopic morphological outcomes in umbilical cord vessels and independent of FGR and PTB. The digital qualitative elastin measurement-technique is novel and accurate and seems feasible for future examinations.

Interpretation. The different associations observed in EOPE and LOPE with

placental and umbilical cord morphology can partly be explained by a shorter gestational age and lower birth weight in the more severe EOPE phenotype. In addition, the positive association between LOPE and placental width is even opposite to the association with EOPE, as observed by others [68]. Kajantie et al. described an association between a smaller placental width and the risk of PE severity, which is in line with our observation in EOPE suggesting that placental width is a marker of placental development [61]. The discrepancy of placental measurements in EOPE and LOPE may be explained by the concept of initial poor and restricted placental development in EOPE versus microvillous overcrowding in term placentas without prior pathology in LOPE [13].

The association of an approximately twofold smaller vein area and approximately one-and-a-half-fold smaller vein wall thickness in EOPE compared to the total control group was much stronger than in LOPE, but appeared only independent of gestational age and birth weight in LOPE. This may be due to the exposure to maternal cardiovascular and metabolic risk factors associated with LOPE (47% in LOPE versus 7% in EOPE pregnancies). However, in the total PE group we also demonstrated that the EOPE and LOPE subgroups may in fact be underpowered, by revealing a strong significant association with a smaller vein area and wall thickness in PE, independent of gestational age and birth weight. Moreover, the low rate of FGR cases within the EOPE pregnancies indicates that a relatively small number of pregnancies complicated with severe placental dysfunction leading to FGR were included, which cannot exclude that the observed association is underestimated.

We do believe that the significantly smaller vein wall thickness is related to the adverse influences originating from PE itself and possibly the additional complications of PTB and FGR. Both gestational age and birthweight are highly related to the severity and moment of onset of PE, suggesting that the most evident findings are appearing in the most severe EOPE cases, who suffered from excessive oxidative stress from the beginning of pregnancy. PTB and FGR have indeed been associated with alterations of cardiovascular risk factors in offspring [69, 70]. However, as suggested by our data and that of others, the intrauterine PE environment seems to be unique and exacerbates or acts in synergy with any risks inferred by PTB or FGR [7]. During normal fetal development, the morphology of the vessel walls changes due to a thickening of the elastic lamellae of the media [71]. PE however deranges the haemodynamic characteristics of the materno-fetal circulation with fluctuations in shear stress, which affects the fetal vascular development [72, 73]. It

has been shown that umbilical perfusion and elastin content of the umbilical veins are decreased in neonates born after PE [62, 65]. Additionally, episodes of placental hypoxia or reperfusion result in excessive oxidative stress and the production of inflammatory cytokines in both maternal and fetal circulation [51]. A disbalance between angiogenic factors and pro-inflammatory chemokines is associated with maternal endothelial cell dysfunction as pregnancy advances with possible consequences for the structure and content of the vessel walls [3]. In PE pregnancies a reduced prostacyclin production in endothelial cells of the umbilical cord vessels resulting in decreased placental perfusion and umbilical cord blood flow has been observed [74]. This substantiates our finding of the smaller umbilical cord vein wall thickness and tendency of decreased elastin content being related to the haemodynamic fluctuations and excessive oxidative stress.

An overexpression of type III and down regulation of type I collagen has been described in umbilical cord veins, arteries and Wharton jelly of neonates exposed to PE, which decreases solubility (water-binding capacity) and may explain the smaller vessel wall thickness and also the decreased elastin content of the umbilical vein walls [64, 65].

Our findings are consistent with Inan et al., who reported a significant reduction in the umbilical vein and artery wall areas of 70 neonates exposed to PE [63]. In contrast, two smaller studies reported an increased umbilical artery wall thickness, which may be due to differences in the definition of PE and umbilical cord sampling methods (at the placental side instead of next to the umbilical cord clamping site) and sample sizes [62, 66].

Conclusion. Our study suggests that PE is associated with a smaller umbilical cord vein area and wall thickness, independent of gestational age and birth weight, which may be considered as a proxy for early features of disturbed cardiovascular development in the newborn.

Periconceptional follow-up studies are needed to ultimately predict the risk of cardiovascular disease in offspring exposed to PE which may create opportunities for early prediction, prevention and treatment in the future.

SUPPLEMENTARY DATA

SUPPLEMENTARY TABLE 1. Macroscopic morphological outcomes of the placenta and umbilical cord vasculature

	Cases		Uncomplicated	Complicated controls		
	EOPE (n=15)	LOPE (n=15)	controls (n=164)	Normotensive FGR (n=28)	Normotensive PTB (n=26)	Overall p-value
Macroscopy of the placenta						
Placental weight (gr)	309 (95.5)	650* (184)	656* (153)	452*† (97)	494* (198)	<0.001
Placental length (cm)	16.4 (4.0)	19.7* (3.9)	20.9* (2.9)	18.1 (2.1)	19.5* (3.7)	<0.001
Placental width (cm)	12.3 (1.8)	19.2* (4.2)	17.7* (2.4)	15.2*† (2.2)	15.8*† (2.5)	<0.001
Macroscopy of the umbilical cord						
Length (cm)	34.8 (8.2)	52.2* (12.0)	51.2* (12.3)	49.9* (12.5)	45.1* (12.9)	<0.001
Diameter (mm)	12.8 (4.0)	13.9 (2.9)	12.8 (3.5)	11.3 (3.8)	13.3 (4.4)	0.197
Coiling index (coils/cm)	0.23(0.12)	0.15 (0.06)	0.20 (0.08)	0.18 (0.01)	0.20 (0.10)	0.149

Data are presented as mean (standard deviation) with corresponding ANOVA testing to examine overall differences between the groups, followed by the post hoc Dunnett t-test for pairwise comparisons of EOPE and LOPE with the uncomplicated and complicated control groups.

* p <0.05 versus EOPE pregnancies. † p <0.05 versus LOPE pregnancies. *ANOVA* analysis of variance; *EOPE* early-onset preeclampsia; *LOPE* late-onset preeclampsia; *FGR* fetal growth restriction; *PTB* preterm birth.

SUPPLEMENTARY TABLE 2. Microscopic morphological outcomes of the umbilical cord

	Cases		Uncomplicated	Complicated controls		Overall p-value
	EOPE (n=15)	LOPE (n=14)	controls (n=24)	Normotensive FGR (n=26)	Normotensive PTB (n=26)	
Total cord area (mm^2)	71.7 (20.1)	78.0 (26.9)	99.8* (35.1)	68.3 (21.9)	85.0 (24.1)	0.001
Missings	1	0	1	0	1	
Wharton jelly area (mm^2)	65.5 (21.3)	67.7 (27.4)	91.0*† (34.3)	51.7 (11.9)	66.1 (18.7)	<0.001
Missings	4	1	5	5	12	
Total vessel area (mm^2)	6.7 (1.8)	9.1 (1.7)	11.6* (3.3)	8.8 (2.9)	9.3 (3.7)	<0.001
Missings	3	1	5	5	11	
Total lumen area (mm^2)‡	0.8 (0.5)	1.5 (1.2)	1.3 (1.1)	0.8 (1.1)	1.4 (1.7)	0.192
Missings	3	1	5	5	11	
Umbilical Vein						
Vein total area (mm^2)	2.9 (1.3)	4.8 (1.4)	6.4* (2.5)	4.9* (2.4)	5.4* (2.7)	0.001
Missings	1	0	2	1	0	
Wall thickness (mm)	0.47 (0.17)	0.60 (0.12)	0.76* (0.20)	0.68* (0.24)	0.73* (0.32)	0.004
Missings	0	0	1	1	0	
Lumen area (mm^2)‡	0.61 (0.58)	1.30 (0.93)	1.13 (1.01)	0.65 (0.95)	0.90 (1.05)	0.086
Missings	1	0	2	1	0	
Elastin content (%)	5.8 (2.1)	5.9 (1.6)	9.0* (2.5)	7.4 (1.9)	7.5 (2.7)	0.033
Missings	0	0	0	1	1	
Umbilical Artery						
Artery total area (mm^2)	2.2 (0.5)	2.7 (0.8)	3.1 (0.9)	2.8 (1.0)	2.8 (1.2)	0.059
Missings	0	0	1	1	0	
External wall layer area (mm^2)	1.4 (0.3)	1.9 (0.5)	2.2* (0.6)	2.0* (0.9)	1.9 (0.8)	0.018
Missings	0	0	1	1	0	
Internal wall layer area (mm^2)‡	0.62 (0.25)	0.79 (0.29)	0.85 (0.59)	0.71 (0.40)	0.69 (0.64)	0.068
Missings	0	0	1	1	0	
Wall thickness (mm)	0.68 (0.11)	0.74 (0.10)	0.80 (0.13)	0.77 (0.17)	0.76 (0.18)	0.206
Missings	0	0	1	1	0	
Lumen area (mm^2)‡	0.03 (0.08)	0.02 (0.08)	0.03 (0.05)	0.02 (0.07)	0.03 (0.13)	0.437
Missings	0	0	1	1	0	
Elastin content (%)	6.7 (1.8)	7.7 (2.2)	5.9 (2.3)	6.3 (1.8)	5.5 (1.6)	0.686
Missings	1	0	1	2	0	

Data are presented as mean (standard deviation) with corresponding ANOVA testing to examine overall differences between the groups, followed by the post hoc Dunnett t-test for pairwise comparisons of EOPE and LOPE with the uncomplicated and complicated control groups.

‡ Skewed data are presented as median (interquartile range) with corresponding Kruskall-Wallis testing.

* p <0.05 versus EOPE pregnancies. † p <0.05 versus LOPE pregnancies. *ANOVA* analysis of variance; *EOPE* early-onset preeclampsia; *LOPE* late-onset preeclampsia; *FGR* fetal growth restriction; *PTB* preterm birth.

CHAPTER 4

Microcirculation in women with severe preeclampsia and HELLP syndrome: a case-control study

J.M.J. Cornette, E.M. Herzog, E.A.B. Buijs, J.J. Duvekot, D. Rizopoulos, W.C.J. Hop, D. Tibboel, E.A.P. Steegers

British Journal of Obstetrics and Gynaecology, 2014. 121: p. 363–370

ABSTRACT

Objective. To compare microcirculatory perfusion in women with severe preeclampsia against that in healthy pregnant women, and secondly in women with severe preeclampsia with or without HELLP syndrome (haemolysis, elevated liver enzymes, and low platelets).

Design. Case–control study.

Setting. University Hospital Rotterdam, the Netherlands.

Population. Twenty-three women with severe preeclampsia and 23 healthy pregnant controls, matched for maternal and gestational age. Out of the 23 women with severe preeclampsia, ten presented with HELLP syndrome.

Methods. Microcirculation was analysed sublingually by a non-invasive sidestream dark-field imaging device (SDF).

Main outcome measures. Perfused vessel density (PVD), microcirculatory flow index (MFI), and heterogeneity index (HI) were calculated for both small vessels (Ø < 20 μm; capillaries) and non-small vessels (Ø > 20 μm; venules and arterioles).

Results. There were no significant differences between women with severe preeclampsia and healthy controls. Women with preeclampsia and HELLP syndrome showed a reduced PVD ($p = 0.045$), MFI ($p = 0.008$), and increased HI ($p = 0.002$) for small vessels, as compared with women with preeclampsia but without HELLP syndrome.

Conclusions. Sidestream dark-field is a novel, promising technique in obstetrics that permits the non-invasive evaluation of microcirculation. We did not observe major differences in sublingual microcirculatory perfusion between women with severe preeclampsia and healthy pregnant controls. In women with severe preeclampsia, the presence of HELLP syndrome is characterised by impaired capillary perfusion.

INTRODUCTION

The microcirculation is a vast network of small vessels with a diameter below 100 μm. It consists of arterioles that regulate flow to the capillaries, which subsequently drain in venules [75]. Exchange of oxygen and nutrients occurs at the level of the capillaries, which mainly consist of a thin layer of endothelium. With the availability of new imaging modalities, the importance of microcirculatory perfusion in the pathophysiology, prognosis, and treatment of conditions with profound haemodynamic imbalance, like sepsis, shock, and cardiac disease, is emerging. Parameters of microcirculatory perfusion seem independent of global haemodynamic status and appear to be strong predictors of outcome [75-80]. Sidestream dark-field (SDF) imaging is a novel technique enabling direct, non-invasive visualisation of microcirculatory perfusion at the bedside in adults, children, and newborns [75-77]. Severe preeclampsia is characterised by a maternal haemodynamic instability caused by generalised endothelial dysfunction [3]. Many of its symptoms and complications strongly suggest microcirculatory dysfunction. A recent study indicates that capillary rarefaction precedes the clinical onset of preeclampsia [81]. HELLP syndrome (haemolysis, elevated liver enzymes, and low platelets) is considered an expression of disease severity [82, 83]. Although its exact pathophysiology is not completely understood, the haemolysis, platelet consumption, and liver cell necrosis might reflect a more profound disturbance in microcirculatory function. Our aim was to explore the potential and reliability of SDF in pregnant women, and to analyse microcirculatory perfusion in women with severe preeclampsia as compared with that in healthy pregnant women. Secondly, we investigated the influence of HELLP syndrome on microcirculation in women with severe preeclampsia.

MATERIALS AND METHODS

Study setting. The study was conducted from November 2009 to September 2012 at the department of Obstetrics and Prenatal Medicine of the Erasmus Medical Centre of the University of Rotterdam. Twenty-three women with severe preeclampsia were included. In ten of these women, preeclampsia was complicated by HELLP syndrome. Four women with severe preeclampsia had a history of systemic lupus erythematosus or chronic hypertension. Twenty-three healthy pregnant women, matched for maternal and gestational age, were included as controls. Informed consent was obtained from all women and the study protocol was approved by the local medical ethical committee.

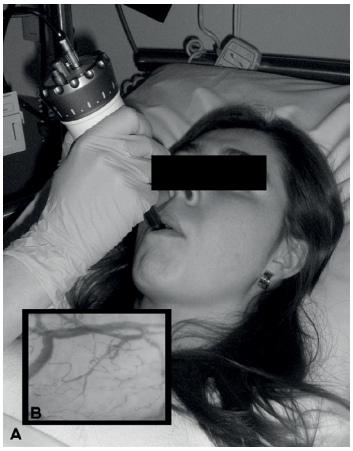

FIGURE 1. Set-up for a sublingual microcirculatory perfusion measurement with SDF. A disposable sterile plastic cap covers the mouthpiece of the probe (A). A frozen video-clip image of sublingual microcirculation as viewed with SDF (B).

Severe preeclampsia was defined as preeclampsia (hypertension and significant proteinuria) with severe hypertension, and/or with symptoms, and/or with biochemical and/or haematological impairment [84]. HELLP syndrome was defined as the presence of at least two components of either haemolysis (lactate dehydrogenase, LDH ≥ 600 U/l), elevated liver enzymes (aspartate aminotransferase, AST ≥ 70 U/l), or thrombocytopenia (thrombocytes < 100 × 10^9/l) [83]. All women with severe preeclampsia were categorised into severe preeclampsia either with or without HELLP syndrome according to previous definitions after expert agreement by three of the authors (J.C., E.H., and J.D.). Women with severe preeclampsia were managed according to our local protocol, as described in **Appendix S1**.

In women with severe preeclampsia we aimed to perform microcirculatory analysis at time points when disease activity was estimated to be maximal and when the interference from treatment was estimated to be as minimal as possible. Therefore, measurements were performed either before intravenous nicardipine, magnesium sulphate bolus, or when laboratory abnormalities consistent with HELLP syndrome occurred, irrespective of other concomitant medication. Age, parity, body mass index (BMI), gestational age, and medical history were obtained for all women.

All measurements were performed in a 15° left lateral tilt. Women were asked to refrain from eating or drinking for 30 minutes before measurements. Blood pressure was determined by manual sphygmomanometry. LDH, AST analysis, and thrombocyte count, as well as haematocrit and haemoglobin counts,

were performed as part of the routine clinical procedure in women with severe preeclampsia on the day of the measurements.

Sidestream dark-field imaging. The sublingual microcirculation was visualized using SDF (**Figure 1A**) [85]. This hand-held video microscope (MicroScan; MicroVision Medical, Amsterdam, the Netherlands) emits stroboscopic green light (530 nm) from an outer ring of light-emitting diodes (LEDs), which penetrates the tissue to a depth of approximately 3 mm. The light is absorbed by the haemoglobin of individual red blood cells in superficial vessels. A negative image is transmitted back, after 5× optical magnification, to an isolated synchronised charge-coupled device camera in the core of the probe. This allows high-contrast video images of circulating erythrocytes to be recorded with a 286× magnification from the microcirculation of organs covered with a thin epithelial layer. (**Figure 1B**) [79]. SDF imaging has been validated against and found to be superior to intravital videomicroscopy [75, 85].

The consensus recommendations on how to best obtain and evaluate SDF measurements were followed [78, 86]. After obtaining good image focus and contrast, with specific attention paid to avoiding pressure artefacts by assuring continuous venous perfusion, one investigator (E.H.) recorded three high-quality video clips per measurement, with a duration of at least 20 seconds, each at a different sublingual site (using a high-definition videocassette recorder: GV-HD700; Sony Instruments, Tokyo, Japan).These were digitalised, blinded, and stored on an external hard drive. After completion of the data set, E.H. performed analysis of the blinded recordings using ava 3.0 (Automated Vascular Analysis, MicroVision Medical, Amsterdam, the Netherlands).

Inter-observer variability was assessed though separate analysis of the 45 recordings of 15 randomly selected cases by a different investigator (E.B.).

As described in the consensus recommendations, the perfused vessel density (PVD), microcirculatory flow index (MFI), and the heterogeneity index (HI) for MFI were calculated, each reflecting distinctive characteristics of microcirculatory perfusion [78, 86]. Each parameter was determined separately for both small vessels ($\emptyset < 20\ \mu m$, capillaries) and non-small vessels ($20\ \mu m \leq \emptyset \leq 100\ \mu m$, mostly venules and arterioles) [86-88]. A detailed description of these parameters and respective methods of calculation is available in **Appendix S2**.

Statistical analysis. Statistical analysis was performed with spss 20.0 (SPSS Inc., Chicago, IL, USA). Variables were tested for normality and compared with the Students' *t*-test or non-parametric Mann–Whitney *U*-test, as appropriate. The effect of parameters with a known potential to influence haemodynamics

FIGURE 2. Bland–Altman plots showing interobserver agreement for PVD in small and non-small vessels.

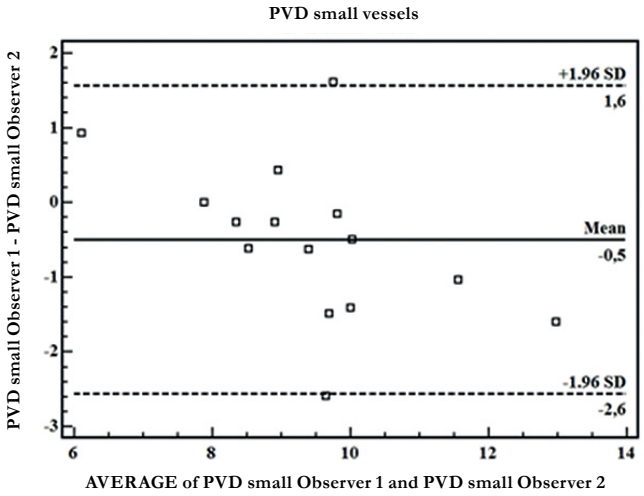

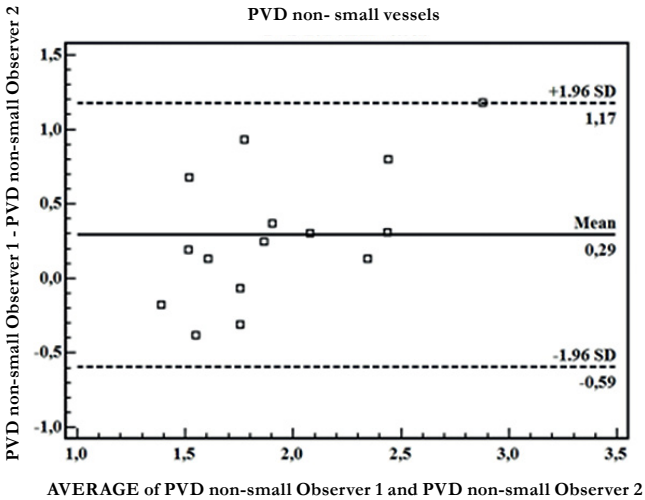

(gestational age, use of oral antihypertensive medication), vascular structure (maternal age, BMI, race), or SDF measurements (haematocrit, haemoglobin) was assessed by analysis of covariance (ancova) or by its non-parametric variant (the Quade test), as appropriate [89-93]. The adjusted *p-value*s, with $P \leq 0.05$ (two-sided) as the limit of significance, were used without correction for multiple comparisons.

Inter-observer reliability was assessed by calculation of the intraclass correlation coefficients from each parameter (PVD, MFI, and HI), separated for small- and non-small vessels in 15 cases. Inter-observer agreement for PVD was shown in Bland–Altman plots.

In the absence of SDF data on microcirculatory perfusion in pregnancy and severe preeclampsia, no power calculation was performed and this study was undertaken as an exploratory pilot.

RESULTS

Adequate recordings and measurements were obtained for all participants. Intraclass correlation coefficients were good for capillary measurements and were moderate for larger vessels **(Table 1). Figure 2** shows the inter-observer agreement for PVD in small and non-small vessels. Twelve women with severe preeclampsia received concomitant oral antihypertensive medication. This included women with and without HELLP syndrome. All received methyldopa, nifedipine, or a combination of both. One woman received additional oral labetalol. The baseline characteristics of women with severe preeclampsia and healthy controls were similar **(Table 2)**. As expected, blood pressure was significantly higher in women with severe preeclampsia. Preeclampsia was considered to be severe in all women either because of the severity of their hypertension (systolic blood pressure, SBP, ≥ 160 mmHg and/or diastolic blood pressure, DBP, ≥ 110 mmHg) or because of the presence of HELLP. Baseline characteristics between women with severe preeclampsia, with or without HELLP, were also comparable, except for the components of HELLP syndrome (**Table 2**).

Women with HELLP syndrome had significantly lower values of PVD and MFI and significantly higher values of HI for small vessels, as compared with women with severe preeclampsia without HELLP (**Figure 3A, B**). These differences remained significant after adjusting for haemoglobin count, haematocrit, BMI, medication use, pre-existent disease, maternal age, and gestational age.

TABLE 1. Intraclass correlation coefficients (ICCs) and 95% CIs for inter-observer reliability

ICC (95% CI)	PVD	MFI	HI
Small vessels	0.87 (0.61–0.96)	0.94 (0.77–0.98)	0.96 (0.84–0.99)
Non-small vessels	0.66 (0.05–0.89)	0.88 (0.63–0.96)	0.73 (0.15–0.91)

TABLE 2. Population characteristics

Characteristics	Severe preeclampsia (n = 23)	Controls (n = 23)	P
Severe preeclampsia versus control pregnancies			
Nulliparous	54.5%	45.5%	ns
Gestational age (weeks) a	33 (21–37)	33 (20–38)	nt
Age (years)	31 (±5)	31 (±5)	nt
BMI a	28 (20–56)	26 (18–41)	ns
Systolic blood pressure (mmHg) a	170 (130–2015)	110 (99–135)	<0.001
Diastolic blood pressure (mmHg) a	102 (76–115)	68 (50–90)	<0.001
Characteristics	**With HELLP (n = 10)**	**Without HELLP (n = 13)**	**P**
Severe preeclampsia with or without HELLP syndrome			
Nulliparous	50%	54%	ns
Gestational age (weeks) a	30 (21–37)	33 (25–37)	ns
Age (years)	31.1 (±3.9)	31.7 (±6.5)	ns
BMI a	26 (20–32)	30 (20–56)	ns
Systolic blood pressure (mmHg)	157 (±31)	174 (±20)	ns
Diastolic blood pressure (mmHg)	96 (±12)	102 (±7)	ns
Oral antihypertensive medication	40%	69%	ns
LDH (U/l) a	850 (602–2964)	426 (265–575)	<0.001
AST (U/l) a	221 (42–1593)	23 (14–52)	<0.001
Thrombocytes (10^9/l) a	99 (41–289)	250 (134–375)	<0.001

ns, not significant; nt, not tested (matching criterion). Values are expressed as means ± standard deviations or medians with ranges according to normality.
a Non-parametric test used.

DISCUSSION

Main findings. In this study we explored microcirculatory perfusion in women with severe preeclampsia with SDF, a novel technique in obstetrics. Microcirculatory research has mainly been hampered by technological limitations. SDF allows the direct recording of high-contrast images and assessment of different aspects of microcirculatory perfusion. In our study, satisfactory images were obtained at the bedside and with minimal discomfort in all women. Inter-observer variability showed good reliability for capillary vessels, but is less evident in non-small vessels given the wide confidence intervals for PVD and HI, despite acceptable intraclass correlation coefficients. These findings are in line with previous results in non-pregnant populations [78, 88, 94, 95]. Fortunately previous research and our results suggest that the capillary compartment is the main area of interest in microcirculatory perfusion. Therefore, SDF seems a preferred method for microcirculatory analysis in obstetrics [75]. Nevertheless, although image recording is relatively straightforwards, offline analysis still requires substantial human input and remains time consuming. Developments in the most recent version of the SDF camera now permit automatic image analysis, which will further improve reliability, and holds promise for bedside recording and analysis in the future.

Despite the increased blood pressure we did not observe any difference in microcirculatory parameters in women with severe preeclampsia, as compared with healthy pregnant controls. Apparently, the major macrocirculatory disturbances of severe preeclampsia are not reflected in significant differences in sublingual microcirculatory perfusion. Interestingly, when comparing women with severe preeclampsia with or without HELLP syndrome, we observed significant differences in all aspects of capillary perfusion, with a decrease in PVD and MFI and an increased HI in women with HELLP syndrome.

Interpretation and relation to other studies. Previous microcirculation studies described a decreased venular diameter and increased postcapillary (venular) resistance in women with preeclampsia using intravital microscopy and plethysmography [96, 97]. Although we did not specifically asses changes in vessel diameters and used different techniques in different organ systems, we did not observe major changes in large vessels, which mostly consist of venules and arterioles to a lesser extent. Hasan, using intravital capillaroscopy, reported a reduced capillary density in 11 women with preeclampsia, as compared with normal healthy pregnant and non-pregnant women [98]. Houben, using a similar set-up, could not confirm these findings, and Vollebregt, using orthogonal polarisation spectral imaging (OPS), did not find any changes in nail fold capillary

FIGURE 3. Scatter plots (A) and box plots (B) depicting differences in PVD, MFI, and HI for small and non-small vessels between women with severe preeclampsia and controls, as well as between women with severe preeclampsia with and without HELLP syndrome.

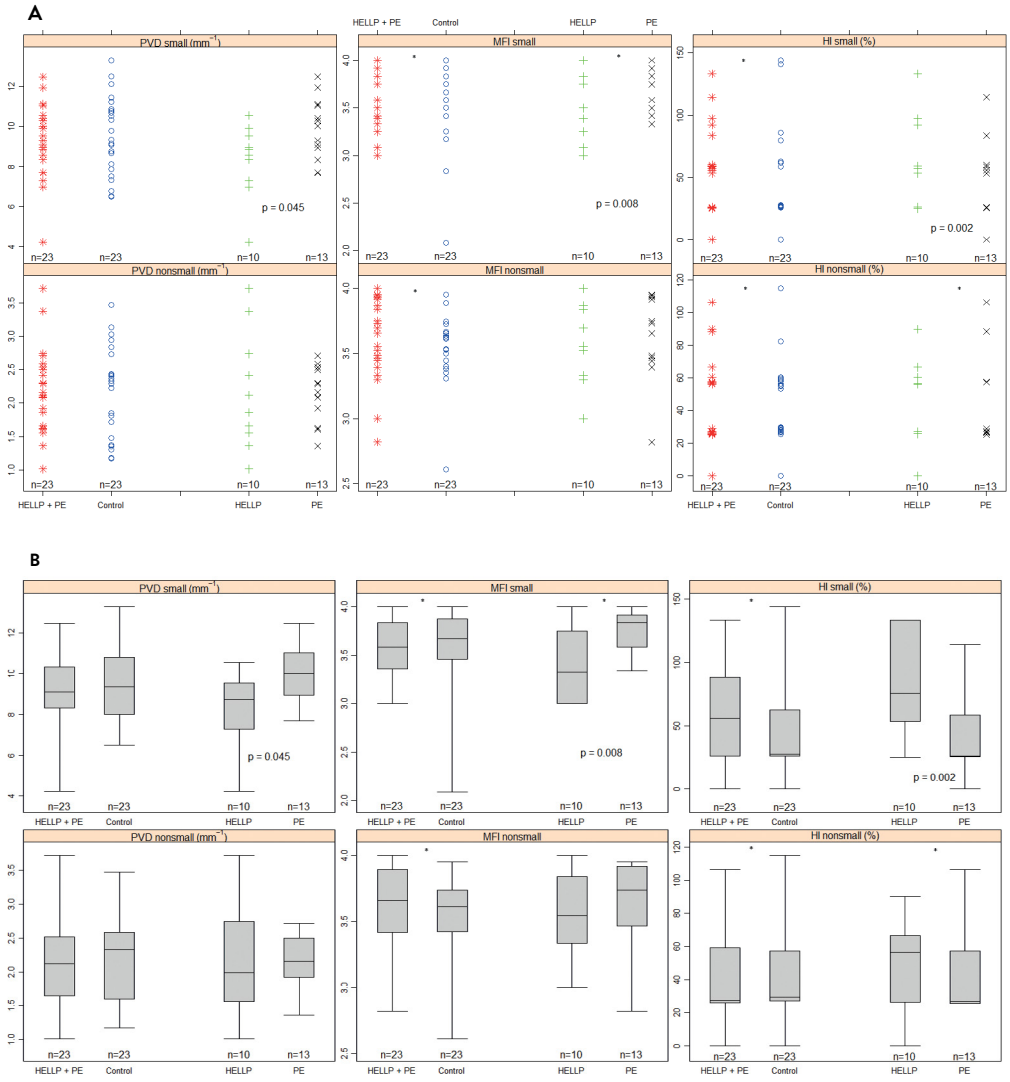

Boxes denote interquartile ranges, bars in boxes represent median values, and error bars represent ranges. *Non-parametric test used. Adjusted P values are depicted for comparisons with statistical significant difference. PVD Perfused vessel density; MFI microcirculatory flow index; HI and heterogeneity index; HELLP, severe preeclampsia with HELLP syndrome; PE, severe preeclampsia without HELLP syndrome.

red blood cell velocity [97, 99]. Neither did we observe any changes at a capillary level between women with severe preeclampsia and healthy pregnant women. This discrepancy may be explained by the use of medication in women with preeclampsia, as Hasan performed the measurements before any intervention. Most women in our, Vollebregt's, and Houben's studies had already received some form of antihypertensive therapy, magnesium sulphate, or steroids for fetal lung maturation. These drugs have the potential to influence capillary perfusion [100]. In further studies, attempts should be made to perform measurements before any treatment; however, this remains difficult, as the maternal condition often does not permit treatment delay in severe preeclampsia.

The suggestion of impaired capillary perfusion in women with both preeclampsia and HELLP syndrome might explain some aspects of the pathophysiology of HELLP syndrome [83]. The reduced PVD and MFI might be a reflection of microvascular erythrocyte fragmentation and platelet adherence to the damaged endothelial surface in narrowed capillaries [101]. The increased heterogeneity could explain the diffuse pattern of liver cell necrosis in HELLP, where fibrin microthrombi and fibrinogen deposits are often observed both in intact hepatic sinusoids and in areas with hepatocellular necrosis upon histology [82]. Heterogeneity of flow is an important characteristic of impaired microcirculation [75, 78]. With heterogeneous flow, a reduced number of capillaries are perfused. Cells close to the capillaries extract the normal quantity of oxygen, but cells too far away become hypoxic. Although the total oxygen delivery is the same, heterogeneous perfusion probably affects tissue oxygenation more than a reduced but homogenous flow.

Future research. Sublingual microcirculation is easily accessible for SDF. It is representative in sepsis, probably because of the embryological and metabolic similarities with the splanchnic mucosa [75, 78]. Even so, preeclampsia is a complex syndrome that groups a broad clinical spectrum with variable degrees of organ dysfunction. It is therefore questionable whether the endothelial dysfunction is always manifested equally in all vascular beds. Our results, both in women with and without HELLP, could be explained by the fact that the sublingual microcirculation may not be the most representative site in all pre-eclamptic women. SDF enables microvascular analysis in different areas (e.g. skin, conjunctiva, nail fold, vagina, cervix, etc.). Further research in obstetrics should explore microcirculatory perfusion at various sites during the haemodynamic adaptation of normal pregnancy, and explore eventual representative areas in pathological conditions.

Besides facilitating (patho) physiological research in larger populations, future improved versions with rapid bedside analysis also offer perspectives for clinical implications. As in sepsis and cardiogenic shock, microcirculatory perfusion analysis has the potential to improve outcome prediction, and assist in the selection of candidates for expectant management or monitoring of medical treatment [80, 102].

Strengths and limitations. This is the largest population of women with preeclampsia investigated for microcirculatory changes in a prospective, case-controlled design. Our control group of 23 pregnant women is also one of the largest investigated populations of healthy subjects using SDF. The significant capillary differences in women with HELLP syndrome seem supported by a large effect size. Although it remains controversial whether this exploratory set-up allows for adjustment, significant differences remained, irrespective of adjustment for confounding factors. The absence of clinically relevant spread in the 95% confidence intervals of most parameters suggest that the size of our population was probably sufficient to exclude differences in sublingual microcirculation between healthy women and women with preeclampsia. Still, the populations remain small and this study should merely be viewed as an exploratory analysis. Our results certainly need further confirmation in a larger trial, separating women with and without HELLP syndrome, and preferably before any intervention.

Conclusion. Sidestream dark-field (SDF) imaging is a promising technique for the study of microcirculatory perfusion in obstetrics. Our study indicates that there are no major differences in sublingual microcirculatory perfusion between women with severe preeclampsia and healthy pregnant controls; however, HELLP syndrome is associated with an impairment of all aspects of capillary perfusion.

SUPPLEMENTARY DATA

Appendix S1. Description of local clinical management protocol for severe pre-eclampsia.

Antihypertensive therapy with oral medication aimed at blood pressure control within safety limits. Intravenous nicardipine was started in case of hypertensive emergency (systolic blood pressure (SBP) ≥ 160 mmHg or diastolic blood pressure (DBP) ≥ 110 mmHg). Magnesium sulphate was administered for seizure prophylaxis in women with hypertensive emergencies, with signs and symptoms of imminent eclampsia or with HELLP syndrome. Fetal lung maturation as induced with steroids before 34 weeks. No steroid treatment for HELLP syndrome or plasma volume expansion occurred.

Appendix S2. Description of microcirculatory perfusion parameters and respective methods of calculation.

PVD was obtained by multiplying the vessel density by the proportion of perfused vessels. The calculation is based on the principle that density is proportional to the number of vessels crossing 3 horizontal and 3 vertical equidistant lines drawn on the screen. Vessel density was calculated as the number of vessels crossing these lines divided by the length of these lines. Perfusion at the crossings was visually scored: 0 = absent flow, 1 = intermittent flow or 2 = continuous flow. The proportion of perfused vessels was calculated as follows: 100 × (total number of vessels – (no flow + intermittent flow)) / total number of vessels. PVD is a good reflection of functional capillary density. For the calculation of MFI an SDF clip was divided in 4 quadrants. The predominant type of flow, characterised as absent, intermittent, sluggish, normal or hyperdynamic, was determined in each quadrant and averaged for all three measurements. The MFI describes the predominant flow pattern of the microcirculatory perfusion. Finally, heterogeneity of microcirculatory perfusion was calculated from the MFI scores of each quadrant of all three sublingual recordings by subtracting the lowest score from the highest score divided by the mean score.

CHAPTER 5

Tissue-specific DNA methylation profiles in newborns (Clinical Epigenetics, 2013. 5: p. 8-12)

CHAPTER 6

The tissue-specific aspect of genome-wide DNA-methylation in newborn and placental tissues: implications for epigenetic epidemiologic studies (submitted)

CHAPTER 7

Early- and late-onset preeclampsia and the tissue-specific epigenome of the placenta and newborn (Placenta, 2017. 58: p. 122-132)

CHAPTER 8

DNA hypomethylation of placental growth factor and decreased SAM:SAH ratio in placental tissue of preeclampsia-complicated pregnancies (submitted)

PART 02

EPIGENETIC STUDIES

CHAPTER 5

Tissue-specific DNA methylation profiles in newborns

E.M. Herzog, J.M. Galvez, A.J.M. Roks, L. Stolk, M.M.P.J. Verbiest, P.H.C. Eilers, J.J. Cornelissen, E.A.P. Steegers, R.P.M. Steegers-Theunissen

Clinical Epigenetics, 2013. 5: p. 8-12.

ABSTRACT

Background. Epidemiological studies demonstrate that fetal growth restriction and low birth weight affect long-term health. Derangements in tissue-specific epigenetic programming of fetal and placental tissues are a suggested underlying mechanism of which DNA methylation is best understood. DNA methylation has been mostly investigated in DNA from white blood cells. To improve baseline understanding of tissue-specific DNA methylation, we examined variation in DNA methylation profiles of the imprinted fetal growth genes *IGF2* and *H19* in three different tissues from the same newborn obtained at the same time.

Findings. We obtained DNA from umbilical cord blood mononuclear cells (MNC), i.e., CD34+ and CD34- (n = 6), the fetal side of the placenta (n = 5) and umbilical cord Wharton jelly (n = 5). DNA methylation of *IGF2* differentially methylation region *(DMR)* and *H19 DMR* was measured using quantitative mass spectrometry. ANOVA testing showed no statistical difference between total mean methylation of CD34+ and CD34- MNC. Further comparisons were made with the pooled total MNC fraction. Mean *IGF2 DMR* methylation of Wharton jelly (p-value 0.001) was 1.3 times higher than mean methylation of the pooled MNC. Placental mean methylation was 0.8 times lower (p-value <0.001) and Wharton jelly 0.9 times lower (p-value <0.001) than the pooled MNC of *H19 DMR*.

Conclusion. Our study shows that the total MNC fraction is a rather homogeneous cell population for methylation studies of imprinted genes in umbilical cord blood white blood cells. However, these blood cells may not always reflect the methylation levels of *IGF2* and *H19* in other organs.

BACKGROUND

The prenatal period is critical for adverse pregnancy outcome and chronic diseases in adulthood [103]. Epigenetic programming of fetal and placental tissues is a suggested underlying mechanism, of which DNA methylation is best understood [26, 104].

DNA methylation profiles are tissue-specific in somatic and germ line tissues [26, 105, 106]. This is important in the tissue-specific regulation of cellular differentiation and lineage maintenance [107-109]. However, human methylation profiles are mostly performed in DNA from an easily accessible, heterogeneous white blood cell population. DNA methylation studies often select imprinted loci as candidate genes, because DNA methylation levels at these loci were assumed to be comparable in different tissues. Recent literature, however, has questioned this assumption [26, 110, 111]. The imprinted *IGF2-H19* gene complex, involved in placental, embryonic and fetal growth and development, has been described extensively in this context. Both genes are located near each other and are reciprocally imprinted [112]. It was demonstrated in mice that placental *Igf2* knockout results in fetal growth restriction, whereas *H19* silencing leads to fetal overgrowth [113, 114]. In human, the phenotype related to the silencing of *IGF2* is Silver Russell Syndrome and *H19* silencing is related to Beckwith Wiedemann Syndrome [110].

From this background, we aimed to improve the baseline understanding of tissue-specific variation in DNA methylation profiles of the imprinted genes *IGF2* and *H19*, and therefore examined umbilical cord blood mononuclear cells (MNC), placental tissue and Wharton jelly derived from the umbilical cord. The rationale for selecting these tissues is that they are easily accessible, MNC consist of a rather homogeneous population of white blood cells, and placental and umbilical cord tissues are involved in fetal programming and development. Moreover, morphological abnormalities in these tissues are related to pregnancy complications, in which epigenetic derangements might be involved [22, 62, 63, 66]. To examine a possible methylation difference between MNC subpopulations, CD34+ and CD34- fractions were also analysed separately.

MATERIALS AND METHODS

Maternal, pregnancy and child characteristics. In this study we analysed samples of 6 pregnancies. Median maternal age was 30.5 years (range: 23.8-37.3) and median parity was 0.5 (0-2). All pregnancies were uncomplicated, except 1 gestational hypertension (peak blood pressure: 140/90 mmHg). Deliveries were at term and spontaneously, median birth weight was 3,303 grams (2,795-3,975). 2 Out of 6 newborns were male. Samples were collected after written informed

TABLE 1. Characteristics of primers per gene

	Forward Primer	Reverse Primer	Base pair length (bp)	Position	CpG sites (no.)
IGF2 DMR	aggaagagagTGGATAGG AGATTGAGGAGAAA	cagtaatacgactcactatagggagaa ggctAAACCCCAACAAAAA CCACT	338	Chr. 11: 2169458-2169796	7
H19 DMR	aggaagagagGGGTTTGG GAGAGTTTGTGAGGT	cagtaatacg actcactatagggagaagg ctATACCT ACTACTCCCTA CCTACCAAC	413	Chr. 11: 2019371-2019784	20

NCBI build: 37. Tags in lower case

consent was obtained before delivery at the Erasmus MC, University Medical Centre Rotterdam, the Netherlands. Ethical approval was given by the Erasmus MC, University Medical Centre Research Ethics Board (MEC-2004-227).

Sample collection. Immediately after delivery of the newborn with the placenta still in situ, umbilical cord blood (n = 6) was collected in cord blood collection bags containing 21 mL anticoagulant Citrate Phosphate Dextrose-solution (CPD). Placenta (n=5) and umbilical cord (n=5) were collected within 10 minutes after delivery of the placenta. Samples of 0.5 cm^3 were taken from the fetal side of the placental villi at 4 different sites in a 3 cm radius around the umbilical cord insertion, after carefully removing the membranes and 2 mm of the top placental layer. Wharton jelly from the umbilical cord was isolated in pieces of 0.5 cm^2 avoiding the umbilical cord vessels. Tissues were frozen immediately in liquid nitrogen and stored at -80°C until DNA extraction. All samples were collected by two researchers.

Blood cell separation. Umbilical cord blood was processed within 48 hours after collection. Using Ficoll gradient centrifugation, the MNC fraction was obtained and washed. CD34+ MNC were isolated from this pool by magnetic-activated cell separation (MACS) using "Direct CD34 Progenitor Cell Isolation Kit" (MACS Miltenyi Biotec, 130-046-702) according to manufacturer's protocols. The remaining cells were collected and further analysed as CD34- MNC.

DNA extraction. Placental and Wharton jelly tissues were grinded on liquid nitrogen and lysed overnight at 55°C using cell lysis buffer. Subsequently, genomic DNA was extracted from all tissues using the Gentra Puregene Tissue Kit (Qiagen, Hilden, Germany), following manufacturer's instructions.

DNA methylation measurement. The amplicons for *IGF2* and *H19* were described previously [115]. The amplicon for *IGF2* is located in the *IGF2 DMR*,

upstream of exon 1 of *IGF2*. For *H19,* the amplicon partly overlaps a CpG island, which is part of the *H19 DMR,* upstream of exon 1 of *H19*. **Table 1** shows the location, length and primers of the amplicons. Firstly, the amplicons were tested on a standard curve constructed from DNA with low and high methylation (EpigenDx, Worcester, MA, USA) at stages of 10% methylation difference. Only amplicons with a good distribution of the methylation percentages were used for measurements of the samples.

Isolated genomic DNA (500 ng) was treated with sodium bisulphite for 16 hours using the EZ-96 DNA methylation kit (Shallow) (Zymo Research, Irvine, CA, USA). This was followed by PCR amplification, reverse transcription, fragmentation and analysis on a mass spectrometer (Sequenom, Inc, San Diego, USA). This generated mass signal patterns that were translated into quantitative DNA methylation levels per CpG site by Mass ARRAY EpiTYPER Analyzer software (v1.0, build1.0.6.88 Sequenom, Inc, San Diego, USA) [116]. Fragments containing one or more CpG sites were called CpG units. Measurements were done in triplicate on DNA from the same bisulphite-treatment batch on different PCR-plates. On every bisulphite plate, standard DNA with low, 25%, 50%, 75% and high methylation was included.

Data cleaning. During quality control (QC), CpG units with a very low mass or very high mass or CpG units with overlapping RNA fragments were excluded from further analysis. Two out of three of the replicate measurements per CpG unit had to be successful, and the standard deviation (SD) of the duplicates or triplicates had to be ≤0.10 to be included in the statistical analysis. CpG units with interference of single-nucleotide polymorphisms were also excluded (dbSNP134). After QC, 3 CpG units for *IGF2 DMR* and 9 for *H19 DMR* remained for further analysis.

Statistical analysis. Possible batch-effects were ruled out by comparing means of the standards per bisulphite-plate and PCR plate with ANOVA-testing. To analyse total methylation per gene and per individual CpG unit between tissues, ANOVA-testing was used, followed by pair-wise comparisons. We adjusted the total methylation per gene for the number of CpG units.

We checked and confirmed the normal distribution by visual inspection of the residuals. Several individual CpG sites showed significant differences in variance of DNA methylation. We excluded one patient and 4 CpGs from further testing for *H19 DMR* to deal with this variation. ANOVA was finally performed on 3 CpG units of *IGF2 DMR* and 5 CpG units of *H19 DMR*.

Firstly, we analysed CD34+ and CD34- MNC separately, followed by a weighted pooled total MNC fraction after these 2 fractions appeared not statistically

TABLE 2. Mean absolute methylation level (SD) of the different tissues per gene and per CpG site

	CD34+ MNC (SD)	CD34- MNC (SD)	Pooled MNC (SD)	placental tissue (SD)	Wharton jelly (SD)
IGF2 DMR (total)	**0.55 (0.14)**	**0.50 (0.13)**	**0.50 (0.13)**	**0.54 (0.16)**	**0.65 (0.13)†***
IGF2 DMR CpG 3	0.59 (0.05)	0.52 (0.02)	0.52 (0.02)	0.59 (0.07)	0.66 (0.07)†
IGF2 DMR CpG 4	0.64 (0.18)	0.59 (0.18)	0.59 (0.18)	0.58 (0.25)	0.77 (0.11)
IGF2 DMR CpG 6.7	0.43 (0.06)	0.39 (0.03)	0.39 (0.03)	0.44 (0.03)	0.52 (0.06)†
H19 DMR (total)	**0.30 (0.02)**	**0.31 (0.02)**	**0.31 (0.02)**	**0.25 (0.02)†**	**0.28 (0.03)†***
H19 DMR CpG 2	0.28 (0.01)	0.29 (0.01)	0.29 (0.01)	0.26 (0.01)	0.27 (0.04)
H19 DMR CpG 9.10	0.31 (0.01)	0.31 (0.02)	0.31 (0.02)	0.26 (0.03)	0.30 (0.04)
H19 DMR CpG 12	0.28 (0.02)	0.29 (0.01)	0.29 (0.01)	0.23 (0.02)†	0.26 (0.02)†
H19 DMR CpG 13	0.30 (0.01)	0.31 (0.01)	0.31 (0.01)	0.24 (0.01)†	0.28 (0.03)
H19 DMR CpG 17	0.34 (0.02)	0.35 (0.01)	0.35 (0.01)	0.25 (0.03)†	0.31 (0.03)*

ANOVA testing between the different tissue groups. Bonferroni correction was applied to all p-values to adjust for multiple comparisons. † p-value <0.05 versus pooled MNC (Pairwise comparisons), * p-value <0.05 versus placenta (Pairwise comparisons)

differently methylated. The original CD34+ and CD34- data was pooled in a 1:100 distribution, comparable to the biological appearance of CD34+ cells in an umbilical cord blood MNC fraction. Bonferroni correction was applied to correct for multiple comparisons. All tests were performed using means of the data in triplicate. Statistical analysis was performed in SPSS version 17.0.2.

RESULTS

The mean methylation of CpG sites of the *IGF2 DMR* and the *H19 DMR* are depicted in **Table 2**. *IGF2 DMR* and *H19 DMR* methylation of CD34+ and CD34- MNC were not statistically different, neither the total mean methylation per amplicon nor the individual CpG units. Therefore, further comparisons were made with the weighted pooled total MNC fraction as a reference group. The mean *IGF2 DMR* methylation of Wharton jelly (p-value 0.001) was statistically significantly higher than the mean methylation of MNC. This was similar in two out of the three individual *IGF2 DMR* CpG units.

The mean *H19 DMR* methylation of both placenta (p-value <0.001) and Wharton jelly (p-value <0.001) was statistically significantly lower than of MNC. This was similar in one out of five individual *H19 DMR* CpG units and only applied

to placenta in two other CpG units. Wharton jelly was statistically significantly higher methylated than placenta in *IGF2 DMR* (p-value 0.032) and *H19 DMR* (p-value <0.001), as well as one individual *H19* CpG unit (**Table 2, Figure 1**).

CONCLUSION

This study provides a basic understanding of tissue-specific variation in DNA methylation of two imprinted genes in easily accessible tissues. The total MNC fraction of CD34+ and CD34- appears rather homogeneous for DNA methylation analysis of these genes in umbilical cord blood. The observed between-tissue methylation differences seem to be small and could be explained by either consistently higher and lower methylation, or by differences in sensitivity of tissues to environmental exposures, fetal and maternal factors. This needs further investigation in a larger sample size and therefore only careful conclusions should be drawn from this data.

Thus, umbilical cord blood MNC are useful and easily accessible to study associations between epigenetic programming and pregnancy course and outcome, but not always exactly reflect the methylation levels of other organs.

FIGURE 1. Mean absolute DNA methylation levels per CpG site for *IGF2 DMR* and *H19 DMR*

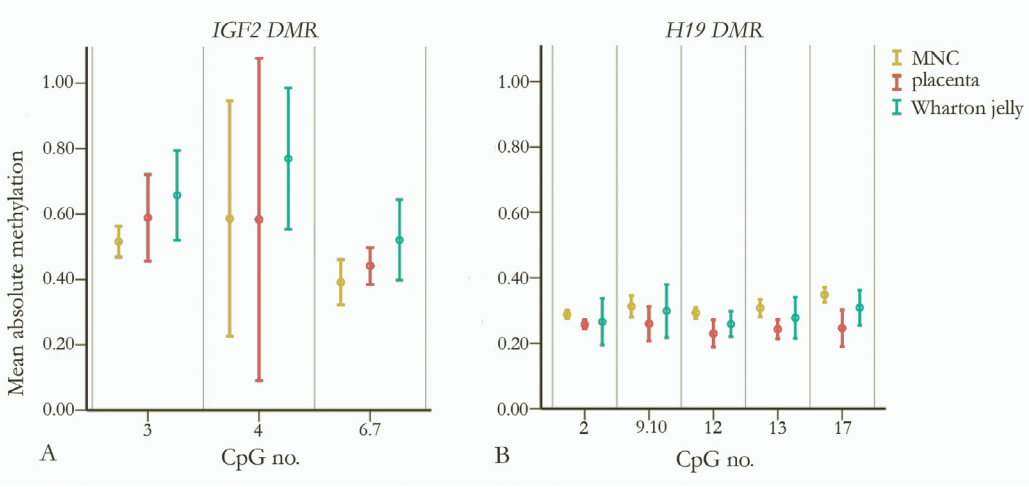

Error Plots of mean methylation levels (coloured dots) of all individuals +/- 2 standard deviations (coloured bars) shown for each CpG unit for each of the three tissues separately for (A) *IGF2 DMR* and (B) *H19 DMR*.

CHAPTER 6

The tissue-specific aspect of genome-wide DNA methylation in newborn and placental tissues: implications for epigenetic epidemiologic studies

E.M. Herzog, A.J. Eggink, S.P. Willemsen, R.C. Slieker, J.F. Felix, A.P. Stubbs, P.J. van der Spek, J.B.J. van Meurs, B.T. Heijmans, R.P.M. Steegers-Theunissen

Submitted

ABSTRACT

Epigenetic programming is essential for lineage differentiation, embryogenesis and placentation in early pregnancy. DNA methylation is the most investigated epigenetic mechanism mainly examined in DNA derived from white blood cells, with little knowledge of its validity to other tissues of interest. Therefore, we investigated the tissue-specificity of epigenome-wide DNA methylation in newborn and placental tissues.

Umbilical cord white blood cells (UC-WBC n=25), umbilical cord blood mononuclear cells (UC-MNC n=10), human umbilical vein endothelial cells (HUVEC n=25) and placental tissue (n=25) were obtained from 36 uncomplicated pregnancies. Genome-wide DNA methylation was measured by the Illumina HumanMethylation450K BeadChip.

Using UC-WBC as reference tissue, we identified 3,595 HUVEC tissue-specific differentially methylated regions (tDMRs) and 11,938 placental tDMRs. Functional enrichment analysis showed that HUVEC- and placental tDMRs were involved in embryogenesis, vascular development and regulation of gene-expression. No tDMRs were identified in UC-MNC.

The extensive amount of genome-wide HUVEC and placental tDMRs underlines the relevance of tissue-specific approaches in future epigenetic association studies, or the use of validated representative tissues for a certain disease of interest, if available. HUVEC may serve as an accessible vascular tissue for studying associations between prenatal exposures and vascular-related pregnancy outcomes and diseases, with epigenetics as underlying mechanism.

INTRODUCTION

Adverse influences during early prenatal development are associated with an increased risk of cardiovascular, metabolic and neurodevelopmental dysfunction in child- and adulthood, which is in line with the 'Developmental Origins of Health and Disease' paradigm (DOHaD) [1]. These associations are potentially mediated by epigenetic mechanisms [1]. Epigenetic reprogramming is essential during early embryonic development and placentation, when active and passive demethylation takes place immediately after fertilization, followed by *de-novo* methylation at the late morula-stage [117, 118].

Epigenetic epidemiological studies are essential to elucidate the role of DNA methylation in the associations between prenatal exposures and health in later life. Most studies however focus on DNA methylation levels in white blood cells as surrogate tissue, because the target tissue of interest is not easily accessible in human studies [119]. In 1983 it was demonstrated in rodents and followed by many other studies that DNA methylation is established in a tissue-specific manner and as such responsible for lineage differentiation [24-26]. Recently, this has been addressed in epigenome-wide analyses of DNA methylation with attempts to identify differentially methylated positions (DMPs) and regions (DMRs) associated with tissue-specificity or disease [120-122].

The rationale for the investigation of tissue-specificity is that disturbed epigenetic programming of embryonic and extra-embryonic tissues may underlie some of the adverse pregnancy outcomes and diseases, such as preeclampsia and offspring born small for gestational age, which are associated with increased cardiovascular and metabolic disease risks in the life course. Tissue-specificity is best studied in newborn tissues since postnatal environmental exposures affecting DNA methylation can be excluded [123]. The placenta is an essential extra-embryonic organ for embryonic and fetal growth and development. The epigenetic programming of the placenta is involved in the regulation of fetal demands and intrauterine conditions [30]. To examine the newborn vasculature as target tissue of linking prenatal exposure to future vascular health, umbilical vein endothelial cells (HUVEC) are the best accessible representative tissue. During initial embryonic development and differentiation, the development of these cells is also highly regulated by various epigenetic mechanisms, influenced by external exposures and the local haemodynamic conditions of the pregnancy [20, 21, 27]. One of the challenges of whole blood epigenetic studies is the variation in blood cell mixtures as potential confounder for DNA methylation differences [124]. This can be investigated by comparing DNA methylation levels between umbilical cord

FIGURE 1. Flowchart of the sample distribution in the study population.

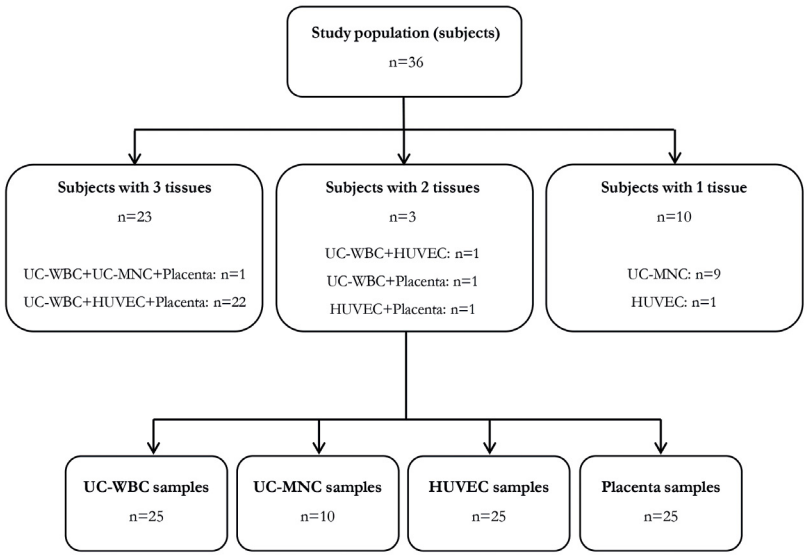

UC-WBC umbilical cord blood white blood cells; *UC-MNC* umbilical cord blood mononuclear cells; *HUVEC* human umbilical vein endothelial cells

white blood cells (UC-WBC) and a subgroup without granulocytes: mononuclear cells (UC-MNC).

Against this background, the objective of this study was to examine the tissue-specificity of placental tissue, HUVEC and UC-MNC in comparison to the widely-used UC-WBC as representative tissue, in order to ultimately increase the use of validated representative tissues for diseases of interest in future epigenome-wide association studies (EWAS).

RESULTS

Tissues from 36 uncomplicated control pregnancies were studied derived from a nested case-control study embedded in The Rotterdam Periconceptional Cohort [32]. From 23 pregnancies we obtained UC-WBC, HUVEC and placental samples, and in four pregnancies one or two tissues were obtained (**Figure 1**). Nine pregnancies provided UC-MNC samples only. This resulted in 25 UC-WBC, 10 UC-MNC, 25 HUVEC and 25 placental samples.

Maternal and newborn characteristics of the four tissue-groups are

shown in **Table 1** and were overall comparable. The mean age of the women was 32 years and 83% were of Western geographic origin. Newborns were born at a mean gestational age of 40 weeks and 58% were male. In the UC-MNC tissue group, comorbidity was present in 10% of the pregnancies and the mean newborn birth weight was 3,352 grams versus the other tissue-groups presenting with comorbidity in 24 to 28% and a mean birth weight around 3800 grams.

tDMP identification. Genome-wide DNA methylation data revealed an overall bimodal distribution (**Figure 2**). In UC-WBC, UC-MNC and HUVEC, only a small amount of cytosine-guanine dinucleotides (CpGs) demonstrated methylation levels around 50%, in contrast to a relatively large amount of CpGs with around 50% methylation in placental tissue. Most annotated regions demonstrated median methylation levels between 50 and 85%, except for CpG islands and proximal promotor regions, which revealed lower median methylation levels of around 10% (**Supplementary table 1**).

Hierarchical cluster analysis using all CpGs revealed clustering of the three different tissues (UCB, HUVEC and placenta) (**Supplementary figure 1**). No distinctive clusters were identified for the two different UCB cell fractions. This is also depicted in the heatmap based on the clustering of methylation according to CpG and sample (**Figure 3**). On an epigenome-wide level we identified tissue-specific CpG methylation using UC-WBC as reference tissue. We observed 1,636 (0.4%) differentially methylated CpGs between UC-WBC and UC-MNC, 193,945 (43%) between UC-WBC and HUVEC and 333,061 (73%) between UC-WBC and placental tissue (all false discovery rate (FDR)-adjusted $p < 0.05$). Those statistically differentially methylated CpGs with an additional effect-size > 1.3 in M-value (logit2 of the β-value: ~ Δ 20% β-value), were defined as tissue-specific differentially methylated positions (tDMPs). This revealed 2 ($4x10^{-6}$ %) MNC-tDMPs, 49,979 (11%) HUVEC tDMPs and 126,482 (28%) placental tDMPs, in comparison to UC-WBC (**Figure 4a, Supplementary table 2**). We provided a Supplementary Table with all tDMPs observed in UC-MNC, HUVEC and placenta, including CpG-identifiers, β-values and p-values (**Supplementary table 3**). A partial replication demonstrated a strong correlation between the estimates (β) for the tissue-effect in our own dataset and the Δ β methylation differences of HUVEC and placenta versus UC-WBC of three independent datasets for all our tDMPs ($r=0.94$ in HUVEC samples and $r=0.98$ in placental samples, $p < 0.0001$) (**Supplementary figure 2**).

CpG-density- and gene-centric enrichment of tDMPs. To evaluate whether tDMPs were enriched in certain genomic annotations, CpG island- and gene-

TABLE 1. Maternal and newborn characteristics of uncomplicated control pregnancies (n=36)

Maternal characteristics	UC-WBC (n=25)	UC-MNC (n=10)	HUVEC (n=25)	Placenta (n=25)	Overall (n=36)
Age (years)	31.8 (5.4)	32.1 (4.7)	31.9 (5.4)	31.8 (5.3)	31.8 (5.1)
Nulliparous, n (%)	7 (28.0)	3 (30.0)	8 (32.0)	8 (32.0)	11 (30.6)
Ethnicity, n (%)					
Western geographic origin	20 (80.0)	9 (90.0)	20 (80.0)	20 (80.0)	30 (83.3)
Non-Western geographic origin	5 (20.0)	1 (10.0)	5 (20.0)	5 (20.0)	6 (16.7)
Preconceptional BMI (kg/m^2)	24.9 (4.4)	23.4 (3.1)	24.9 (4.4)	24.7 (4.5)	24.3 (4.0)
Smoking during pregnancy (yes), n (%)	0 (0.0)	0 (0.0)	0 (0.0)	0 (0.0)	0 (0.0)
Co-morbidity (yes), n (%)	6 (24.0)	1 (10.0)	7 (28.0)	7 (28.0)	8 (22.2)
Newborn characteristics					
Male gender, n (%)	14 (56.0)	5 (50.0)	16 (64.0)	14 (56.0)	21 (58.3)
Gestational age at birth* (weeks)	39.9 (1.9)	39.8 (1.9)	39.9 (1.7)	39.9 (1.9)	39.7 (1.1)
Birth weight (grams)	3,815 (396)	3,352 (377)	3,811 (364)	3,788 (398)	3,691 (418)

Data are presented as mean (standard deviation) or number (%).
* Non-parametric data are presented as median (interquartile range). No statistical testing has been performed due to overlapping pregnancies between the tissue-groups.
BMI body mass index; *UC-WBC* umbilical cord white blood cells; *UC-MNC* umbilical cord blood mononuclear cells; *HUVEC* human umbilical vein endothelial cells.

centric annotations of HUVEC and placental tDMR genes were examined (**Figure 5**, **Supplementary table 4**). tDMP annotation relative to CpG islands showed that tDMPs were significantly enriched in CpG shores, shelves and especially in non-CpG island regions (non-CPG-island OR^{HUVEC} 2.02, 95% CI 1.98-2.06, $OR^{Placenta}$ 1.54, 95% CI 1.52-1.56) and strongly depleted in CpG islands (CpG island OR^{H} 0.47, 95% CI 0.47-0.48, OR^{P} 0.27, 95%CI 0.26-0.27). Both annotation patterns were concordant for HUVEC- and placental tDMPs.

tDMPs were significantly enriched in all gene-centric regions except for a strong depletion of tDMPs in proximal promotors (Odds ratio $(OR)^{HUVEC}$ 0.55, 95% Confidence Interval (CI) 0.54-0.57, $OR^{Placenta}$ 0.49, 95% CI 0.48-0.50). The strongest placental enrichment was observed in intergenic regions. HUVEC' strongest enrichment was observed in gene bodies (**Figure 5**, **Supplementary table 4**).

A combined gene- and CpG-island annotation of tDMPs is depicted in **Supplementary table 5** and in **Supplementary figure 3**. A prominent depletion of tDMPs in proximal promotors due to a strong underrepresentation of tDMPs in CpG-island proximal promotors was observed ($OR^{Placenta}$ 0.21, 95%CI 0.21-0.22, OR^{HUVEC} 0.12, 95%CI 0.11-0.12). The combined annotation enrichment analysis

also revealed opposite annotation patterns for HUVEC and placental tDMPs, mainly in various gene-centric regions situated in CpG-islands and CpG-shelves.

tDMR identification. To obtain a more robust measure of genomic regions with a large proportion of tissue-specific sites, we used the tDMPs to generate tDMRs with DMRfinder. This revealed 3,595 HUVEC tDMRs with a mean length of 639 basepairs (bp) and 11,938 placental tDMRs with a mean length of 894 bp. The numbers of overlapping HUVEC and placental tDMRs are presented in **Figure 4b**. **Supplementary figure 4** shows that HUVEC and placental tissue demonstrate a similar distribution of tDMRs over the genome, without a clear preference towards certain genomic regions.

Gene-ontology (GO)-term enrichment of tDMR genes. To gain insight in tDMR functional categories, tDMRs were mapped to their nearest gene. This yielded 2,882 unique (without duplicate genes) HUVEC genes and 7,629 unique placental genes. The 2,882 HUVEC tDMR genes mapped to 2,296 genes in The Database for Annotation, Visualization and Integrated Discovery (DAVID), because the remaining annotations were mainly transcripts. The 2,296 genes were enriched for involvement in embryogenesis, regulation of gene expression, cell motility and vascular development. The top 3,000 placental tDMR genes were selected based on the regions with the largest absolute mean value of each tDMP M-value difference within the DMR, to meet the maximum number of genes for the Functional Annotation Clustering tool in DAVID. After excluding transcripts, DAVID mapped 2,208 placental tDMR genes and revealed enriched GO term involvement in embryogenesis, regionalisation and regulation of gene expression. HUVEC and placental highest significantly enriched GO terms are presented in **Table 2**.

Qiagen Ingenuity Pathway Analysis (IPA) of tDMR genes. Ingenuity software mapped 2,523 of the 2,881 HUVEC tDMR genes and identified enriched canonical pathways. Top-ranked pathways were mainly involved in immune response processes. We further conducted network analyses, using Fischer's Exact test, revealing that the top networks were mainly associated with cellular function, movement and signalling, immune response and embryonic development.

Out of 7,629 placental tDMR genes, 6,333 were mapped by Ingenuity, demonstrating top 5 enriched pathways involved in a broad spectrum of cell-signalling processes and embryonic stem cell pluripotency. The top networks were mainly associated with cardiovascular disease, embryonic development and cellular movement and function. The highest significantly enriched HUVEC and placental pathways and networks are presented in **Table 3**.

FIGURE 2. Density plot of mean methylation β-values per tissue.

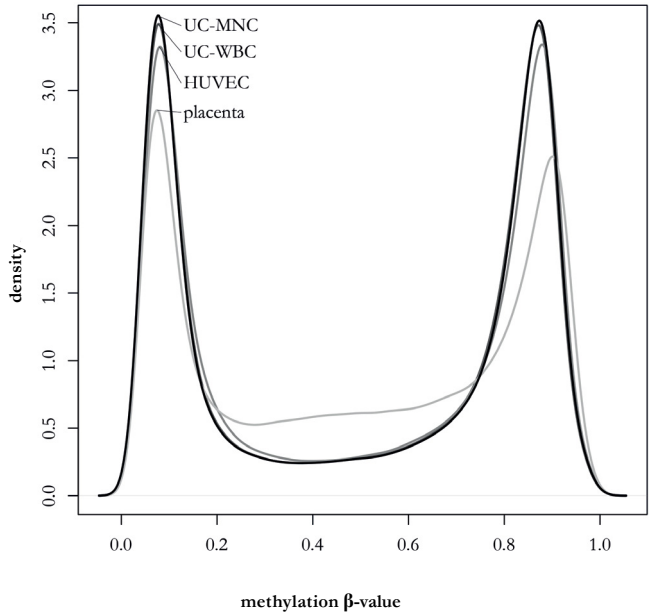

Genome-wide DNA methylation data revealed an overall bimodal distribution of methylation levels. In addition, the placenta demonstrated a larger amount of CpGs with methylation levels around 50%, in contrast to the other tissues. *UC-WBC* umbilical cord blood white blood cells; *UC-MNC* umbilical cord blood mononuclear cells; *HUVEC* human umbilical vein endothelial cells; *CpGs* cytosine-guanine dinucleotides.

FIGURE 3. Heatmap based on clustering of methylation (β-value) of all differentially methylated CpGs.

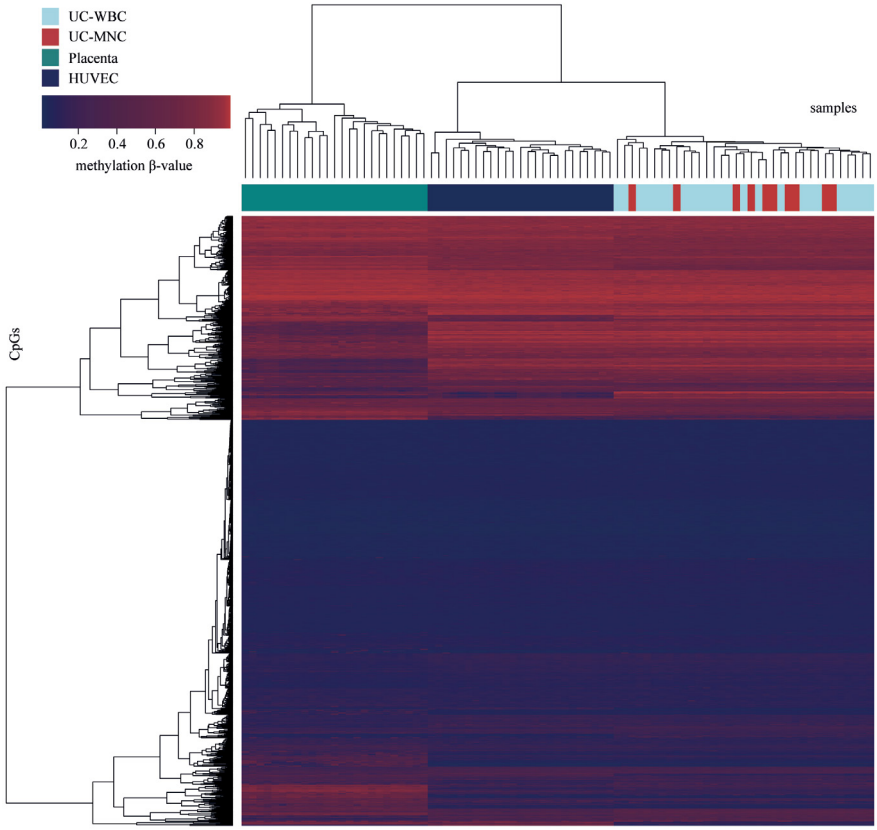

Samples are depicted on the horizontal axis and CpGs on the vertical axis. Samples cluster by tissue type, without distinctive clustering for the two different UCB cell fractions. β-Values are depicted for a better biological understanding of the figure.
UC-WBC umbilical cord white blood cells; *UC-MNC* umbilical cord blood mononuclear cells; *HUVEC* human umbilical vein endothelial cells.

FIGURE 4. Venn diagram of the number of unique and overlapping HUVEC and placental tDMPs (A) and tDMRs (B), relative to UC-WBC.

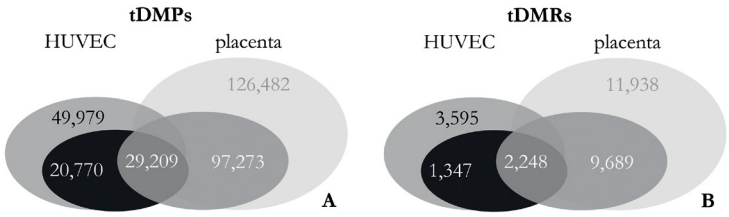

tDMPs tissue-specific differentially methylated positions; *tDMRs* tissue-specific differentially methylated regions; *HUVEC* human umbilical vein endothelial cells.

FIGURE 5. HUVEC and placental- tDMP enrichment in the CpG-density (A) and gene-centric (B) annotation, in comparison to UC-WBC.

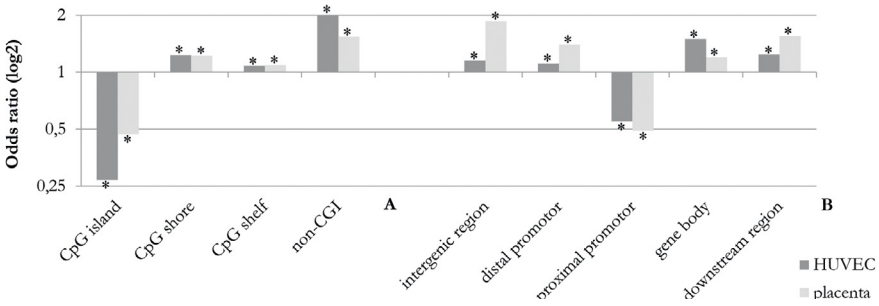

A. tDMP annotation relative to CpG islands showed that tDMPs were significantly enriched in CpG shores, shelves and especially in non-CpG island regions and strongly depleted in CpG islands. Annotation patterns in relation to CpG islands were concordant for HUVEC- and placental tDMPs.
B. tDMP annotation relative to genes, demonstrated that tDMPs were significantly enriched in all gene-centric regions except for a strong depletion of tDMPs in proximal promotors. The strongest placental enrichment was observed in intergenic regions. HUVEC' strongest enrichment was observed in gene bodies. * $p<0.05$. non-CGI *non*-CpG island; *HUVEC* human umbilical vein endothelial cells.

TABLE 2. Top 10 DAVID GO Functional annotation clusters of HUVEC and placental tDMR nearest genes

HUVEC	Annotation Cluster Enrichment score
1. Embryonic morphogenesis	8.4
2. Negative regulation of gene expression	8.4
3. Positive regulation of gene expression	8.3
4. Cell motility	7.6
5. Vascular development and morphogenesis	7.1
6. Embryonic development	7.1
7. Haematopoiesis	7.0
8. Inflammatory response	6.7
9. Bone development	5.7
10. Cell adhesion	5.1
Placenta	**Annotation Cluster Enrichment score**
1. Embryonic development	13.9
2. Embryonic morphogenesis	12.9
3. Regionalisation	11.7
4. Negative regulation of gene expression	10.7
5. Embryonic organ development	9.3
6. Regulation of transcription	8.9
7. Embryonic development and morphogenesis	8.5
8. Positive regulation of gene expression	8.3
9. Cellular morphogenesis	8.3
10. Cell motility	7.2

HUVEC and placental tDMRs were mapped to the nearest gene using Ensembl annotations from UCSC database. Assigned Ensembl genes were uploaded to the DAVID tool to examine possible enrichment of corresponding GO terms using the GO_BP_FAT annotation category. Fisher Exact was applied to measure the gene-enrichment of annotated GO terms of the uploaded gene list, against the whole human genome list as a background. To focus on the biology of the annotated GO terms, clusters of similar annotations were examined from the DAVID Functional annotation Clustering table tool. The clustering algorithm is based on the hypothesis that similar annotations have similar gene members, resulting in a Group Enrichment Score to rank their biological significance, which is based on the Fisher Exact p-values of each GO term within the cluster. The higher the enrichment score, the more enriched. *tDMRs* tissue-specific differentially methylated regions; *DAVID* Database for Annotation, Visualization and Integrated Discovery; *HUVEC* human umbilical vein endothelial cells.

TABLE 3. Top 10 Ingenuity networks and pathways of HUVEC and placental tDMR nearest genes

HUVEC Canonical pathways	**-log p-value**
1. Dendritic Cell Maturation	4.48
2. Antigen Presentation Pathway	4.48
3. T Helper Cell Differentiation	4.48
4. Role of NFAT in Regulation of the Immune Response	4.48
5. PKCθ Signalling in T Lymphocytes	4.48
6. iCOS-iCOSL Signalling in T Helper Cells	4.48
7. OX40 Signalling Pathway	4.05
8. Hepatic Fibrosis / Hepatic Stellate Cell Activation	4.04
9. Altered T Cell and B Cell Signalling in Rheumatoid Arthritis	3.23
10. Allograft Rejection Signalling	3.11
HUVEC networks	**Score**
1. Behaviour, Reproductive System Development and Function, Cellular Function and Maintenance	31/35
2. Cell-To-Cell Signalling and Interaction, Inflammatory Response, Lipid Metabolism	31/35
3. Cellular Function and Maintenance, Inflammatory Response, Digestive System Development and Function	29/34
4. Cellular Movement, Immune Cell Trafficking, Cell Morphology	27/33
5. Skeletal and Muscular System Development and Function, Embryonic Development, Organismal Development	25/32
6. Infectious Diseases, DNA Replication, Recombination, and Repair, Gene Expression	25/32
7. Glomerular Injury, Organismal Injury and Abnormalities, Renal Fibrosis	25/32
8. Cell-To-Cell Signalling and Interaction, Haematological System Development and Function, Immune Cell Trafficking	23/31
9. Cell Signalling, Molecular Transport, Vitamin and Mineral Metabolism	23/31
10. Connective Tissue Development and Function, Skeletal and Muscular System Development and Function, Tissue Development	23/31
Placenta Canonical pathways	**-log p-value**
1. G-Protein Coupled Receptor Signalling	5.18
2. Glutamate Receptor Signalling	5.14
3. Neuropathic Pain Signalling In Dorsal Horn Neurons	5.02
4. Human Embryonic Stem Cell Pluripotency	5.02
5. cAMP-mediated signalling	5.01
6. Regulation of the Epithelial-Mesenchymal Transition Pathway	5.01
7. Axonal Guidance Signalling	4.78
8. Transcriptional Regulatory Network in Embryonic Stem Cells	4.43
9. Hepatic Fibrosis / Hepatic Stellate Cell Activation	4.26
10. Antigen Presentation Pathway	3.38

continues on next page

continuing from previous page

Placenta networks	Score
1. Cardiovascular Disease, Organismal Injury and Abnormalities, Reproductive System Disease	21/35
2. Cellular Movement, Cell Morphology, Cellular Assembly and Organization	21/35
3. Cardiovascular Disease, Cellular Movement, Developmental Disorder	21/35
4. Cell-To-Cell Signalling and Interaction, Cellular Function and Maintenance, Embryonic Development	21/35
5. Cell Death and Survival, Cellular Compromise, Neurological Disease	21/35
6. Cardiovascular System Development and Function, Small Molecule Biochemistry, Connective Tissue Development and Function	19/34
7. Cell Death and Survival, Infectious Diseases, Inflammatory Disease	19/34
8. Haematological System Development and Function, Organismal Functions, Cell-To-Cell Signalling and Interaction	19/34
9. Cellular Movement, Cell Death and Survival, Cardiovascular System Development and Function	19/34
10. Connective Tissue Disorders, Cancer, Gastrointestinal Disease	19/34

canonical pathways were calculated using the Fisher's Exact test and subjected to Benjamini-Hochberg procedure for controlling FDR ($p<0.05$). Networks were generated based on network eligible molecules, which were encoded by our DMP genes and also interact with other molecules in the Ingenuity Pathways Knowledge Base. A high score for a network indicates a more approximate fit between network eligible molecules and the molecules that constitute the network, calculated using the right-tailed Fisher's Exact test.
tDMRs tissue-specific differentially methylated regions; *HUVEC* human umbilical vein endothelial cells.

DISCUSSION

This epigenome-wide DNA methylation study shows 43% HUVEC- and 73% placental tissue-specific DNA methylation out of all measured CpGs, in comparison to UC-WBC. Enrichment of tDMPs was demonstrated in gene bodies and non-CpG-islands. No tDMRs were observed in UC-MNC compared to UC-WBC.

The more pronounced identification of placental compared to HUVEC tDMRs might be explained by the time-point of placental-specific development. After fertilisation and global demethylation of the paternally and maternally derived genome, the very first *de novo* DNA methylation at the late morula-stage determines the initial developmental lineage differentiation of the inner cell mass that will give rise to the embryo, and the trophectoderm that will evolve into placental tissue. The inner cell mass methylation is more pronounced than the relatively hypomethylated trophectoderm, resulting in an asymmetrical methylation status from this developmental stage onwards, which is consistent with the observed extent of genome-wide placental-specific methylation and in line with previous studies [117, 118, 125]. The relatively hypomethylated state of the trophectoderm is necessary for the highly proliferative and invasive process of

first trimester placentation requiring an active transcription of genes [118]. Schroeder et al. recently described a novel finding of partially methylated regions (PMRs) in the placenta, characterised by methylation levels around 45%, in contrast to most human tissues demonstrating mainly a high methylation (>70%) of the majority of the genome [126]. This is in line with the relatively abundant placenta-specific intermediate methylation levels around 50% in our data, especially since the PMRs were annotated to genes with tissue-specific functions.

HUVEC displayed another substantial tissue-specific methylation pattern compared to UC-WBC, but less extreme then placental tissue. This may be explained by the fact that HUVEC and the surrounding umbilical cord originate from the inner cell mass [127]. Umbilical cord blood (UCB) originates from endothelial cells in the ventral aorta of the developing embryo during initial haematopoiesis and thus displays a more common background with HUVEC, substantiating the less diverging methylation profiles of UC-WBC and HUVEC [52]. These observations in HUVEC suggest that carefully selected tDMR-poor genomic regions may be represented adequately by UC-WBC in terms of DNA methylation in candidate-gene studies, but this needs further functional validation.

In comparison to peripheral blood, Slieker et al. identified 3,500 DMRs in peripheral tissues and 5,400 DMRs in post-mortem internal tissues, mainly situated in CpG-poor regions, which is in agreement with our data considering HUVEC tDMR- quantity and genomic occurrence [121]. Also in line with our observations are the recently published data of Lowe et al. showing highly distinctive epigenome-wide methylation levels in whole blood DNA versus several somatic tissues using publicly available Illumina450K-databases [120, 128]. Although other studies have identified tDMRs to examine tissue-specificity, these studies are limited in terms of comparability, due to the use of post-mortem tissues or cultured cells and a wide variety of statistical approaches [105, 122, 129]. There exists partial overlap between tDMRs identified in our study and in previous EWAS. These potentially represent highly tissue-specific sites throughout several different tissues and suggest a certain degree of reproducibility of our results (**Supplementary table 3**).

We expected to find substantial differences in DNA methylation of the two blood cell fractions since DNA methylation is important in haematopoiesis and blood cell differentiation, and MNC represent a strongly different subgroup as they lack the largest proportion of total WBC: granulocytes [130]. A genome-wide profiling study using Illumina 27K Methylation arrays compared haematopoietic pluripotent cells (HPC) with granulocytes and monocytes from the same

UCB and demonstrated that further differentiation of HPC is associated with demethylation of certain epigenetic programs, depending on the cell type [130]. In our data however, only 0.4% of all epigenome-wide measured CpG sites were statistically differentially methylated, resulting in only two tDMPs and no tDMRs. This is partly explained by the decreased power as a result of the 2.5 times lower UC-MNC sample size, but mainly by the smaller effect sizes we find when studying the UC-MNC group and the biological origin being much more similar to the UC-WBC than the other tissues. It seems therefore equally adequate to perform DNA methylation studies in DNA derived from UC-WBC as from UC-MNC, if the use of homogeneous blood cells is not feasible. Nevertheless, adjustment for WBC mixtures should always be applied in whole blood EWAS to avoid confounding of underlying WBC mixtures [124]. To this purpose, a cord blood specific algorithm was recently developed to estimate cell proportions [131].

Our observations concerning UC-WBC seem in agreement with the study of Wu et al., demonstrating significantly correlated methylation levels within the same individuals for MNC and WBC in adult peripheral blood, although these were measured by repetitive element methylation levels in different assays [132].

Enrichment analysis of the identified HUVEC- and placental tDMPs showed that tDMPs in general occur quite randomly relative to CpG density and genes. However, a strong depletion of tDMPs in CpG-islands and proximal promotors and a strong enrichment in non-CpG-islands was evident. Additionally, we demonstrated HUVEC tDMP enrichment in gene body regions, in agreement with Lokk et al. [122]. Gene bodies and non-CpG island regions seem to be more tissue-specific and susceptible to variation in DNA methylation, and may therefore represent interesting genomic regions for future epidemiologic epigenetic association studies. This also suggests that we should focus less on the concept of DNA methylation resulting in complete silencing of transcription which is related to DNA methylation of promotor regions. Methylation of gene bodies does in fact not block transcription, and is associated with transcription stimulation [23]. Evidence emerges that CpG island methylation of promoter regions, the main region of interest in previous work, is mostly associated with long-term repression of gene expression (Imprinting, X-chromosome inactivation i.a.), which is in line with the shown depletion of tDMPs in CpG-island proximal promotors [23, 121, 129].

Gene-ontology functional annotations of the tDMRs demonstrated that tissue-specific DNA-methylation is involved in specific tissue-related biological functions such as vascular development in HUVEC, suggesting that DNA derived from HUVEC might be more informative than from UC-WBC if one would

be interested in epigenetic involvement during prenatal vascular development. Moreover, general biological functions and early developmental processes were also observed in association with tDMR genes, such as the regulation of gene expression, cellular function and signalling and embryonic development Both categories underline that the tissue-specific aspect should be considered in future epigenetic association studies.

The Ingenuity Knowledge database validated most GO functional annotations in revealing a broad spectrum of housekeeping and embryonic development pathways. In addition, HUVEC tDMR genes were annotated to immune response processes which fit to the known immune cell adhesion and migration function of endothelial cells [21]. This, however, also demonstrates that a certain reference tissue might reveal corresponding tDMR genes and one could argue that the annotated immune response genes might in fact be more attributable to our reference tissue UC-WBC than to HUVEC-specific methylation. It should also be noted, that pathway enrichment analyses may be susceptible to bias due to the design of the array, but we believe this is unlikely given the strength of the enrichments consistent between DAVID and IPA [133].

This data provide novel insights into the tissue-specificity of epigenome-wide DNA-methylation in newborn and placental tissues without confounding of postnatal exposures. The study was performed in human tissues with a much larger sample size than used in previous studies. Moreover, we standardised the tissue sampling and different tissues were obtained mostly from the same pregnancies, to avoid possible inter-tissue variation due to inter-individual variability. Additionally, we applied an optimised tDMR identification technique. We therefore believe that our findings support and contribute to the existing evidence demonstrating the importance of tissue-specificity in genome-wide DNA-methylation measurements.

The following concerns however, need to be addressed. The absence of expression data to validate our findings and the lack of information on external validity are limitations of our study. Furthermore, full replication of our analysis was not possible because a comparable independent dataset with similar patients, tissues and an almost full within-subject statistical study design is not available. A strong correlation was however observed between the estimates of the tissue-effect in our own dataset and $\Delta\beta$ methylation differences of HUVEC and placenta versus UC-WBC of three independent datasets, suggesting partial replication of our tDMPs (**Supplementary figure 2**). Moreover, our findings could have been more relevant with the use of homogeneous cell types of UCB

and placental tissue, thereby avoiding any confounding of methylation differences due to underlying cell mixture differences [134, 135]. However, upon examination of the potential influence of underlying cell variation in UC-WBC and placental tissue on our model, we did see a high correlation with and without adjusting for cell heterogeneity, suggesting that the effect was marginal. A minor limitation is that we did not exclude the published list of potential cross-reactive probes that are present on the array, prior to further analysis [136]. However, given the number of cross-reactive probes in comparison to the number of identified loci, the effect will be very limited. Although we initially intended to obtain all tissues from each patient, due to logistic reasons it appeared not feasible to perform a full within-subject analysis. The collection of sufficient blood in cord blood collection bags for UC-MNC isolation appeared extremely challenging. This seemed a result of random factors such as stressful deliveries, caesarean sections or night shifts, but did not seem systematic. The majority of study subjects were eventually overlapping in the comparisons between UC-WBC versus placenta (24 out of 25 subjects in each group) and UC-WBC versus HUVEC (23 out of 25 subjects in each group), but the UC-MNC group only shares one patient with the UC-WBC. Fortunately, this resulted in maternal and fetal characteristics that were highly comparable between all different tissue groups (**Table 1**). However, this does not exclude some residual confounding, especially in the UC-MNC analysis.

Further research with repeated measurements is needed to gain insights in the maintenance and stability of tissue-specific methylation differences throughout pregnancy and postnatal life, which may increase or decrease due to accumulating environmental exposures, ageing in general and stochastically [137]. Also the degree of correlation between tissue-specific epigenetic programming and the possibility to observe effects of environmental exposures on epigenetic features remains to be elucidated.

Conclusions. We demonstrated an extensive amount of genome-wide HUVEC and placental tDMRs in comparison to UC-WBC. This underlines the relevance of tissue-specific approaches in future epigenetic association studies, or the use of a profound and validated representative tissue for a certain disease of interest, if available. Especially the potentially limited predictive value of extra-embryonic placental tissue on epigenetic programming in fetal tissues should be considered.

The HUVEC tDMR gene involvement in vascular programming suggests that HUVEC may serve as a representative tissue for studying associations between prenatal vascular programming and the prediction of the development of vascular-related diseases during the life course. Further validation in functional

studies is therefore needed to establish the usability of this data in future epigenetic epidemiological birth cohort studies.

METHODS

Study design. Pregnant women and their newborn babies were recruited between June 2011 and June 2013 in a nested case-control study embedded in The Rotterdam Periconceptional Cohort (Predict Study), at the Erasmus MC, University Medical Centre Rotterdam, the Netherlands [32].

Maternal and newborn characteristics. The case-control study aimed to examine genome-wide DNA-methylation in pregnancies with various pregnancy-induced diseases. For the current study we analysed 36 uncomplicated control pregnancies of the case-control study, that provided the tissues of interest and met the inclusion criteria as outlined below. Uncomplicated pregnancies were defined as pregnancies without the following pregnancy-specific complications: preeclampsia, gestational hypertension, fetal growth restriction or preterm birth. Due to the tertiary hospital setting where the study was carried out, chronic comorbidities including endocrine-, metabolic-, auto-immune-, renal- or cardiovascular diseases were no exclusion criterion. Women with HIV infection, those aged < 18 years, those not able to read or understand the Dutch language, multiple birth pregnancies or women with pregnancies complicated by fetal congenital malformations were excluded. Maternal and newborn characteristics were obtained from hospital medical records. All women gave written informed consent before participation and parental informed consent was obtained for the child. All methods were performed in accordance with relevant guidelines and regulations and ethical approval for the study was given by the Erasmus MC, University Medical Centre Research Ethics Board (MEC-2004-227).

Data collection. Immediately after delivery of the newborn, UCB samples from the umbilical vein were collected in anticoagulant vacutainer tubes (Ethylenediaminetetraacetic acid) and cord blood collection bags containing 21 mL anticoagulant Citrate Phosphate Dextrose-solution (CPD) with the placenta still *in situ*. The complete umbilical cord was cut at the placental insertion and immediately stored in umbilical cord buffer (HBSS with 1% Penicillin/Streptomycin) at 4 to 8 °C until further HUVEC isolation within 24 hours after delivery. Umbilical cord and placental samples were collected within 10 minutes after delivery of the placenta. Placental samples of 0.5 cm^3 were taken from the fetal side of the villi at four different sites in a 3 cm radius around the umbilical cord insertion, after carefully removing the membranes and 2 mm of the top placental

layer. After washing in phosphate buffered saline-solution (PBS) to remove maternal blood, placental samples were snap frozen in liquid nitrogen and stored at -80°C until DNA extraction. All samples were collected by trained researchers.

UCB processing. UCB vacutainer tubes and cord blood collection bags were stored at 4 to 8 °C and processed within 48 hours after delivery. Total UC-WBC were isolated after centrifugation of the vacutainer tubes. UC-MNC represent a subgroup of UC-WBC and were obtained from the cord blood collection bags using Ficoll gradient centrifugation to remove granulocytes from the total WBC fraction. The UC-WBC- and MNC pellets were stored at -80 °C until DNA extraction.

HUVEC isolation. The umbilical cord vein was connected to infusion tubes on both extremes and rinsed with cord buffer. Once all remaining umbilical cord blood was removed, the umbilical vein was filled with collagenase solution (1mg/ml) and incubated for 15 minutes in a PBS water bath at 37°C. Detached HUVEC were obtained in suspension and further purified by magnetic activated cell separation (MACS) with CD146 MACS MicroBeads (Miltenyi Biotec GmbH, Bergisch Gladbach, Germany). PBS washed HUVEC cell pellets were snap frozen in liquid nitrogen and stored at -80 °C until DNA extraction.

DNA extraction. Thawed UC-WBC and UC-MNC pellets were subjected to erythrocyte lysis by use of an Erythrocyte Lysis Buffer (Qiagen, Hilden, Germany), following manufacturer's protocols. Thirty mg frozen placental tissue was grinded manually on dry ice using a tissue grinder. The placental powder was immediately added to a cell lysis buffer and stored at -80 °C until further processing. Subsequently, genomic DNA was extracted from all tissues using the Allprep DNA/RNA isolation mini kit (Qiagen, Hilden, Germany), according to manufacturer's instructions.

DNA methylation measurement. Isolated genomic DNA (500 ng) was treated with sodium bisulphite using the EZ-96 DNA methylation kit (Shallow) (Zymo Research, Irvine, CA, USA). Hybridization was performed following manufacturer's instructions. DNA methylation of CpGs was measured by the Illumina HumanMethylation450K BeadChip using the manufacturer's protocol (Illumina, Inc., San Diego, CA, USA) [138-140].

Data quality control and pre-processing. All data pre-processing and statistical analyses were performed in R software version 3.2.2 and Bioconductor version 3.1 [141]. A quality control protocol was conducted in Illumina GenomeStudio software using the methylation module. It included a sample call rate check, colour balance check and control dashboard checks. Probes targeting a CpG with documented single-nucleotide polymorphisms in the C or G nucleotides were removed

(n=17,196) (Minor allele frequency > 0.05, European population, 1000 Genomes Project). Probes directed at the sex chromosomes (n=11,648) and with a detection p-value >0.01 in more than 1% of samples (n=2,773) were also excluded. Out of 485,512 probes, a total of 454,892 were left for further analysis. Normalisation was performed for all samples together by the Dasen method, which consists of background adjustment and between-array normalization, applied to Type I and Type II probes separately (Bioconductor package watermelon version 1.80) [142]. The effect of the Dasen normalisation procedure was checked by plotting raw and normalised density plots per tissue, where the β-values with and without Dasen normalisation showed a very high correlation (r>0.99, **Supplementary figure 5**).

tDMP identification. Methylation β-values were converted to M-values using: M-value = $\log_2$ (β-value/(1-β-value)) [143]. For every CpG on the array we estimated a linear mixed model with the M-value as response, tissue as categorical predictor and a random intercept for each subject, adjusted for bisulphite-plate batch and gestational age to compare each tissue with the UC-WBC (R package 'lme4') [36]. Sensitivity analyses were performed for the following covariates: batch-effect of the bisulphite-plate, gestational age, birth weight, fetal gender, comorbidity and moment of inclusion for the study in or >1st trimester. Only gestational age and bisulphite-plate were thereafter included in our statistical model as potential confounders. The effect of all potential technical and biological covariates on the methylation β-values is depicted in a correlation-heatmap (**Supplementary figure 6**). It is demonstrated that the first three principle components are represented by the different tissues, explaining 98.7% of total variation present in our data. We additionally checked whether adjustment for variation in underlying cell populations in UC-WBC and placenta demonstrated an effect on our model. For this we rerun our final model with additional covariates representing the first two principle components of imputed blood cell populations and imputed placental underlying cell variation using Houseman-data [124, 144]. These additional covariates were not applied to our final model due to the very strong correlation that was demonstrated between the two models in HUVEC (r=0.996) and placental samples (r=0.998). The correlation in the UC-MNC samples is lower due to the initial very low tissue-effect in this comparison, which is attenuated after correction for the different blood cell populations in UC-WBC (r=0.770) (**Supplementary figure 7**). The potential effect of 'mode of delivery' was also excluded after comparing our final statistical model with and without additional covariate 'mode of delivery' (vaginal delivery versus caesarean section) and observing a very strong

correlation between the two models in UC-MNC (r=0.95), HUVEC (r>0.99) and placental samples (r>0.99) (**Supplementary figure 8**).

We used the following model:

$$M_{ij} = b_i + \beta_0 + \beta_1 T_{HUVEC} + \beta_2 T_{PLACENTA} + \beta_3 T_{UC\text{-}MNC} + \beta_4 GA + \beta_5 PLATE_2 + \beta_6 PLATE_3 + \varepsilon_{ij.}$$

M_{ij} is the logit of the methylation of individual i in tissue j, where j is UC-WBC, UC-MNC, HUVEC or placenta. b_i is the subject specific intercept which is assumed to follow a normal distribution, T_{HUVEC}, $T_{PLACENTA}$ and $T_{UC\text{-}MNC}$ are tissue specific indicator variables, GA is the gestational age and $PLATE_2$ and $PLATE_3$ are indicator variables for the sample plates. β_0 Is the intercept and β_1 to β_7 are the regression coefficients indicating the effect of the various covariates. ε_{ij} Is the measurement error, assumed to be independently normally distributed with a constant variance and mean of zero. All tissues were compared against one reference tissue: UC-WBC.

A False Discovery Rate (FDR) adjusted p-value below 0.05 was considered significant. CpG sites were classified as tDMP if statistically significant and presenting with a minimal effect-size ΔM of 1.3 versus UC-WBC. We considered various M-value cut-off values for further data analysis and applied the widely used robust cut-off of 20% $\Delta\beta$ (~ 1.3 on M-value scale) [145] (**Supplementary table 2**, **Supplementary figure 9**). For the comparison with the smallest number of samples (n=10 UC-WBC samples), we were able to measure methylation differences of at least 9.4% $\Delta\beta$), with a power of 0.7 (sd of 0.05 and $p < 0.05$). The lambda-values for the different EWAS performed include 0.02 for UC-WBC versus UC-MNC, 6.4 for UC-WBC versus HUVEC and 76.6 for UC-WBC versus placenta. These values are to be expected looking at the amount of CpGs that were found significantly different and based on the underlying biology of our study samples.

A partial replication was performed by a correlation analysis between the estimates (β) for the tissue-effect in our dataset with the $\Delta\beta$ of three publicly available GEO-datasets for UC-WBC (GSE69176: n=152 samples), HUVEC (GSE82234: n=6 samples) and placental tissue (GSE75248: n=174 samples with adequate gestational age range) [146, 147]. $\Delta\beta$ was calculated as the $\Delta\beta$ mean methylation of HUVEC or placenta versus UC-WBC for all our tDMPs. To check the reproducibility of our tDMRs we compared our results to three previous EWAS with available tDMR datasets and similar study designs with respect to type of methylation array and tissues. We were able to compare our tDMR genes

in HUVEC to tDMR genes in vascular tissue of Lokk et al, our tDMR genes in placenta to amniotic tDMR genes of Slieker et al 2015 (both extraembryonic tissues), and all our tDMR genes in HUVEC and placenta to those of Slieker et al 2013 by using the online Jvenn-tool [121, 122, 125, 148].

CpG-density- and gene-centric enrichment analysis of tDMPs. tDMPs were annotated according to their position relative to CpG-islands and relative to genes using UCSC-database. In relation to CpG islands, we identified CpG shores as the 2 kb CpG island flanking region and shelves as the 2 kb CpG shore flanking region. Remaining tDMPs were annotated as non-CGI regions [121]. Enrichment analysis was applied to tDMPs. Relative to genes, tDMPs were annotated as gene body (+500 bp to 3' end of the gene), distal promotor (> 10 to 1.5 kb from the nearest transcription start site (TSS)), proximal promotor (-1.5 to +500 bp from the nearest TSS), intergenic (> 10kb from the nearest TSS), and downstream regions (3' end to +5 kb from 3' end). Human genome build 37 was used for all annotations.

tDMR identification. tDMRs were generated according to a previously published algorithm as regions in which at least three tDMPs were detected with an inter-CpG distance ≤ 1 kb, and not interrupted by more than three non-DMPs within the DMR (DMRfinder) [121].

GO-term enrichment analysis and IPA of tDMR genes. HUVEC and placental tDMRs were mapped to the nearest gene based on Ensembl annotations from UCSC, also when facing multiple genes. Assigned Ensembl genes were uploaded to the DAVID tool to examine possible enrichment of corresponding GO terms using the GO_BP_FAT annotation category (DAVID Bioinformatics Resources 6.7 [149, 150]. Fisher Exact was applied to measure the gene-enrichment of annotated GO terms of the uploaded gene list, against the whole human genome list as a background. To focus on the biology of the annotated GO terms, clusters of similar annotations were examined from the DAVID Functional annotation Clustering table tool. The clustering algorithm is based on the hypothesis that similar annotations have similar gene members, resulting in a Group Enrichment Score to rank their biological significance.

We additionally conducted IPA with the annotated DMP Ensembl gene lists to validate the DAVID enrichment and focussed on canonical pathways and networks. Associated canonical pathways were subjected to Benjamini-Hochberg procedure for controlling FDR ($p < 0.05$). Networks were generated based on network eligible molecules, which were encoded by our DMP genes and also interact with other molecules in the Ingenuity Pathways Knowledge Base. A high score for a network indicates a more approximate fit between network eligible

molecules and the molecules that constitute the network, calculated using the right-tailed Fisher's Exact Test.

SUPPLEMENTARY DATA

SUPPLEMENTARY FIGURE 1. Hierarchical cluster analysis of methylation (M-value), visualised per tissue type.

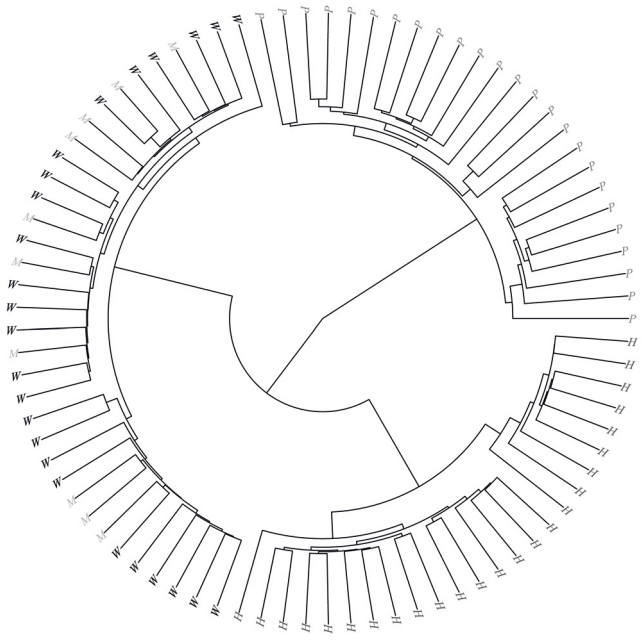

Samples cluster by tissue type, without distinctive clustering for the two different UCB cell fractions. *W* umbilical cord white blood cells; *M* umbilical cord blood mononuclear cells; *H* human umbilical vein endothelial cells; *P* placental tissue.

SUPPLEMENTARY FIGURE 2. Correlation of the estimates (β) for the tissue-effect in our dataset against the Δ β of publicly available GEO-datasets (HUVEC and placental tissue compared to UC-WBC) in all our tDMPs.

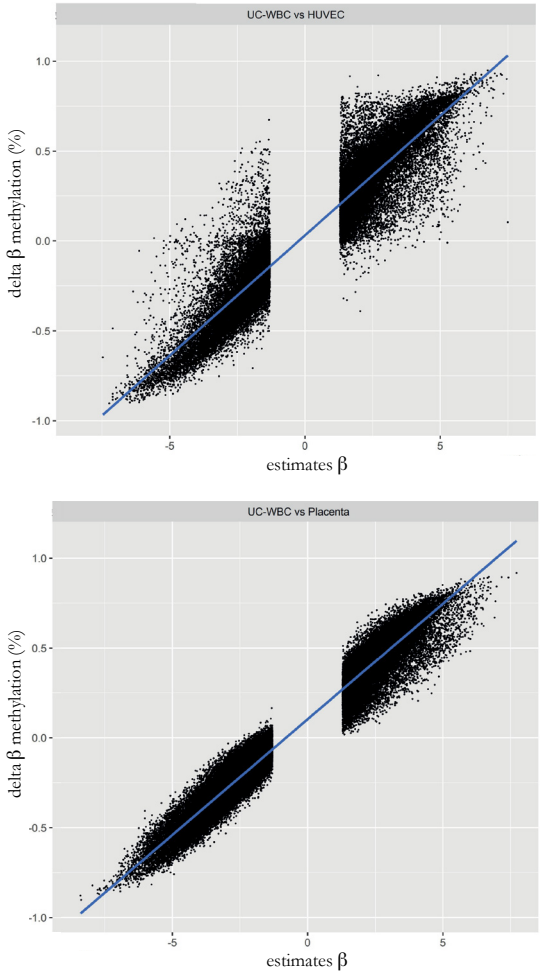

Estimates (β) for the tissue-effect in our dataset are depicted on the x-axis and Δ β of the independent datasets (calculated as the Δ β mean methylation (%) of HUVEC or placenta versus UC-WBC) are depicted on the y-axis, for all HUVEC and placental tDMPs observed in our dataset. A strong correlation is observed between both datasets (r=0.94 in HUVEC samples and r=0.98 in placental samples, p<0.0001). β-Values are depicted for a better biological understanding of the figure. UC-WBC umbilical cord white blood cells; HUVEC human umbilical vein endothelial cells.

SUPPLEMENTARY FIGURE 3. Combined tDMP enrichment in the CpG-density and gene-centric annotation.

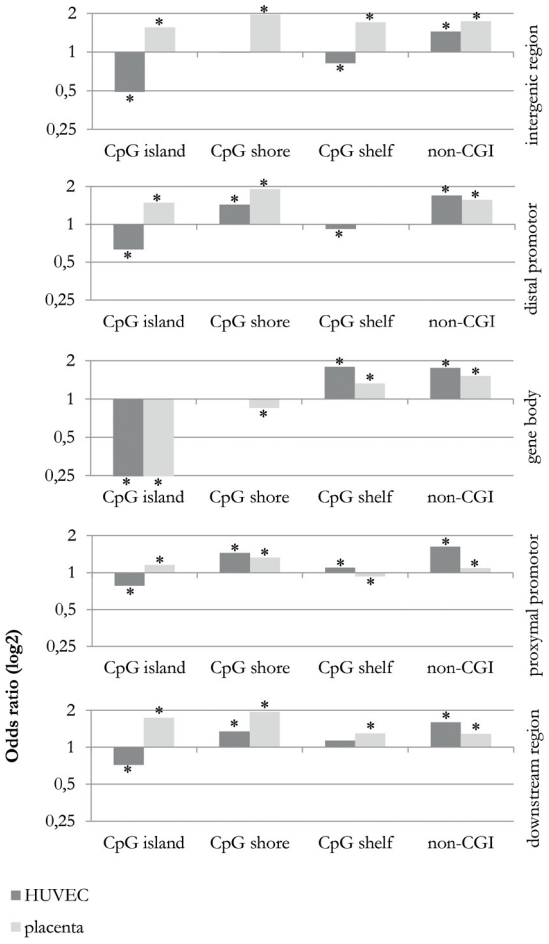

A prominent depletion of tDMPs in proximal promotors due to a strong underrepresentation of tDMPs in CpG-island proximal promotors was observed. The combined annotation enrichment analysis also revealed opposite annotation patterns for HUVEC and placental tDMPs, mainly in various gene-centric regions situated in CpG-islands and CpG-shelves. * $p<0.05$. non-CGI non-CpG island; HUVEC human umbilical vein endothelial cells.

SUPPLEMENTARY FIGURE 4. Representation of the location of the HUVEC tDMRs (A) and placental tDMRs (B) (represented as red dots) on the genome, depicted per chromosome. The darker the colour of the dots, the higher the density of tDMRs on a certain position on the chromosome.

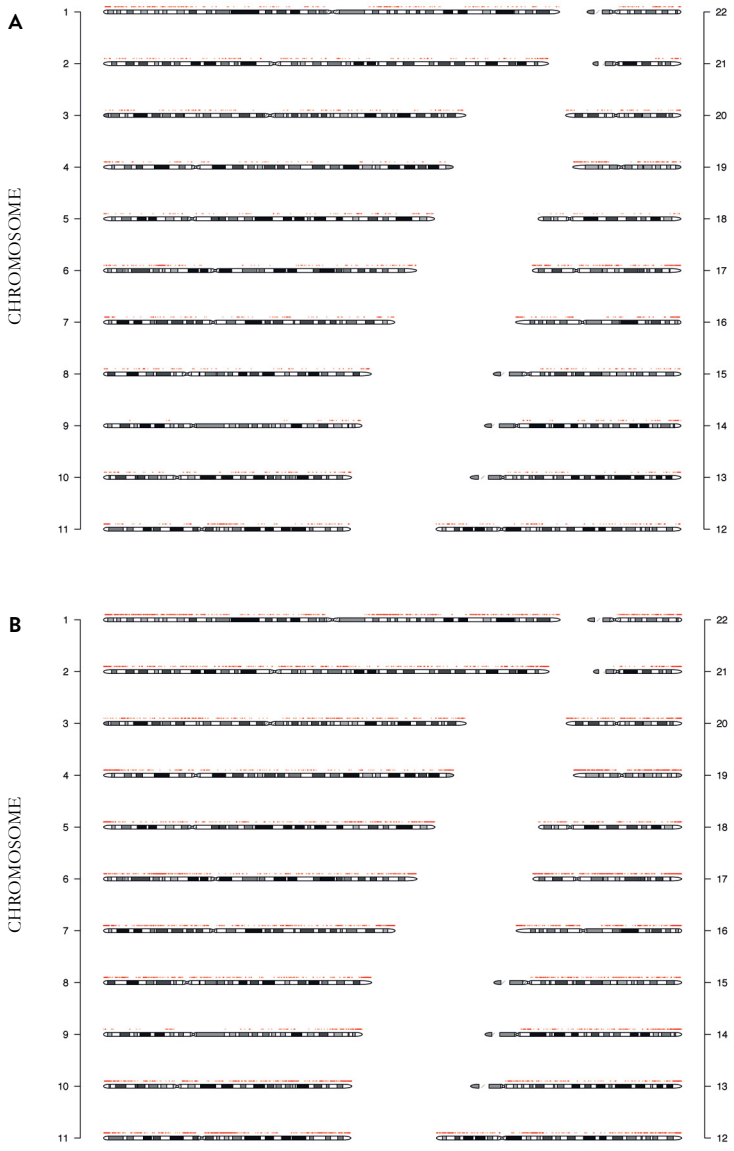

SUPPLEMENTARY FIGURE 5. Density plots of raw and Dasen normalised methylation β-values in UC-MNC samples (A), UC-WBC samples (B), placental samples (C) and HUVEC samples (D).

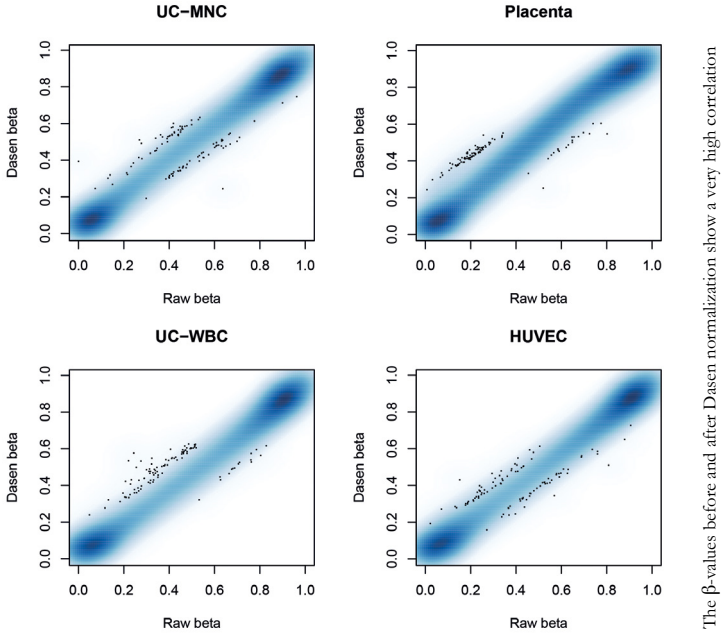

The β-values before and after Dasen normalization show a very high correlation (r>0.99).

SUPPLEMENTARY FIGURE 6. Correlation-heatmap of the first principle components of the β-values against all potential technical and biological covariates.

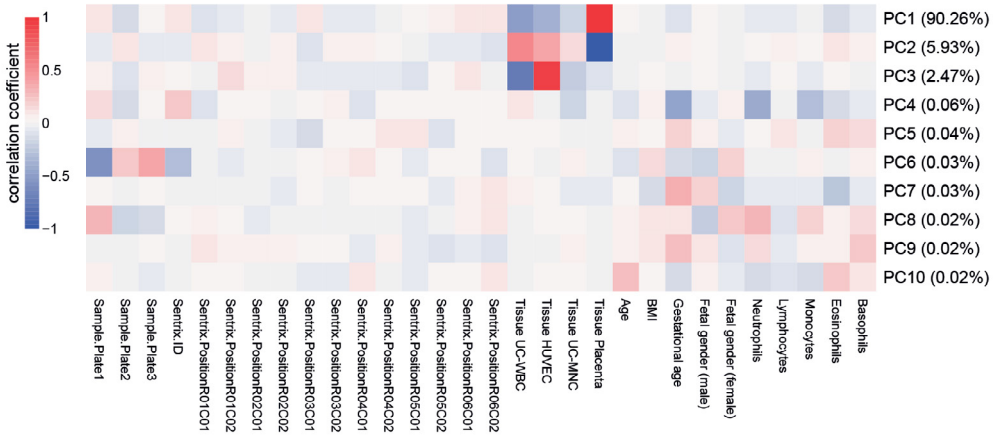

All potential technical and biological covariates are depicted on the x-axis and the first 10 principle components of the β-values are depicted on the y-axis. The stronger the correlation, the darker the colour of the corresponding box. It is clearly demonstrated that the first three principle components are represented by the different tissues, explaining 98.7% of total variation present in our data. PC principle component.

SUPPLEMENTARY FIGURE 7. Relation of β-values representing the tissue-effect of the final statistical model with and without additional covariates for underlying cell populations in UC-MNC samples (A), HUVEC samples (B) and placental samples (C) compared to UC-WBC.

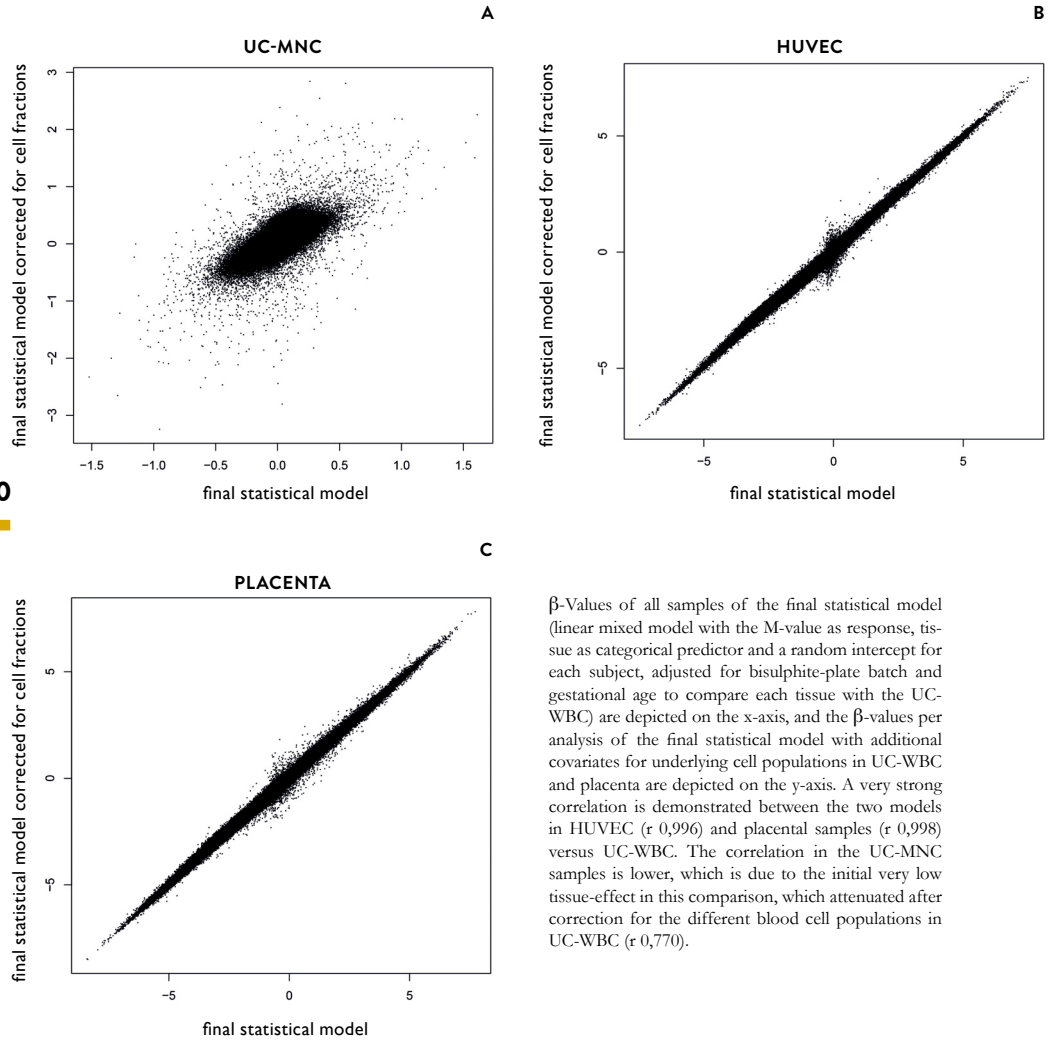

β-Values of all samples of the final statistical model (linear mixed model with the M-value as response, tissue as categorical predictor and a random intercept for each subject, adjusted for bisulphite-plate batch and gestational age to compare each tissue with the UC-WBC) are depicted on the x-axis, and the β-values per analysis of the final statistical model with additional covariates for underlying cell populations in UC-WBC and placenta are depicted on the y-axis. A very strong correlation is demonstrated between the two models in HUVEC (r 0,996) and placental samples (r 0,998) versus UC-WBC. The correlation in the UC-MNC samples is lower, which is due to the initial very low tissue-effect in this comparison, which attenuated after correction for the different blood cell populations in UC-WBC (r 0,770).

SUPPLEMENTARY FIGURE 8. Relation of β-values representing the tissue-effect of the final statistical model with and without additional covariate mode of delivery in UC-MNC samples (A), HUVEC samples (B) and placental samples (C) compared to UC-WBC.

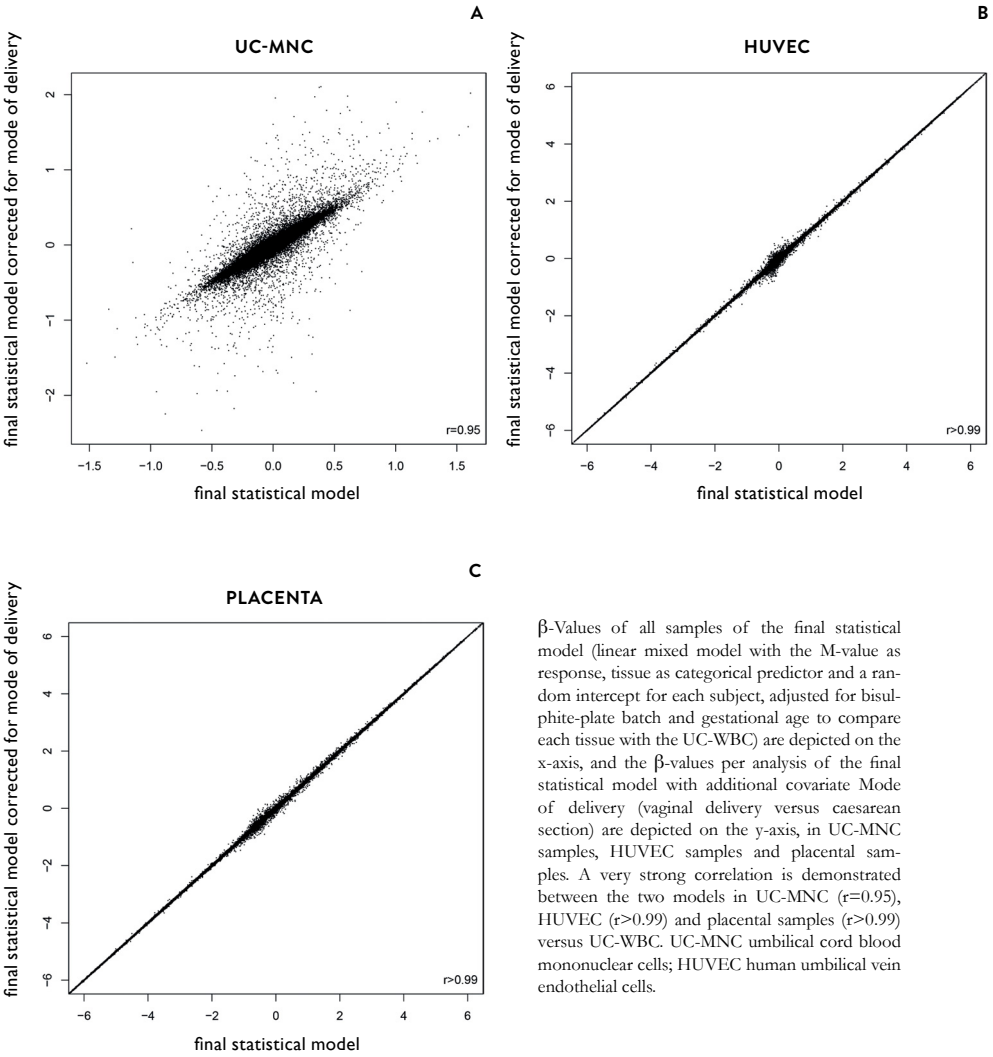

β-Values of all samples of the final statistical model (linear mixed model with the M-value as response, tissue as categorical predictor and a random intercept for each subject, adjusted for bisulphite-plate batch and gestational age to compare each tissue with the UC-WBC) are depicted on the x-axis, and the β-values per analysis of the final statistical model with additional covariate Mode of delivery (vaginal delivery versus caesarean section) are depicted on the y-axis, in UC-MNC samples, HUVEC samples and placental samples. A very strong correlation is demonstrated between the two models in UC-MNC (r=0.95), HUVEC (r>0.99) and placental samples (r>0.99) versus UC-WBC. UC-MNC umbilical cord blood mononuclear cells; HUVEC human umbilical vein endothelial cells.

SUPPLEMENTARY FIGURE 9. Relation of methylation β-value and M-value and visualisation of genome-wide significantly differentially methylated CpGs (represented as red dots) and insignificant CpGs (represented as blue dots).

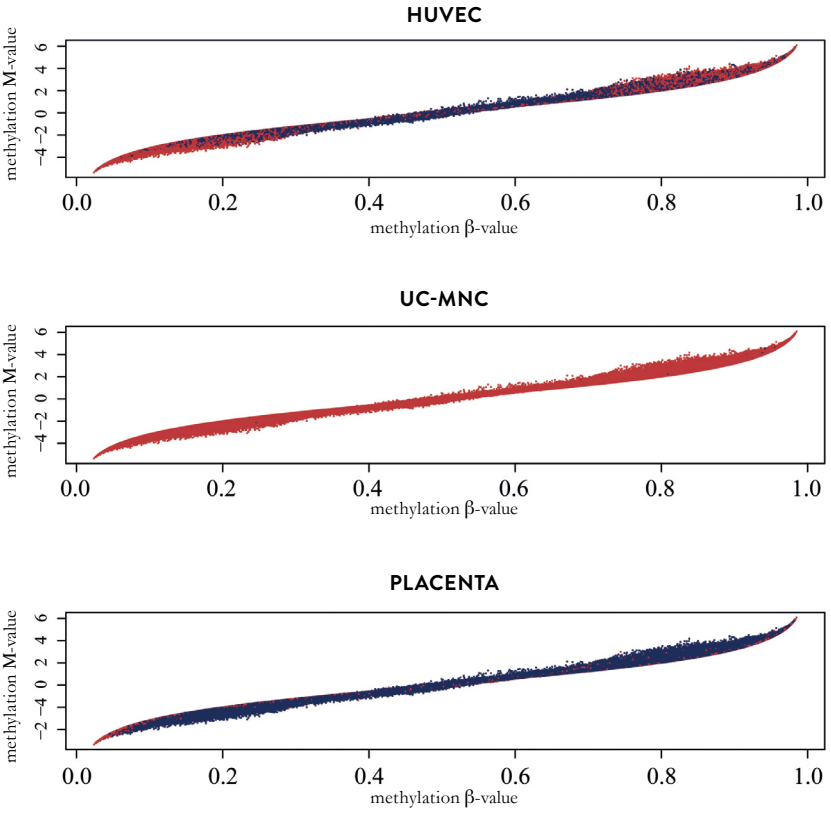

The vast majority of statistical significant CpGs were represented on the M-value scale with a linear correlation to the β-scale, that is between 0.2 and 0.8 methylation on the β-scale. This enabled using a single effect-size M-value cut-off without introducing a bias based on the absence of linearity between M- and β –values in the methylation extremities. *UC-MNC* umbilical cord blood mononuclear cells; *HUVEC* human umbilical vein endothelial cells.

SUPPLEMENTARY TABLE 1. Median methylation β-value per tissue

	UC-WBC	UC-MNC	HUVEC	Placenta
Overall, % (IQR)	66.1 (10.6-85.4)	66.1 (10.4-85.7)	63.6 (11.2-85.8)	54.8 (13.6-84.3)
CpG islands, % (IQR)	9.5 (6.6-19.3)	9.3 (6.6-18.9)	9.8 (6.8-19.5)	10.7 (6.8-36.6)
CpG shores, % (IQR)	49.9 (11.9-83.1)	49.3 (11.7-83.3)	49.2 (12.5-83.3)	49.8 (16.4-81.4)
CpG shelves, % (IQR)	83.8 (11.9-87.9)	84.0 (11.7-88.1)	84.2 (12.5-88.5)	82.1 (61.0-89.6)
Non-CpG island, % (IQR)	82.9 (67.4-87.6)	83.2 (67.3-87.8)	82.7 (63.9-88.1)	77.2 (51.1-88.1)
Intergenic region, % (IQR)	78.1 (40.9-86.2)	78.3 (40.4-86.4)	77.1 (36.7-86.6)	63.2 (36.6-82.3)
Distal promotor, % (IQR)	73.8 (17.5-85.8)	73.9 (17.3-86.0)	74.0 (19.0-86.1)	65.6 (32.5-84.9)
Proximal promotor, % (IQR)	10.9 (7.2-56.0)	10.7 (7.1-55.6)	11.4 (7.4-54.9)	13.1 (7.4-53.0)
Gene body, % (IQR)	82.5 (53.4-87.8)	82.8 (53.2-88.0)	82.3 (48.2-88.3)	78.7 (46.6-89.3)
Downstream region, % (IQR)	73.6 (17.2-86.1)	73.8 (16.7-83.3)	71.1 (17.5-83.3)	65.2 (33.2-81.4)

Data are presented as median methylation β-value % (interquartile range).*IQR* interquartile range; *UC-WBC* umbilical cord white blood cells; *UC-MNC* umbilical cord blood mononuclear cells; *HUVEC* Human Umbilical Vein Endothelial Cell

SUPPLEMENTARY TABLE 2. Number of tDMPs with different effect-size cut-off values

Effect-size cut-off	UC-WBC vs UC-MNC	UC-WBC vs HUVEC	UC-WBC vs placenta
None	1,636 (0.4%)	193,945 (43%)	333,061 (73%)
10% β ~0.6 m-value	65	98,571	224,250
15% β ~ 1.0 m-value	8	64,747	155,097
20% β ~ 1.3 m-value	**2**	**49,979 (11%)**	**126,482 (28%)**
30% β ~ 2.0 -value	0	29,618	78,418

The effect-size cut-off value 20% β ~ 1.3 m-value and corresponding tDMPs depicted in bold were applied during final data analysis.
tDMPs tissue-specific differentially methylated positions; *UC-WBC* umbilical cord white blood cells; *UC-MNC* umbilical cord blood mononuclear cells; *HUVEC* Human Umbilical Vein Endothelial Cells.

SUPPLEMENTARY TABLE 3 will be available at the website of the scientific journal in which this part of the thesis will be published.

SUPPLEMENTARY TABLE 4. tDMP enrichment in the CpG-density and gene-centric annotation

	UC-WBC vs UC-MNC	UC-WBC vs HUVEC		UC-WBC vs Placenta	
tDMP enrichment in the CpG-density annotation		**n (%)**	**OR (95% CI)**	**n (%)**	**OR (95% CI)**
CpG island	-	5,871 (12%)	0.27* (0.26-0.27)	25,767 (20%)	0.47* (0.47-0.48)
CpG shore	-	13,220 (26%)	1.23* (1.20-1.25)	32,537 (26%)	1.22* (1.21-1.24)
CpG shelf	-	5,159 (10%)	1.08* (1.05-1.12)	12,914 (10%)	1.09* (1.06-1.11)
non-CpG island	-	25,729 (51%)	2.02* (1.98-2.06)	55,264 (44%)	1.54*(1.52-1.56)
tDMP enrichment in the gene-centric annotation					
Intergenic region	-	8,968 (18%)	1.15* (1.12-1.18)	28,745 (23%)	1.86* (1.83-1.89)
Distal promotor	-	2,682 (5%)	1.11* (1.07-1.16)	7,733 (6%)	1.40* (1.36-1.44)
Proximal promotor	-	13,177 (26%)	0.55* (0.54-0.57)	33,342 (26%)	0.49* (0.48-0.50)
Gene body	-	23,965 (48%)	1.50* (1.48-1.53)	53,338 (42%)	1.20* (1.18-1.21)
Downstream region	-	1,187 (2%)	1.24* (1.17-1.32)	3,324 (3%)	1.55* (1.48-1.61)

No results were available for the UC-MNC tDMP enrichment analysis, due to the low number of UC-MNC tDMPs (n=2). *tDMPs* tissue-specific differentially methylated positions; *UC-WBC* umbilical cord white blood cells; *UC-MNC* umbilical cord blood mononuclear cells; *HUVEC* Human Umbilical Vein Endothelial Cells; *OR* Odds ratio; *CI* Confidence interval. * $p < 0.05$.

SUPPLEMENTARY TABLE 5. tDMP enrichment of the combined CpG-density and gene-centric annotation

	Island- HUVEC	Island- placenta	Shore- HUVEC	Shore- placenta	Shelf- HUVEC	Shelf- placenta	non-CGI HUVEC	non-CGI placenta
IR, n (%)	701 (1%)	4,513 (4%)	1,188 (2%)	4,631 (4%)	554 (1%)	2,382 (2%)	6,525(13%)	17,219(14%)
OR (95% CI)	0.49* (0.45-0.53)	1.56* (1.50-1.62)	0.99 (0.93-1.05)	1.96* (1.88-2.03)	0.82* (0.75-0.89)	1.71* (1.63-1.81)	1.45* (1.41-1.49)	1.74* (1.70-1.77)
DP, n (%)	321 (0.6%)	1,615 (1%)	739 (1%)	2,092 (2%)	888 (2%)	2,427 (2%)	734 (1%)	1,599 (1%)
OR (95% CI)	0.63* (0.56-0.70)	1.48* (1.39-1.58)	1.43* (1.32-1.54)	1.91* (1.81-2.03)	0.92* (0.86-0.99)	1.01 (0.96-1.06)	1.70* (1.56-1.84)	1.57* (1.47-1.67)
PP, n (%)	1,502 (3%)	7,942 (6%)	5,385 (11%)	12,264 (10%)	656 (1%)	1,225 (1%)	5,634 (11%)	11,911 (9%)
OR (95% CI)	0.12* (0.11-0.12)	0.21* (0.21-0.22)	1.00 (0.97-1.03)	0.85* (0.84-0.87)	1.79* (1.64-1.95)	1.32* (1.23-1.41)	1.75* (1.70-1.80)	1.51* (1.48-1.55)
GB, n (%)	3,174 (6%)	10,848 (9%)	5,601 (11%)	12,629 (10%)	2,875 (6%)	6,374 (5%)	12,315 (25%)	23,487 (19%)
OR (95% CI)	0.78* (0.75-0.81)	1.16* (1.13-1.18)	1.45* (1.41-1.50)	1.33* (1.30-1.36)	1.10*(1.06-1.14)	0.93* (0.90-0.95)	1.63* (1.59-1.66)	1.09* (1.08-1.11)
DR, n (%)	173 (0.3%)	849 (0.7%)	307 (0.6%)	921 (0.7%)	186 (0.4%)	506 (0.4%)	521 (1%)	1,048 (0.8%)
OR (95% CI)	0.72* (0.61-0.84)	1.74* (1.59-1.90)	1.35* (1.19-1.52)	1.94* (1.78-2.11)	1.13 (0.97-1.32)	1.30*(1.17-1.45)	1.60* (1.46-1.76)	1.29* (1.20-1.39)

tDMPs tissue-specific differentially methylated positions*; UC-WBC* umbilical cord blood white blood cells; *UC-MNC* umbilical cord blood mononuclear cells; *HUVEC* Human Umbilical Vein Endothelial Cells; *OR* Odds ratio; *CI* Confidence interval; *IR* intergenic region; *DP* distal promotor; *PP* proximal promotor; *GB* gene body; *DR* downstream region. * $p < 0.05$.

CHAPTER 7

Early- and late-onset preeclampsia and the tissue-specific epigenome of the placenta and newborn

E.M. Herzog, A.J. Eggink, S.P. Willemsen, R.C. Slieker, K.P.J. Wijnands, J.F. Felix, J. Chen, A.P. Stubbs, P.J. van der Spek, J.B. van Meurs, R.P.M. Steegers-Theunissen

Placenta, 2017. 58: p. 122-132

ABSTRACT

Introduction. Preeclampsia (PE) carries increased risks of cardiovascular- and metabolic diseases in mothers and offspring during the life course. While the severe early-onset PE (EOPE) phenotype originates from impaired placentation in early pregnancy, late-onset PE (LOPE) is in particular associated with pre-existing maternal cardiovascular- and metabolic risk factors. We hypothesize that PE is associated with altered epigenetic programming of placental and fetal tissues and that these epigenetic changes might elucidate the increased cardiovascular- and metabolic disease susceptibility in PE offspring.

Methods. A nested case-control study was conducted in The Rotterdam Periconceptional Cohort comprising 13 EOPE, 16 LOPE, and three control groups of 36 uncomplicated pregnancies, 27 normotensive fetal growth restricted and 20 normotensive preterm birth (PTB) complicated pregnancies. Placental tissue, newborn umbilical cord blood white blood cells (UC-WBC) and umbilical vein endothelial cells were collected and DNA methylation of cytosine-guanine dinucleotides was measured by the Illumina HumanMethylation450K BeadChip. An epigenome-wide analysis was performed by using multiple linear regression models.

Results. Epigenome-wide tissue-specific analysis between EOPE and PTB controls revealed 5001 mostly hypermethylated differentially methylated positions (DMPs) in UC-WBC and 869 mostly hypomethylated DMPs in placental tissue, situated in or close to genes associated with cardiovascular-metabolic developmental pathways.

Discussion. This study shows differential methylation in UC-WBC and placental tissue in EOPE as compared to PTB, identifying DMPs that are associated with cardiovascular system pathways. Future studies should examine these loci and pathways in more detail to elucidate the associations between prenatal PE exposure and the cardiovascular disease risk in offspring.

INTRODUCTION

Preeclampsia (PE) is a major cause of maternal and fetal morbidity and mortality and is suggested to be associated with the future risk of cardiovascular- and metabolic diseases in mothers and offspring [7]. Two main disease entities have been identified. Early-onset PE (EOPE) is the more severe phenotype originating from impaired placentation during the first trimester of pregnancy; late-onset PE (LOPE) occurs in the third trimester mainly as a consequence of exposure to pre-existing maternal cardiovascular- and metabolic risk factors [3, 11]. The exact pathophysiology of PE is not understood, but it is known that in EOPE inadequate spiral artery remodelling leads to ischaemia-reperfusion-type placental insults [14]. This induces an excessive production of oxidative radicals. As a result, pro-inflammatory cytokines are released into the maternal circulation inducing endothelial dysfunction that leads to the clinical symptoms of PE [14]. Excessive placental oxidative stressors are also produced in LOPE but more towards the end of pregnancy [11].

PE is considered a complex disease induced by gene- and environmental interactions [18, 19]. Altered epigenetic programming of specific tissues, induced by excessive oxidative stress, has been suggested to be an underlying mechanism [18]. Impaired placental perfusion, excessive production of oxidative radicals, endothelial dysfunction and immune modifications in PE may disturb epigenetic programming in offspring tissues as well, resulting in derangements of the vascular epigenome and function in the offspring [15-17, 151]. From this background *we hypothesize* that altered epigenetic programming of especially placental tissues is associated with the pathogenesis of PE (as cause or consequence) and with cardiovascular and metabolic risks in the offspring over the life course [22].

Although PE has been associated with DNA methylation changes of candidate genes in placental and newborn tissue, only a few epigenome-wide association studies (EWAS) have found new loci of interest and most of these did not examine multiple tissues per patient [25, 152-156]. In this study we examined tissue-specific genome-wide DNA methylation of umbilical cord white blood cells (UC-WBC), placental tissue and human umbilical cord endothelial cells (HUVEC) in relation to EOPE and LOPE.

Considering that PE is complicated by fetal growth restriction (FGR) in 12 % of cases and associated with iatrogenic preterm birth (PTB) in 20 %, which are conditions that can independently affect epigenetic programming, we examined the epigenome of PE and uncomplicated controls but also that of controls complicated by FGR and PTB [34-36].

MATERIALS AND METHODS

Study design. Pregnant women and their newborn babies were recruited between June 2011 and June 2013 in a nested case-control study embedded in The Rotterdam Periconceptional Cohort (Predict study), at the Erasmus MC, University Medical Centre Rotterdam, the Netherlands [32]. Cases comprised of EOPE and LOPE, and unmatched controls comprised of uncomplicated pregnancies and FGR and PTB complicated pregnancies. Patients were recruited for our case-control study by two different pathways. The first pathway contains subjects that were included in the Predict study in the first trimester and developed PE later in pregnancy. The second pathway contains subjects that were admitted to our hospital because of PE after the first trimester, and were specifically recruited in the Predict Study for our case-control study. This also applies to our (un)complicated control groups.

Maternal and fetal characteristics. PE was defined according to the International Society for the Study of Hypertension in Pregnancy as gestational hypertension of at least 140/90 mmHg accompanied by a urine protein/creatinine ratio of ≥ 30 mg/mmol arising de novo after the 20th week of gestation [44]. EOPE and LOPE were defined as being diagnosed before and after 34 weeks of gestation, respectively [45]. Uncomplicated pregnancies were defined as pregnancies without the following pregnancy-specific complications: PE, gestational hypertension, FGR or PTB. FGR was defined as an estimated fetal weight below the 10th percentile for gestational age based on ultrasound measurements performed between 20 and 38 weeks gestational age [46]. Birth weight percentiles were calculated using the reference curves of the Dutch Perinatal Registry to validate birth weight < 10th percentile [47]. Spontaneous preterm deliveries between 22 and 37 weeks of gestation were defined as PTB [48]. Women with HIV infection, aged < 18 years, not able to read and understand the Dutch language, multiple birth pregnancies or women with pregnancies complicated by fetal congenital malformations were excluded.

Maternal and newborn characteristics were obtained from hospital medical records. All women gave written informed consent before participation and parental informed consent was obtained for the child. The research has been carried out in accordance with the Declaration of Helsinki (2013) of the World Medical Association.

Data collection. UC-WBC samples from the umbilical vein were collected with the placenta still in situ. Thereafter, placental tissue was obtained and HUVEC were isolated and stored until DNA extraction. A detailed description of the

data collection, UC-WBC processing, HUVEC isolation and DNA extraction is provided in **Appendix 1**.

DNA methylation measurement. Isolated genomic DNA (500 ng) was treated with sodium bisulphite using the EZ-96 DNA methylation kit (Shallow) (Zymo Research, Irvine, CA, USA). Hybridization was performed following manufacturer's instructions. DNA methylation of CpGs was measured by the Illumina HumanMethylation450K BeadChip using the manufacturer's protocol (Illumina, Inc., San Diego, CA, USA) [138-140]. Data quality control and pre-processing is described in **Appendix 2**.

Differentially methylated position (DMP) identification. To improve statistical power, prior to further statistical analysis a selection of probes containing at least ≥0.05 SD variability in methylation β-values across all samples was applied for each tissue separately [157]. This resulted in a remaining total of 43,488 UC-WBC probes, 134,700 placental probes and 42,352 HUVEC probes. Methylation β-values were converted to M-values using: M-value = $\log_2$ (β-value/(1-β-value)) [143]. A multiple linear regression model was used predicting methylation M-values by disease state for EOPE and LOPE versus (un)complicated controls, adjusted for bisulphite-plate batch and gestational age as covariates for each tissue separately (R package 'CpGassoc'). Sensitivity analyses were performed for the following covariates: batch-effect of the bisulphite-plate, gestational age, birth weight, fetal gender, comorbidity, mode of delivery and moment of inclusion for the study in or >1st trimester. Only gestational age and bisulphite-plate were thereafter included in our statistical model as potential confounders.

UC-WBC analyses were performed with additional adjustment for total number of UC-WBC leucocytes (x10^9/L), available from our flow-cytometric data (n=61, 70 %) or otherwise imputed (n=27, 30 %) [158]. Missing leucocyte numbers were imputed by 'Multiple Imputations with Chained Equations' using other available UC-WBC variables and all contributing maternal and fetal characteristics with maternal age^2 as the best predictive variable (package mice) [159]. Additionally, Houseman-data was applied during imputation, further predicting proportions of lymphocytes, monocytes and granulocytes based on a community cohort of 94 non-diseased, non-smoking, predominantly female individuals between 24 to 45 years old, which improved the Akaike Information Criterion by 11 [124]. Imputed leucocyte concentrations are given in **Supplementary table 1**. Due to sample size constraints we could not adjust for further differentiated white blood cell counts.

FIGURE 1. Overview of the study population and sample distribution.

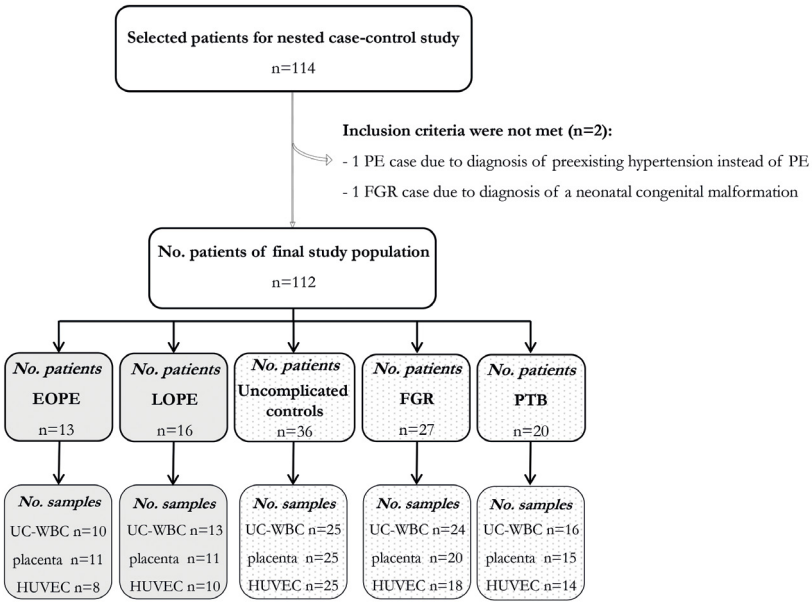

EOPE early-onset preeclampsia; *LOPE* late-onset preeclampsia; *FGR* fetal growth restriction; *PTB* preterm birth; *UC-WBC* umbilical cord white blood cells; *HUVEC* human umbilical vein endothelial cells; no. number of.

We used the following model:

$$M_i = \beta_0 + \beta_1 G + \beta_2 GA + \beta_3 PLATE_2 + \beta_4 PLATE_3 + (+_5 UC\text{-}WBC\text{-}leucocytes) + \varepsilon_i$$

where M_i is the (base 2) logit of the methylation of individual i. G is the group indicator variable (that is one if the sample corresponds to EOPE or LOPE and zero otherwise), GA is gestational age and $PLATE_2$ and $PLATE_3$ are indicator variables for the sample plates. β_5 is only applied for the UC-WBC analysis. ε_i is the residual error assumed to derive from a normal distribution.

A False Discovery Rate (FDR) adjusted p-value below 0.05 was considered significant. CpG sites were classified as DMP if statistically significant and presenting with a minimal effect-size ΔM of 0.8. We considered various M-value cut-off values for further data analysis and applied the widely used robust cut-off of 12.5 % Δβ (~ 0.8 on M-value scale) (**Supplementary table 2**, **Supplementary figure 2**) [145, 153]. For the comparison with the smallest number of

samples (n=8 HUVEC samples in EOPE), we were able to measure methylation differences of at least 10% $\Delta\beta$ or higher, with a power of 0.7 (sd of 0.05 and FDR<0.05). An arbitrary selection of 100 epigenome-wide significant hits was subjected to a critical assessment of M-value plots to exclude potential outlier-driven hits or residual single nucleotide polymorphism-interference.

A detailed description of the DMP CpG-density- and gene-centric enrichment analysis, Gene Ontology (GO) term enrichment analysis and Ingenuity Pathway Analysis (IPA) is provided in **Appendix 3**.

RESULTS

All eligible pregnancies that met the inclusion criteria and provided sufficient tissues were included for the case-control analysis. After exclusion of 2 misclassified pregnancies the final study population consisted of 112 pregnancies. The 29 PE pregnancies comprised of 13 EOPE and 16 LOPE pregnancies, and controls included 36 uncomplicated and 27 FGR- and 20 PTB complicated control pregnancies (**Figure 1**). This number of patients is a result of the initially aimed number of 25 samples per tissue per case-control group. Because we were unable to collect this exact amount of samples and because we obtained often more samples from one patient, the number of corresponding patients differs for each case-control group.

Maternal and newborn characteristics are shown in **Table 1**. In addition to significantly different PE-specific parameters, such as blood pressure, proteinuria, gestational age and birth weight, nulliparity was more frequent in EOPE (84.6 %) and LOPE (81.3 %) than in uncomplicated controls (30.6 %, overall p = 0.001). Caesarean section was more frequent in EOPE (84.6 %) than in both LOPE (31.3 %) and (un)complicated controls (20.0-33.3 %, overall p = 0.002). In the EOPE group, one pregnancy was complicated by FGR (7.7 %) and all by PTB; in the LOPE group, three pregnancies (18.8 %) were complicated by FGR (p = 0.606, in comparison to the EOPE group) and three (18.8 %) by PTB (p <0.001, in comparison to the EOPE group).

DMP identification. Genome-wide DNA methylation data revealed an overall bimodal distribution for UC-WBC and HUVEC (**Figure 2**). In these tissues, only a small amount of cytosine-guanine dinucleotides (CpGs) demonstrated methylation levels around 50 %. In placental tissue however, more CpGs presented 50 % methylation levels. Methylation levels in placental tissue and HUVEC were comparable in all groups, but in EOPE the methylation levels in UC-WBC clearly deviated from those in all other groups.

TABLE 1. Maternal and newborn characteristics

				Complicated controls		
	EOPE	LOPE	Uncomplicated controls	Normoten-sive FGR	Normotensive PTB	Overall
Maternal characteristics	**(n=13)**	**(n=16)**	**(n=36)**	**(n=27)**	**(n=20)**	**p-value**
Age (years)	30.0 (4.7)	33.3 (4.5)	31.8 (5.1)	29.7 (6.0)	31.0 (5.1)	0.187
Nulliparous, n (%)	11 (84.6)	13 (81.3)	11*# (30.6)	17 (63.0)	10 (50.0)	0.001
Caesarean section, n (%)	11 (84.6)	5* (31.3)	10* (27.8)	9* (33.3)	4* (20.0)	0.002
Ethnicity, n (%)						
Western geographic origin	12 (92.3)	9 (56.3)	30 (83.4)	17 (63.0)	18 (90.0)	0.074
Non-Western geographic origin	1 (7.7)	7 (43.8)	6 (16.7)	10 (37.0)	2 (10.0)	
Preconception BMI[a] (kg/m^2)	24.7 (10.1)	24.1 (4.4)	23.7 (4.8)	23.0 (6.5)	23.8 (6.1)	0.668
Smoking during pregnancy (yes), n (%)	2 (18.2)	0 (0.0)	0 (0.0)	2 (8.0)	2 (10.5)	0.132
Co-morbidity (yes), n (%)	1 (7.7)	7 (43.8)	8 (22.2)	7 (25.9)	4 (20.0)	0.260
Newborn characteristics						
Male gender, n (%)	3 (23.1)	7 (43.8)	21 (58.3)	15 (55.6)	10 (50.0)	0.253
Gestational age at birth[a] (weeks)	30.7 (3.4)	37.4* (1.9)	39.9*# (1.9)	38.9* (2.6)	35.4*# (7.9)	<0.001
Birth weight[a] (grams)	1,185 (481)	3,183* (1244)	3,713*# (551)	2,630*# (595)	2,660*# (1805)	<0.001
Birth weight <10th percentile, n (%)	1 (7.7)	3 (18.8)	0# (0.0)	27*# (100.0)	0 (0.0)	<0.001

Data are presented as mean (standard deviation) with corresponding ANOVA testing to examine overall differences between the groups, followed by the post hoc Dunnett t-test for pairwise comparisons of EOPE and LOPE with (un)complicated controls.
Data are presented as number (%) with corresponding Chi^2/Fischer's exact testing.
[a] Non-parametric data are presented as median (interquartile range) with corresponding Kruskall-Wallis testing and posthoc Mann-Whitney testing.
* p <0.05 versus EOPE pregnancies. # p <0.05 versus LOPE pregnancies.
ANOVA analysis of variance; *BMI* body mass index; *EOPE* early-onset preeclampsia; *LOPE* late-onset preeclampsia; *FGR* fetal growth restriction; *PTB* preterm birth.

A heatmap based on the clustering of methylation according to CpG and sample depicts prominent clustering of the three different tissues (**Figure 3A**). We therefore also examined clustering per tissue, which demonstrated EOPE clustering in UC-WBC but no clustering in the placental- and HUVEC samples (**Figure 3B-D**). This was validated by a principal component analysis (PCA) (**Supplementary figure 1**).

Differences between EOPE, LOPE and (un)complicated controls were examined in an epigenome-wide analysis. In the comparison of EOPE and PTB we found 12,040 (28 %) differentially methylated CpGs in UC-WBC and 5,668 (0.5 %) differentially methylated CpGs in placenta. One differentially methylated CpG each

was found in the comparison of EOPE and uncomplicated controls in placental tissue and in HUVEC, and in the comparison of EOPE and FGR in placental tissue (all FDR-adjusted p <0.05). No epigenome-wide significant CpGs were found in the comparisons of LOPE and (un)complicated controls. Differentially methylated CpGs with an effect size > 0.8 in M-value (logit2 of the β-value), representing an approximate change in β-value of 12.5 %, were defined as differentially methylated positions (DMPs), which left 5,001 DMPs in UC-WBC and 869 DMPs in placenta in EOPE compared to PTB (**Supplementary table 2**). 25 DMPs are overlapping between UC-WBC and placenta, which corresponds to 152 shared genes between UC-WBC and placenta. In UC-WBC, 71 % of DMPs were hypermethylated; in contrast, hypomethylation was seen in 67 % of the placental DMPs. Of the shared set of DMPs, 13 (52%) share the same methylation direction in both tissues and 54 (36%) genes are overlapping in methylation direction (**Figure 4**). All (overlapping) UC-WBC and placental DMP identifiers are listed in **Supplementary table 3**.

CpG-density- and gene-centric enrichment of DMPs. To evaluate whether DMPs were enriched in certain genomic annotations, CpG island- and gene-centric annotations of UC-WBC- and placental DMPs were examined (**Figure 5** and **Supplementary table 4**). DMP enrichment analysis relative to CpG islands revealed exactly opposite patterns for UC-WBC and placental DMPs with the strongest enrichment in non-CpG island regions and strongest depletion in CpG islands in UC-WBC ($OR^{UC\text{-}WBC}$ 1.61, 95 % CI 1.52-1.71 and $OR^{UC\text{-}WBC}$ 0.23, 95 % CI 0.20-0.26, respectively) versus strongest enrichment in CpG island regions and strongest depletion in non-CpG islands in placenta ($OR^{Placenta}$ 1.33, 95 % CI 1.15-1.54 and $OR^{Placenta}$ 0.72, 95 % CI 0.62-0.83, respectively) (**Figure 5** and **Supplementary table 4**).

The location of DMPs relative to genes revealed the strongest enrichment in gene bodies with additional high enrichment in downstream regions of the placenta. A strong depletion of DMPs in intergenic regions was observed in both UC-WBC and placental tissue ($OR^{UC\text{-}WBC}$ 0.53, 95 % CI 0.49-0.58, $OR^{Placenta}$ 0.63, 95 % CI 0.53-0.75).

Gene-ontology (GO) term enrichment of DMP genes. To gain more insight in functionality, the DMPs were mapped to the nearest gene. This yielded 3,444 unique UC-WBC genes and 697 unique placental genes. The 3,444 UC-WBC DMP genes mapped to 2,744 genes in The Database for Annotation, Visualization and Integrated Discovery (DAVID) after discarding the remaining DMP annotations as transcripts. These genes were enriched for involvement in cell signalling processes and regulation of cell death, gene expression,

FIGURE 2. Density plot of β-values per tissue and per group.

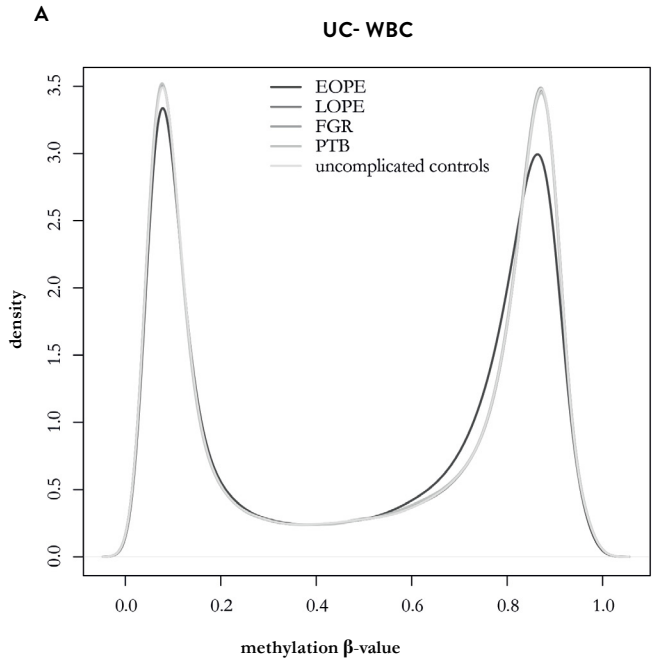

Density plots show the β-value-densities for UC-WBC (A), placenta (B) and HUVEC (C). Genome-wide DNA methylation data revealed an overall bimodal distribution of methylation levels. In addition, the placenta demonstrated a larger amount of CpGs with methylation levels around 50%, in contrast to the other tissues. In UC-WBC, EOPE deviates from LOPE and (un)complicated control pregnancies.
EOPE early-onset preeclampsia; *LOPE* late-onset preeclampsia; *FGR* fetal growth restriction; *PTB* preterm birth; *UC-WBC* umbilical cord white blood cells; *HUVEC* human umbilical vein endothelial cells; *CpGs* cytosine-guanine dinucleotides.

B

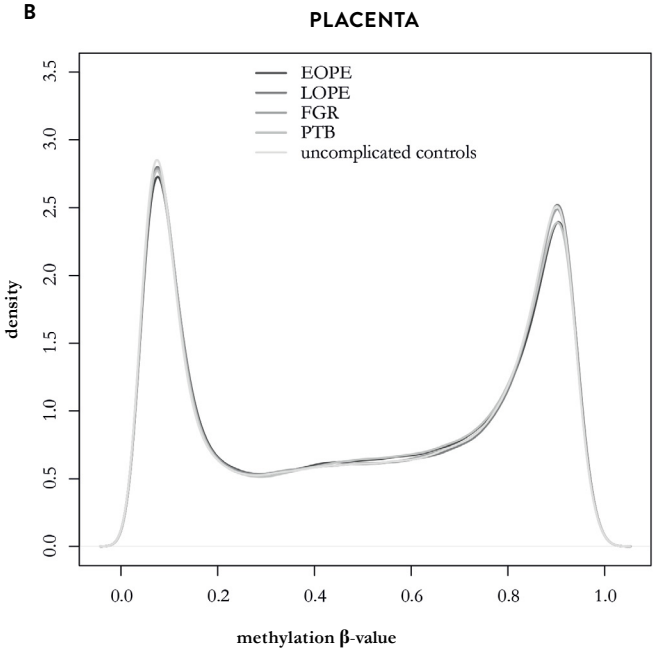
PLACENTA
EOPE
LOPE
FGR
PTB
uncomplicated controls
density
0.0
0.5
1.0
1.5
2.0
2.5
3.0
3.5
0.0
0.2
0.4
0.6
0.8
1.0
methylation β-value

C

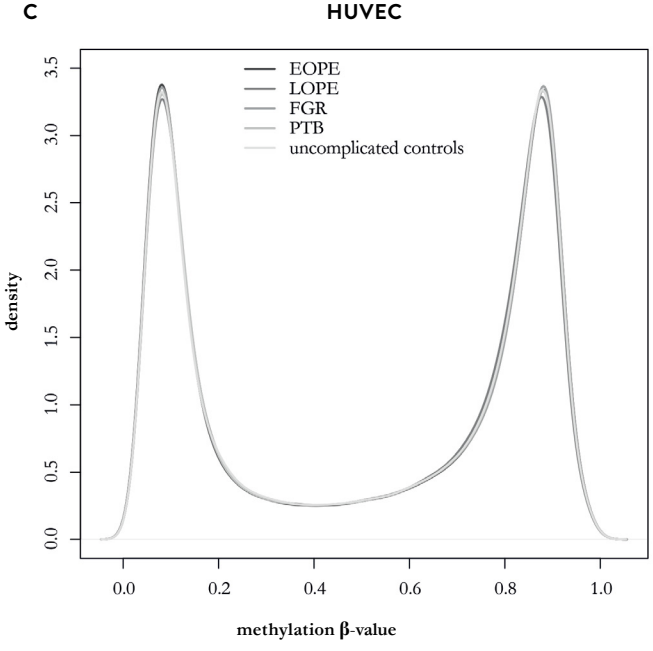
HUVEC
EOPE
LOPE
FGR
PTB
uncomplicated controls
density
0.0
0.5
1.0
1.5
2.0
2.5
3.0
3.5
0.0
0.2
0.4
0.6
0.8
1.0
methylation β-value

FIGURE 3. Heatmap based on clustering of methylation (β-value) of all differentially methylated CpGs.

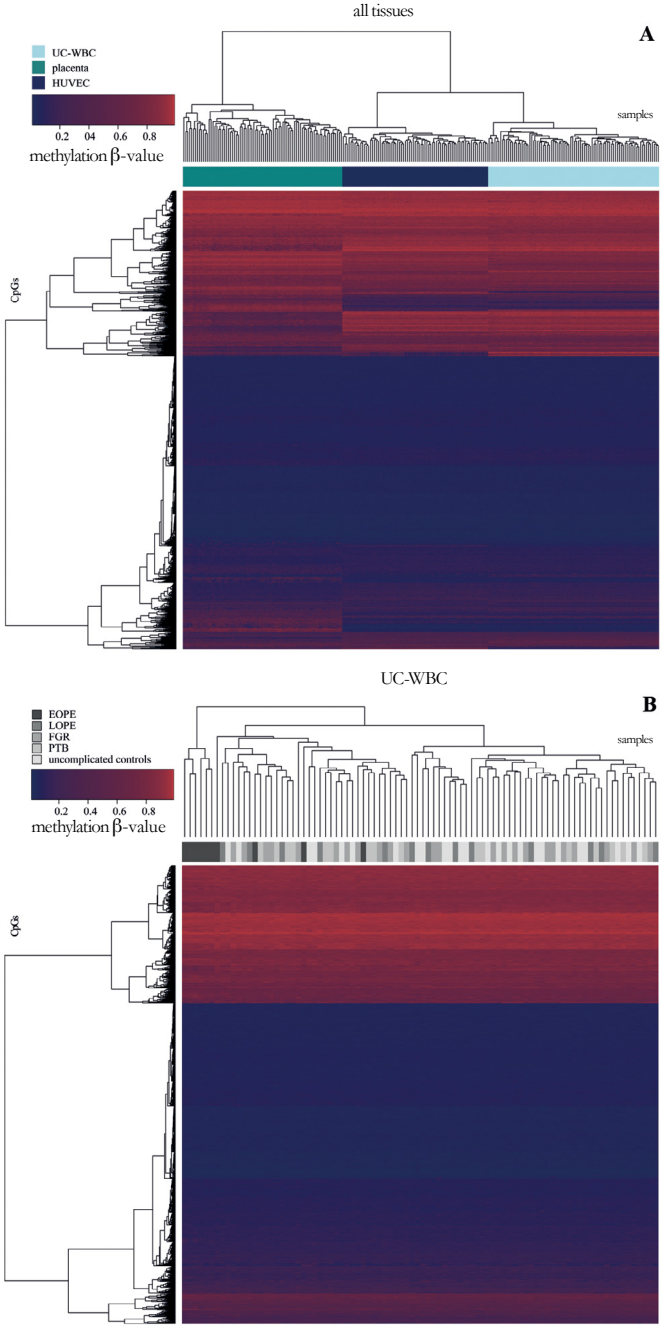

Heatmap plots show the clustering results of the EWAS using all significant CpGs in all tissues (A), UC-WBC samples (B), placental samples (C) and HUVEC samples (D). Samples are plotted on the horizontal axis and CpGs on the vertical axis. Samples cluster between the different tissues (A) and between EOPE and the (un) complicated control groups in UC-WBC samples (B). β-values are depicted for a better biological understanding of the figure. *EOPE* early-onset preeclampsia; *LOPE* late-onset preeclampsia; *FGR* fetal growth restriction; *PTB* preterm birth; *UC-WBC* umbilical cord white blood cells; *HUVEC* human umbilical vein endothelial cells.

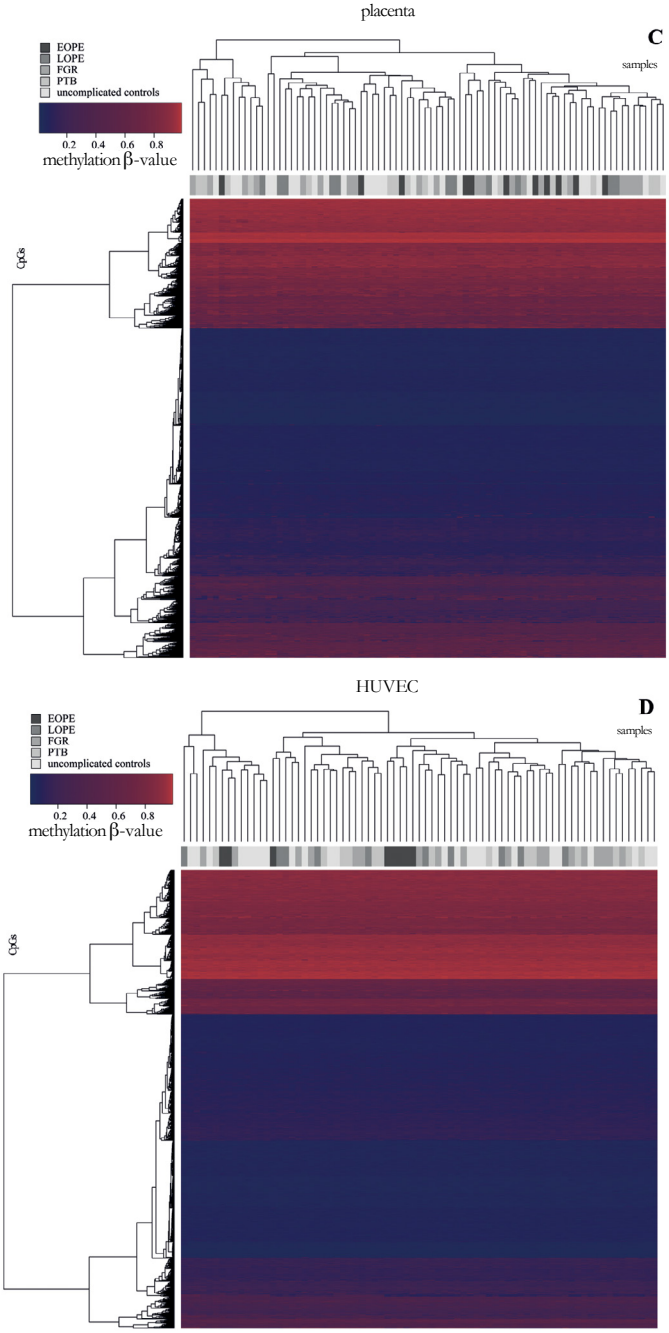
placenta
C
EOPE
LOPE
FGR
PTB
uncomplicated controls
0.2 0.4 0.6 0.8
methylation β-value
samples
CpGs
HUVEC
D
EOPE
LOPE
FGR
PTB
uncomplicated controls
0.2 0.4 0.6 0.8
methylation β-value
samples
CpGs

FIGURE 4. Venn diagram of the number of (overlapping) UC-WBC- and placental DMPs in EOPE compared with PTB complicated pregnancies.

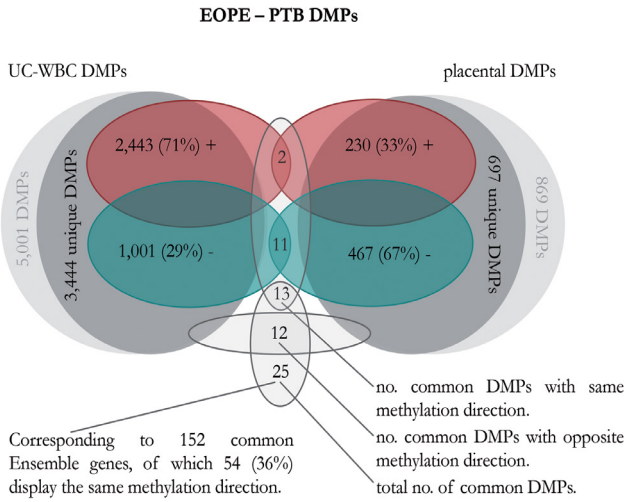

Red circles display the number of hypermethylated DMPs relative to PTB (+), green circles display the number of hypomethylated DMPs relative to PTB (-). *UC-WBC* umbilical cord white blood cells; *DMPs* differentially methylated positions; *EOPE* early-onset preeclampsia; *PTB* preterm birth; *no.* number of.

RAS-activity, inflammatory responses and erythrocyte development. After excluding those DMPs that were mapped to transcripts instead of genes, DAVID mapped 536 placental DMP genes and revealed enriched GO term involvement in embryogenesis, regulation of transcription and cellular differentiation. UC-WBC and placental highest enriched GO terms are presented in **Table 2**.

Ingenuity Pathway Analysis (IPA) of DMP genes. We applied IPA to validate the GO findings from DAVID. Ingenuity software mapped 3,011 UC-WBC DMP genes and a canonical pathway analysis identified enrichment of top-ranked pathways all involved in cascade-signalling mechanisms. We further conducted network analyses, which revealed that the top networks were mainly associated with cardiovascular system development, cellular function and development, haematological system development and infectious diseases.

596 placental DMP genes were mapped by Ingenuity, of which enriched canonical pathways did not reach statistical significance. The top ten enriched networks were mainly associated with embryonic development, cellular development, regulation of gene expression, cardiovascular system development,

FIGURE 5. UC-WBC- and placental- DMP enrichment in the CpG-density (A) and gene-centric (B) annotation, in EOPE compared to PTB complicated pregnancies.

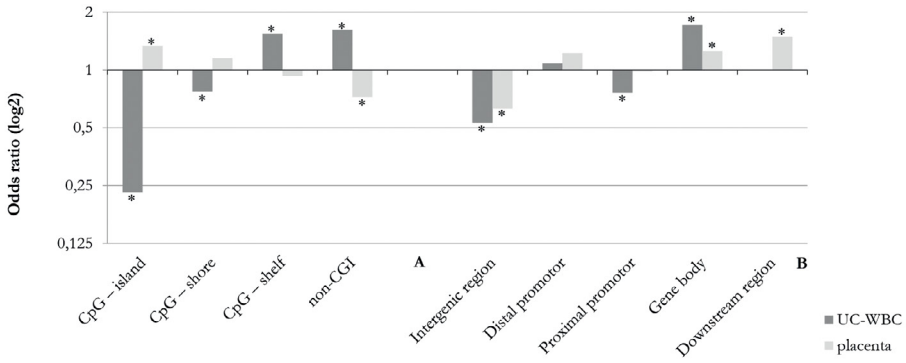

A. DMP annotation relative to CpG islands showed exactly opposite patterns for UC-WBC as compared to placental DMPs with the strongest enrichment in non-CpG island regions and strongest depletion in CpG islands in UC-WBC versus strongest enrichment in CpG island regions and strongest depletion in non-CpG islands in placenta.
B. DMP annotation relative to genes, revealed strongest enrichment in gene body regions, with additional high enrichment in downstream regions of the placenta. A strong depletion of DMPs in intergenic regions was observed in both UC-WBC and placental tissue.
* $p<0.05$. *UC-WBC* umbilical cord white blood cells; *EOPE* early-onset preeclampsia; *PTB* preterm birth; *non-CGI* non-CpG island; *DMP* differentially methylated position.

cell death and survival and haematological system development. The highest enriched pathways and networks are presented in **Table 3**.

DISCUSSION

In this study we demonstrate significant differences in genome-wide UC-WBC and placental DNA methylation between EOPE and PTB controls but not between EOPE and FGR controls or uncomplicated controls. Significant differences were also not found between LOPE and all other (un)complicated control pregnancies.

EOPE differential methylation in comparison to PTB, in UC-WBC and placental tissue. Our most evident observation was the large difference in the level of differential methylation observed in EOPE but not in LOPE. This may be best explained by the excessive oxidative stress exposure in EOPE and LOPE pregnancies, suggested to be highly involved in the disturbance of epigenetic programming [15]. In response to various forms of stress, cells increase the production of important protective proteins while reducing the translation of other less relevant proteins to restore cellular homeostasis [12]. We observed both hyper- and

TABLE 2. Top 10 DAVID GO Functional annotation clusters of EOPE UC-WBC- and placental DMP nearest genes

UC-WBC	Enrichment score
1. Phosphorylation	4.6
2. Programming of cell death	3.9
3. Cytoskeleton organization	3.9
4. Positive regulation of gene expression	3.6
5. Regulation of RAS (GTPase) activity	3.3
6. Endocytose	2.8
7. Regulation of phosphate metabolic process	2.7
8. Defence/inflammatory response	2.4
9. Erythrocyte differentiation and development	2.1
10. Regulation of endocytosis and phagocytosis	2.0
Placenta	**Enrichment score**
1. Embryonic development	7.3
2. Regulation of transcription	7.2
3. Neuron development	6.3
4. Embryonic morphogenesis	5.7
5. Positive regulation of transcription	4.9
6. Negative regulation of transcription	4.2
7. Embryonic morphogenesis	4.1
8. Respiratory development	3.9
9. Regulation of cell differentiation and development	3.5
10. Embryonic development: dorsal/ventral pattern formation	3.4

UC-WBC- and placental DMPs in EOPE were mapped to the nearest gene using Ensembl annotations from UCSC database. Assigned Ensembl genes were uploaded to the DAVID tool to examine possible enrichment of corresponding GO terms using the GO_BP_FAT annotation category. Fisher Exact was applied to measure the gene-enrichment of annotated GO terms of the uploaded gene list, against the whole human genome list as a background. To focus on the biology of the annotated GO terms, clusters of similar annotations were examined from the DAVID Functional annotation Clustering table tool. The clustering algorithm is based on the hypothesis that similar annotations have similar gene members, resulting in a Group Enrichment Score to rank their biological significance, which is based on the Fisher Exact p-values of each GO term within the cluster. The higher the enrichment score, the more enriched.

DMPs differentially methylated positions; *DAVID* Database for Annotation, Visualization and Integrated Discovery; *GO-term*, gene-ontology term; *HUVEC* human umbilical vein endothelial cells.

hypomethylation in association with EOPE in UC-WBC and placenta tissue, and enrichment of both positive and negative regulation of transcription among the functional annotations of DMP genes, in line with these cellular stress responses. Moreover, if cellular stress responses fail or a sudden excessive stress event occurs, cellular death might occur, through apoptosis or necrosis [13]. Also this cellular death- and survival pathway was identified among the DMP gene functional annotations, underlining the potential involvement of excessive oxidative stress.

TABLE3. Top 10 Ingenuity networks and pathways of EOPE UC-WBC- and placental DMP nearest genes

UC-WBC Canonical pathways	**-log p-value**
1. Molecular Mechanisms of Cancer	4,49
2. Tec Kinase Signalling	4,37
3. Relaxin Signalling	4,37
4. IL-1 Signalling	4,00
5. Fcγ Receptor-mediated Phagocytosis in Macrophages and Monocytes	3,87
6. PPAR Signalling	3,78
7. Renal Cell Carcinoma Signalling	3,74
8. G Beta Gamma Signalling	3,67
9. G-Protein Coupled Receptor Signalling	3,67
10. HGF Signalling	3,49
UC-WBC networks	**Score**
1. Cardiovascular System Development and Function, Lymphoid Tissue Structure and Development, Cell Morphology	29/35
2. Cardiovascular System Development and Function, Tissue Morphology, Cellular Movement	26/34
3. Cell Cycle, Cellular Development, Haematological System Development and Function	24/33
4. Connective Tissue Disorders, Developmental Disorder, Skeletal and Muscular Disorders	24/33
5. Cancer, Organismal Injury and Abnormalities, RNA Post-Transcriptional Modification	24/33
6. Cardiovascular Disease, Cellular Compromise, Organismal Injury and Abnormalities	23/32
7. Infectious Diseases, Antigen Presentation, Protein Synthesis	23/32
8. RNA Damage and Repair, Post-Translational Modification, Cellular Development	23/32
9. Cell Morphology, Cellular Function and Maintenance, Infectious Diseases	23/32
10. Cancer, Organismal Injury and Abnormalities, Reproductive System Disease	23/32
placental networks	**Score**
1. Embryonic Development, Hereditary Disorder, Neurological Disease	45/32
2. Cellular Development, Cellular Growth and Proliferation, Organismal Development	36/28
3. Gene Expression, Cancer, Organismal Injury and Abnormalities	36/28
4. Cell Cycle, Cellular Movement, Developmental Disorder	30/25
5. Cardiovascular System Development and Function, Cellular Movement, Carbohydrate Metabolism	25/22
6. Molecular Transport, Inflammatory Response, Haematological System Development and Function	14/15
7. Metabolic Disease, Organismal Injury and Abnormalities, Respiratory Disease	12/14
8. Cellular Development, Cellular Growth and Proliferation, Cellular Movement	12/14
9. Cell Death and Survival, Cell Cycle, Cellular Assembly and Organization	12/14
10. Cell Death and Survival, Cardiovascular System Development and Function, Cell Morphology	12/14

Ingenuity pathway analysis was performed with the annotated UC-WBC- and placental DMP Ensembl gene lists in EOPE with focus on canonical pathways and networks. Enriched canonical pathways were calculated using the Fisher's Exact test and subjected to Benjamini-Hochberg procedure for controlling FDR ($p<0.05$). Networks were generated based on network eligible molecules, which were encoded by our DMP genes and also interact with other molecules in the Ingenuity Pathways Knowledge Base. A high score for a network indicates a more approximate fit between network eligible molecules and the molecules that constitute the network, calculated using the right-tailed Fisher's Exact Test. No significant EOPE placental canonical pathways were observed.
DMPs differentially methylated positions; *HUVEC* human umbilical vein endothelial cells; *FDR*, false discovery rate.

From our data it appears that oxidative stress may have more consequences for EOPE pregnancies, where placental and newborn tissues are indeed subjected to this adverse exposure from early pregnancy onwards. In EOPE, chorionic villi are exposed to oxidative stress at 8-9 weeks of gestation through contact with maternal oxygenated blood due to early unplugging of spiral arteries, disturbing the formation of the definitive placenta by restricted invasion and impaired remodelling of spiral arteries [12]. One might hypothesize that the epigenetic programming involved in this initial placental formation and differentiation is in fact already affected, perhaps inducing the further development of EOPE, rather than being a consequence of the disease. We suggest that perhaps the very initial process of epigenetic reprogramming between fertilisation and formation of the blastocyst is already affected in EOPE, explaining the observed extensive involvement of placental DMPs and also suggesting a more causative epigenetic involvement. In general, impaired placentation seems to play a much larger role in the pathophysiology of EOPE than LOPE, with more adverse consequences for the fetus, such as FGR, supporting the current results [11]. Also the maternal and fetal pro-inflammatory milieu is more pronounced in EOPE than in LOPE, with more potential consequences for UC-WBC epigenetic programming, as substantiated by our data [15].

Although we would have expected to establish some degree of differential methylation in LOPE, the lack of differential methylation is in accordance to previous literature [152, 153, 160-162]. Only Zhu et al. identified DMRs in placental tissue of severe LOPE pregnancies as compared to that of gestational age- and parity-matched controls. They however used different techniques (DNA immunoprecipitation and deep sequencing) and included only severe cases of LOPE, potentially explaining the discrepancy with our findings [156].

A possible reason for observing associations between EOPE and PTB only, is that these two groups are least affected by a larger gestational age range and additional comorbidity and hence easier to compare than the other control groups. The lack of any significantly differential methylation in HUVEC obtained from EOPE pregnancies might be partly explained by the decreased power as a result of the lower HUVEC sample size (n=8) and the larger variation, compared to (un)complicated controls.

The majority of DMPs in placental tissue was hypomethylated, which is substantiated by literature [153, 160-163], whereas the more prominent hypermethylation in UC-WBC is in contrast to previous studies [154, 164]. These

studies did not adjust for potential confounders such as gestational age or leucocyte-count, which may explain the discrepancy of the results. Compared to the total number of DMPs, the relatively small shared set of 25 DMPs and 152 corresponding genes suggests that UC-WBC and placenta are behaving rather differently in association to EOPE. This is substantiated by the fact that only 52% of the shared DMPs and 36% of the shared genes in UC-WBC and placental tissue are behaving in the same methylation direction relative to PTB, and by the opposite enrichment patterns described below. In certain overlapping genes it appears that different CpGs are affected in UC-WBC than in placental tissue.

CpG-density- and gene-centric enrichment of EOPE UC-WBC- and placental DMPs. Enrichment analysis of the identified EOPE DMPs showed opposite patterns for the positions of UC-WBC- and placental DMPs relative to CpG-islands. EOPE was associated with strong differential methylation of non-CpG island regions in UC-WBC and depletion in CpG islands, whereas in placental tissue differential methylation was observed in CpG islands and depletion in non-CpG islands, which is in line with previous studies [153, 154]. Evidence emerges that CpG island methylation is mostly associated with long-term repression of gene expression such as imprinting, which is an important process for normal placental development [22, 23]. Indeed, a supporting role of imprinting in the development of PE has been observed in previous studies [165].

UC-WBC- and placental DMPs display strong enrichment in gene bodies and evident depletion in intergenic regions. Previous studies describe enrichment of EOPE DMPs in placental enhancer- and UC-WBC 'open sea'-regions, classified according to the Illumina gene-centric annotation which is not directly comparable to our UCSC gene-centric annotation results. Gene body regions seem to be more susceptible to variation in DNA methylation, and may therefore represent interesting genomic regions for future epidemiologic epigenetic association studies [23]. Because methylation of gene bodies is generally associated with stimulation of transcription, the strong placental hypomethylation suggests mainly repression of transcription and the contrary for UC-WBC [23].

GO-term enrichment and IPA of EOPE DMP genes. DMP GO functional annotations demonstrated that genes linked to UC-WBC DMPs were involved in many processes associated with the pathogenesis of PE, such as regulation of inflammatory responses and RAS-activity [3, 166]. We and others have previously described decreased leucocytes and increased nucleated red blood cells in EOPE UC-WBC, indeed suggesting inflammatory response involvement and disturbed fetal haematopoiesis [53, 167]. Therefore, of particular interest is the enriched GO

term of erythrocyte development. The observed enriched GO-term of cellular death regulation might be related to flawing of the endothelial vessel wall in PE, causing apoptosis of endothelial cells, which has been related to the increased presence of endothelial microparticles in PE [15]. One of the most enriched UC-WBC GO terms covers a broad spectrum of cell signalling processes involved in many general processes, which is likely a result of general excessive oxidative stressors. The latter was confirmed by all highest significant canonical pathways from IPA. Placental DMP GO functions covered general functions such as cellular differentiation and cell death, embryogenesis and regulation of gene expression, which is in agreement to the impaired placentation and compromised fetal growth in EOPE and substantiated by literature [153].

The involvement of DNA methylation differences in cardiovascular programming of PE offspring was strongly suggested by many identified gene-ontology (GO) functional annotations and pathways associated with the DMP genes. Repeated enrichment of IPA genetic networks associated with development of cardiovascular and metabolic disease was observed. This is partly substantiated by previous PE EWAS, describing differential methylation in the fatty acid synthase pathway and in collagen-related genes [152, 154]. There exists partial overlap between identified genes in association with EOPE in previous EWAS in both UC-WBC and placental DMP-genes, as depicted in **Supplementary table 3**. We believe these overlapping genes might represent interesting loci for further research and suggest a certain degree of reproducibility of our results. Yuen et al identified hypomethylation of the *TIMP3* gene in EOPE placentas, suggesting reduced angiogenesis and trophoblast invasiveness by use of the Illumina GoldenGate Methylation assay [162]. In other vascular-related candidate gene studies, altered DNA methylation in association with PE was found of *LEP*, *VEGF*, *FLT-1*, *KDR*-genes and collagen-metabolism genes [161, 163, 168], substantiating the role of disturbed vascular programming in PE. All of these previously identified candidate genes were also present among our DMPs in UC-WBC and/or placental tissue.

Several studies have demonstrated that epigenetic programming may indeed be involved in the development of cardiovascular disease, as reviewed by Casanello et al. [21]. One of these studies showed increased DNA methylation of estrogen receptor beta promotors in endothelial cells of atherosclerotic plaques [169]. Alexander at al. showed that in smooth muscle cells epigenetic mechanisms were involved in the phenotypic switch to less contractility with vascular dysfunction as a result [170].

Strengths and limitations. The design of our EWAS is unique in that it addresses tissue-specific methylation levels of EOPE and LOPE and uses both uncomplicated and FGR- and PTB-complicated normotensive control pregnancies. The different tissues were obtained mostly from the same pregnancies and therefore the data provide novel insights in the tissue-specific epigenome-wide DNA-methylation in PE-exposed newborn tissues. Moreover, we adjusted for gestational age and UC-WBC cell mixtures [36, 162], which has not often been done in previous studies [152, 154, 155]. The UC-WBC cell populations were however partly estimated, based on our own and external populations. Our description of the standardised tissue sampling is more extensive than in most other studies, and this is relevant because the method of tissue sampling can be an important potential confounder or effect modifier of DNA methylation [171, 172].

Inherent to the observational and case-control character of the study, residual confounding cannot be fully excluded. The addition of birthweight as potential confounder did not improve our statistical model and was discarded also because of the limited sample size. Moreover, we had no expression data to validate our findings and the external validity is reduced by the relatively high presence of comorbidities in uncomplicated controls in our tertiary hospital setting. Our findings could have improved with the use of larger sample sizes and homogeneous cell types of placental tissue (and UC-WBC), thereby avoiding potential confounding by cell mixture variation [134, 135].

Conclusion. We found a large number of genome-wide DMPs in UC-WBC and placental tissue that were associated with EOPE. The enrichment in several cardiovascular system developmental pathways implies that epigenetic programming may be an underlying mechanism explaining the association with increased cardiovascular disease risks in EOPE offspring. Future follow-up studies in offspring should address whether these pathways represent potential targets for intervention or prevention of the enhanced cardiovascular disease susceptibility.

SUPPLEMENTARY DATA

Appendix 1.

Data collection. Immediately after delivery of the newborn, UC-WBC samples from the umbilical vein were collected in anticoagulant vacutainer tubes (Ethylenediaminetetraacetic acid) with the placenta still in situ. The complete umbilical cord was cut at the placental insertion and immediately stored in umbilical cord buffer (HBSS with 1 % penicillin/streptomycin) at 4 to 8 °C until further HUVEC isolation within 24 hours after delivery. Umbilical cord and placental samples were collected within 10 minutes after delivery of the placenta. Placental samples of 0.5 cm^3 were taken from the fetal side of the villi at four different sites in a 3 cm radius around the umbilical cord insertion, after carefully removing the membranes and 2 mm of the top placental layer. After washing in phosphate buffered saline-solution (PBS) to remove maternal blood, placental samples were snap frozen in liquid nitrogen and stored at -80 °C until DNA extraction. All samples were collected by trained researchers.

UC-WBC processing. UC-WBC vacutainer tubes were stored at 4 to 8 °C and processed within 48 hours after delivery. Total white blood cells were isolated after centrifugation of the vacutainer tubes. The white blood cell-pellets were stored at -80 °C until DNA extraction.

HUVEC isolation. The umbilical cord vein was connected to infusion tubes on both extremes and rinsed with cord buffer. Once all remaining umbilical cord blood was removed, the umbilical vein was filled with collagenase solution (1mg/ml) and incubated for 15 minutes in a PBS water bath at 37 °C. Detached HUVEC were obtained in suspension and further purified by magnetic activated cell separation (MACS) with CD146 MACS MicroBeads (Miltenyi Biotec GmbH, Bergisch Gladbach, Germany). PBS washed HUVEC cell pellets were snap frozen in liquid nitrogen and stored at -80 °C until DNA extraction.

DNA extraction. Thawed WBC pellets were subjected to erythrocyte lysis by use of an Erythrocyte Lysis Buffer (Qiagen, Hilden, Germany), following manufacturer's protocols. Thirty mg frozen placental tissue was grinded manually on dry ice using a tissue grinder. The powder was immediately added to a cell lysis buffer and stored at -80 °C until further processing. Subsequently, genomic DNA was extracted from all tissues using the Allprep DNA/RNA isolation mini kit (Qiagen, Hilden, Germany), according to manufacturer's instructions.

Appendix 2.

Data quality control and pre-processing. All data pre-processing and statistical analyses were performed in R software version 3.2.2 and Bioconductor version 3.1 [141]. We checked performance of built-in internal quality controls in the Control Dashboard using the methylation module of GenomeStudio (Illumina Inc., San Diego, USA). It included a sample call rate check, colour balance check and control dashboard checks. Probes targeting a CpG with documented single-nucleotide polymorphisms in the C or G nucleotides were removed (n=17,196) (Minor allele frequency > 0.05, European population, 1000 Genomes Project). Probes directed at the sex chromosomes (n=11,648) and with a detection P value >0.01 in more than 1% of samples (n=2,773) were also excluded. Out of all 485,512 probes, a total of 454,892 were left for further analysis. Normalisation was performed for all samples together by the Dasen method, which consists of background adjustment and between-array normalization, applied to Type I and Type II probes separately (Bioconductor package watermelon version 1.80) [142].

Appendix 3.

CpG-density- and gene-centric enrichment analysis of DMPs. DMPs were annotated according to their position relative to CpG-islands and relative to genes using UCSC-database. In relation to CpG islands, we identified CpG shores as the 2 kb CpG island flanking region and shelves as the 2 kb CpG shore flanking region. Remaining DMPs were annotated as non-CpG island regions [121]. Relative to genes, DMPs were annotated as gene body (+500 basepairs (bp) to 3' end of the gene), distal promotor (> 10 to 1.5 kb from the nearest TSS), proximal promotor (-1.5 to +500 bp from the nearest TSS), intergenic (> 10kb from the nearest TSS), and downstream regions (3' end to +5 kb from 3' end). Human genome build 37 was used for all annotations. The DMP enrichment analyses were performed using the selected 43,488 UC-WBC probes and 134,700 placental probes, respectively.

Gene Ontology (GO) term enrichment analysis and Ingenuity Pathway Analysis (IPA) of DMP genes. UC-WBC- and placental DMPs were mapped to the nearest gene based on Ensemble annotations from UCSC, also when facing multiple genes. Assigned Ensembl genes were uploaded to the DAVID

tool to examine possible enrichment of corresponding GO terms using the GO_BP_FAT annotation category (DAVID Bioinformatics Resources 6.7, http://david.abcc.ncifcrf.gov/) [149, 150]. Fisher Exact was applied to measure the gene-enrichment of annotated GO terms of the uploaded gene list, against the whole human genome list as a background. To focus on the biology of the annotated GO terms, clusters of similar annotations were examined from the DAVID Functional annotation Clustering table tool. The clustering algorithm is based on the hypothesis that similar annotations have similar gene members, resulting in a Group Enrichment Score to rank their biological significance.

We additionally conducted IPA with the annotated DMP Ensembl gene lists to validate the DAVID enrichment and focussed on canonical pathways and networks. Associated canonical pathways were subjected to Benjamini-Hochberg procedure for controlling FDR ($p<0.05$). Networks were generated based on network eligible molecules, which were encoded by our DMP genes and also interact with other molecules in the Ingenuity Pathways Knowledge Base. A high score for a network indicates a more approximate fit between network eligible molecules and the molecules that constitute the network, calculated using the right-tailed Fisher's Exact Test.

To check the reproducibility of our DMPs we compared our results to three previous EWAS with available DMP datasets and similar study designs with respect to patients and tissues. We were able to compare our DMPs in UC-WBC to results of Ching et al and our DMPs in placental tissue to Blair et al and Anton et al by using jvenn web application [148, 152-154].

SUPPLEMENTARY FIGURE 1. Relation of methylation β-value and M-value and visualisation of genome-wide significantly differentially methylated CpGs (represented as red dots) and insignificant CpGs (represented as blue dots) in UC-WBC (A) and placenta (B).

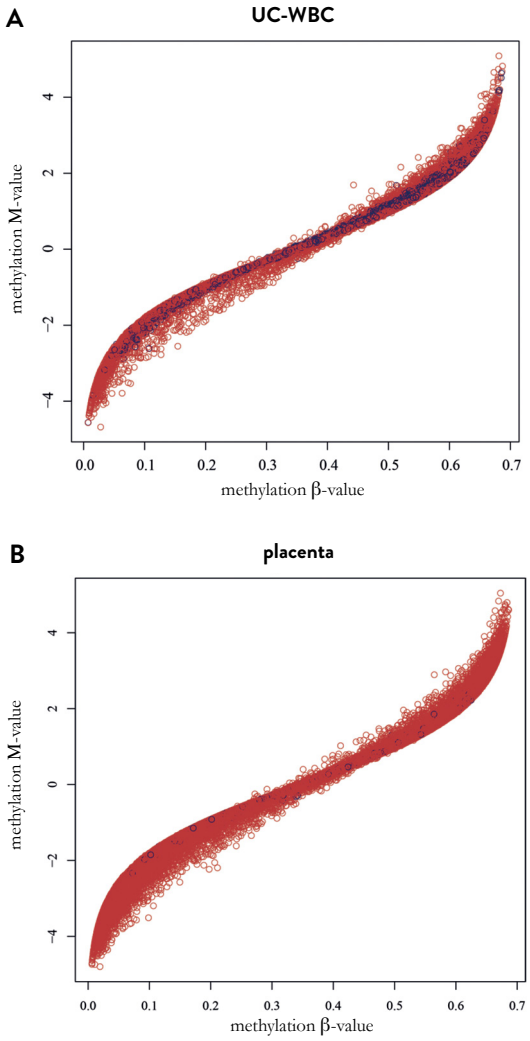

The vast majority of statistical significant CpGs were represented on the M-value scale with a linear correlation to the β-scale; that is between 0.2 and 0.8 methylation on the β-scale. This enabled using a single effect-size M-value cut-off without introducing a bias based on the absence of linearity between M- and β –values in the methylation extremities. *UC-WBC* umbilical cord white blood cells.

SUPPLEMENTARY FIGURE 2. Principal Component Analysis (PCA) of EOPE, LOPE and (un)complicated control pregnancies.

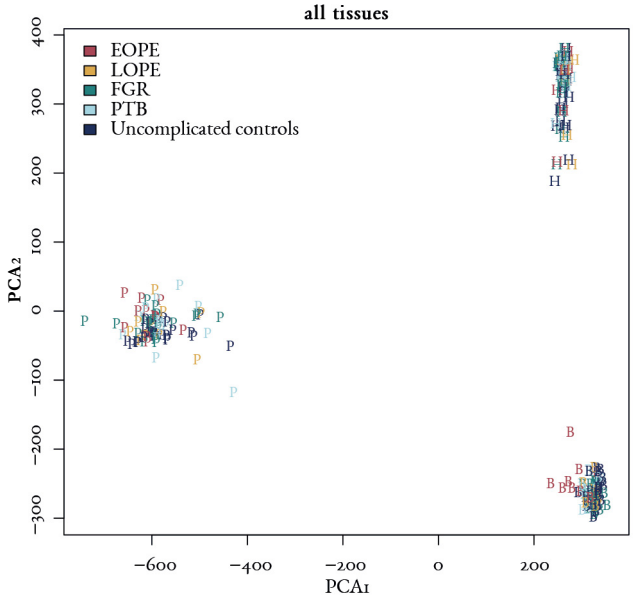

A

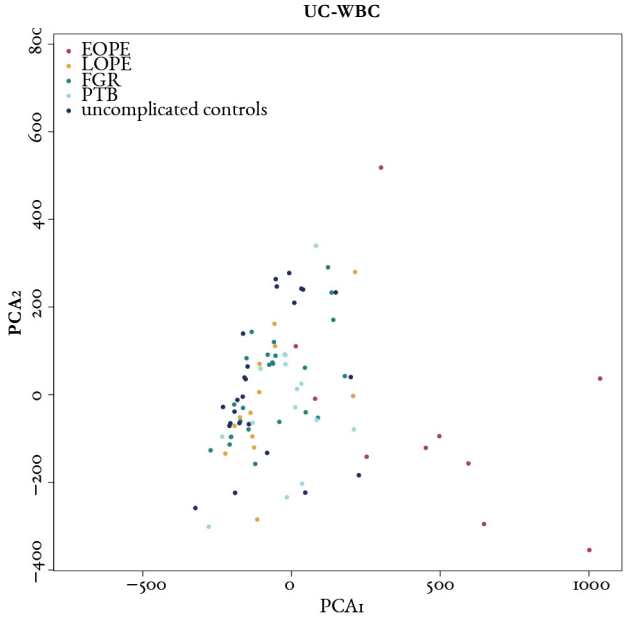

B

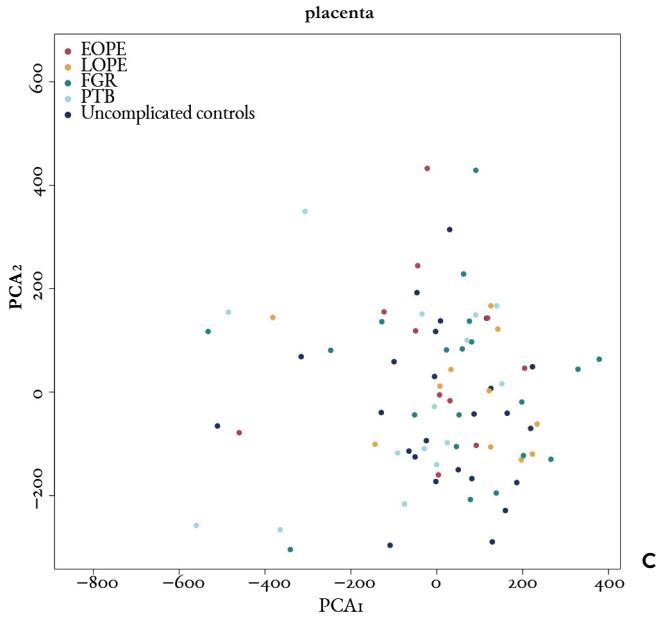

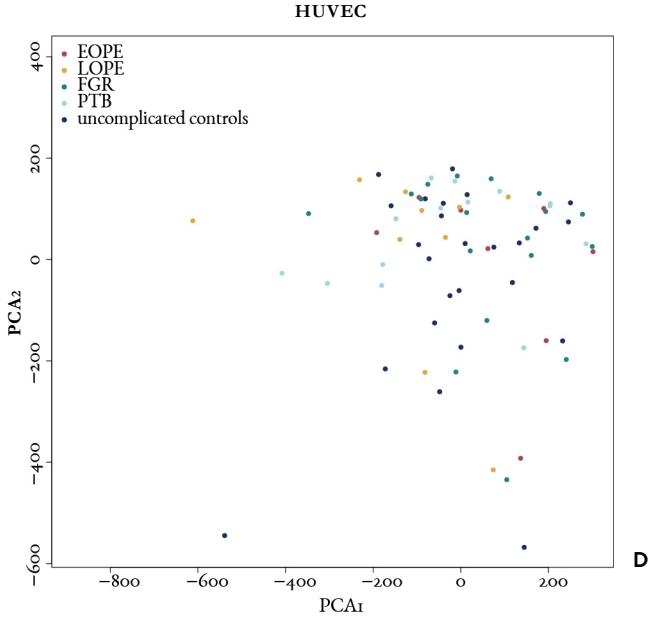

PCA plots show the results of the EWAS using all tissues (A), using only UC-WBC samples (B), using only placental samples (C) and using only HUVEC samples (D). Each dot represents a single patient sample. Red dots represent EOPE-, dark blue dots represent LOPE-, black dots represent uncomplicated control-, green dots represent FGR- and light blue dots represent PTB samples. Distinct clustering is observed between different tissues (A) and between EOPE and (un)complicated controls in UC-WBC samples (B). *EOPE* early-onset preeclampsia; *LOPE* late-onset preeclampsia; *FGR* fetal growth restriction; *PTB* preterm birth; *UC-WBC* umbilical cord white blood cells; *HUVEC* human umbilical vein endothelial cells.

SUPPLEMENTARY TABLE 1. UC-WBC cell leucocyte counts

	EOPE	LOPE	Uncomplicated controls	Complicated controls	
				Normotensive FGR	Normotensive PTB
	(n=13)	(n=16)	(n=36)	(n=27)	(n=20)
Total leucocytes (x10^9/L)	6.39 (2.14)	12.41* (2.92)	13.67* (3.57)	12.38* (3.74)	10.38 (5.40)
Missings of total group	7	7	9	9	8
Missings of group with UC-WBC	4	4	8	6	5
Imputed total leucocytes (x10^9/L)	6.43 (2.11)	11.98 (3.4)	13.22 (3.96)	12.96 (4.17)	9.61 (4.60)

Data are presented as mean (standard deviation).
UC-WBC umbilical cord white blood cells; *EOPE* early-onset preeclampsia; *LOPE* late-onset preeclampsia; *FGR* fetal growth restriction; *PTB* preterm birth.

SUPPLEMENTARY TABLE 2. Number of EOPE DMPs per comparison with different effect-size cut-off values

Effect-size cut-off	EOPE - unc. controls placenta	EOPE - unc. controls HUVEC	EOPE - FGR placenta	EOPE - PTB UC-WBC	EOPE - PTB placenta
None	1 (7x10^{-6} %)	1 (2x10^{-5} %)	1 (7x10^{-6} %)	12,040 (28 %*)	5,668 (0.5 %*)
Hypomethylated	1	1	1	3,457 (29 %)	4,684 (83 %)
Hypermethylated	0	0	0	8,583 (71 %)	984 (17 %)
12.5 % β ~ 0.8 m-value	**1**	**1**	**1**	**5,001**	**869**
(Without duplicate DMPs)				**3,444**	**697**
Hypomethylated				1,417 (28 %)	566 (65 %)
(Hypomethylated without duplicate DMPs)				1,001 (29 %)	467 (67 %)
Hypermethylated				3,584 (72 %)	303 (35 %)
(Hypermethylated without duplicate DMPs)				2443 (71 %)	230 (33 %)
20 % β ~ 1.3 m-value	1	1	1	569	58

EOPE DMPs versus (un)complicated control groups per tissue. No LOPE DMPs were identified. The effect-size cut-off value 12.5 % β ~ 0.8 m-value and corresponding DMPs depicted in bold were applied during final data analysis
EOPE early-onset preeclampsia; *LOPE* late-onset preeclampsia; *FGR* fetal growth restriction; *PTB* preterm birth; *UC-WBC* Umbilical Cord Blood; *HUVEC* Human Umbilical Vein Endothelial Cells; *DMPs* differentially methylated positions.
* This % is calculated by dividing the number of significant CpGs by the total number of probes used per tissue: n=43,488 UC-WBC probes, n=134,700 placental probes.

SUPPLEMENTARY TABLE 3. is available at the website of the scientific journal in which this part of the thesis has been published.

SUPPLEMENTARY TABLE 4. EOPE DMP enrichment in the gene-centric and CpG-density annotation of UC-WBC- and placental DMPs

	EOPE-PTB UC-WBC		EOPE-PTB placenta	
	n (%)	OR (95% CI)	n (%)	OR (95% CI)
DMP enrichment in the gene-centric annotation				
Intergenic region	635 (13 %)	0.53* (0.49-0.58)	151 (17 %)	0.63* (0.53-0.75)
Distal promotor	306 (6 %)	1.08 (0.96-1.23)	63 (7 %)	1.22 (0.93-1.58)
Proximal promotor	1,071 (22 %)	0.76* (0.71-0.82)	231 (27 %)	0.98 (0.84-1.15)
Gene body	2,870 (57 %)	1.71* (1.61-1.82)	393 (45 %)	1.25* (1.09-1.44)
Downstream region	119 (2 %)	1.00 (0.82-1.22)	31 (4 %)	1.49* (1.01-2.14)
DMP enrichment in the CpG-density annotation				
CpG island	213 (4 %)	0.23* (0.20-0.26)	263 (30 %)	1.33* (1.15-1.54)
CpG shore	1,043 (21 %)	0.77* (0.71-0.83)	233 (27 %)	1.15 (0.98-1.34)
CpG shelf	797 (16 %)	1.54* (1.41-1.67)	75 (9 %)	0.93 (0.73-1.18)
non-CpG island	2,948 (59 %)	1.61* (1.52-1.71)	298 (34 %)	0.72* (0.62-0.83)

UC-WBC Umbilical Cord Blood; *HUVEC* Human Umbilical Vein Endothelial Cells; *OR* Odds ratio; *CI* Confidence interval. * $p < 0.05$.

CHAPTER 8

DNA hypomethylation of placental growth factor and decreased SAM:SAH ratio in placental tissue of preeclampsia-complicated pregnancies

S.G. Heil, E.M. Herzog, P.H. Griffioen, B.D. van Zelst, S.P. Willemsen,
R.P.M. Steegers-Theunissen and E.A.P. Steegers

Submitted

ABSTRACT

Introduction. The pathophysiology of preeclampsia is largely unknown. Aberrant DNA methylation might be involved in the etiology of preeclampsia (PE). Serum placental induced growth factor (PlGF) levels are decreased during second trimester pregnancy. We hypothesize that placental levels of *PlGF* DNA methylation are lower in PE pregnancies. In addition, we measured long-interspersed nuclear element-1 (*LINE*-1) and S-adenosylmethionine (SAM) and S-adenosylhomocysteine (SAH) levels in placental tissue to assess global methylation status.

Methods. Placental tissue of 22 PE pregnancies (11 early onset PE (EOPE) and 11 late onset PE (LOPE)) and 60 controls (25 uncomplicated controls and 35 complicated controls including 20 fetal growth restriction and 15 preterm births) was collected from a nested case-control study in The Rotterdam Periconceptional Cohort. DNA was isolated from placental tissue and was treated with sodium bisulfite. Methylation of *LINE-1* and *PlGF* genes was analyzed by Sequenom Epityper and SAM and SAH were measured by LC-ESI-MS/MS.

Results. Placental SAM levels were significantly lower in placental tissue of PE pregnancies compared to uncomplicated and complicated controls resulting in a lower SAM:SAH ratio (β -0.30 and β -0.29 respectively, $p < 0.05$). *PlGF* DNA hypomethylation was observed in PE cases versus controls (β -0.30, $p = 0.005$). Stratification according to onset of PE showed that these effects were more pronounced in EOPE (β -0.42, β -0.46 and β -0.47 respectively for SAM, SAM:SAH ratio and *PlGF* DNA methylation, $p < 0.05$). No significant differences were observed for SAH and *LINE-1* DNA methylation.

Discussion. Placental *PlGF* gene is hypomethylated in preeclampsia. Together with disturbed SAM:SAH ratio this underlines the possible role of placental DNA methylation in the pathophysiology of PE, which needs to be further addressed.

INTRODUCTION

Preeclampsia (PE) is one of the most severe maternal pregnancy complications worldwide and affects 2-8% of all pregnancies [3]. The pathophysiological mechanism is not fully understood and therapy is mostly aimed at reducing blood pressure rather than to cure the disease. The molecular mechanism is thought to involve defective invasion of the spiral arteries into the maternal blood stream, which leads to maternal endothelial dysfunction and concomitant high blood pressure [3, 173]. However, preeclampsia is a heterogeneous disorder: it can occur as early-onset (EOPE; ≤34 weeks of gestation) or late-onset (LOPE; >34 weeks of gestation) disease. Both phenotypes share common risk factors but differences also exists: EOPE is associated with more adverse (fetal) effects compared to LOPE [174].

Several studies demonstrated an imbalance in the release of soluble fms-like tyrosine kinase (sFlt-1) and placental growth factor (PIGF) into the maternal blood stream in preeclamptic women [175-177]. The presence of sFlt-1 competes with Flt-1 in the binding of *PlGF* and causes maternal endothelial dysfunction resulting in preeclampsia. During second trimester pregnancy elevated levels of sFLt-1 and decreased levels of PIGF have been observed in preeclamptic complicated pregnancies compared to normotensive pregnancies resulting in an increased sFlt-1/PlGF ratio [175, 178, 179].

Previously, we and others demonstrated a role of one-carbon metabolism in relation to PE [3, 180-183]. This metabolism donates methyl groups for cellular methylation reactions. S-adenosylmethionine (SAM) donates its methyl group to DNA after which S-adenosylhomocysteine (SAH) is formed. SAH can be hydrolyzed into homocysteine by SAH hydrolase by a reversible reaction. SAH is suggested to be a potent inhibitor of methylation reactions [184]. Elevated levels of plasma homocysteine, which is a sensitive marker of disturbed 1-carbon metabolism, has been shown to be associated with elevated levels of SAM and SAH, decreased global DNA methylation (such as methylation of *LINE*-1 repetitive elements) and decreased methylation of imprinted genes [184-186].

We hypothesized that DNA methylation is decreased in placental tissue of PE pregnancies and assessed SAM and SAH levels, global DNA methylation and methylation of the *PlGF* gene in placental tissue of PE pregnancies compared to uncomplicated and complicated control pregnancies.

METHODS

Placental material. Between June 2011 and June 2013 placental tissue was collected as part of the Rotterdam Periconceptional Cohort (Predict study), an ongoing prospective tertiary hospital-based cohort conducted at the Erasmus MC University Medical Centre Rotterdam [32]. EOPE and LOPE cases were both selected as PE cases. Uncomplicated pregnancies were selected as controls. In addition, we selected placental tissue from fetal growth restricted (FGR) pregnancies and preterm births (PTB) to reduce confounding.

PE was defined according to the International Society for the Study of Hypertension in Pregnancy as gestational hypertension of at least 140/90 mmHg accompanied by an urine protein/creatinine ratio of ≥ 30 mg/mmol, arising de novo after the 20th week of gestation. EOPE and LOPE were defined as being diagnosed before and after 34 weeks of gestation, respectively [44]. Uncomplicated control pregnancies were defined as pregnancies without PE, gestational hypertension, FGR or PTB. FGR was defined as estimated fetal weight below the 10th percentile for gestational age. Birthweight percentiles were calculated according to the reference curves of the Dutch Perinatal Registry [47]. PTB was defined as spontaneous delivery between 22 and 37 weeks of gestation. Woman with multiple birth pregnancies or pregnancies complicated by fetal congenital malformations were excluded from this study. All women agreed to take part of this study and the study protocol was approved by the medical ethical committee of the ErasmusMC (METC number 2004-227).

Sample collection. Within 30 minutes after delivery of the placenta, samples of 0.5 cm^3 were taken from the fetal side of the placental tissue at 4 different sites in a 3 cm radius around the umbilical cord insertion, after carefully removing the membranes and 2 mm of the top placental layer. Placental tissue from 4 different sites was quickly rinsed in PBS and was snap frozen in liquid nitrogen in Eppendorf tubes and was stored at -80° until further analysis. Placental tissue was grinded from 30 mg tissue and frozen placental powder was directly added to a cell lysis buffer and stored in Eppendorf tubes at -80 °C until DNA analysis. Subsequently, genomic DNA was extracted using the Allprep DNA/RNA isolation mini kit (Qiagen, Hilden, Germany), according to manufacturer's instructions. SAM and SAH measurements were performed in a different biopsy from the fetal side as described above. One aliquot of grinded placental tissue was mixed in an acidic saline solution (800µl saline, 80µl 1M Acetic Acid) for SAM, SAH and total protein measurement. A second grinded tissue aliquot was mixed

in cell lysis (600µl) solution Puregene core kit A (Qiagen, Germany) for DNA extraction. Cell lysis was performed overnight (55 °C) and DNA extraction was performed accordingly to the instructions of the manufacturer.

SAM and SAH measurements. In short, the acidified placental extracts were neutralized with 1 M NH_3 and subjected to an SPE sample clean-up. 10 µl of sample was then injected on a 50x2.1 mm HPLC Atlantis C_{18} column (Waters, Etten-Leur, the Netherlands) and eluted using a methanol gradient in 0.1% aqueous acetic acid. Detection was performed on a Quattro Premier XE mass spectrometer (Waters, Etten-Leur, the Netherlands). The concentration of total protein in the grinded placental extracts was determined on a Cobas 701 analyzer using the urine/CSF total protein test kit (Roche Diagnostics, Almere, the Netherlands). The amount of SAM and SAH was expressed as nmol/g protein.

Quantification of DNA methylation. Global DNA methylation was measured by *LINE*-1 repetitive elements (Genbank: X58075) as previously described by Wang et al [187]. Primers of *PLGF* gene were designed according to genbank sequences NC_000014.9 (*PLGF*). The following primers were selected: L1-FOR: 5'-aggaagagagGTGTGAGGTGTTAGTGTGTTTTGTT -3', L1-REV 5' -cagtaatacgactcactatagggagaaggctATATCCCACACCTAACTCAAAAAAT -3', *PLGF*-FOR 5'-aggaagagagGTTGGATTTTTGGATGTTTTTATTT -3', and *PLGF*-REV 5'-cagtaatacgactcactatagggagaaggctCAAACAACAACTCCCTTCT AAAACT -3'. DNA (500ng) was bisulfite treated with EZ DNA methylation kit (Zymo research, USA) according to the instructions of the manufacturer. Bisulfite treated DNA was dissolved in a Tris/0.1xEDTA buffer in a final concentration between 5 and 7 ng/µL. All bisulfite treated DNA samples were stored at -80 °C. PCR was performed in quadruplicate within 30 days after bisulfite treatment and all PCR reactions were performed simultaneously. Methylated DNA and unmethylated DNA control (Zymo research, USA) were mixed in a 4:1 ratio as a positive control. In addition, genomic DNA isolated from blood leucocytes was used throughout the whole procedure as a positive control. Bisulfite treatment was performed for 20 samples each run and contained both the zymo control as well as the blood sample control besides 18 placental samples. PCR (quadruplicate) was performed in a total volume of 12µl. Reaction mixture contained buffer 1x, dNTP (0.2mM), $MgCl_2$ (1.5mM), forward/research primer (4 pmol), Amplitaq Gold (0.5 units, Life Technologies, the Netherlands) and 2µl bisulfite treated DNA. PCR program followed a touch down procedure with an initial denaturation at 95° for 10 min. First 5 cycles of denaturation at 95° for 20 sec, annealing at 65° for 30 sec, elongation at 72°

for 1 min. Second 5 cycles of denaturation at 95° for 20 sec, annealing at 58° for 30 sec, elongation at 72° for 1 min. Followed by 39 cycles of denaturation at 95° for 20 sec, annealing at 53° for 30 sec, elongation at 72° for 1 min and a final elongation at 72° for 3 min. 3µl of the PCR product was tested on gel. All PCR products were stored at -20 °C until sequenom analysis. Sequenom analysis (triplicate) was performed accordingly to the instructions of the manufacturer. All samples for *LINE*-1 measurement were analyzed on a single spectrochip, the same was done for *PlGF* measurement. Methylation percentage was called by MassARRAY Epityper Analyzer Software (Sequenom, USA).

Validation of LINE-1 and PlGF methylation assays. *LINE*_1 amplicon detected 8 CpG sites of which CpG site 4 was omitted because of a silent signal and CpG_10 could not be measured because of low mass. Mean percentage of methylation, standard deviation (SD), and coefficient of variation (CV) were calculated from triplicate measurements of each CpG site. Triplicates with CV>10% were checked for outliers (±3SD) and I single outliers were removed if the remaining duplicate measurement resulted in a CV<10%. The *PlGF* amplicon consisted of 15 CpG sites of which 6 CpG sites were omitted due to low/high mass or silent signal. Of the 9 CpG sites that potentially could be quantified only CpG site 1 could be quantified. Other 8 CpG sites had a methylation of less than 5%, which resulted in a CV>20%. Mean percentage of methylation, SD, and CV were calculated from triplicate measurements of each CpG site. Mean methylation of *PLGF* was lower than *LINE-1* methylation and for this reason we could not measure *PLGF* methylation with the same precision as *LINE*-1. We therefore used <CV20% as cut-off instead of 10%. Triplicates with CV>20% were checked for outliers (±3SD) and single outliers were removed if the remaining duplicate measurement resulted in a CV<20%.

Measurement of global and gene specific DNA methylation. S-adenosylmethionine (SAM) and S-adenosylhomocysteine (SAH) concentrations were determined in grinded placental tissue with an isotope dilution liquid chromatography tandem MS method (ID-LC-MS/MS) as adapted from Gellekink et al. [188]. Global DNA methylation was measured by *LINE*-1 repetitive elements as previously described by Wang et al [187]. *PLGF* methylation was quantified by Sequenom Epityper. DNA (500ng) was bisulfite treated with EZ DNA methylation kit (Zymo research, USA) according to the instructions of the manufacturer and was used for Sequenom Epityper measurements.

Statistical analysis. Means with SD were calculated from normal distributed variables and median with range were presented for skewed variables. Differences

in maternal and neonatal characteristics between different groups were calculated with ANOVA for normal distributed variables and Kruskal-Wallis test for skewed variables. To assess whether differences occurred in DNA methylation markers between PE complicated pregnancies and control pregnancies an univariate linear model was applied which was corrected for birthweight and gestational age. *LINE*-1 amplicon was analyzed as the mean of all CpGs per sample to assess methylation of the whole differentially methylated region (DMR). In order to assess whether differences existed between EOPE, LOPE and controls an univariate analysis of variance was applied with correction for birthweight and gestational age followed by post-hoc Bonferroni analysis to correct for multiple comparisons. Standardized betas with corresponding p-values were calculated with linear regression analysis. P <0.05 was considered to be significantly. Bonferroni correction was applied to correct for multiple comparisons of independent methylation markers. We accounted for five independent multiple comparisons (SAM, SAH, SAM:SAH ratio, *LINE-1* methylation and *PlGF* methylation). P <0.01 was considered significant after Bonferroni correction (i.e. p = 0.05/5). Correlation between methylation markers was assessed with Pearson correlation. P <0.05 was considered significant. Data are available on request with the first author.

RESULTS

Baseline descriptives. Descriptives of the cohort are depicted in **Table 1**. Gestational age and birthweight were significantly different between groups (p <0.05). In addition, PE cases had lower gestational age and lower birthweight compared to uncomplicated and complicated controls (p <0.05). 50% of PE women exhibited EOPE (p <0.05). Nulliparity occurred more frequently in PE cases than controls.

Placental SAM and SAH levels. SAM levels and SAM:SAH ratio were significantly lower in placental tissue from PE pregnancies compared to controls (β -0.30 and β -0.29 respectively, p <0.05, **Table 2**). SAH was not significantly different. Post-hoc analysis demonstrated lower placental SAM levels and lower SAM:SAH ratio in EOPE compared to controls (β -0.42 and β -0.46 respectively, p <0.05, **Table 2, 3** and **Figure 1**). SAM and SAM:SAH ratio in LOPE was not significantly different from controls, **Table 3**).

Placental PlGF and LINE-1 DNA methylation. Placental *PlGF* DNA methylation was significantly lower in PE pregnancies compared to controls (β -0.30, p = 0.005, **Table 2** and **Table 3**). Additional analysis according to the origin of PE

TABLE 1. Maternal and neonatal characteristics

	Cases		Controls			
	EOPE N=11	LOPE N=11	Uncomplicated controls N=25	Normotensive FGR controls N=20	Normotensive PTB controls N=15	p-value*
Maternal						
Age (y)	31.2 ± 4.0	33.6 ± 4.7	31.8 ± 5.3	29.6 ± 6.3	31.4 ± 3.3	0.30
SBD (mm/Hg)	174 ± 19	150 ± 10	129 ± 12	130 ± 14	126 ± 17	<0.001#
DBD (mm/Hg)	99 ± 16	94 ± 11	76 ± 6	75 ± 9	79 ± 14	<0.001#
Nulliparous, n (%)	9 (82)	11 (100)	8 (32)	13 (65)	8 (53)	0.001#
Neonatal						
Sex (male), N (%)	3 (27)	5 (45)	14 (56)	12 (60)	7 (47)	0.46
Gestational age (days)$	215 (58)	265 (46)	279 (30)	267 (27)	245 (101)	<0.001#
Birthweight (grams)	1181 ± 356	3363 ± 662	3788 ± 398	2451 ± 362	2259 ± 958	<0.001#
Birthweight <10th percentile, N (%)	0 (0)	1 (9)	0 (0)	20 (100)	0 (0)	<0.001#

Data are presented as mean ± standard deviation or as $median (range) for skewed variables for continuous variables and as number and percentage for dichotomous variables. *ANOVA p-value to examine differences for normal distributed variables and Kruskal Wallis test p-value for skewed variables between all groups; #p <0.05 for cases versus controls

TABLE 2. Methylation markers in cases and controls

	Cases		Controls			
	EOPE N=11	LOPE N=11	Uncomplicated controls N=25	Normotensive FGR controls N=20	Normotensive PTB controls N=15	p-value*
SAM (nmol/g protein)	397 ± 109	345 ± 119	384 ± 147	360 ± 128	568 ± 241	0.02#
SAH (nmol/g protein)	95.8 ± 27.0	79.7 ± 29.0	78.5 ± 28.4	76.5 ± 31.8	84.1 ± 27.1	0.75
SAM:SAH ratio	4.4 ± 1.4	4.9 ± 2.4	5.3 ± 2.0	5.1 ± 2.3	6.8 ± 2.1	0.07#
LINE-1 DMR methylation(%)	22.1 ± 2.4	22.7 ± 1.9	22.8 ± 2.1	22.0 ± 2.5	22.3 ± 2.9	0.15
PIGF methylation (%)$	13.3 [9.7)	13.0 [5.7]	14.0 [12.0]	12.2 [14.0]	15.2 [22.3]	<0.001#

Data are presented as mean ± standard deviation or as $median (range) for skewed variables. *p-value of univariate analysis of variance between all groups corrected for differences for birthweight and gestational age; #p <0.05 for difference between cases and controls of univariate analyses corrected for birthweight and gestational age

TABLE 3. Univariate linear regression analysis of methylation markers in placental DNA from PE, EOPE and LOPE versus controls

	PE N=22		EOPE N=11		LOPE N=11	
	Beta	p-value	Beta	p-value	Beta	p-value
SAM	-0.30	0.006*	-0.42	0.002*	-0.12	0.27
SAH	0.07	0.58	0.11	0.49	0.03	0.81
SAM:SAH ratio	-0.29	0.01	-0.46	0.002*	-0.11	0.36
LINE-1 DMR methylation	-0.04	0.74	-0.17	0.27	0.04	0.73
PIGF methylation	-0.30	0.005*	-0.47	0.001*	-0.09	0.38

Adjusted standardized beta of linear regression analysis corrected for birth weight and gestational age compared to uncomplicated and complicated

showed lower levels of placental *PlGF* methylation in EOPE compared to controls (β -0.47, p = 0.001, **Table 2, 3** and **Figure 1**). Placental *PlGF* DNA methylation was not significantly lower in LOPE placentas compared to controls (table 3). Placental *LINE*-1 methylation was not significantly different between cases and controls.

Correlation of methylation markers. *PlGF* DNA methylation was significantly correlated to SAM levels (R = 0.35, p = 0.002) and *LINE-1* DNA methylation (R = 0.42, p <0.001), although correlation coefficients were weak (R<0.80). No significant correlation was present between *PlGF* DNA methylation, SAH levels (R = 0.13, p = 0.26) and SAM:SAH ratio (R = 0.21, p = 0.06) and between *LINE*-1 methylation and SAM (R=-0.04, p = 0.72), SAH (R= 0.012, p = 0.92) or SAM:SAH ratio (R=-0.11 p = 0.34).

DISCUSSION

The pathophysiological mechanism of PE is unknown and studies have suggested a role of epigenetics. However, results are contradictory as some studies show placental hypomethylation and others show hypermethylation. We show significantly lower SAM and SAM:SAH ratio and *PlGF* hypomethylation in placental tissues from PE pregnancies, which is most pronounced in EOPE pregnancies.

Several studies have investigated DNA methylation at a global scale or focused on candidate genes [163, 189, 190]. Results from genome-wide studies using methylation arrays provided evidence for a role of some novel epigenetic loci although these results need to be validated in larger cohorts [153, 191]. In these studies *PlGF* was not identified as target locus in PE. However, most studies were underpowered or were not able to correct for differences in gestational age, which might have contributed to type I or II errors.

In our study we assessed placental methylation status of *PlGF* in PE complicated pregnancies and compared this to uncomplicated pregnancies and pregnancies complicated by FGR and PTB. We demonstrated *PlGF* hypomethylation in placental tissue from PE pregnancies compared to uncomplicated and complicated controls. Stratification according to moment of disease onset demonstrated *PlGF* DNA hypomethylation in EOPE pregnancies whereas no significant changes were observed in LOPE pregnancies. After correction for multiple testing with Bonferroni adjustment significance remained, which underlines a pathophysiological role of *PlGF* hypomethyation in PE. A previous study by Gao et al. demonstrated DNA hypermethylation of *LINE*-1 and *H19* promoter hypermethylation in placental tissue of EOPE pregnancies compared to uncomplicated controls [189]. However, in that study differences in

FIGURE 1. Placental methylation markers in EOPE, LOPE and controls

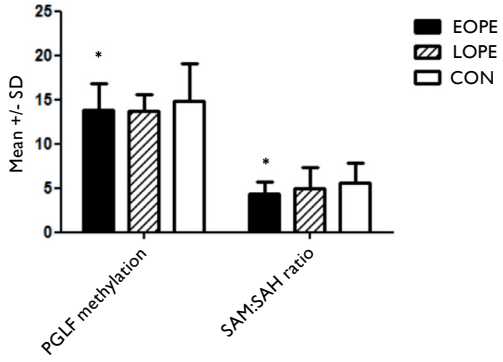

Mean PlGF DNA methylation (%) and SAM:SAH ratio in placental tissue of EOPE (n=22, black bar), LOPE (n=11, hatched bar) and controls (n=42, white bar). *P<0.05 Univariate analysis of variance corrected for gestational age and birthweight.

gestational age between PE cases and controls might have accounted for the observed differences. In our study we analyzed, in addition to uncomplicated controls, also complicated controls to adjust for differences in gestational age and birthweight. However, as differences in gestational age and birthweight still existed between PE pregnancies and uncomplicated and complicated controls we corrected all analyses for gestational age and birthweight. We observed lower SAM and SAM:SAH levels and *PlGF* hypomethylation in PE versus controls. We were not able to demonstrate differences in placental *LINE-1* methylation between PE pregnancies and controls. Not many studies have investigated the role of global methylation measured by *LINE*-1 repeats in preeclampsia. Placental *LINE-1* DNA hypermethylation was found in two studies [189, 192]. In addition, Nomura et al. reported lower levels of global placental methylation in preeclampsia by using an Luminometric Methylation Assay (LUMA) [193]. In another study, placental *LINE*-1 methylation was not altered in hypertensive disorders compared to normotensive controls. This is in agreement with our result that *LINE*-1 methylation in placental tissue of PE complicated pregnancies is not different from control pregnancies. However, more studies are necessary to draw a firm conclusion.

Placental *PlGF* mRNA expression has been demonstrated to be lower

in PE [194]. In our study we found DNA hypomethylation of *PlGF*, which might be a promising biomarker in early prediction of PE. In line with the general idea that DNA methylation of regulatory parts of genes are associated with lower expression, our findings of lower methylation would suggest increased mRNA expression of *PlGF*. In addition, the mean difference in *PlGF* methylation in PE cases compared to controls is relatively modest (~1%) and therefore future studies are necessary to replicate *PlGF* hypomethylation and to assess whether it is associated with altered *PlGF* mRNA and *PlGF* protein levels.

Based on the previous described role of one-carbon metabolism in relation to PE we hypothesized that placental levels of SAM, SAH and SAM:SAH ratio would be altered in PE. Indeed we showed lower SAM with concomitant lower SAM:SAH ratio in placental tissue of PE cases compared to complicated and uncomplicated controls. SAM:SAH ratio has been described as the methylation potential of the cell and a lower SAM:SAH ratio is expected to be associated with less methylation. Our finding of lower SAM:SAH ratio is in line with our finding of *PlGF* hypomethylation, although we were not able to demonstrate a strong correlation between these markers.

This is the first study that assessed placental DNA methylation of *PLGF* and global markers of methylation in preeclampsia. We showed placental *PLGF* DNA hypomethylation and lower SAM and SAM:SAH ratio in PE woman compared to controls.

CHAPTER 9
General discussion

CHAPTER 10
Summary / Samenvatting
De dans van DNA: een aanvulling op de Nederlandse samenvatting

PART 03

CHAPTER 9

General discussion

PE is one of the major pregnancy disorders associated with maternal and fetal morbidity and mortality and an increased risk of cardiovascular disease in later life for both mother and child. In this thesis we have investigated the cardiovascular development and epigenetic programming of placental and newborn tissues after exposure to EOPE and LOPE, in order to provide novel insights into the association with later cardiovascular disease risk, and its underlying mechanisms. The following objectives have been studied:

1. The development of placental and newborn cardiovascular tissues in association with EOPE and LOPE (a), and of the maternal microcirculation in association with PE (b) (**Part I**)
2. The tissue-specific DNA methylation in placental and newborn cardiovascular tissues in association with EOPE and LOPE (**Part II**)

We have performed flow-cytometric, histological and (genome-wide) epigenetic analysis. The main findings, the clinical implications and directions for future research are discussed below.

MAIN FINDINGS

1a. The association between EOPE and LOPE and a disturbed development of placental and newborn cardiovascular tissues

During embryonic and fetal development, haematopoiesis and vasculogenesis are closely related and influenced by environmental conditions, such as blood flow, oxygen tension, oxidative stress and epigenetic factors [52] [21]. We observed that EOPE exposure is associated with disturbed haematopoiesis by revealing a four to sevenfold decrease of neutrophil count and fivefold increase of NRBC count in UCB (**chapter 2**). Additionally, we found that PE exposure was associated with a smaller umbilical vein area and vein wall thickness and LOPE with a larger placental width (**chapter 3**).

These findings suggest that PE exposure results in poor intrauterine conditions that are related to a disturbed development of both haematopoiesis and vasculogenesis. In PE pregnancies, early placental morphology is assumed to be characterised by superficial trophoblast invasion and insufficient remodelling of spiral arteries in the myometrium, causing suboptimal placentation with episodes of placental hypoxia and reperfusion [31]. As a result, the production of inflammatory cytokines in the maternal and fetal circulation increases, which promotes the production of reactive oxygen species (ROS) by up to 40% in comparison to normal placentas [31, 51]. The developing embryo and fetus are thus

exposed to excessive levels of oxidative stress, partly because the suboptimal placenta during PE also displays a reduced antioxidant capacity [31]. Various important developmental processes are however dependent on tightly controlled oxidative stress exposure, such as cellular signalling, differentiation and proliferation [12, 195]. Haematopoiesis and vasculogenesis are therefore believed to be highly affected by the excessive oxidative stress exposure during PE pregnancies. Especially the vascular endothelium is known to be extremely susceptible to oxidative damage, due to its low cytoprotective capacity, as demonstrated in rodents [31].

Not only the exposure of tissues to excessive oxidative stress, but also to the dysbalance of angiogenic and antiangiogenic factors of placental origin could contribute to the disturbance of several developmental processes, later in pregnancy. The antiangiogenic factors soluble fms-like tyrosine kinase-1, (sFlt-1, also known as soluble vascular growth factor (VEGF) receptor -1) and soluble endoglin (sEng) are increased in plasma of PE patients. sFlt-1 and sEng promote vascular dysfunction, capillary permeability, liver dysfunction and neurological abnormalities via antagonisation of proangiogenic factors such as VEGF and placental growth factor (PlGF) and are therefore potential underlying factors for especially the decreased umbilical vein wall thickness in PE [12, 31]. In chapter 8 of this thesis we describe lower DNA methylation of *PlGF* in EOPE exposed placental tissue, supporting the involvement of these (anti)angiogenetic factors in our data.

Furthermore, the exposure to excessive oxidative stress and (anti) angiogenic factors results in a general enhanced inflammatory state of the maternal and fetal circulation, inducing endothelial cell dysfunction. Because prenatal haematopoiesis originates from endothelial cells in the ventral aorta of the developing embryo, fetal endothelial damage may therefore not only affect fetal vasculogenesis, but also the maturation and development of fetal haematopoiesis. Another reason to suggest a close relationship between disturbed haematopoiesis and vasculogenesis in PE, is the known involvement of placental over-expression of protein HIF-1α, due to the early suboptimal placental perfusion and prolonged hypoxic placental state in EOPE pregnancies [59, 60]. HIF-1α regulates several processes such as angiogenesis, glycolysis and erythropoiesis, through erythropoietin-release [59]. Although we did not measure HIF-1α, placental over-expression of HIF-1α may explain both the enhanced NRBC counts in UCB in EOPE and the decreased umbilical vein wall thickness in PE.

Interestingly, the above findings from our clinical studies suggesting disturbed haematopoiesis and vasculogenesis are largely substantiated by

the results of our epigenome-wide analysis in Part II of this thesis, where we observed differential DNA methylation in association with EOPE in placental tissue and umbilical cord white blood cells (UC-WBC), in genes associated with inflammatory responses, haematological system development, erythrocyte differentiation in particular and regulation of cell differentiation and cardiovascular development.

EOPE and LOPE demonstrated pronounced differences in our data on UCB cell populations and morphology of the placenta and umbilical cord, and have been proposed as two distinct disease entities [11]. The difference is best understood by the placental involvement in both phenotypes, and is clearly illustrated by the opposite placental measurements in EOPE and LOPE in chapter 3. A negative association was demonstrated with placental weight, length and width in EOPE, dependent of gestational and birth weight, in contrast to a positive association with placental width in LOPE. This discrepancy may be explained by the concept of initial poor and restricted placental development in EOPE, whereas in LOPE, trophoblast dysfunction at the end of gestation may be due to villous overcrowding in large, term placentas without prior pathology [13]. Additionally, in term placentas an increasing uterine contractility occurs, causing suboptimal intervillous perfusion and a potential degree of hypoxia-reperfusion injury thereby inducing ROS production [196]. Both phenotypes are thus characterised by placental induced generation of excessive oxidative stress, but this occurs much later in gestation in LOPE, explaining why the fully developed fetal haematopoiesis as well as the fully developed umbilical cord (vasculature) at term are less affected in LOPE than in EOPE (**Figure 2A and B, association A1 and B1**).

Although EOPE displayed more severe features of disturbed vasculogenesis than LOPE, a higher dependency of gestational age and birth weight was observed. Indeed, also FGR and PTB have been associated with increased cardiovascular risk factors in offspring [69, 70]. However, as suggested by our data and that of others, the intrauterine environment in PE complicated pregnancies seems to be unique and exacerbates or acts in synergy with any risks inferred by PTB or FGR [7, 197]. The strong significant association with a smaller vein area and wall thickness in the total PE group, independent of gestational age and birth weight, demonstrates that the EOPE and LOPE subgroups may in fact be underpowered. Moreover, the dependency of comorbidities FGR and PTB suggests that the severity of placental pathology is relevant in the

association between EOPE and umbilical vascular alterations. The low rate of FGR cases within the EOPE pregnancies however indicates that a relatively small number of pregnancies complicated by severe placental dysfunction leading to FGR was included, which cannot exclude that the observed association is underestimated.

The combination of disturbed leucocyte and NRBC counts in UCB and a decreased umbilical vein wall thickness may actually represent very early features of the increased cardiovascular risk profile in PE offspring in later life, based on the suggested involvement of the following mechanisms. **Firstly,** the observed altered UCB populations in EOPE suggest the involvement of systemic inflammation, which is known to play an important role in cardiovascular disease and metabolic syndrome development. **Secondly**, both observations clearly suggest impaired endothelial function, which is confirmed in PE offspring in childhood and adolescence and has been proposed as the mechanistic link between PE and later cardiovascular disease risk [198-201]. **Thirdly,** the reduced umbilical vein wall thickness may in fact be a proxy for early fetal vascular alterations, explaining why EOPE children have an increased blood pressure or an increased carotid intima media thickness in young adulthood, which is considered a subclinical marker of atherosclerosis [201]. Concentric remodelling has also been observed by increased cardiac wall thickness measurements in offspring at adolescence. This may not seem in agreement with reduced umbilical vein wall measurements, but could be a compensatory mechanism to the exposure of maternal hypertension in utero or the abnormal uteroplacental haemodynamic state in PE [202]. Indeed, a high resistance in the umbilical artery has been associated with low cardiac mass in preschool offspring, substantiating the association between heamodynamics in utero and later structure and function of the cardiovascular system [203]. The observed trend of elastin reduction in the umbilical cord vein in EOPE may be an early feature of arterial stiffness, which is a key determinant of increased blood pressure in adults [204].

Interestingly, the increased risk of high blood pressure and stroke is higher in offspring exposed to EOPE than offspring exposed to LOPE, which is in line with our observations [197]. The current discussion in the literature centers around the potential genetic, behavioural or intrauterine origin of cardiovascular disease development in PE offspring. In response to this discussion, we propose that offspring exposed to EOPE develop a suboptimal cardiovascular phenotype during pregnancy, predisposing them to cardiovascular disease in a relatively

FIGURE 2. A

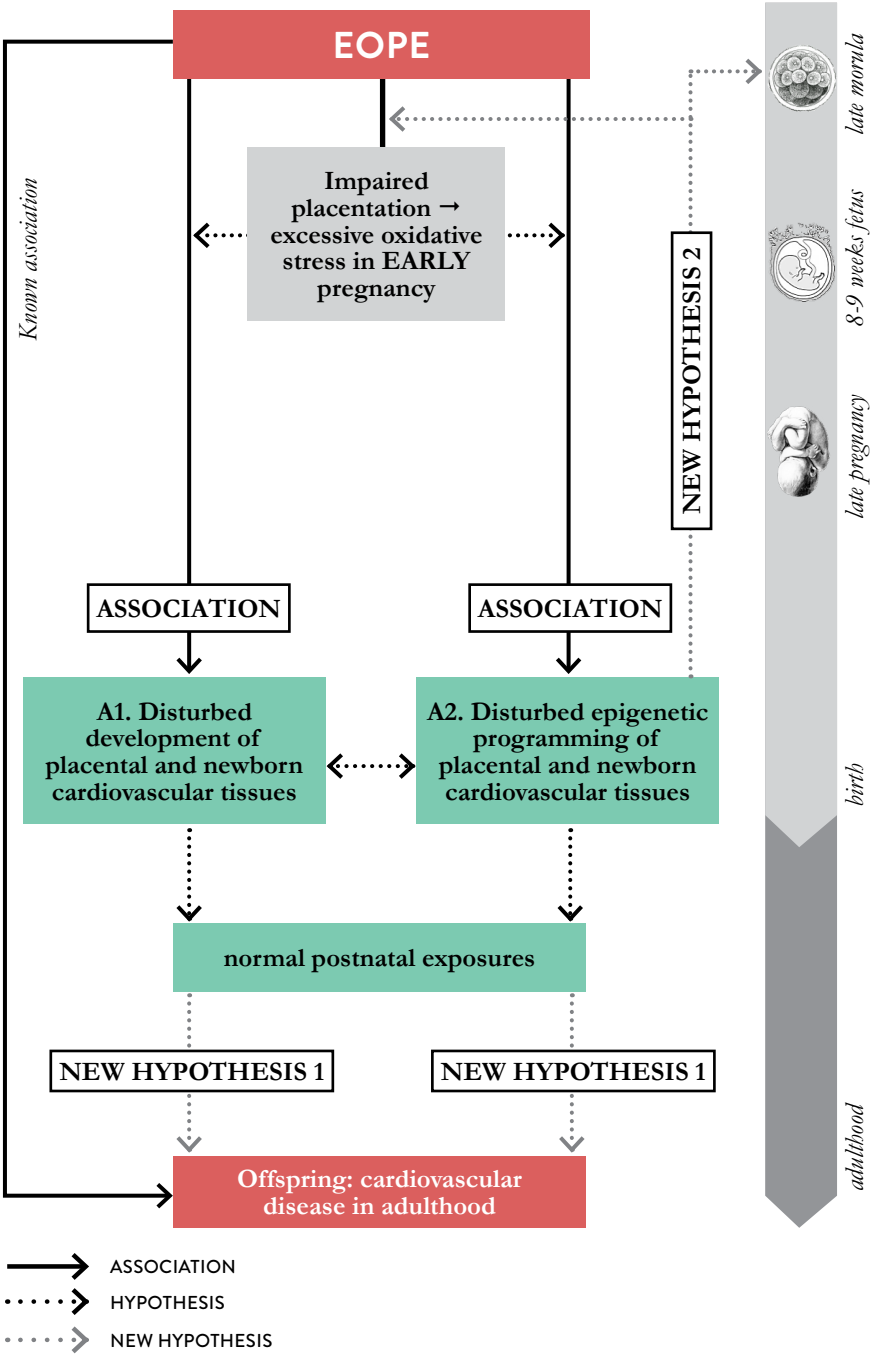
EOPE
Impaired placentation → excessive oxidative stress in EARLY pregnancy
Known association
NEW HYPOTHESIS 2
late morula
8-9 weeks fetus
late pregnancy
birth
adulthood
ASSOCIATION
ASSOCIATION
A1. Disturbed development of placental and newborn cardiovascular tissues
A2. Disturbed epigenetic programming of placental and newborn cardiovascular tissues
normal postnatal exposures
NEW HYPOTHESIS 1
NEW HYPOTHESIS 1
Offspring: cardiovascular disease in adulthood
ASSOCIATION
HYPOTHESIS
NEW HYPOTHESIS

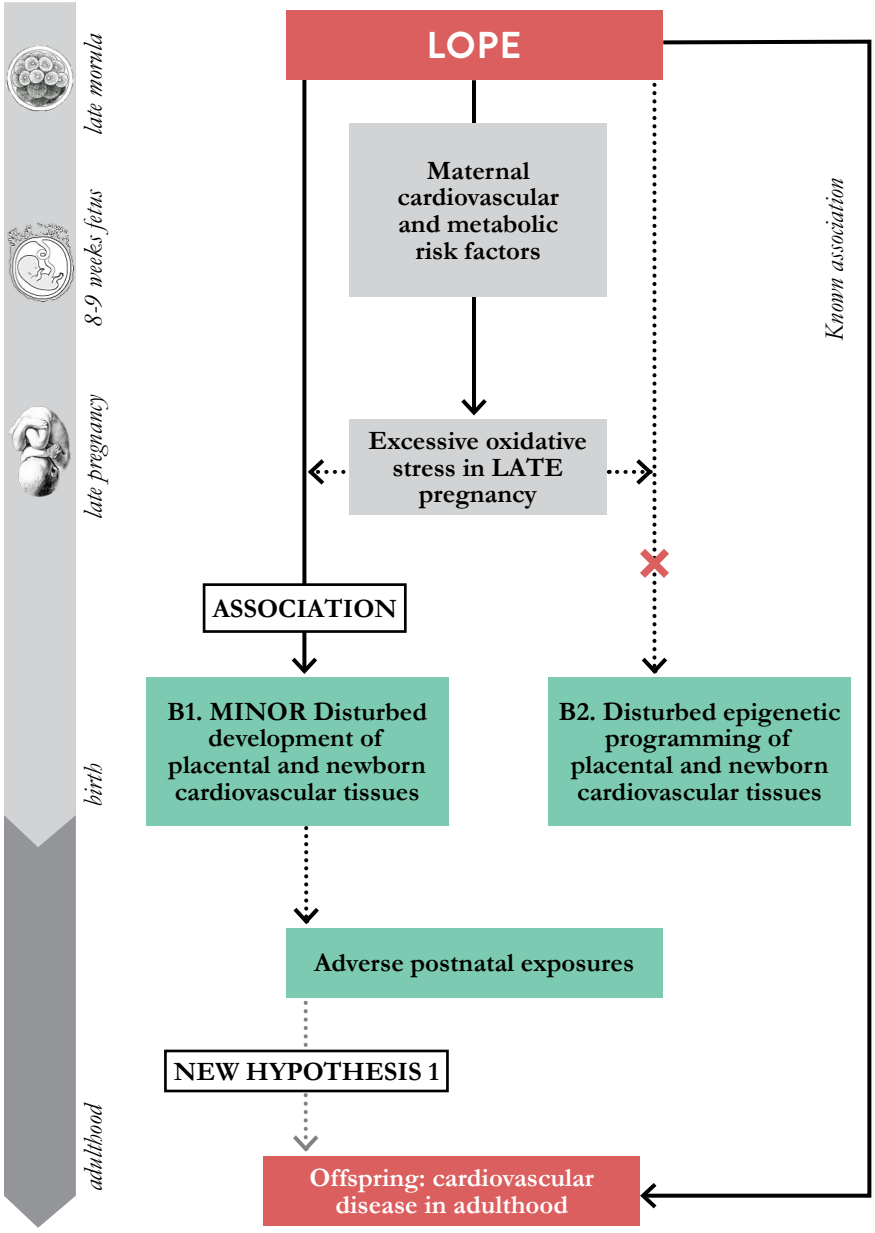
late morula
8-9 weeks fetus
late pregnancy
birth
adulthood
LOPE
Maternal cardiovascular and metabolic risk factors
Excessive oxidative stress in LATE pregnancy
Known association
ASSOCIATION
B1. MINOR Disturbed development of placental and newborn cardiovascular tissues
B2. Disturbed epigenetic programming of placental and newborn cardiovascular tissues
Adverse postnatal exposures
NEW HYPOTHESIS 1
Offspring: cardiovascular disease in adulthood

normal postnatal environment, whereas offspring exposed to LOPE develop a relatively normal cardiovascular phenotype during pregnancy, possibly developing cardiovascular disease merely as an effect of behavioural and environmental risk factors postnatally [197, 205] (**Figure 2A and B, new hypothesis 1**). This is further substantiated by our PE EWAS findings, demonstrating an evident involvement of differential DNA methylation in genes related to cardiovascular, inflammatory and metabolic pathways, in UC-WBC and placental tissue of EOPE pregnancies only (**Part II**).

1b. The association between PE and maternal microcirculation

In severe PE, maternal endothelial dysfunction can results in haemodynamic instability with possible consequences for microcirculatory functioning [3]. The microcirculation consists of vessels with a diameter < 100 μm and is essential for oxygen and nutrient exchange, especially at the level of capillaries. Sublingual microcirculation measurements demonstrated that women with severe PE and HELLP syndrome showed a reduced perfused vessel density, a reduced flow velocity and increased heterogeneity of flow in capillaries, compared with women with severe PE without HELLP syndrome. No statistically significant differences were observed in microcirculatory perfusion between severe PE and healthy controls (**chapter 4**).

The reduced density and velocity of capillary perfusion may be a reflection of microvascular erythrocyte fragmentation and platelet adherence to the damaged endothelial surface of narrowed capillaries, explaining the haemolytic aspect and platelet decrease of HELLP syndrome. Heterogeneity of flow is an important and harmful characteristic of impaired microcirculation, suggesting that the number of perfused capillaries is reduced which results in a disturbance of tissue oxygenation. This may be related to the observed endothelial dysfunction five-eight years after delivery in mothers who experienced PE, accompanied by increased inflammatory and antiangiogenic maternal biomarkers such as sFlt-1 and CRP [199]. The lack of differences in microvascular measurements between severe PE and healthy controls may be related to the fact that endothelial dysfunction is not equally manifested in all vascular beds during PE, and sublingual microcirculation may not be the most representative site of disease. Sublingual microcirculation is believed to be informative in severe haemodynamic imbalanced conditions like sepsis, shock and cardiac disease, because it reflects the splanchnic circulation given their shared embryologic origin, and splanchnic hypoperfusion is an early indicator of systemic hypoperfusion [78].

Evidence is emerging that not only macrocirculatory measures such as blood pressure, but also microcirculatory outcome measures are relevant in the light of adult cardiovascular disease development. The risk of maternal cardiovascular disease is particularly high after EOPE pregnancies, where various maternal cardiac and vascular characteristics are disturbed during pregnancy including the impaired uteroplacental blood flow, increased peripheral resistance and reduced cardiac output [197]. Because impaired maternal microcirculation seems to be involved in the pathophysiology of severe PE/HELLP syndrome [206], this may be an informative measure in light of the cardiovascular disease risk in mothers who experienced PE.

2. The association between EOPE and LOPE and tissue-specific DNA methylation in placental and newborn cardiovascular tissues

Altered programming of the placental and newborn epigenome may be an underlying mechanism for the disturbed development of fetal haematopoiesis and vasculogenesis (**Part I**) and as such, elucidate the association between prenatal PE exposure and cardiovascular disease risk in later life. Because epigenetic programming is essential for lineage differentiation, embryogenesis and placentation in early pregnancy, we aimed to optimize our epigenetic studies by initially addressing the tissue-specific characteristics of DNA methylation in pregnancies without major pregnancy complications such as PE, gestational hypertension, FGR or PTB.

The tissue-specificity of DNA methylation. Firstly we describe significant tissue-specific DNA methylation of imprinted genes *IGF2* in Wharton jelly and *H19* in placental tissue and Wharton jelly, in comparison to UC-WBC methylation patterns. No statistically significant differences were observed between total mean *IGF2/H19* methylation of CD34+ and CD34- UC-MNC fractions (**chapter 5**). Next on a genome-wide level, HUVEC and placental tissue displayed large tissue-specific differences versus UC-WBC in 43% and 73% of the total number of genome-wide measured CpGs respectively, but no differentially methylated regions were identified between UC-MNC and UC-WBC (**chapter 6**).

A comparison between the candidate gene- and genome-wide findings is difficult because we applied different laboratory- and statistical analysis and used different tissues in both studies. However, the similarities between CD34+ and CD34- UC-MNC and between UC-MNC and UC-WBC are in agreement and suggest that DNA methylation levels in different UC-WBC subsets in general seem rather comparable.

The genome-wide analysis revealed the most prominent tissue-specific observations in placental tissue, which is best explained by the time-point of placental-specific development. After fertilisation followed by the global demethylation of the paternally and maternally derived genome, the very first de novo DNA methylation at the late morula-stage determines the initial differential developmental event: lineage separation of the inner cell mass that will give rise to the embryo, and the trophectoderm that will evolve into most of the placental tissue. Inner cell mass methylation is more pronounced than the relatively hypomethylated trophectoderm, resulting in an asymmetrical methylation status from this developmental stage onwards [117, 118, 125]. HUVEC displayed another substantial genome-wide tissue-specific methylation pattern compared to UC-WBC, but less extreme than placental tissue. This can be argued by the fact that HUVEC and the surrounding umbilical cord originate from the inner cell mass [127], thus displays a more common background with UC-WBC [52]. In line with the extensive amount of identified genome-wide HUVEC and placental tDMRs in comparison to UC-WBC, we applied a tissue-specific approach in our EWAS in PE as well.

The association between EOPE and LOPE and tissue-specific DNA methylation in newborns. EOPE demonstrated extensive genome-wide DNA methylation differences in UC-WBC and placental tissue in comparison to PTB pregnancies, whereas in LOPE no significant differential methylation was observed (**chapter 7**). In the candidate-gene study we observed an association between PE and hypomethylation of the *PlGF* gene and lower levels of the SAM:SAH ratio in placental tissue, more pronounced in EOPE than in LOPE **(chapter 8)**.

The PE-related excessive oxidative stress exposure during pregnancy is suggested to be highly involved in the disturbance of epigenetic programming [15]. In response to various forms of stress, cells increase the production of important protective proteins while reducing the translation of others that are temporarily less essential to conserve energy, aiming at restoring cellular homeostasis [12]. We observed both hyper- and hypomethylation in association with EOPE in UC-WBC and placenta, and enrichment of both positive and negative regulation of transcription among the functional annotations of DMP genes, in line with these cellular stress responses. Moreover, in case of partial failure to restore cellular homeostasis or a sudden excessive stress event, cellular death might occur, through apoptosis or necrosis [13]. Also this cellular death- and survival pathway was identified among the DMP gene functional annotations, underlining the potential involvement of excessive oxidative stress.

In our genome-wide and *PlGF* gene methylation studies, altered DNA methylation seems to be more pronounced in EOPE pregnancies, where placental and newborn tissues are indeed exposed to excessive oxidative stress very early in pregnancy, in contrast to the oxidative stress exposure later in pregnancy in LOPE [11, 12]. If early unplugging of spiral arteries occurs already at eight-to-nine weeks of gestation like in EOPE, chorionic villi are not mature enough to withstand the oxidative stress through contact with maternal oxygenated blood, disturbing the formation of the definitive placenta by restricted invasion and impaired remodelling of spiral arteries [12]. One might hypothesize that the epigenetic programming involved in this initial placental formation and differentiation is in fact already affected, perhaps inducing the further development of EOPE, rather than being a consequence of the disease (**Figure 2A, new hypothesis 2**). Perhaps, even the essential process of epigenetic reprogramming at the late-morula stage (at 3-4 days after fertilisation) is already disturbed, also suggesting a more causative epigenetic involvement (**Figure 2A, new hypothesis 2**). Whether cause or consequence, the evident involvement of impaired placentation in EOPE may explain the large extent of differential DNA methylation in the placenta [11]. Also the maternal and fetal pro-inflammatory milieu is more pronounced in EOPE than in LOPE, with more potential consequences for UC-WBC epigenetic programming, as substantiated by our data [15]. The lack of genome-wide differentially methylation in LOPE is in accordance to previous literature [152, 153, 160-162]. A possible reason for only observing associations between EOPE and PTB is that these groups are least affected by a large gestational age range and additional comorbidities and hence easier to compare than the other control groups.

The involvement of DNA methylation differences in cardiovascular programming of PE offspring was strongly suggested by many identified gene-ontology (GO) functional annotations and pathways associated with the DMP genes. Repeated enrichment of genetic networks associated with the development of cardiovascular and metabolic disease was observed. This is partly substantiated by previous PE EWAS, describing differential methylation in the fatty acid synthase pathway and in collagen-related genes [152, 154]. Yuen et al identified hypomethylation of the *TIMP3* gene in EOPE placentas, suggesting reduced angiogenesis and trophoblast invasiveness by use of the Illumina GoldenGate Methylation assay [162]. Moreover, further evidence for cardiovascular programming involvement is available in our *PlGF* candidate-gene study. Here, hypomethylation of the *PlGF* gene in placental tissue demonstrated that (anti)

angiogenic factors are likely to be involved in the pathophysiology of EOPE in particular. The additional lower placental SAM:SAH ratio represents a lower cellular methylation potential, which is in line with both the placental hypomethylation of *PlGF* and the observed genome-wide predominant hypomethylated state of the placenta in EOPE. *PlGF* is considered as one of the major proangiogenic factors, essential for controlling placental growth and maintaining normal endothelial structure and function. PE is associated with lower levels of *PlGF* due to increased *sFlt-1* levels in plasma and declined placental *PlGF* production [12]. Our results are in agreement with the candidate gene study by Sundrani et al., describing altered placental DNA methylation of (anti)angiogenic factors *VEGF* and *FLT-1* in association with PE [163].

Enrichment of other relevant pathways involved in systemic inflammation, cell differentiation and development and erythropoiesis may specifically explain the decreased leucocytes and increased NRBC that we observed in UCB of EOPE pregnancies and decreased umbilical vein wall thickness in PE. The respiratory development pathway enrichment may explain the suggested association of PE with neonatal bronchopulmonary dysplasia development [207]. Also the renin-angiotensin system (RAS) pathway was enriched and seems important in PE pathophysiology, underlining the generally suggested potential role of DNA methylation in the process of cardiovascular programming in PE offspring.

METHODOLOGICAL CONSIDERATIONS

The data used for this thesis were collected in The Rotterdam Periconceptional Cohort, a prospective tertiary hospital-based cohort study. Both the clinical and epigenetic studies are based on the same samples derived from the same nested case-control study. This enables us to correlate the epigenetic findings to the clinical findings. Inherent to the tertiary hospital setting is the limited external validity due to the proportion of high-risk pregnancies. Case- and control pregnancies presented with a relatively high percentage of concurrent comorbidity. In particular pregnancies included in the first trimester of pregnancy that were afterwards enrolled as uncomplicated pregnancies (without PE, gestational hypertension, FGR and PTB) showed a high frequency of relevant maternal chronic comorbidity, including endocrine-, metabolic-, auto-immune-, renal- or cardiovascular disease. Complicated EOPE, LOPE, FGR and PTB pregnancies were more often included in the second half of pregnancy and presented with a lower frequency of additional maternal comorbidity.

Although we initially intended to enrol FGR- and PTB complicated

control groups to avoid additional adjustment for gestational age and birth weight, unfortunately EOPE and LOPE still appeared to have a lower birth weight and shorter gestational age than FGR and PTB. This turned out to be a significant limitation for our analysis, because we had to apply adjustments despite the small sample sizes in each subgroup. Due to the unmatched inclusion we were not able to conduct a matched analysis afterwards, nor was it possible to adjust for all potential confounders and therefore also inherent to the observational study design residual confounding cannot be excluded. Selection bias due to the relatively high percentage of missing samples in (the most severe) EOPE and LOPE pregnancies may have occurred, which seemed a result of random factors such as stressful deliveries, caesarean sections or night shifts, but did not seem systematic.

A limitation of the epigenetic studies is the absence of expression data to validate our findings and the absence of validation by alternative DNA methylation techniques. Secondly, the implications of our findings would have been improved by using homogeneous cell types of placental tissue and UC-WBC, thereby avoiding any potential confounding of methylation differences due to underlying cell mixture differences [134, 135].

In general, the studies discussed in this thesis cannot distinguish whether observed umbilical cord (blood) and placental characteristics are causes or consequences of EOPE or LOPE. We did establish important associations in line with our hypothesis, but we therefore cannot draw conclusions on causal relationships between our findings and PE and the increased cardiovascular disease risk, as depicted in **Figure 2**. However, this generates new hypotheses and provides an important background for future studies.

CLINICAL IMPLICATIONS AND RECOMMENDATIONS FOR FUTURE RESEARCH

This thesis implies that newborns of pregnancies complicated by especially EOPE, may possess a cardiovascular phenotype characterised by disturbed haematopoiesis, impaired endothelial function and early structural vascular alterations. Given the increased risk to develop hypertension and stroke in adulthood, these children might therefore benefit from clinical follow-up, aiming at life-style interventions to lower and possibly prevent the risk of adult cardiovascular events. Not only postnatal risk-management is needed, but also prenatal or even periconceptional intervention programmes are warranted to optimise the environment for the developing placenta and cardiovascular system of the embryo and fetus. This may be particularly beneficial for the maternal

metabolic- and cardiovascular risk profile in LOPE pregnancies, helping both mother and child throughout pregnancy and beyond.

The observed epigenetic involvement in EOPE pregnancies may be useful in this context. By measuring validated epigenetic marks in early pregnancy in cell-free fetal DNA obtained from maternal peripheral blood, or at delivery from placental tissue or umbilical cord (blood), a clinical predictive value may be available [18]. Epigenetic marks could also serve as possible targets for intervention and prevention, given that epigenetic changes are potentially dynamic [208, 209]. An example of an epigenetic-driven preventive measure may be to optimise periconceptional maternal folic acid intake, thereby providing an important source of methylgroups necessary for various cellular developmental processes, such as DNA methylation. The identified lower SAM:SAH ratio in PE pregnancies indeed suggests a lower cellular methylation potential, and folic acid supplementation has proven to decrease maternal homocysteine levels and thereby the risk of PE [210].

New research questions to be addressed in future clinical and epigenetic association studies are provided by this thesis. The evident difference in EOPE and LOPE presented throughout this thesis, implies that the two phenotypes should be considered as different disease entities in future studies, also with respect to the associated cardiovascular disease risk in offspring. Control groups should preferably be matched for gestational age and birthweight to avoid extensive adjustment in small sample size association studies examining PE.

The use of umbilical cord (vascular) tissue and DNA methylation measurements seems promising for studying associations between adverse antenatal environmental factors such as PE, FGR, PTB and disease-outcome within the DOHaD concept. The relationship between umbilical cord vasculature and newborn vasculature could be examined by (functional) studies addressing haemodynamic, hormonal and morphological (dis)agreements to establish the predictive value of this tissue. Potential associations with early predictive umbilical cord ultrasound measures may also be useful to investigate in this context and the relation with upcoming (anti)angiogenic biomarkers *sFlt-1* and *PlGF*. Additionally, due to its non-invasive character, microcirculatory measurements may provide real-time information on cardiovascular features of newborn vascular sites that would otherwise be inaccessible.

With respect to future EWAS, firstly, the observed heterogeneity of UCB cell populations in EOPE, LOPE, FGR and PTB implies that UC-WBC

mixtures should always be considered as potential confounder. The marginal genome-wide UC-MNC and UC-WBC methylation differences seem negligible, supporting the use of easily accessible UC-WBC over UC-MNC. However, the observed (genome-wide) tissue-specific aspect of DNA methylation calls into question whether certain representative tissues such as UC-WBC, can be generally used in epigenetic epidemiological studies examining placental and/or vascular-related diseases of pregnancy. HUVEC is suggested to serve as an accessible vascular tissue for human studies investigating associations between prenatal exposures and vascular-related pregnancy outcome and future diseases, with epigenetic programming as underlying mechanism. In order to optimise the benefits of EWAS, we should apply a universal approach concerning study design and statistics, enhance the use of functional and technical validation, and stimulate the collaboration between research groups to achieve larger sample sizes. Moreover, further research with repeated measurements is needed to cover the maintenance and stability of (tissue-specific) methylation differences throughout pregnancy and postnatal life. Finally, gene-body regions appeared most susceptible to (tissue-specific) variation in DNA methylation, highlighting their potential significance in future EWAS.

GENERAL CONCLUSION

The associations demonstrated in this thesis support our hypothesis that the development and epigenetic programming of placental and newborn cardiovascular tissues is disturbed in EOPE offspring, and as such suggest that this (partly) explains their increased susceptibility to cardiovascular disease in later life. This seems to be less applicable for LOPE.

We emphasize that those newborns at increased cardiovascular risk should be identified in order to establish targeted therapeutic risk management to lower and possibly prevent cardiovascular events in adulthood. This should be incorporated in a larger sample set prospective cohort study with long-term cardiovascular follow-up in mothers and offspring. Prenatal and periconceptional interventions are needed to improve intrauterine conditions for placental, embryonic and fetal development, especially in mothers at risk to develop LOPE. Although (genome-wide) epigenetic studies are challenging and need to be optimised, they may provide novel genomic loci or pathways of interest that could contribute to a better understanding of cardiovascular disease development in PE, and perhaps methylation-based early prediction of cardiovascular risk in offspring.

CHAPTER 10

Summary / Samenvatting

SUMMARY

Evidence is accumulating that mothers and offspring exposed to pregnancies complicated by preeclampsia (PE) have an enhanced risk to develop cardiovascular disease in later life. PE complicates 2-8% of all pregnancies and is defined as gestational hypertension accompanied by significant proteinuria arising *de novo* at or after 20 weeks of pregnancy. Pregnancies complicated by PE are characterised by high maternal and perinatal morbidity and mortality. According to the moment of disease-onset, two main disease entities have been identified, with early-onset PE (EOPE) as the more severe phenotype, diagnosed before 34 weeks of gestation and late-onset PE (LOPE) diagnosed at or after 34 weeks of gestation.

Currently, the exact pathophysiology of both phenotypes is not yet fully understood, but there is extensive evidence that EOPE originates from poor first trimester placentation, causing episodes of placental hypoxia and reperfusion, often resulting in fetal growth restricted fetuses. LOPE however, is considered a more maternal disorder originating from underlying maternal cardiovascular- and metabolic risk factors and associated with typically well-grown fetuses. In both phenotypes, the developing embryo and fetus are exposed to excessive oxidative stress, although in LOPE this occurs more towards the end of gestation. As a result, pro-inflammatory cytokines and (anti)angiogenic factors are released into the maternal circulation inducing maternal endothelial dysfunction, leading to the clinical symptoms of PE.

The adverse prenatal PE environment may disturb the development and programming of placental and newborn cardiovascular tissues, resulting in a cardiovascular phenotype of the newborn that is more susceptible to develop future cardiovascular diseases. The process of developmental programming is strongly mediated by various epigenetic mechanisms such as DNA methylation, which involves the attachment of a methyl group on the DNA sequence, thereby regulating gene-expression. The aim of the present thesis was to gain more insight into the following topics:

1. The development of placental and newborn cardiovascular tissues in association with EOPE and LOPE (a), and of the maternal microcirculation in association with PE (b) (**Part I**)
2. The tissue-specific DNA methylation in placental and newborn cardiovascular tissues in association with EOPE and LOPE (**Part II**) (**Figure 1,** page 12-13)

The majority of data described in this thesis was obtained from a nested case-control study embedded in The Rotterdam Periconceptional Cohort, a prospective hospital-

based cohort study conducted at the Department of Obstetrics and Gynaecology of the Erasmus MC, University Medical Centre Rotterdam, the Netherlands.

The association between EOPE and LOPE and the development of placental and newborn tissues was examined by flow-cytometry measurements of UCB cell populations, revealing a four to sevenfold decreased neutrophil count and a fivefold increased nucleated red blood cell count in association with EOPE (**chapter 2**). Moreover, we investigated the relation between EOPE and LOPE and (histo-) morphologic measurements of the placenta and umbilical cord (vasculature). This data demonstrated that PE exposure was associated with a smaller umbilical vein area and vein wall thickness and LOPE with a larger placental width. These findings suggest that the prenatal development of haematopoiesis and vasculogenesis is disturbed in especially EOPE (**chapter 3**) (**Figure 2, association A1 and B1**, page 156-157).

To investigate if the known maternal endothelial dysfunction during PE exposure may be associated with real-time maternal cardiovascular disturbances, maternal sublingual microcirculatory measurements were performed. We demonstrated that women with severe PE and HELLP syndrome showed a reduced perfused vessel density, a reduced flow velocity and increased heterogeneity of flow in capillaries, compared with women with severe PE without HELLP syndrome. This suggests an involvement of microcirculatory dysfunction in the development of PE/HELLP syndrome, potentially related to endothelial dysfunction and the increased maternal cardiovascular disease risk after PE pregnancies (**chapter 4**).

In order to examine whether epigenetic mechanisms may be underlying these findings and whether they are associated with PE, (genome-wide) tissue-specific DNA methylation studies were performed. We initially demonstrated the tissue-specific aspect of DNA methylation of imprinted *IGF2/H19* genes in Wharton jelly of the umbilical cord and placental tissue, versus UC-MNC (**chapter 5**). Next on a genome-wide level, HUVEC and placental tissue displayed large tissue-specific differences in 43% and 73% of all measured CpGs respectively, versus UC-WBC. No differentially methylated regions were identified between UC-MNC and UC-WBC (**chapter 6**).

The relation between EOPE, LOPE and DNA methylation alterations was therefore investigated in a tissue-specific manner and demonstrated extensive genome-wide UCB- and placental DNA methylation differences in EOPE, in comparison to PTB pregnancies. Moreover, functional annotations of DMP genes revealed a strong enrichment of pathways associated with cellular stress responses, cardiovascular- and metabolic system development, systemic

inflammation, cellular differentiation and erythropoiesis, the latter substantiating our findings in chapter 2 and 3. No significant differential methylation was observed in LOPE pregnancies (**chapter 7**) (**Figure 2, association A2**, page 156). Finally, we revealed that PE was associated with hypomethylation of the *PlGF* gene and a lower placental SAM:SAH ratio, more pronounced in EOPE than LOPE (**chapter 8**).

In conclusion, this thesis provides evidence for associations between prenatal exposure to particularly EOPE and a disturbed development and epigenetic programming of placental and newborn cardiovascular tissues, as potentially underlying mechanism for the association with future cardiovascular risk in offspring. We therefore emphasize the need for periconceptional and prenatal intervention programmes to optimise the environment for the developing placenta and the cardiovascular system of the embryo and fetus. These programmes should in particularly target future mothers with metabolic- and cardiovascular risk factors and an increased risk of especially LOPE.

SAMENVATTING

In toenemende mate is aangetoond dat vrouwen en kinderen die blootgesteld werden aan een zwangerschap gecompliceerd door preeclampsie (PE) een verhoogd risico hebben op het ontwikkelen van cardiovasculaire ziekten op latere leeftijd. PE manifesteert zich in 2-8% van alle zwangerschappen en wordt gedefinieerd als een hoge bloeddruk in combinatie met eiwitverlies in de urine, optredend vanaf de 20e zwangerschapsweek. Zwangerschappen die gecompliceerd worden door PE hebben een hoge maternale en perinatale morbiditeit en mortaliteit. Naar gelang het moment waarop de ziekte ontstaat wordt onderscheid gemaakt tussen twee vormen van PE: vroege en late PE. De vroeg in de zwangerschap optredende vorm van PE laat vaak een ernstiger verloop zien en wordt gediagnosticeerd voor de 34^{e} zwangerschapsweek; de later optredende vorm van PE wordt vanaf 34 weken zwangerschapsduur gediagnosticeerd.

De exacte ontstaanswijze van PE is nog niet volledig bekend, maar er zijn sterke aanwijzingen dat vroege PE ontstaat door een verstoorde aanleg van de placenta in het eerste trimester van de zwangerschap, waardoor er een suboptimale zuurstoftoevoer in de placenta optreedt, en het ontwikkelende kind vaak groeivertraging vertoont. Late PE wordt meer gezien als een maternale ziekte, omdat de moeder zelf vaak diverse predisponerende cardiovasculaire risicofactoren heeft en het kind tijdens de zwangerschap een normale groei vertoont. Bij beide vormen van PE wordt het ontwikkelende kind aan overmatige hoeveelheden oxidatieve stress blootgesteld, echter bij late PE in een veel later stadium van de zwangerschap dan bij vroege PE. Dit veroorzaakt een verhoogde ontstekingsreactie in de maternale circulatie, resulterend in het dysfunctioneren van het endotheel (de binnenbekleding van bloedvaten) en de klinische symptomen van PE.

Een zwangerschap die gecompliceerd wordt door PE staat dus onder invloed van diverse suboptimale intra-uteriene omgevingsfactoren, die zouden kunnen leiden tot een verstoorde ontwikkeling van de placenta en de cardiovasculaire weefsels van de pasgeborene, resulterend in een verhoogd risico op het ontwikkelen van cardiovasculaire ziekten op latere leeftijd. De ontwikkeling van deze weefsels wordt sterk gereguleerd door verschillende epigenetische mechanismen waaronder DNA methylering, een proces dat gen-expressie kan reguleren (zie voor een uitgebreide Nederlandse uitleg hiervan pagina 176-177). Het doel van dit proefschrift is om meer inzicht te krijgen in:

1. De ontwikkeling van de placenta en cardiovasculaire weefsels van de pasgeborene in associatie met vroege en late PE (a), en de maternale microcirculatie in associatie met PE (b) (**Deel 1**)

2. De weefsel-specifieke DNA methylering in de placenta en cardiovasculaire weefsels van de pasgeborene in associatie met vroege en late PE (**Deel II**) (**Figuur 1**, pagina 12-13)

Het grootste deel van de data die gebruikt werden voor dit proefschrift is afkomstig van een case-control studie die werd uitgevoerd binnen het Rotterdam Periconceptie Cohort, een prospectieve cohort-studie gebaseerd op de ziekenhuispopulatie van de afdeling Verloskunde en Gynaecologie van het Erasmus MC in Rotterdam.

De associatie tussen vroege en late PE en de ontwikkeling van de placenta en de cardiovasculaire weefsels van de pasgeborene werd onderzocht middels flow-cytometrie op verschillende bloedcellen uit navelstrengbloed, waarbij een 4 tot 7-maal lagere neutrofielen hoeveelheid en een 5-maal hogere kernhoudende erythrocyten hoeveelheid werd aangetoond in associatie met EOPE (**hoofdstuk 2**). Vervolgens onderzochten we de relatie tussen vroege en late PE en (histo-) morphologische metingen van de placenta en navelstreng (vasculatuur). Er werd een associatie aangetoond tussen PE en een kleinere navelstrengvene-oppervlakte- en wanddikte en tussen late PE en een grotere placenta-breedte. Deze bevindingen suggereren dat de prenatale ontwikkeling van haematopoiese en vasculogenese (aanmaak van bloedcellen en bloedvaten) verstoord is bij vooral EOPE (**hoofdstuk 3**) (**Figuur 2, association A1 and B1**, pagina 156-157).

Om te onderzoeken of de maternale endotheel dysfunctie gedurende een zwangerschap die gecompliceerd wordt door PE gepaard gaat met maternale cardiovasculaire afwijkingen, hebben we maternale sublinguale microcirculatoire metingen uitgevoerd. Daarmee toonden we aan dat in het capillaire vaatbed (allerkleinste bloedvaatjes) van vrouwen met ernstige PE en HELLP syndroom een lagere dichtheid van goed doorstroomde capillairen bestaat, met een lagere stroomsnelheid van het bloed en een toegenomen heterogeniteit van de bloedstroom, i.c.m. vrouwen zonder HELLP syndroom. Dit suggereert dat het suboptimaal functioneren van het capillaire vaatbedsysteem betrokken zou kunnen zijn in de ontwikkeling van PE/HELLP en mogelijk gerelateerd is aan de maternale endotheel dysfunctie en het verhoogde cardiovasculaire risico van vrouwen na een zwangerschap gecompliceerd door PE (**hoofdstuk 4**).

Met als doel te onderzoeken of epigenetische mechanismen aan deze bevindingen ten grondslag liggen en geassocieerd zijn met PE, hebben we (genoomwijde) weefselspecifieke studies naar DNA methylering verricht. Allereerst hebben we de weefselspecificiteit van DNA methylering aangetoond van geimprinte genen *IGF2/H19* in DNA afkomstig van de Wharton jelly

van de navelstreng (gelei-achtige substantie om de navelstrengvaten) en de placenta, in vergelijking met leucocyten in navelstrengbloed (**hoofdstuk 5**). Vervolgens observeerden we op genoom-wijde schaal, dat endotheelcellen van de navelstrengvene en placentaweefsel een grote hoeveelheid weefselspecifiek gemethyleerde regio's vertonen ten opzichte van DNA uit navelstrengbloed leucocyten, respectievelijk in 43% en 73% van de totale hoeveelheid gemeten posities. Er werden geen verschillend gemethyleerde regio's aangetoond tussen DNA uit navelstrengbloed leucocyten en navelstrengbloed mononucleaire cellen (**hoofdstuk 6**).

De relatie tussen vroege en late PE en veranderingen in DNA methylering werd daarom ook in verschillende weefsels onderzocht. We observeerden uitgebreide genoomwijde verschillen in DNA methylering in navelstrengbloed en placentaweefsel van zwangerschappen gecompliceerd door vroege PE, i.c.m. zwangerschappen die gecompliceerd werden door spontane vroeggeboorte. De verschillend gemethyleerde posities bleken onder meer in of bij genen te liggen die cellulaire stress reguleren, evenals de ontwikkeling van het cardiovasculair-metabole systeem, ontstekingsreacties, celdifferentiatie en de ontwikkeling van rode bloedcellen. Dit laatste komt overeen met de bevindingen uit hoofdstukken 2 en 3. Er werden geen significante epigenetische bevindingen aangetoond in navelstrengbloed en placentaweefsel van zwangerschappen met late PE (**hoofdstuk 7**) (**Figuur 2, association A2**, pagina 156). Tot slot beschrijven we de associatie tussen PE en lagere methylering van het *PlGF*-gen en een lagere SAM:SAH ratio in placentaweefsel, beide meer uitgesproken in vroege dan late PE (**hoofdstuk 8**).

Concluderend toont dit proefschrift aan dat er een associatie bestaat tussen prenatale blootstelling aan vroege PE en een verstoring van de ontwikkeling en programmering van de placenta en cardiovasculaire weefsels van de pasgeborene. Deze verstoring zou een mogelijke verklaring kunnen vormen voor het verhoogde cardiovasculaire risicoprofiel van de pasgeborene op latere leeftijd. We benadrukken daarom het belang van lange-termijn cardiovasculaire screening in vrouwen en kinderen na blootstelling aan PE, om het risico op cardiovasculaire ziekten op volwassen leeftijd te kunnen verlagen of voorkomen. Met behulp van periconceptionele en prenatale interventieprogramma's zou gestreefd moeten worden naar een optimalisering van de intra-uteriene omgeving van de ontwikkelende placenta en het cardiovasculaire systeem van het ontwikkelende kind. Dit laatste zou zich vooral moeten richten op toekomstige moeders met predisponerende cardiovasculaire risicofactoren en een verhoogd risico op met name late PE.

DE DANS VAN DNA: een aanvulling op de Nederlandse samenvatting

Omdat ik de afgelopen jaren heb gemerkt dat het voor geïnteresseerde buitenstaanders niet altijd makkelijk te begrijpen is waar ik me als promovendus nu eigenlijk mee bezig heb gehouden, heb ik hier geprobeerd de begrippen *Epigenetica* en *DNA methylering* zo eenvoudig mogelijk uit te leggen, als aanvulling op de Nederlandse samenvatting. Ik gebruik hierbij een analogie die volgens mij bijzonder mooi past: dans.

Zoals we ons waarschijnlijk allemaal ongeveer kunnen voorstellen, zit in alle kernhoudende cellen van ons lichaam DNA. Het DNA is een lange opgevouwen slinger met daarop een uitgestrekte code waarin alle mogelijke processen en bestanddelen van ons lichaam zijn vastgelegd. De code bestaat uit een specifieke volgorde van verschillende letters die onze genen vormen. We zouden onze DNA code kunnen vergelijken met een choreografie, waarin alle dansbewegingen in plaats en tijd zijn vastgelegd. Wanneer we onze DNA code aflezen is het eindproduct een eiwit, en als we de choreografie opvolgen is het eindproduct een dans.

Het DNA is in principe niet te veranderen en in alle cellen gelijk. Toch is het niet zo dat een cel de hele DNA code met alle genen nodig heeft. Afhankelijk van het type cel, het type weefsel en allerlei omgevingsfactoren, is er in een cel behoefte aan specifieke eiwitten, dus bepaalde stukjes van de DNA code. Ook een choreografie is in principe niet te veranderen, en toch bestaat er een grote variatie aan uitvoeringen, doordat een choreograaf de artistieke vrijheid heeft om de choreografie te interpreteren naar zijn/haar wensen. Als we bijvoorbeeld op kerstavond naar een hedendaagse uitvoering van *De Notenkraker* gaan, is de choreografie van de oorspronkelijke choreografen Marius Petipa en Lev Ivanov onveranderd, maar de interpretatie van de choreograaf van nu waarschijnlijk heel anders dan tijdens de premiere in 1892.

Zoals een choreograaf kan bepalen hoe hij/zij de choreografie tot expressie wil laten komen tot een dans, kunnen de cellen in ons lichaam iets vergelijkbaars. Het is namelijk mogelijk om bepaalde stukjes van de DNA-code aan of uit te zetten en meer of minder tot expressie te laten komen (te *programmeren*), om zo alleen die eiwitten te produceren die nodig zijn. Dit proces van het programmeren van onze genen op de DNA code heet *epigenetische programmering* (*epi* is Grieks voor *op*, dus op onze genen).

De epigenetische programmering en de interpretatie van een choreografie worden beide sterk beïnvloed door omgevingsfactoren. Omgevingsfactoren

die de epigenetische programmering kunnen beïnvloeden zijn bijvoorbeeld leeftijd, voeding, zwangerschap, lichamelijke activiteit, roken of alcohol. Bij de interpretatie van een choreografie kunnen we bij omgevingsfactoren denken aan de theaterruimte, muziek, kostuums en ten slotte de kwaliteit van de dansers zelf. Als de omgevingsfactoren niet optimaal zijn - de muziek hapert of de dansers weinig getraind of gegeten hebben - dan is de dans niet optimaal.

Tijdens een zwangerschap die gecompliceerd wordt door preeclampsie, zijn de ontwikkelende placenta en het kind blootgesteld aan diverse negatieve omgevingsfactoren, vooral gekenmerkt door een verstoorde zuurstoftoevoer in de placenta. In deel II van dit proefschrift heb ik daarom onderzocht of blootstelling aan preeclampsie tijdens de zwangerschap geassocieerd is met veranderingen in de epigenetische programmering van het DNA.

Er zijn diverse mechanismen die zorgen voor de epigenetische programmering van het DNA. Daarvan heb ik er in dit proefschrift één onderzocht: DNA methylering. Hierbij gaat het om een chemische verbinding (methylgroep) op de DNA code, die ervoor zorgt dat een bepaald gen meer of minder makkelijk kan worden afgelezen en tot expressie kan komen. Ik heb onderzocht in hoeverre de aanwezigheid van deze methylgroepen tussen verschillende cellen en weefsels verschilt, en of dit verschilt in zwangerschappen blootgesteld aan vroege en late PE en controle zwangerschappen.

ADD END UM

REFERENCES

AUTHORS AND AFFILIATIONS

LIST OF ABBREVIATIONS

LIST OF PUBLICATIONS

ABOUT THE AUTHOR

PHD PORTFOLIO

ACKNOWLEDGEMENTS

REFERENCES

1. Gluckman PD, Hanson MA, Cooper C, Thornburg KL. Effect of in utero and early-life conditions on adult health and disease. *N Engl J Med.* 2008;359:61-73
2. Jaddoe VW, de Jonge LL, Hofman A, Franco OH, Steegers EA, Gaillard R. First trimester fetal growth restriction and cardiovascular risk factors in school age children: Population based cohort study. *BMJ.* 2014;348:g14
3. Steegers EA, von Dadelszen P, Duvekot JJ, Pijnenborg R. Pre-eclampsia. *Lancet.* 2010;376:631-644
4. Davis EF, Lazdam M, Lewandowski AJ, Worton SA, Kelly B, Kenworthy Y, et al. Cardiovascular risk factors in children and young adults born to preeclamptic pregnancies: A systematic review. *Pediatrics.* 2012;129:e1552-1561
5. Lawlor DA, Macdonald-Wallis C, Fraser A, Nelson SM, Hingorani A, Davey Smith G, et al. Cardiovascular biomarkers and vascular function during childhood in the offspring of mothers with hypertensive disorders of pregnancy: Findings from the avon longitudinal study of parents and children. *European Heart Journal.* 2012;33:335-345
6. Kajantie E, Eriksson JG, Osmond C, Thornburg K, Barker DJP. Pre-eclampsia is associated with increased risk of stroke in the adult offspring: The helsinki birth cohort study. *Stroke.* 2009;40:1176-1180
7. Davis EF, Newton L, Lewandowski AJ, Lazdam M, Kelly BA, Kyriakou T, et al. Pre-eclampsia and offspring cardiovascular health: Mechanistic insights from experimental studies. *Clin Sci (Lond).* 2012;123:53-72
8. Mosca L, Benjamin EJ, Berra K, Bezanson JL, Dolor RJ, Lloyd-Jones DM, et al. Effectiveness-based guidelines for the prevention of cardiovascular disease in women--2011 update: A guideline from the american heart association. *Circulation.* 2011;123:1243-1262
9. McDonald SD, Malinowski A, Zhou Q, Yusuf S, Devereaux PJ. Cardiovascular sequelae of preeclampsia/eclampsia: A systematic review and meta-analyses. *American heart journal.* 2008;156:918-930
10. American College of O, Gynecologists, Task Force on Hypertension in P. Hypertension in pregnancy. Report of the american college of obstetricians and gynecologists' task force on hypertension in pregnancy. *Obstet Gynecol.* 2013;122:1122-1131
11. Raymond D, Peterson E. A critical review of early-onset and late-onset preeclampsia. *Obstet Gynecol Surv.* 2011;66:497-506
12. Redman CW, Staff AC. Preeclampsia, biomarkers, syncytiotrophoblast stress, and placental capacity. *Am J Obstet Gynecol.* 2015;213:S9 e1, S9-11
13. Redman CW, Sargent IL, Staff AC. Ifpa senior award lecture: Making sense of pre-eclampsia - two placental causes of preeclampsia? *Placenta.* 2014;35 Suppl:S20-25
14. Burton GJ, Yung HW, Cindrova-Davies T, Charnock-Jones DS. Placental endoplasmic reticulum stress and oxidative stress in the pathophysiology of unexplained intrauterine growth restriction and early onset preeclampsia. *Placenta.* 2009;30 Suppl A:S43-48
15. Hakim J, Senterman MK, Hakim AM. Preeclampsia is a biomarker for vascular disease in both mother and child: The need for a medical alert system. *International journal of pediatrics.* 2013;2013:953150
16. Schulz E, Gori T, Munzel T. Oxidative stress and endothelial dysfunction in hypertension. *Hypertension research : official journal of the Japanese Society of Hypertension.* 2011;34:665-673
17. Yang P, Dai A, Alexenko AP, Liu Y, Stephens AJ, Schulz LC, et al. Abnormal oxidative stress responses in fibroblasts from preeclampsia infants. *PLoS One.* 2014;9:e103110
18. Choudhury M, Friedman JE. Epigenetics and micrornas in preeclampsia. *Clinical and experimental hypertension.* 2012;34:334-341

19. Nejatizadeh A, Stobdan T, Malhotra N, Pasha MA. The genetic aspects of pre-eclampsia: Achievements and limitations. *Biochemical genetics*. 2008;46:451-479
20. Krause B, Sobrevia L, Casanello P. Epigenetics: New concepts of old phenomena in vascular physiology. *Current vascular pharmacology*. 2009;7:513-520
21. Casanello P, Schneider D, Herrera EA, Uauy R, Krause BJ. Endothelial heterogeneity in the umbilico-placental unit: DNA methylation as an innuendo of epigenetic diversity. *Front Pharmacol*. 2014;5:49
22. Nelissen EC, van Montfoort AP, Dumoulin JC, Evers JL. Epigenetics and the placenta. *Hum Reprod Update*. 2011;17:397-417
23. Jones PA. Functions of DNA methylation: Islands, start sites, gene bodies and beyond. *Nature reviews. Genetics*. 2012;13:484-492
24. Gama-Sosa MA, Midgett RM, Slagel VA, Githens S, Kuo KC, Gehrke CW, et al. Tissue-specific differences in DNA methylation in various mammals. *Biochimica et biophysica acta*. 1983;740:212-219
25. Herzog E, Galvez J, Roks A, Stolk L, Verbiest M, Eilers P, et al. Tissue-specific DNA methylation profiles in newborns. *Clin Epigenetics*. 2013;5:8
26. Ollikainen M, Smith KR, Joo EJ, Ng HK, Andronikos R, Novakovic B, et al. DNA methylation analysis of multiple tissues from newborn twins reveals both genetic and intrauterine components to variation in the human neonatal epigenome. *Hum Mol Genet*. 2010;19:4176-4188
27. Jin SW, Patterson C. The opening act: Vasculogenesis and the origins of circulation. *Arteriosclerosis, thrombosis, and vascular biology*. 2009;29:623-629
28. Marino M, Beny JL, Peyter AC, Bychkov R, Diaceri G, Tolsa JF. Perinatal hypoxia triggers alterations in k+ channels of adult pulmonary artery smooth muscle cells. *Am J Physiol Lung Cell Mol Physiol*. 2007;293:L1171-1182
29. Peyter AC, Delhaes F, Baud D, Vial Y, Diaceri G, Menetrey S, et al. Intrauterine growth restriction is associated with structural alterations in human umbilical cord and decreased nitric oxide-induced relaxation of umbilical vein. *Placenta*. 2014;35:891-899
30. Sandovici I, Hoelle K, Angiolini E, Constancia M. Placental adaptations to the maternal-fetal environment: Implications for fetal growth and developmental programming. *Reprod Biomed Online*. 2012;25:68-89
31. Stojanovska V, Scherjon SA, Plosch T. Preeclampsia as modulator of offspring health. *Biol Reprod*. 2016;94:53
32. Steegers-Theunissen RP, Verheijden-Paulissen JJ, van Uitert EM, Wildhagen MF, Exalto N, Koning AH, et al. Cohort profile: The rotterdam periconceptional cohort (predict study). *Int J Epidemiol*. 2016;45:374-381
33. Duley L. The global impact of pre-eclampsia and eclampsia. *Semin Perinatol*. 2009;33:130-137
34. Hillman SL, Finer S, Smart MC, Mathews C, Lowe R, Rakyan VK, et al. Novel DNA methylation profiles associated with key gene regulation and transcription pathways in blood and placenta of growth-restricted neonates. *Epigenetics*. 2015;10:50-61
35. Menon R, Conneely KN, Smith AK. DNA methylation: An epigenetic risk factor in preterm birth. *Reproductive Sciences*. 2012;19:6-13
36. Novakovic B, Yuen RK, Gordon L, Penaherrera MS, Sharkey A, Moffett A, et al. Evidence for widespread changes in promoter methylation profile in human placenta in response to increasing gestational age and environmental/stochastic factors. *BMC Genomics*. 2011;12:529
37. Canzoneri BJ, Lewis DF, Groome L, Wang Y. Increased neutrophil numbers account for leukocytosis in women with preeclampsia. *Am J Perinatol*. 2009;26:729-732
38. Lurie S, Frenkel E, Tuvbin Y. Comparison of the differential distribution of leukocytes in preeclampsia versus uncomplicated pregnancy. *Gynecol Obstet Invest*. 1998;45:229-231

39. Davies NP, Buggins AG, Snijders RJ, Jenkins E, Layton DM, Nicolaides KH. Blood leucocyte count in the human fetus. *Arch Dis Child.* 1992;67:399-403
40. Dzierzak E, Robin C. Placenta as a source of hematopoietic stem cells. *Trends Mol Med.* 2010;16:361-367
41. Morrison SJ, Uchida N, Weissman IL. The biology of hematopoietic stem cells. *Annu Rev Cell Dev Biol.* 1995;11:35-71
42. Proytcheva MA. Issues in neonatal cellular analysis. *American Journal of Clinical Pathology.* 2009;131:560-573
43. Sashida G, Iwama A. Epigenetic regulation of hematopoiesis. *International journal of hematology.* 2012;96:405-412
44. Brown MA, Lindheimer MD, de Swiet M, Van Assche A, Moutquin JM. The classification and diagnosis of the hypertensive disorders of pregnancy: Statement from the international society for the study of hypertension in pregnancy (isshp). *Hypertension in Pregnancy.* 2001;20:IX-XIV
45. Tranquilli A, Brown M, Zeeman G, Dekker G, Baha M. The definition of severe and early-onset preeclampsia. Statements from the international society for the study of hypertension in pregnancy (isshp). *Pregnancy Hypertension: An International Journal of Women's Cardiovascular Health.* 2013;3:44-47
46. Battaglia FC, Lubchenco LO. A practical classification of newborn infants by weight and gestational age. *J Pediatr.* 1967;71:159-163
47. Visser GH, Eilers PH, Elferink-Stinkens PM, Merkus HM, Wit JM. New dutch reference curves for birthweight by gestational age. *Early Hum Dev.* 2009;85:737-744
48. Acog committee opinion no 579: Definition of term pregnancy. *Obstet Gynecol.* 2013;122:1139-1140
49. Perrone S, Vezzosi P, Longini M, Marzocchi B, Tanganelli D, Testa M, et al. Nucleated red blood cell count in term and preterm newborns: Reference values at birth. *Arch Dis Child Fetal Neonatal Ed.* 2005;90:F174-175
50. Catarino C, Santos-Silva A, Belo L, Rocha-Pereira P, Rocha S, Patricio B, et al. Inflammatory disturbances in preeclampsia: Relationship between maternal and umbilical cord blood. *J Pregnancy.* 2012;2012:684384
51. Mellembakken JR, Aukrust P, Hestdal K, Ueland T, Abyholm T, Videm V. Chemokines and leukocyte activation in the fetal circulation during preeclampsia. *Hypertension.* 2001;38:394-398
52. Adamo L, Garcia-Cardena G. The vascular origin of hematopoietic cells. *Dev Biol.* 2012;362:1-10
53. Aali BS, Malekpour R, Sedig F, Safa A. Comparison of maternal and cord blood nucleated red blood cell count between pre-eclamptic and healthy women. *J Obstet Gynaecol Res.* 2007;33:274-278
54. Akercan F, Cirpan T, Saydam G. Nucleated red blood cells in infants of women with preterm labor and pre-eclampsia. *Int J Gynaecol Obstet.* 2005;90:138-139
55. Catarino C, Rebelo I, Belo L, Rocha-Pereira P, Rocha S, Bayer Castro E, et al. Erythrocyte changes in preeclampsia: Relationship between maternal and cord blood erythrocyte damage. *J Perinat Med.* 2009;37:19-27
56. Hebbar S, Misha M, Rai L. Significance of maternal and cord blood nucleated red blood cell count in pregnancies complicated by preeclampsia. *J Pregnancy.* 2014;2014:496416
57. Bayram F, Ozerkan K, Cengiz C, Develioglu O, Cetinkaya M. Perinatal asphyxia is associated with the umbilical cord nucleated red blood cell count in pre-eclamptic pregnancies. *Journal of obstetrics and gynaecology : the journal of the Institute of Obstetrics and Gynaecology.* 2010;30:383-386
58. Jauniaux E, Poston L, Burton GJ. Placental-related diseases of pregnancy: Involvement of oxidative stress and implications in human evolution. *Hum Reprod Update.* 2006;12:747-755
59. Rath G, Aggarwal R, Jawanjal P, Tripathi R, Batra A. Hif-1 alpha and placental growth factor in pregnancies complicated with preeclampsia: A qualitative and quantitative analysis. *Journal of clinical laboratory analysis.* 2016;30:75-83
60. Sezer SD, Kucuk M, Doger FK, Yuksel H, Odabasi AR, Turkmen MK, et al. Vegf, pigf and hif-1alpha in placentas of early- and late-onset pre-eclamptic patients. *Gynecological endocrinology : the official journal of*

the International Society of Gynecological Endocrinology. 2013;29:797-800
61. Kajantie E, Thornburg KL, Eriksson JG, Osmond C, Barker DJ. In preeclampsia, the placenta grows slowly along its minor axis. *The International journal of developmental biology*. 2010;54:469-473
62. Junek T, Baum O, Lauter H, Vetter K, Matejevic D, Graf R. Pre-eclampsia associated alterations of the elastic fibre system in umbilical cord vessels. *Anat Embryol (Berl)*. 2000;201:291-303
63. Inan S, Sanci M, Can D, Vatansever S, Oztekin O, Tinar S. Comparative morphological differences between umbilical cords from chronic hypertensive and preeclamptic pregnancies. *Acta Med Okayama*. 2002;56:177-186
64. Romanowicz L, Jaworski S. Collagen of umbilical cord vein and its alterations in pre-eclampsia. *Acta Biochim Pol*. 2002;49:451-458
65. Romanowicz L, Sobolewski K. Extracellular matrix components of the wall of umbilical cord vein and their alterations in pre-eclampsia. *J Perinat Med*. 2000;28:140-146
66. Blanco MV, Vega HR, Giuliano R, Grana DR, Azzato F, Lerman J, et al. Histomorphometry of umbilical cord blood vessels in preeclampsia. *J Clin Hypertens (Greenwich)*. 2011;13:30-34
67. Abramoff M, Magalhaes P, Ram S. Image processing with image j. *Biophotonics International*. 2004;11:36-42
68. Dahlstrom B, Romundstad P, Oian P, Vatten LJ, Eskild A. Placenta weight in pre-eclampsia. *Acta obstetricia et gynecologica Scandinavica*. 2008;87:608-611
69. Norman M. Preterm birth--an emerging risk factor for adult hypertension? *Semin Perinatol*. 2010;34:183-187
70. Huxley RR, Shiell AW, Law CM. The role of size at birth and postnatal catch-up growth in determining systolic blood pressure: A systematic review of the literature. *J Hypertens*. 2000;18:815-831
71. Cheng JK, Wagenseil JE. Extracellular matrix and the mechanics of large artery development. *Biomechanics and modeling in mechanobiology*. 2012;11:1169-1186
72. Cockell AP, Poston L. Flow-mediated vasodilatation is enhanced in normal pregnancy but reduced in preeclampsia. *Hypertension*. 1997;30:247-251
73. Culver JC, Dickinson ME. The effects of hemodynamic force on embryonic development. *Microcirculation*. 2010;17:164-178
74. Klockenbusch W, Goecke TW, Krussel JS, Tutschek BA, Crombach G, Schror K. Prostacyclin deficiency and reduced fetoplacental blood flow in pregnancy-induced hypertension and preeclampsia. *Gynecol Obstet Invest*. 2000;50:103-107
75. De Backer D, Ospina-Tascon G, Salgado D, Favory R, Creteur J, Vincent JL. Monitoring the microcirculation in the critically ill patient: Current methods and future approaches. *Intensive care medicine*. 2010;36:1813-1825
76. Genzel-Boroviczeny O, Strotgen J, Harris AG, Messmer K, Christ F. Orthogonal polarization spectral imaging (ops): A novel method to measure the microcirculation in term and preterm infants transcutaneously. *Pediatr Res*. 2002;51:386-391
77. Top AP, Tasker RC, Ince C. The microcirculation of the critically ill pediatric patient. *Critical care*. 2011;15:213
78. Trzeciak S, Dellinger RP, Parrillo JE, Guglielmi M, Bajaj J, Abate NL, et al. Early microcirculatory perfusion derangements in patients with severe sepsis and septic shock: Relationship to hemodynamics, oxygen transport, and survival. *Annals of emergency medicine*. 2007;49:88-98, 98 e81-82
79. Bezemer R. KM, Ince C. Recent advencements in microcirculatory image acquisition and analysis. *Yearbook of Intensive Care and Emergency Medicine*. 2008;2008
80. De Backer D, Ortiz JA, Salgado D. Coupling microcirculation to systemic hemodynamics. *Current opinion in critical care*. 2010;16:250-254
81. Nama V, Manyonda IT, Onwude J, Antonios TF. Structural capillary rarefaction and the onset of preeclampsia. *Obstet Gynecol*. 2012;119:967-974
82. Barton JR, Sibai BM. Gastrointestinal complications of pre-eclampsia. *Semin Perinatol*. 2009;33:179-188

83. Sibai BM. Diagnosis, controversies, and management of the syndrome of hemolysis, elevated liver enzymes, and low platelet count. *Obstet Gynecol.* 2004;103:981-991
84. . *Hypertension in pregnancy: The management of hypertensive disorders during pregnancy*. London; 2010.
85. Goedhart PT, Khalilzada M, Bezemer R, Merza J, Ince C. Sidestream dark field (sdf) imaging: A novel stroboscopic led ring-based imaging modality for clinical assessment of the microcirculation. *Optics express.* 2007;15:15101-15114
86. De Backer D, Hollenberg S, Boerma C, Goedhart P, Buchele G, Ospina-Tascon G, et al. How to evaluate the microcirculation: Report of a round table conference. *Critical care.* 2007;11:R101
87. Elbers PW, Ozdemir A, van Iterson M, van Dongen EP, Ince C. Microcirculatory imaging in cardiac anesthesia: Ketanserin reduces blood pressure but not perfused capillary density. *Journal of cardiothoracic and vascular anesthesia.* 2009;23:95-101
88. Boerma EC, Mathura KR, van der Voort PH, Spronk PE, Ince C. Quantifying bedside-derived imaging of microcirculatory abnormalities in septic patients: A prospective validation study. *Critical care.* 2005;9:R601-606
89. Yuruk K, Almac E, Bezemer R, Goedhart P, de Mol B, Ince C. Blood transfusions recruit the microcirculation during cardiac surgery. *Transfusion.* 2011;51:961-967
90. Cornette J, Duvekot JJ, Roos-Hesselink JW, Hop WC, Steegers EA. Maternal and fetal haemodynamic effects of nifedipine in normotensive pregnant women. *BJOG.* 2011;118:510-540
91. Magriples U, Boynton MH, Kershaw TS, Duffany KO, Rising SS, Ickovics JR. Blood pressure changes during pregnancy: Impact of race, body mass index, and weight gain. *Am J Perinatol.* 2013;30:415-424
92. Duvekot JJ, Peeters LL. Maternal cardiovascular hemodynamic adaptation to pregnancy. *Obstet Gynecol Surv.* 1994;49:S1-14
93. Gaillard R, Bakker R, Steegers EA, Hofman A, Jaddoe VW. Maternal age during pregnancy is associated with third trimester blood pressure level: The generation r study. *American journal of hypertension.* 2011;24:1046-1053
94. Hubble SM, Kyte HL, Gooding K, Shore AC. Variability in sublingual microvessel density and flow measurements in healthy volunteers. *Microcirculation.* 2009;16:183-191
95. De Backer D, Creteur J, Preiser JC, Dubois MJ, Vincent JL. Microvascular blood flow is altered in patients with sepsis. *Am J Respir Crit Care Med.* 2002;166:98-104
96. Anim-Nyame N, Gamble J, Sooranna SR, Johnson MR, Sullivan MH, Steer PJ. Evidence of impaired microvascular function in pre-eclampsia: A non-invasive study. *Clin Sci (Lond).* 2003;104:405-412
97. Houben AJ, de Leeuw PW, Peeters LL. Configuration of the microcirculation in pre-eclampsia: Possible role of the venular system. *J Hypertens.* 2007;25:1665-1670
98. Hasan KM, Manyonda IT, Ng FS, Singer DR, Antonios TF. Skin capillary density changes in normal pregnancy and pre-eclampsia. *J Hypertens.* 2002;20:2439-2443
99. Vollebregt KC, Boer K, Mathura KR, de Graaff JC, Ubbink DT, Ince C. Impaired vascular function in women with pre-eclampsia observed with orthogonal polarisation spectral imaging. *BJOG.* 2001;108:1148-1153
100. Schauf B, Becker S, Abele H, Klever T, Wallwiener D, Aydeniz B. Effect of magnesium on red blood cell deformability in pregnancy. *Hypertens Pregnancy.* 2005;24:17-27
101. Haram K, Svendsen E, Abildgaard U. The hellp syndrome: Clinical issues and management. A review. *BMC pregnancy and childbirth.* 2009;9:8
102. Verdant C, De Backer D. How monitoring of the microcirculation may help us at the bedside. *Current opinion in critical care.* 2005;11:240-244
103. Hanson MA, Gluckman PD. Developmental origins of health and disease: New insights. *Basic Clin Pharmacol Toxicol.* 2008;102:90-93
104. Godfrey KM, Sheppard A, Gluckman PD, Lillycrop KA, Burdge GC, McLean C, et al. Epigenetic gene

promoter methylation at birth is associated with child's later adiposity. *Diabetes*. 2011;60:1528-1534

105. Rakyan VK, Down TA, Thorne NP, Flicek P, Kulesha E, Graf S, et al. An integrated resource for genome-wide identification and analysis of human tissue-specific differentially methylated regions (tdmrs). *Genome Res*. 2008;18:1518-1529

106. Ghosh S, Yates AJ, Fruhwald MC, Miecznikowski JC, Plass C, Smiraglia D. Tissue specific DNA methylation of cpg islands in normal human adult somatic tissues distinguishes neural from non-neural tissues. *Epigenetics*. 2010;5:527-538

107. Khavari DA, Sen GL, Rinn JL. DNA methylation and epigenetic control of cellular differentiation. *Cell Cycle*. 2010;9:3880-3883

108. Bird A. DNA methylation patterns and epigenetic memory. *Genes Dev*. 2002;16:6-21

109. Rugg-Gunn PJ. Epigenetic features of the mouse trophoblast. *Reprod Biomed Online*. 2012;25:21-30

110. Tabano S, Colapietro P, Cetin I, Grati FR, Zanutto S, Mando C, et al. Epigenetic modulation of the igf2/h19 imprinted domain in human embryonic and extra-embryonic compartments and its possible role in fetal growth restriction. *Epigenetics*. 2010;5:313-324

111. Prickett AR, Oakey RJ. A survey of tissue-specific genomic imprinting in mammals. *Mol Genet Genomics*. 2012;287:621-630

112. Vu TH, Li T, Nguyen D, Nguyen BT, Yao XM, Hu JF, et al. Symmetric and asymmetric DNA methylation in the human igf2-h19 imprinted region. *Genomics*. 2000;64:132-143

113. Angiolini E, Fowden A, Coan P, Sandovici I, Smith P, Dean W, et al. Regulation of placental efficiency for nutrient transport by imprinted genes. *Placenta*. 2006;27 Suppl A:S98-102

114. Constancia M, Hemberger M, Hughes J, Dean W, Ferguson-Smith A, Fundele R, et al. Placental-specific igf-ii is a major modulator of placental and fetal growth. *Nature*. 2002;417:945-948

115. Heijmans BT, Kremer D, Tobi EW, Boomsma DI, Slagboom PE. Heritable rather than age-related environmental and stochastic factors dominate variation in DNA methylation of the human igf2/h19 locus. *Hum Mol Genet*. 2007;16:547-554

116. Ehrich M, Nelson MR, Stanssens P, Zabeau M, Liloglou T, Xinarianos G, et al. Quantitative high-throughput analysis of DNA methylation patterns by base-specific cleavage and mass spectrometry. *Proc Natl Acad Sci U S A*. 2005;102:15785-15790

117. Senner CE. The role of DNA methylation in mammalian development. *Reprod Biomed Online*. 2011;22:529-535

118. Koukoura O, Sifakis S, Spandidos DA. DNA methylation in the human placenta and fetal growth (review). *Mol Med Rep*. 2012;5:883-889

119. Mill J, Heijmans BT. From promises to practical strategies in epigenetic epidemiology. *Nature reviews. Genetics*. 2013;14:585-594

120. Lowe R, Slodkowicz G, Goldman N, Rakyan VK. The human blood DNA methylome displays a highly distinctive profile compared with other somatic tissues. *Epigenetics*. 2015;10:274-281

121. Slieker RC, Bos SD, Goeman JJ, Bovee JV, Talens RP, van der Breggen R, et al. Identification and systematic annotation of tissue-specific differentially methylated regions using the illumina 450k array. *Epigenetics Chromatin*. 2013;6:26

122. Lokk K, Modhukur V, Rajashekar B, Martens K, Magi R, Kolde R, et al. DNA methylome profiling of human tissues identifies global and tissue-specific methylation patterns. *Genome biology*. 2014;15:r54

123. Gomes MV, Pelosi GG. Epigenetic vulnerability and the environmental influence on health. *Exp Biol Med (Maywood)*. 2013;238:859-865

124. Koestler DC, Christensen B, Karagas MR, Marsit CJ, Langevin SM, Kelsey KT, et al. Blood-based profiles of DNA methylation predict the underlying distribution of cell types: A validation analysis. *Epigenetics*. 2013;8:816-826

125. Slieker RC, Roost MS, van Iperen L, Suchiman HE, Tobi EW, Carlotti F, et al. DNA methylation

landscapes of human fetal development. *PLoS genetics*. 2015;11:e1005583
126. Schroeder DI, Blair JD, Lott P, Yu HO, Hong D, Crary F, et al. The human placenta methylome. *Proc Natl Acad Sci U S A*. 2013;110:6037-6042
127. Bruce M. Carlson BC. *Human embryology and developmental biology*. MOSBY; 2009.
128. Lowe R, Gemma C, Beyan H, Hawa MI, Bazeos A, Leslie RD, et al. Buccals are likely to be a more informative surrogate tissue than blood for epigenome-wide association studies. *Epigenetics*. 2013;8:445-454
129. Byun HM, Siegmund KD, Pan F, Weisenberger DJ, Kanel G, Laird PW, et al. Epigenetic profiling of somatic tissues from human autopsy specimens identifies tissue- and individual-specific DNA methylation patterns. *Hum Mol Genet*. 2009;18:4808-4817
130. Bocker MT, Hellwig I, Breiling A, Eckstein V, Ho AD, Lyko F. Genome-wide promoter DNA methylation dynamics of human hematopoietic progenitor cells during differentiation and aging. *Blood*. 2011;117:e182-189
131. Bakulski KM, Feinberg JI, Andrews SV, Yang J, Brown S, S LM, et al. DNA methylation of cord blood cell types: Applications for mixed cell birth studies. *Epigenetics*. 2016;11:354-362
132. Wu HC, Delgado-Cruzata L, Flom JD, Kappil M, Ferris JS, Liao Y, et al. Global methylation profiles in DNA from different blood cell types. *Epigenetics*. 2011;6:76-85
133. Harper KN, Peters BA, Gamble MV. Batch effects and pathway analysis: Two potential perils in cancer studies involving DNA methylation array analysis. *Cancer epidemiology, biomarkers & prevention : a publication of the American Association for Cancer Research, cosponsored by the American Society of Preventive Oncology*. 2013;22:1052-1060
134. Grigoriu A, Ferreira JC, Choufani S, Baczyk D, Kingdom J, Weksberg R. Cell specific patterns of methylation in the human placenta. *Epigenetics*. 2011;6:368-379
135. Joo JE, Hiden U, Lassance L, Gordon L, Martino DJ, Desoye G, et al. Variable promoter methylation contributes to differential expression of key genes in human placenta-derived venous and arterial endothelial cells. *BMC Genomics*. 2013;14:475
136. Chen YA, Lemire M, Choufani S, Butcher DT, Grafodatskaya D, Zanke BW, et al. Discovery of cross-reactive probes and polymorphic cpgs in the illumina infinium humanmethylation450 microarray. *Epigenetics*. 2013;8:203-209
137. Cencioni C, Spallotta F, Martelli F, Valente S, Mai A, Zeiher AM, et al. Oxidative stress and epigenetic regulation in ageing and age-related diseases. *International journal of molecular sciences*. 2013;14:17643-17663
138. Dedeurwaerder S, Defrance M, Calonne E, Denis H, Sotiriou C, Fuks F. Evaluation of the infinium methylation 450k technology. *Epigenomics*. 2011;3:771-784
139. Sandoval J, Heyn H, Moran S, Serra-Musach J, Pujana MA, Bibikova M, et al. Validation of a DNA methylation microarray for 450,000 cpg sites in the human genome. *Epigenetics*. 2011;6:692-702
140. Bibikova M, Barnes B, Tsan C, Ho V, Klotzle B, Le JM, et al. High density DNA methylation array with single cpg site resolution. *Genomics*. 2011;98:288-295
141. Huber W, Carey VJ, Gentleman R, Anders S, Carlson M, Carvalho BS, et al. Orchestrating high-throughput genomic analysis with bioconductor. *Nat Methods*. 2015;12:115-121
142. Pidsley R, CC YW, Volta M, Lunnon K, Mill J, Schalkwyk LC. A data-driven approach to preprocessing illumina 450k methylation array data. *BMC Genomics*. 2013;14:293
143. Du P, Zhang X, Huang CC, Jafari N, Kibbe WA, Hou L, et al. Comparison of beta-value and m-value methods for quantifying methylation levels by microarray analysis. *BMC Bioinformatics*. 2010;11:587
144. Houseman EA, Kile ML, Christiani DC, Ince TA, Kelsey KT, Marsit CJ. Reference-free deconvolution of DNA methylation data and mediation by cell composition effects. *BMC Bioinformatics*. 2016;17:259
145. Marabita F, Almgren M, Lindholm ME, Ruhrmann S, Fagerstrom-Billai F, Jagodic M, et al. An evaluation of analysis pipelines for DNA methylation profiling using the illumina humanmethylation450 beadchip platform. *Epigenetics*. 2013;8:333-346

146. Franzen J, Zirkel A, Blake J, Rath B, Benes V, Papantonis A, et al. Senescence-associated DNA methylation is stochastically acquired in subpopulations of mesenchymal stem cells. *Aging cell*. 2017;16:183-191
147. Paquette AG, Houseman EA, Green BB, Lesseur C, Armstrong DA, Lester B, et al. Regions of variable DNA methylation in human placenta associated with newborn neurobehavior. *Epigenetics*. 2016;11:603-613
148. Bardou P, Mariette J, Escudie F, Djemiel C, Klopp C. Jvenn: An interactive venn diagram viewer. *BMC Bioinformatics*. 2014;15:293
149. Huang da W, Sherman BT, Lempicki RA. Bioinformatics enrichment tools: Paths toward the comprehensive functional analysis of large gene lists. *Nucleic acids research*. 2009;37:1-13
150. Huang da W, Sherman BT, Lempicki RA. Systematic and integrative analysis of large gene lists using david bioinformatics resources. *Nature protocols*. 2009;4:44-57
151. Herzog EM, Eggink AJ, Reijnierse A, Kerkhof MA, de Krijger RR, Roks AJ, et al. Impact of early- and late-onset preeclampsia on features of placental and newborn vascular health. *Placenta*. 2017;49:72-79
152. Anton L, Brown AG, Bartolomei MS, Elovitz MA. Differential methylation of genes associated with cell adhesion in preeclamptic placentas. *PLoS One*. 2014;9:e100148
153. Blair JD, Yuen RK, Lim BK, McFadden DE, von Dadelszen P, Robinson WP. Widespread DNA hypomethylation at gene enhancer regions in placentas associated with early-onset pre-eclampsia. *Molecular human reproduction*. 2013;19:697-708
154. Ching T, Ha J, Song MA, Tiirikainen M, Molnar J, Berry MJ, et al. Genome-scale hypomethylation in the cord blood dnas associated with early onset preeclampsia. *Clin Epigenetics*. 2015;7:21
155. Ching T, Song MA, Tiirikainen M, Molnar J, Berry M, Towner D, et al. Genome-wide hypermethylation coupled with promoter hypomethylation in the chorioamniotic membranes of early onset pre-eclampsia. *Molecular human reproduction*. 2014;20:885-904
156. Zhu L, Lv R, Kong L, Cheng H, Lan F, Li X. Genome-wide mapping of 5mc and 5hmc identified differentially modified genomic regions in late-onset severe preeclampsia: A pilot study. *PLoS One*. 2015;10:e0134119
157. van Dongen J, Ehli EA, Slieker RC, Bartels M, Weber ZM, Davies GE, et al. Epigenetic variation in monozygotic twins: A genome-wide analysis of DNA methylation in buccal cells. *Genes (Basel)*. 2014;5:347-365
158. Reinius LE, Acevedo N, Joerink M, Pershagen G, Dahlen SE, Greco D, et al. Differential DNA methylation in purified human blood cells: Implications for cell lineage and studies on disease susceptibility. *PLoS One*. 2012;7:e41361
159. van Buuren S, Groothuis-Oudshoorn K. Mice: Multivariate imputation by chained equations in r. *J Stat Softw*. 2011;45:1-67
160. Hogg K, Blair JD, McFadden DE, von Dadelszen P, Robinson WP. Early onset pre-eclampsia is associated with altered DNA methylation of cortisol-signalling and steroidogenic genes in the placenta. *PLoS One*. 2013;8:e62969
161. Hogg K, Blair JD, von Dadelszen P, Robinson WP. Hypomethylation of the lep gene in placenta and elevated maternal leptin concentration in early onset pre-eclampsia. *Molecular and cellular endocrinology*. 2013;367:64-73
162. Yuen RK, Penaherrera MS, von Dadelszen P, McFadden DE, Robinson WP. DNA methylation profiling of human placentas reveals promoter hypomethylation of multiple genes in early-onset preeclampsia. *European journal of human genetics : EJHG*. 2010;18:1006-1012
163. Sundrani DP, Reddy US, Joshi AA, Mehendale SS, Chavan-Gautam PM, Hardikar AA, et al. Differential placental methylation and expression of vegf, flt-1 and kdr genes in human term and preterm preeclampsia. *Clin Epigenetics*. 2013;5:6
164. He X, Chatterjee R, John S, Bravo H, Sathyanarayana BK, Biddie SC, et al. Contribution of nucleosome

binding preferences and co-occurring DNA sequences to transcription factor binding. *BMC Genomics*. 2013;14:428

165. Monk D. Genomic imprinting in the human placenta. *Am J Obstet Gynecol*. 2015;213:S152-162
166. James JL, Whitley GS, Cartwright JE. Pre-eclampsia: Fitting together the placental, immune and cardiovascular pieces. *Journal of Pathology*. 2010;221:363-378
167. Herzog EM, Eggink AJ, van der Zee M, Lagendijk J, Willemsen SP, de Jonge R, et al. The impact of early- and late-onset preeclampsia on umbilical cord blood cell populations. *Journal of reproductive immunology*. 2016;116:81-85
168. Mousa AA, Cappello RE, Estrada-Gutierrez G, Shukla J, Romero R, Strauss JF, 3rd, et al. Preeclampsia is associated with alterations in DNA methylation of genes involved in collagen metabolism. *The American journal of pathology*. 2012;181:1455-1463
169. Kim J, Kim JY, Song KS, Lee YH, Seo JS, Jelinek J, et al. Epigenetic changes in estrogen receptor beta gene in atherosclerotic cardiovascular tissues and in-vitro vascular senescence. *Biochimica et biophysica acta*. 2007;1772:72-80
170. Alexander MR, Owens GK. Epigenetic control of smooth muscle cell differentiation and phenotypic switching in vascular development and disease. *Annual review of physiology*. 2012;74:13-40
171. Burton GJ, Sebire NJ, Myatt L, Tannetta D, Wang YL, Sadovsky Y, et al. Optimising sample collection for placental research. *Placenta*. 2014;35:9-22
172. Janssen AB, Tunster SJ, Savory N, Holmes A, Beasley J, Parveen SA, et al. Placental expression of imprinted genes varies with sampling site and mode of delivery. *Placenta*. 2015;36:790-795
173. Brosens IA, Robertson WB, Dixon HG. The role of the spiral arteries in the pathogenesis of preeclampsia. *Obstet Gynecol Annu*. 1972;1:177-191
174. Lisonkova S, Joseph KS. Incidence of preeclampsia: Risk factors and outcomes associated with early- versus late-onset disease. *Am J Obstet Gynecol*. 2013;209:544 e541-544 e512
175. Maynard SE, Min JY, Merchan J, Lim KH, Li J, Mondal S, et al. Excess placental soluble fms-like tyrosine kinase 1 (sflt1) may contribute to endothelial dysfunction, hypertension, and proteinuria in preeclampsia. *J Clin Invest*. 2003;111:649-658
176. Levine RJ, Maynard SE, Qian C, Lim KH, England LJ, Yu KF, et al. Circulating angiogenic factors and the risk of preeclampsia. *N Engl J Med*. 2004;350:672-683
177. Karumanchi SA, Maynard SE, Stillman IE, Epstein FH, Sukhatme VP. Preeclampsia: A renal perspective. *Kidney Int*. 2005;67:2101-2113
178. Bouwland-Both MI, Steegers EA, Lindemans J, Russcher H, Hofman A, Geurts-Moespot AJ, et al. Maternal soluble fms-like tyrosine kinase-1, placental growth factor, plasminogen activator inhibitor-2, and folate concentrations and early fetal size: The generation r study. *Am J Obstet Gynecol*. 2013;209:121 e121-111
179. Coolman M, Timmermans S, de Groot CJ, Russcher H, Lindemans J, Hofman A, et al. Angiogenic and fibrinolytic factors in blood during the first half of pregnancy and adverse pregnancy outcomes. *Obstet Gynecol*. 2012;119:1190-1200
180. Zusterzeel PL, Visser W, Blom HJ, Peters WH, Heil SG, Steegers EA. Methylenetetrahydrofolate reductase polymorphisms in preeclampsia and the hellp syndrome. *Hypertens Pregnancy*. 2000;19:299-307
181. Bergen NE, Jaddoe VW, Timmermans S, Hofman A, Lindemans J, Russcher H, et al. Homocysteine and folate concentrations in early pregnancy and the risk of adverse pregnancy outcomes: The generation r study. *Bjog*. 2012;119:739-751
182. van Mil NH, Bouwland-Both MI, Stolk L, Verbiest MM, Hofman A, Jaddoe VW, et al. Determinants of maternal pregnancy one-carbon metabolism and newborn human DNA methylation profiles. *Reproduction*. 2014;148:581-592
183. Steegers-Theunissen RP, Twigt J, Pestinger V, Sinclair KD. The periconceptional period, reproduction and long-term health of offspring: The importance of one-carbon metabolism. *Hum Reprod Update*. 2013

184. Castro R, Rivera I, Struys EA, Jansen EE, Ravasco P, Camilo ME, et al. Increased homocysteine and s-adenosylhomocysteine concentrations and DNA hypomethylation in vascular disease. *Clin Chem.* 2003;49:1292-1296

185. Ingrosso D, Cimmino A, Perna AF, Masella L, De Santo NG, De Bonis ML, et al. Folate treatment and unbalanced methylation and changes of allelic expression induced by hyperhomocysteinaemia in patients with uraemia. *Lancet.* 2003;361:1693-1699

186. Mandaviya PR, Stolk L, Heil SG. Homocysteine and DNA methylation: A review of animal and human literature. *Mol Genet Metab.* 2014;113:243-252

187. Wang L, Wang F, Guan J, Le J, Wu L, Zou J, et al. Relation between hypomethylation of long interspersed nucleotide elements and risk of neural tube defects. *Am J Clin Nutr.* 2010

188. Kok RM, Smith DE, Barto R, Spijkerman AM, Teerlink T, Gellekink HJ, et al. Global DNA methylation measured by liquid chromatography-tandem mass spectrometry: Analytical technique, reference values and determinants in healthy subjects. *Clin Chem Lab Med.* 2007;45:903-911

189. Gao WL, Li D, Xiao ZX, Liao QP, Yang HX, Li YX, et al. Detection of global DNA methylation and paternally imprinted h19 gene methylation in preeclamptic placentas. *Hypertens Res.* 2011;34:655-661

190. Xiang Y, Zhang J, Li Q, Zhou X, Wang T, Xu M, et al. DNA methylome profiling of maternal peripheral blood and placentas reveal potential fetal DNA markers for non-invasive prenatal testing. *Mol Hum Reprod.* 2014;20:875-884

191. Chu T, Bunce K, Shaw P, Shridhar V, Althouse A, Hubel C, et al. Comprehensive analysis of preeclampsia-associated DNA methylation in the placenta. *PLoS One.* 2014;9:e107318

192. Kulkarni A, Chavan-Gautam P, Mehendale S, Yadav H, Joshi S. Global DNA methylation patterns in placenta and its association with maternal hypertension in pre-eclampsia. *DNA Cell Biol.* 2011;30:79-84

193. Nomura Y, Lambertini L, Rialdi A, Lee M, Mystal EY, Grabie M, et al. Global methylation in the placenta and umbilical cord blood from pregnancies with maternal gestational diabetes, preeclampsia, and obesity. *Reprod Sci.* 2014;21:131-137

194. Maebayashi A, Yamamoto T, Azuma H, Kato E, Kuno S, Murase T, et al. Pp121. Expression of plgf, sflt, mtf-1, ho-1 and hif-1 alpha mrnas in preeclampsia placenta and effect of preeclampsia sera on their expression of choriocarcinoma cells. *Pregnancy Hypertens.* 2012;2:304-305

195. Dennery PA. Oxidative stress in development: Nature or nurture? *Free radical biology & medicine.* 2010;49:1147-1151

196. Burton GJ, Jauniaux E. Placental oxidative stress: From miscarriage to preeclampsia. *Journal of the Society for Gynecologic Investigation.* 2004;11:342-352

197. Lazdam M, de la Horra A, Diesch J, Kenworthy Y, Davis E, Lewandowski AJ, et al. Unique blood pressure characteristics in mother and offspring after early onset preeclampsia. *Hypertension.* 2012;60:1338-1345

198. Davidge ST, Signorella AP, Lykins DL, Gilmour CH, Roberts JM. Evidence of endothelial activation and endothelial activators in cord blood of infants of preeclamptic women. *Am J Obstet Gynecol.* 1996;175:1301-1306

199. Kvehaugen AS, Dechend R, Ramstad HB, Troisi R, Fugelseth D, Staff AC. Endothelial function and circulating biomarkers are disturbed in women and children after preeclampsia. *Hypertension.* 2011;58:63-69

200. Jayet P-Y, Rimoldi SF, Stuber T, Salmòn CS, Hutter D, Rexhaj E, et al. Pulmonary and systemic vascular dysfunction in young offspring of mothers with preeclampsia. *Circulation.* 2010;122:488-494

201. Lazdam M, de la Horra A, Pitcher A, Mannie Z, Diesch J, Trevitt C, et al. Elevated blood pressure in offspring born premature to hypertensive pregnancy: Is endothelial dysfunction the underlying vascular mechanism? *Hypertension.* 2010;56:159-165

202. Timpka S, Macdonald-Wallis C, Hughes AD, Chaturvedi N, Franks PW, Lawlor DA, et al. Hypertensive

disorders of pregnancy and offspring cardiac structure and function in adolescence. *Journal of the American Heart Association.* 2016;5

203. Gaillard R, Steegers EA, Tiemeier H, Hofman A, Jaddoe VW. Placental vascular dysfunction, fetal and childhood growth, and cardiovascular development: The generation r study. *Circulation.* 2013;128:2202-2210

204. Mitchell GF, Conlin PR, Dunlap ME, Lacourciere Y, Arnold JM, Ogilvie RI, et al. Aortic diameter, wall stiffness, and wave reflection in systolic hypertension. *Hypertension.* 2008;51:105-111

205. Alsnes IV, Vatten LJ, Fraser A, Bjorngaard JH, Rich-Edwards J, Romundstad PR, et al. Hypertension in pregnancy and offspring cardiovascular risk in young adulthood: Prospective and sibling studies in the hunt study (nord-trondelag health study) in norway. *Hypertension.* 2017;69:591-598

206. Task Force M, Montalescot G, Sechtem U, Achenbach S, Andreotti F, Arden C, et al. 2013 esc guidelines on the management of stable coronary artery disease: The task force on the management of stable coronary artery disease of the european society of cardiology. *Eur Heart J.* 2013;34:2949-3003

207. Bi GL, Chen FL, Huang WM. The association between hypertensive disorders in pregnancy and bronchopulmonary dysplasia: A systematic review. *World journal of pediatrics : WJP.* 2013;9:300-306

208. Lewandowski AJ, Davis EF, Lazdam M, Leeson P. From gene to epigene-based therapies targeting the vascular endothelium. *Current vascular pharmacology.* 2012;10:125-137

209. Weaver IC, Champagne FA, Brown SE, Dymov S, Sharma S, Meaney MJ, et al. Reversal of maternal programming of stress responses in adult offspring through methyl supplementation: Altering epigenetic marking later in life. *The Journal of neuroscience : the official journal of the Society for Neuroscience.* 2005;25:11045-11054

210. Wen SW, Chen XK, Rodger M, White RR, Yang Q, Smith GN, et al. Folic acid supplementation in early second trimester and the risk of preeclampsia. *Am J Obstet Gynecol.* 2008;198:45 e41-47

AUTHORS AND AFFILIATIONS

Erasmus MC, University Medical Centre, Rotterdam, the Netherlands

Department of Obstetrics and Gynaecology

Prof. dr. R.P.M. Steegers-Theunissen
Prof. dr. E.A.P. Steegers
Dr. A.J. Eggink
Dr. J.J. Duvekot
Dr. J.M.J. Cornette
Dr. K.P.J. Wijnands
Dr. J.M. Galvez
A. Reijnierse
M.A.M. Kerkhof
J. Lagendijk

Department of Internal Medicine

Dr. J.B.J. van Meurs
Dr. L. Stolk
M.M.P.J. Verbiest

Department of Internal Medicine, Section of Vascular Medicine and Pharmacology

Dr. A.J.M. Roks

Department of Immunology

Dr. M. van der Zee

Department of Clinical Chemistry

Dr. R. de Jonge
Dr. S.G. Heil
P.H. Griffioen
B.D. van Zelst

Department of Neonatology

Prof. dr. I.K.M. Reiss

Department of Pathology

Prof. dr. R.R. de Krijger

A.L. Nigg

Department of Biostatistics

Prof. dr. ing. P.H.C. Eilers

S.P. Willemsen

Dr. D. Rizopoulos

Dr. W.C.J. Hop

Department of Haematology

Prof. dr. J.J. Cornelissen

Department of Epidemiology

Dr. J.F. Felix

Department of Bioinformatics

Prof. dr. P.J. van der Spek

Dr. A.P. Stubbs

Department of Intensive Care and Paediatric Surgery

Prof. dr. D. Tibboel

Dr. E.A.B. Buijs

Leiden University Medical Centre, Leiden, the Netherlands

Department of Molecular Epidemiology

Dr. B.T. Heijmans

Dr. R.C. Slieker

Harvard School of Public Health, Boston, US

Department of Biostatistics

Dr. J. Chen

LIST OF ABBREVIATIONS

AST	Aspartate aminotransferase
ANCOVA	Analysis of Covariance
ANOVA	Analysis of Variance
BMI	Body mass index
bp	Base pairs
BP	Blood pressure
SBP	Systolic blood pressure
DBP	Diastolic blood pressure
BW	Birth weight
CI	Confidence interval
CPD	Citrate Phosphate Dextrose-solution
CpG	Cytosine phosphate Guanine nucleotides
CV	Coefficient of variation
DMR	Differentially methylated region
DMP	Differentially methylated position
EOPE	Early-onset preeclampsia
EWAS	Epigenome-wide association study
EVG	Elastica Von Gieson
FGR	Fetal growth restriction
GA	Gestational age
GO	Gene-ontology
HE	Hematoxylin/eosin
HELLP	Haemolysis, Elevated Liver enzymes and Low Platelets
HI	Heterogeneity Index
HIF-1α	Hypoxia-Inducible Factor 1α
IEL	Internal elastic lamina
IGF2	Insulin-like growth factor 2
Immature gran.	Immature granulocytes
LDH	Lactate Dehydrogenase
LED	Light-Emitting Diodes
LINE-1	Long-Interspersed Nuclear Element-1
LOPE	Late-onset preeclampsia
LUMA	Luminometric Methylation Assay
MFI	Microcirculatory Flow Index
MNC	Mononuclear cells
NRBC	Nucleated red blood cells
OPS	Orthogonal Polarisation Spectral imaging

OR	Odds ratio
PE	Preeclampsia
PlGF	Placental Growth Factor
PCR	Polymerase Chain Reaction
PTB	Preterm birth
PVD	Perfused Vessel Density
QC	Quality control
RAS	Renin-angiotensin System
ROS	Reactive oxygen species
SAH	S-adenosylhomocysteine
SAM	S-adenosylmethionine
SD	Standard deviation
SDF	Sidestreeam Darkfield
sFLT-1	Soluble Fms-Like Tyrosine kinase-1 receptor-1
sEng	Soluble Endoglin
UCB	Umbilical cord blood
UCBC	Umbilical cord blood cell
UC-MNC	Umbilical cord mononuclear cells
UC-WBC	Umbilical cord white blood cells
UCI	Umbilical coiling index
VEGF	Vascular Endothelial Growth Factor

LIST OF PUBLICATIONS

This thesis

Chapter 2

E.M. Herzog, A.J. Eggink, M. van der Zee, J. Lagendijk, S.P. Willemsen, R. de Jonge, E.A.P. Steegers, R.P.M. Steegers-Theunissen: *The impact of early- and late-onset preeclampsia on umbilical cord blood cell populations.* Journal of Reproductive Immunology, 2016 Aug. 116: p. 81-85

Chapter 3

E.M. Herzog, A.J. Eggink, A. Reijnierse, M.A.M. Kerkhof, R.R. de Krijger, A.J.M. Roks, I.K.M. Reiss, A.L. Nigg, P.H.C. Eilers, E.A.P. Steegers, R.P.M. Steegers-Theunissen: *Impact of early- and late-onset preeclampsia on features of placental and newborn vascular health.* Placenta, 2017 Jan. 49: p. 72-79

Chapter 4

J.M.J. Cornette, E.M. Herzog, E.A.B. Buijs, J.J. Duvekot, D. Rizopoulos, W.C.J. Hop, D. Tibboel, E.A.P. Steegers: *Microcirculation in women with severe preeclampsia and HELLP syndrome: a case-control study*. British Journal of Obstetrics and Gynaecology, 2014. 121: p. 363–370

Chapter 5

E.M. Herzog, J.M. Galvez, A.J.M. Roks, L. Stolk, M.M.P.J. Verbiest, P.H.C. Eilers, J.J. Cornelissen, E.A.P. Steegers, R.P.M. Steegers-Theunissen: *Tissue-specific DNA methylation profiles in newborns*. Clinical Epigenetics, 2013. 5: p. 8-12

Chapter 6

E.M. Herzog, A.J. Eggink, S.P. Willemsen, R.C. Slieker, J.F. Felix, A.P. Stubbs, P.J. van der Spek, J.B.J. van Meurs, B.T. Heijmans, R.P.M. Steegers-Theunissen: *The tissue-specific aspect of genome-wide DNA-methylation in newborn and placental tissues: implications for epigenetic epidemiologic studies.* (submitted)

Chapter 7

E.M. Herzog, A.J. Eggink, S.P. Willemsen, R.C. Slieker, K.P.J. Wijnands, J.F. Felix, J. Chen, A.P. Stubbs, P.J. van der Spek, J.B.J. van Meurs, R.P.M. Steegers-Theunissen: *Early- and late-onset preeclampsia and the tissue-specific epigenome of the placenta and newborn.* Placenta, 2017 Oct. 58: p. 122-132

Chapter 8

S.G. Heil, E.M. Herzog, P.H. Griffioen, B.D. van Zelst, S.P. Willemsen, R.P.M. Steegers-Theunissen and E.A.P. Steegers: *Hypomethylation of placental growth factor and decreased SAM:SAH ratio in placental tissue of preeclampsia-complicated pregnancies*. (submitted)

Other publications

C.B. van den Berg, I. Chaves, E.M. Herzog, E.A.P. Steegers, S.P. Willemsen, G.T.J. van der Horst, R.P.M. Steegers-Theunissen: *Early- and late-onset preeclampsia and the DNA methylation of circadian clock and clock controlled genes in placental and newborn tissues.* Chronobiology International, 2017 Jun. 14: p. 1-12

J.M.J. Cornette, E.A.B. Buijs, J.J. Duvekot, E.M. Herzog, J.W. Roos-Hesselink, D. Rizopoulos, M. Meima, E.A.P. Steegers: *Hemodynamic effects of intravenous nicardipine in severely preeclamptic women with a hypertensive crisis*. Ultrasound in Obstetrics and Gynecology, 2016 Jan. 47: p. 89-95.

ABOUT THE AUTHOR

Emilie Marjolein Herzog was born in 1983 in Amersfoort, the Netherlands, where she attended high school at *Het Nieuwe Eemland College*. During her graduation year she started professional preparatory dance training at CODARTS, University of the Arts, Rotterdam. After her gymnasium graduation in 2001, she performed two years of professional dance education at *De Theaterschool*, Amsterdam School of the Arts. In 2004 she started medical school at Erasmus University Rotterdam and simultaneously founded her Ballet- and Dance school in Woudenberg where she taught ballet classes to children during the weekends.

During her medical internships she became interested in the field of Obstetrics and Gynaecology and performed her last-year elective internships at the Obstetrics and Gynaecology department at the *Charité – Universitätsmedizin* in Berlin and her elective research thesis on microcirculation in preeclamptic patients at the Erasmus MC, University Medical Centre Rotterdam, under the supervision of dr. J.M.J. Cornette.

She graduated from medical school in 2010 and started her PhD project described in this thesis in 2011 under the supervision of prof. dr. R.P.M. Steegers-Theunissen. As board member of the *Arts-Assistenten Vereniging*, she organised the 2013 Erasmus MC Research Day for medical residents and PhD-students.

In 2014 she started working as a junior resident at the department of Obstetrics and Gynaecology at the *Maasstad* Hospital Rotterdam. After obtaining a research-grant from *Stichting Gezond Geboren*, she completed the last phase of her PhD project. In 2016, she started her specialty training in Obstetrics and Gynaecology at the *St. Joseph Krankenhaus* in Berlin, Germany.

PHD PORTFOLIO

Name PhD candidate:	Emilie M. Herzog
Erasmus MC department:	Obstetrics and Gynaecology
PhD period:	2011-2017
Promotor:	Prof. dr. R.P.M. Steegers-Theunissen
Co-promotor:	Dr. A.J. Eggink

General courses	Year
Principles of Research in Medicine (ESP01)	2011
Principles of Genetic Epidemiology (ESP43)	2011
Genomics in Molecular Medicine (ESP57)	2011
Biostatistical Methods I: Basic Principles (CCO2)	2011
English Biomedical Writing and Communication	2012
Literature search	2013

Seminars and workshops	
Epigenetics and Developmental Programming Conference, Newcastle upon Tyne, UK	2011
Weekly research meetings, department of Obstetrics and Prenatal Medicine, Erasmus MC, Rotterdam, the Netherlands	2011-2014
2-Weekly research meetings, department of Epidemiology, Erasmus MC, Rotterdam, the Netherlands	2015
Wladimiroff Research Day, Rotterdam, the Netherlands	2011-2014
Coordinator of Erasmus MC Research Day for residents and PhD students	2013

Presentations

Society of Gynecological Investigations 59th Scientific Meeting, San Diego, USA	2012
2nd European Congress on Preconception Care and Health, Rotterdam, the Netherlands	2012
International Society for the Study of Hypertension in Pregnancy, European Congress, Trømso, Norway	2013
8th World Congress on Developmental Origins of Health and Disease, Singapore	2013
Society of Gynecological Investigations 61st Scientific Meeting, Florence, Italy	2014
Research meeting department of Obstetrics and Prenatal Medicine, Rotterdam, the Netherlands	2011-2014
Research meeting department of Epidemiology, Rotterdam, the Netherlands	2015
9th World Congress on Developmental Origins of Health and Disease, Cape Town, South Africa	2015
International Society for the Study of Hypertension in Pregnancy, European Congress, Berlin, Germany	2017

Teaching

Supervising master thesis M. Galvez, medical doctor	2011
Supervising master thesis J. Lagendijk, 6th year medical student	2011
Supervising master thesis A. Reijnierse, 4th year medical student	2012

Supervising master thesis N. Hou, 6th year medical student	2012-2013
Supervising master thesis M. Kerkhof, 4th year medical student	2013
Clinical lessons nurses, doctors, PhD students, medical students, Erasmus MC, Rotterdam, the Netherlands	2011-2013

Awards

Best Poster award (Basic/Translational research) at International Society for the Study of Hypertension in Pregnancy, European Congress, Trømso, Norway	2013

Grant

Grant from Foundation '*Gezond Geboren*' for PhD project: '*Epigenome-wide analysis of DNA methylation in placental and neonatal tissues in preeclamptic pregnancies*'	2015

Other

Preconception counselling of subfertile couples	2011-2013

ACKNOWLEDGEMENTS

During last summer, my first summer in Berlin, there was a trumpetist practicing one of my favourite songs, 'Summertime' by Gershwin, almost daily from an open window close to my apartment. I enjoyed it from my tiny balcony and realised that this song represents the feeling of my PhD period in the best way possible: it drags forward, feels intense, uncomfortable, and a little melancholic, until the tone changes after the third sentence… Then it feels alright, reassuring, and extremely beautiful. Then you are glad you did it, feel a tiny bit proud, and you realise how much you have learned. You also realise, how many people were of extreme importance during that period, both professionally and privately. Of these people, I would like to thank the following in particular (in their own language):

Mijn promotor, Prof. dr. R.P.M. Steegers-Theunissen, Régine, heel blij verrast las ik eind 2010 je mailtje ter uitnodiging voor een gesprek voor deze promotieplek. Ondanks de voor mij toen nog abstracte begrippen *DOHaD* en *epigenetica*, begreep ik meteen dat dit een heel mooi en sexy (zoals je zelf zei) project was, met een erg hippe professor. Al moest je mij geregeld wat afremmen in mijn enthousiasme, ik ben dankbaar dat we ondanks (of dankzij) mijn koppigheid daarin, toch dit project hebben kunnen uitvoeren. Heel erg bedankt voor je vertrouwen, het altijd zien van nieuwe mogelijkheden en je geduld tijdens de afgelopen tijd, en vooral alle kansen die je me hebt geboden.

Mijn co-promotor, Dr. A.J. Eggink, Alex, je raakte in een wat later stadium betrokken bij mijn promotie, maar jouw input vanuit de kliniek en vooral ook je zeer gedetailleerde en kritische blik tijdens het schrijfproces (zelfs de hele referentie-lijst!) waren van grote waarde.

De leden van mijn leescommissie, Prof. dr. A.H.J. Danser, Prof. dr. A. Franx en Prof. dr. C.M. van Duijn, ik voel mij vereerd dat u bereid bent geweest mijn proefschrift te beoordelen en wil u daarvoor ontzettend bedanken. Ook wil ik de grote commissie bedanken voor uw bereidheid hierin plaats te nemen, mijn proefschrift te beoordelen en uw inbreng tijdens de plechtigheid.

Prof. dr. M. Abou-Dakn, ich fühle mich sehr dankbar, dass ich unter Ihrer begeisterten Leitung in einer so tonangebenden Klinik die Geburtshilfe und Gynäkologie lernen darf und hoffe auf eine noch lange weitere Zusammenarbeit.

Prof. dr. E.A.P. Steegers, Eric, veel dank voor uw inbreng bij de opzet van de klinische studies uit mijn proefschrift. Een Berlijn-Rotterdam symposium

zouden we wellicht in de toekomst nog eens kunnen organiseren, want het is zoals u terecht zei bijzonder fascinerend en verrijkend om van elkaar te leren.

De hulptroepen bij de epigenetica-projecten: Dr. J.F. Felix en Dr. R.C. Slieker. Janine en Roderick, ik ben jullie ongelooflijk dankbaar voor jullie onmisbare inbreng bij de opzet, de statistische analyse en het schrijven en reviseren van beide epigenetica-projecten (en de waardevolle skypegesprekken). Roderick, mijn naaste omgeving kent jou als mijn held, dat je dat even weet; veel dank voor de ontelbare momenten dat je iets schijnbaar onoplosbaars in een split-second hebt opgelost. Ik hoop dat dit niet onze laatste gezamenlijke projecten waren!

Dr. A.J.M. Roks, beste Anton, je hebt ervoor gezorgd dat ik mij als simpele dokter die niet kon pipetteren heel snel thuis ging voelen in jullie super gezellige laboratorium, en mij en Marcela bovendien heel veel geleerd. Ik vond het vaak jammer wanneer *my precious endothelial cells* weer gewonnen waren en ik terug moest kruipen achter mijn computer.

Prof. dr. ing. P.H.C. Eilers en S.P. Willemsen, beste Paul en Sten, wat moeten wij als onderzoekers zonder statistici? Bedankt voor jullie beider hulp, en Sten natuurlijk in het bijzonder voor je zeer intensieve inzet tijdens de genoomwijde epigenetica analyses.

Dr. J.M.J. Cornette, Jerôme, je hebt een grote rol gespeeld in het ontstaan van mijn interesse in de verloskunde, gynaecologie en onderzoek doen in het bijzonder. Ik kijk met veel plezier terug op onze gezamenlijke PICO tijdens mijn coschap, het microcirculatie-project, en jouw uiterst heldere en eerlijke inzichten over de toekomst, zowel op privé als professioneel vlak.

Alle medewerkers van het pathologie-laboratorium in het Erasmuc MC, in het bijzonder prof. dr. R.R. de Krijger, Frieda Uijtdewilligen en Alex Nigg, voor jullie inzet tijdens de grote hoeveelheden navelstrengcoupes die Anniek en ik in korte tijd moesten produceren en analyseren en onze regen aan vragen over het snij-, plak-, kleur-, scan- en digitaal beoordeel-proces.

Michael en Mila! Zonder jullie was deel II van mijn proefschrift er nooit geweest, en waren al die maanden DNA- en RNA- isolaties bovendien een heel stuk minder gezellig geweest. Bedankt voor al jullie hulp en geduld met die onhandige dokters in het lab. Lang leve Zwitsal!

Prof. dr. I.K.M. Reiss, bedankt voor uw inbreng en bijzonder aanstekelijke enthousiasme tijdens de overleggen binnen ons gezamenlijk neonaten-project, weliswaar niet in dit proefschrift opgenomen, maar m.i. nog steeds spannend om nader te onderzoeken. Prof. dr. P.J. van der Spek and Dr. A.P. Stubbs, Andrew, many thanks for helping me to perform and interpret the extensive bioinformatic

analysis of both epigenetic projects. Prof. dr. B.T. Heijmans, Dr. M. van der Zee, Martin, Dr. R. de Jonge, Dr. S.G. Heil, Sandra, Prof. dr. J.J. Cornelissen, Dr. L. Duinhouwer, Lucia, Dr. R.C.J. de Jonge, Rogier, veel dank voor het samen opzetten, uitwerken en meeschrijven aan verschillende onderzoeken binnen mijn proefschrift.

De verloskundigen, verpleegkundigen, medisch studenten en artsen van de verloskamers in het Erasmus MC, die mij (meestal) keurig opbelden wanneer er bijna een Predict-placenta geboren zou worden zodat ik vaak halfslapend op de fiets moest springen. Gelukkig zijn die Predict-placenta's vanaf een zeker moment ook in zeer goede handen gekomen van het fantastische 'Predictteam', te herkennen aan de flitsende step met roze fietsmand, die bij tij en ontij met klotsende vloeibare stikstof onderweg was. Ik geef toe dit misschien iets romantischer klinkt dan het op sommige momenten was... Voor het slagen van dit logistiek zeer uitdagende project waren onze fijne researchverpleegkundigen Joke en Titia onmisbaar.

De groep wisselende bewoners op de 22e verdieping van de oude faculteitstoren van het Erasmus MC. Deze bewoners hebben een aantal bijzondere rituelen, zoals het drinken van overmatige hoeveelheden thee, het nuttigen van overmatige hoeveelheden Cake in de Week en gefrituurde kaasstengels en het zeer punctueel opvolgen van het lunchmoment, dat begint met een groot verzamelspectakel om 12:13u stipt. Ik heb o.a. van de volgende karakteristieke bewoners mogen genieten: strenge maar hele lieve Predict- en borrelqueen Eef, kleurrijke sprankelende Babsie, ballerina/mede-methylerings-nerd Kim, professor Twigt, Matthijs mijn secret-computer-helpdesk, my dear Eline en Jorine, cara Franceska, mijn veel te lieve kamergenootje Nic (bedankt voor alle mandarijnen, bezoekjes aan Dordrecht en discussies over waarom we nu eigenlijk promoveren), reisgenootje Caro (bedankt voor de vele gesprekken over waarom we nu eigenlijk in God moeten geloven en van de man moeten houden), en mede-dansfanaat Ireen (zo cool dat jij gewoon meedoet als ik voorstel mee te dansen in een gothic christmas-chick dansje op University College of een flashmop tussen een zaal vol psychiaters!). Ik mis jullie!

De fantastische medisch studenten, die van grote hulp waren bij een groot deel van deze projecten: Anniek, Martina en Jacky. Special thanks goes to Dr. J.M. Galvez, dear dear Marcela, it was so much fun working with you! I loved all our very first bloopers in the laboratory of Anton and our desperate attempts to obtain those bloody endothelial cells.... I think you are a very talented researcher and wish we were still working together!

Liebe liebe Oberärzte und Kollegen aus dem St. Joseph Krankenhaus, es ist mir sehr wichtig, mich bei euch für die sehr angenehme Zusammenarbeit, eure Unterstützung und die Freiheit zu bedanken, die ich sogar in einigen Nachtdiensten, versteckt hinter meinem Laptop, für dieses PhD Projekt gebraucht habe. Dr. T. Lehmann, unsere leitende Oberärztin, liebe Tina, ich bin sehr dankbar dass ich von dir lernen darf und dass du zu meiner Verteidigung nach Rotterdam kommst!

Marleentje, mijn paranimf! Ik op mijn beurt, mis jou ook veel te vaak en te veel en verlang geregeld naar onze kookfestijnen, ons urenlange gezever over PhD perikelen onder het genot van jullie drankvoorraad, onze licht-snobistische koffie-gesprekken, en vooral dat ik even snel op de fiets naar je toe kan komen voor een pizza al Michèle, en een Limoncello in de voortuin. Je bent een ontzettend waardevolle vriendin, ver weg of niet.

Mijn hele fijne en bijzondere vrienden en vriendinnen: Geer en Oliver, Benno, Leo en Lisa (laten we de appelboor uit de microbiologie-les en de Bailey's in laboratorium-ijs voor altijd blijven eren), Floor en Ro, Desiree en Roeland (met een speciaal kusje voor Felix), Frederique, RJ, Annelies, Wytse, Willemijn, Sjoerd, Stella, Robert (O&N op mijn dakterras?), Anna en Casper, Renée en Floris, Magdalena (waiting for your Placental Art exhibition...), en de veel te luidruchtige, rete-gezellige Familie Starrenburg-Herzog: ik ben blij dat ik hier nog een keer zwart op wit tegen jullie kan zeggen dat jullie van ontzettende waarde geweest zijn tijdens dit uitdagende project, Dankjulliewel!

Mijn lieve zusjes Adrienne en Marcella. Alle drie zijn we een beetje eigenwijs en vol met onze eigen dromen en ambities. Dat maakt onze levens soms heel verschillend, en ook nog zo ver uit elkaar... maar destemeer bewonder ik jullie doorzettingsvermogen, doelgerichtheid en vooral jullie enorme talent. Op naar het EK 2018! Veelzijdige Marcella'tje, ja zeker, voor altijd mijn kleine zusje, maar ook mijn paranimf. Ik ben inderdaad een zondagskind zoals je altijd zegt, dat jij bij de verdediging van dit celmembranen-proefschrift naast mij staat. Heb je wel even opgezocht wat een paranimf precies is...?

Lieve lieve pap en mam. Op vakantie zei een Zuid-Afrikaanse vrouw met drie kinderen die verspreid over de wereld woonden tegen mij: 'Well, I guess we did something good in raising our children in such a way, that they are brave enough to discover the world'. Misschien helpt het een beetje om dit zo te zien, want zo is het echt! Ik ben jullie heel dankbaar voor alles dat jullie ons lieten zien, alles dat jullie voor ons mogelijk maakten, en hoe jullie ons vrij lieten in het langzaam ontdekken van onze dromen en talenten. Maar vooral ook dat

jullie dat stimuleerden en ons lieten geloven dat misschien wel alles mogelijk was... Als kind wilde ik soms dat we een wat normaler doorsnee Woudenbergs gezinnetje waren, maar het is juist helemaal goed zo. Ik kijk al uit naar de eerste avond met zijn allen voor de open haard in de boerderij...

Allerliefste Frank. Ik vrees dat het een illusie is dat de geliefde van een promovendus voldoende bedankt kan worden in enkele regels van het dankwoord. Maar dit wat hier ligt is iets van ons samen, en het belichaamt vele lange uren, die overal te vinden waren, schrijvend op de meest uiteenlopende locaties: in de rook bij Wohnzimmer, op de trap aan het water langs de Donau, voor de open haard in Zuid-Duitsland en in de zon op het terras bij Kaffee A. Horn. Als ik eraan terug denk weet ik heel zeker, dat jij degene bent waardoor het lichter leek, waardoor we zo veel moesten lachen en ik de mooie dingen niet uit het oog verloor. Het is wel wat vreemd, maar ook goed dat het voorbij is voor mij, en bijna voor jou. Jouw proefschrift wordt tenminste een écht boek, coming up soon... Ik kijk uit naar alles dat nog komen gaat, met jou.

PRE
ECL
AMP
SIA